Nitric oxide reactivity of copper(II) complexes with N-donor ligands: Formation of [Cu^{II}-$NO^{\bullet}$] intermediate

A Dissertation submitted to the
Indian Institute of Technology Guwahati as
partial fulfillment for the Degree of
Doctor of Philosophy in Chemistry

Submitted by

Moushumi Sarma
(Roll No. 07612220)

Supervisor

Dr. Biplab Mondal

Department of Chemistry
Indian Institute of Technology Guwahati

December, 2011

Dedicated to My Family
&
Friends.....

Statement

I hereby declare that this thesis entitled "**Nitric oxide reactivity of copper(II) complexes with N-donor ligands: Formation of [Cu^{II}-$NO^{\bullet}$] intermediate**" is the outcome of research work carried out by me under the supervision of Dr. Biplab Mondal, in the Department of Chemistry, Indian Institute of Technology Guwahati, India.

In keeping with the general practice of reporting scientific observations, due acknowledgement has been made whenever work described here has been based on the findings of other investigators.

December, 2011 **Moushumi Sarma**

Certificate

This is to certify that Miss Moushumi Sarma has been working under my supervision since January, 2008 as a regular Ph. D. student in the Department of Chemistry, Indian Institute of Technology Guwahati. I am forwarding her thesis entitled "**Nitric oxide reactivity of copper(II) complexes with N-donor ligands: Formation of [Cu^{II}-$NO^{\bullet}$] intermediate**" being submitted for the Ph. D. degree.

I certify that she has fulfilled all the requirements according to the rules of this Institute regarding the investigations embodied in her thesis and this work has not been submitted elsewhere for a degree.

December, 2011 **Dr. Biplab Mondal**

Acknowledgement

The enlightening experience of doing science under the guidance of Dr. Biplab Mondal can hardly be described in words. The numerous discussions and interactions I had with him provided me the opportunity and resources to be creative, inspired me to do my best, making sure I am progressing along a forward path. These are the things that have given me the most confidence in my scientific abilities.

I would like to acknowledge my sincere gratitude to all my doctoral committee members Dr. Gopal Das, Dr. Parameswar K. Iyer and Dr. Aiyagari Ramesh for their insightful advices and valuable suggestions. I am also grateful to the entire faculty and staff in the Department of Chemistry, Indian Institute of Technology Guwahati for providing a wonderful work atmosphere throughout this period.

I would like to thank my labmates Amardeep da, Pankaj, Apurba, Aswini, Vikash, Kanhu, Somnath, Hemanta, Pushperdra, Ananya and Rajib da whom I had an opportunity to work with. No words can express my thankfulness for giving me their time and companionship, which made the time spent in the laboratory and outside pleasant and memorable.

I would like to give my special thanks to my friends Rupam, Pranab, Dipjyoti and Priyanka, for their timely help, support and for the wonderful time we shared during this period.

The financial support from University Grants Commission (UGC), New Delhi for the research fellowship is duly acknowledged.

Finally, I like to thank my parents, without their love and support this work would not have been completed. I like to thank my younger brother, Samiran for his love and moral support during my research work.

December, 2011 **Moushumi Sarma**

CONTENTS

Synopsis

The thesis entitled, "**Nitric oxide reactivity of copper(II) complexes with N-donor ligands: Formation of [Cu^{II}-$NO^{\bullet}$] intermediate**" is divided into six chapters.

Chapter 1: ***Introduction***

The coordination of nitric oxide (NO) to the transition metal ions and its activation have attracted chemists attention as its various biological and physiological reactivity are attributed to the formation of nitrosyl complexes of metallo-proteins, mostly iron or copper-proteins. For instance, it is believed that a [Cu^{I}-NO^{+} $\leftrightarrow$ Cu^{II}-$NO^{\bullet}$] intermediate is involved in the conversion of nitrite to NO or, in some cases to N_2O by nitrite reductase e.g. from *Achromobacter cycloclastes*. On the other hand, metal-nitrosyl adducts presumably play important roles in nitrosation reactions of various thiols to give S-nitrosothiols which are proposed as important carriers of NO equivalents in cellular systems. In this direction, the iron-nitrosyls, both in protein and synthetic model systems have been studied extensively. Ferriheme proteins are known to undergo reduction in aqueous media in the presence of NO. These reactions proceed through two distinct steps: (i) formation of iron(III)-nitrosyl adduct; (ii) followed by the pH dependent reduction of Fe^{III} to Fe^{II} with a simultaneous attack of hydroxide ion to the activated nitrosonium group, [Fe^{III}-$NO^{\bullet}$ $\leftrightarrow$ Fe^{II}-NO^{+}] leading to the formation of nitrite. NO reductions of Cu^{II} are also known though have not been studied as extensively as iron-nitrosyls. A few examples of reduction of Cu^{II} by NO and their use for NO detection are reported in recent years. However, there are hardly any example which shows the distinct spectral evidence of formation of [Cu^{II}-$NO^{\bullet}$] intermediate except one reported by Diaz et. at. and recently by Hayton et. al. Furthermore, there is no report on the coordination of NO in aqueous solution though

it gives a better approach to in vivo conditions than the organic solvents. Thus, the study of the formation of [Cu^{II}-$NO^{\bullet}$] species becomes very important to understand the complex biological processes.

In this chapter, a general introduction of NO with respect to its structural and spectroscopic properties followed by a brief account on its coordination and activation by copper ions has been discussed based on available literature.

Chapter 2: ***Reduction of copper(II) complex of tris-(2-isopropyl aminoethyl)amine by nitric oxide and tri-nitrosation of the ligand***

The reaction of copper(II)perchlorate hexahydrate, $[Cu(H_2O)_6](ClO_4)_2$, with *tris*-(2-isopropylaminoethyl)amine ($\mathbf{L_1}$) in acetonitrile afforded the mononuclear complex **2.1**. It was characterized by various spectroscopic techniques as well as by X-ray single crystal structure determination. The structure of the complex **2.1** (Figure S.2.1) indicates its distorted trigonal bipyramidal shape ($\tau \sim 0.6$) in the solid state.

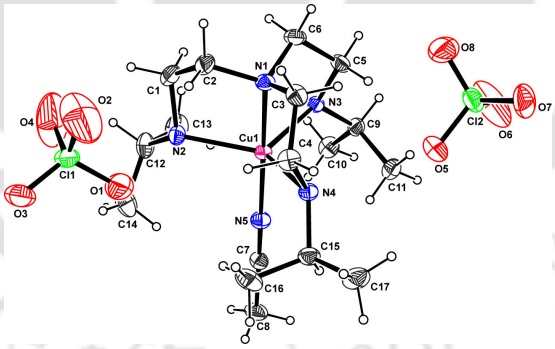

Figure S.2.1: ORTEP diagram of complex **2.1** (50% thermal ellipsoid plot).

The complex **2.1** exhibited a broad *d-d* band with λ_{max} at 826 nm (ε, 340 $M^{-1}cm^{-1}$) along with a relatively strong intra-ligand absorption in the UV-region (λ_{max}, 294 nm, ε, 4775 $M^{-1}cm^{-1}$) in acetonitrile solvent. It displayed one electron paramagnetism and characteristic signals in X-band EPR spectroscopy.

To a degassed acetonitrile solution of complex **2.1**, bubbling of NO leads to the reduction of Cu^{II} center to Cu^{I}. The *d-d* transition for complex **2.1** at 826 nm was found to shift to 640 nm suggesting the formation of [Cu^{II}-$NO^{\bullet}$] intermediate. The unstable nature of the intermediate precludes its further characterization. The absorption intensity of the intermediate was found to decrease with time indicating the reduction of Cu^{II} center to Cu^{I}. This has been monitored by UV-visible (Figure S.2.2a), EPR (Figure S.2.2b), and ^{1}H-NMR spectroscopic studies. The rate of decomposition of [Cu^{II}-$NO^{\bullet}$] intermediate was found to be 5.64×10^{-2} sec^{-1} at 298K.

The reduction of Cu^{II} center was found to be accompanied with the N-nitrosation of the ligand leading to the formation of $\mathbf{L_1}'$ exclusively (yield~30%) (Scheme S.2.1). $\mathbf{L_1}'$ was isolated from the reaction mixture as its perchlorate salt and was characterized by X-ray single crystal structure determination, ^{1}H-NMR and ^{13}C-NMR studies. The ORTEP diagram is shown in figure S.2.3.

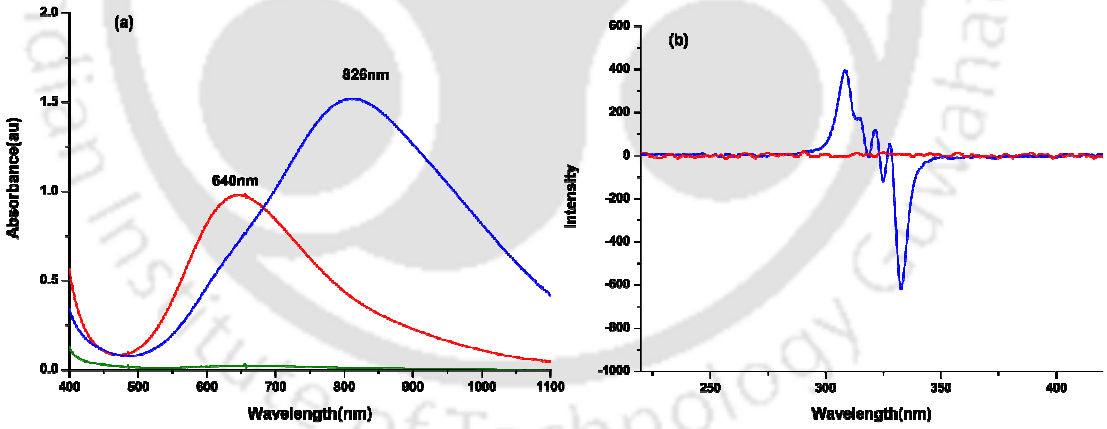

Figure S.2.2: (a) UV-visible spectra of the reaction of complex **2.1** (blue trace) with NO in acetonitrile solvent at room temperature. Red and green traces represent the [Cu^{II}-$NO^{\bullet}$] intermediate and complete reduction of Cu^{II} to Cu^{I}, respectively. (b) X-band EPR spectra of the complex **2.1** (blue trace) and immediately after its reaction with NO (red trace) in acetonitrile solvent at room temperature.

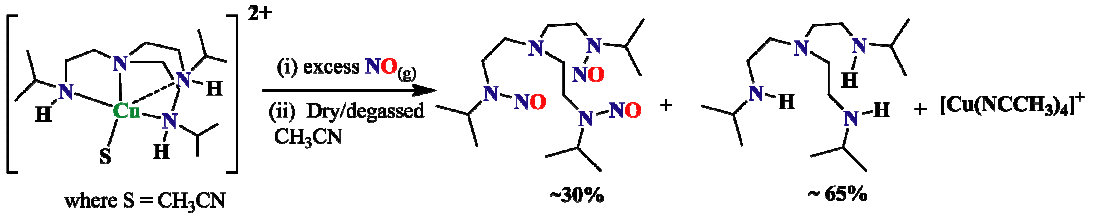

Scheme S.2.1

It should be noted that in methanol solution, the reduction of Cu^{II} to Cu^{I} by NO was also observed. The reduction was found to be accompanied with mono- and dinitrosation (~10% and 20%, respectively) of the terminal amine, but no trinitrosation. In water medium, the reduction of the Cu^{II} to Cu^{I} took place, but no modification of the ligand was observed.

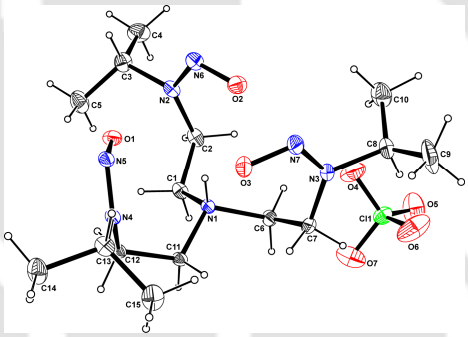

Figure S.2.3: ORTEP diagram of $\mathbf{L_1}'$- perchlorate (50% thermal ellipsoid plot).

Thus, this chapter describes the reduction of Cu^{II} to Cu^{I} by NO in acetonitrile through the formation of an unstable [Cu^{II}-$NO^{\bullet}$] intermediate. Ligand N-nitrosation was observed in acetonitrile and methanol solvents.

Chapter 3: ***Nitric oxide reactivity of copper(II) complexes of tris-[2-aminethyl]amine and ethylenediamine***

In the previous chapter, the formation of [Cu^{II}-$NO^{\bullet}$] intermediate was observed prior to the reduction of Cu^{II} to Cu^{I}. It is, thus, logical to assume that the N-nitrosation was a result of attack of NO^{+} formed during the reduction of Cu^{II} to Cu^{I} by NO. To have

further insight into the mechanistic details and the formation of NO^+, tren, [*tris*-(2-aminoethyl)amine] ligand (**L_2**) and ethylenediamine (**L_3**) have been chosen for the present study. Both the ligands have terminal primary amine center which are susceptible to diazotization in presence of NO^+.

In this chapter, two Cu^{II} complexes, **3.1** and **3.2** with **L_2** and **L_3**, respectively, were prepared. These complexes were characterized by various spectroscopic techniques as well as X-ray single crystal structure determination. Both the complexes were reported earlier, also. The complex **3.1** exhibited a broad *d-d* band with λ_{max} at 828 nm (ε, 158 M^{-1} cm^{-1}), along with relatively strong intra-ligand absorptions in the UV-region at λ_{max}, 274 nm (ε, 3600 M^{-1} cm^{-1}) in acetonitrile solvent; whereas complex **3.2** shows *d-d* band at λ_{max} at 550 nm (ε, 187 $M^{-1}cm^{-1}$). Both the complexes displayed one electron paramagnetism and characteristic signals in X-band EPR spectroscopy.

In degassed acetonitrile solution of the complexes, addition of NO was found to generate unstable intermediate prior to the reduction of Cu^{II} to Cu^{I}. This has been evidenced by UV-visible, X-band EPR and solution FT-IR spectroscopy.

In the present cases, the reduction of the Cu^{II} centers by NO afforded ligand transformation through diazotization at the primary amine coordination site (Scheme S.3.1). The modified ligands, in each case, were isolated and characterized by various spectroscopic studies.

However, when the reaction was carried out in aqueous solution, along with the reduction of the Cu^{II} to Cu^{I}, formation of NO_2^- /NO_3^- was observed.

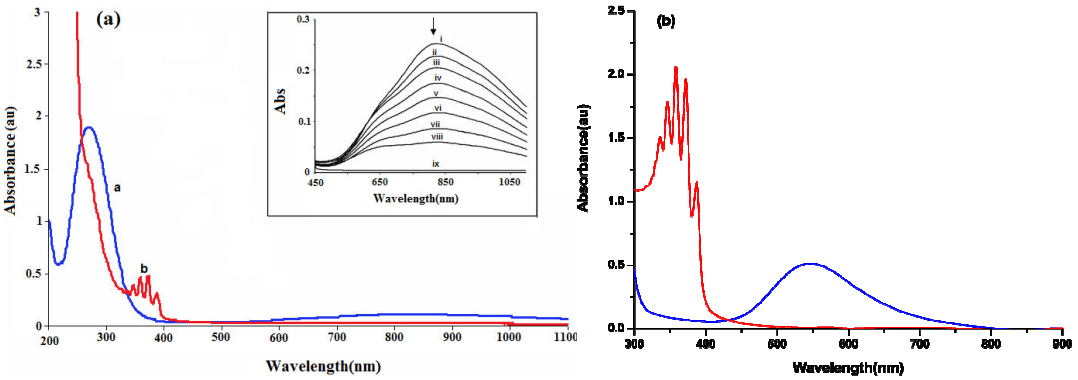

Figure S.3.1: UV-visible spectra of complexes (a) **3.1** and (b) **3.2** [blue traces for the complex before purging NO and red trace showing the reduction of Cu^{II} to Cu^{I} after the reaction with NO].

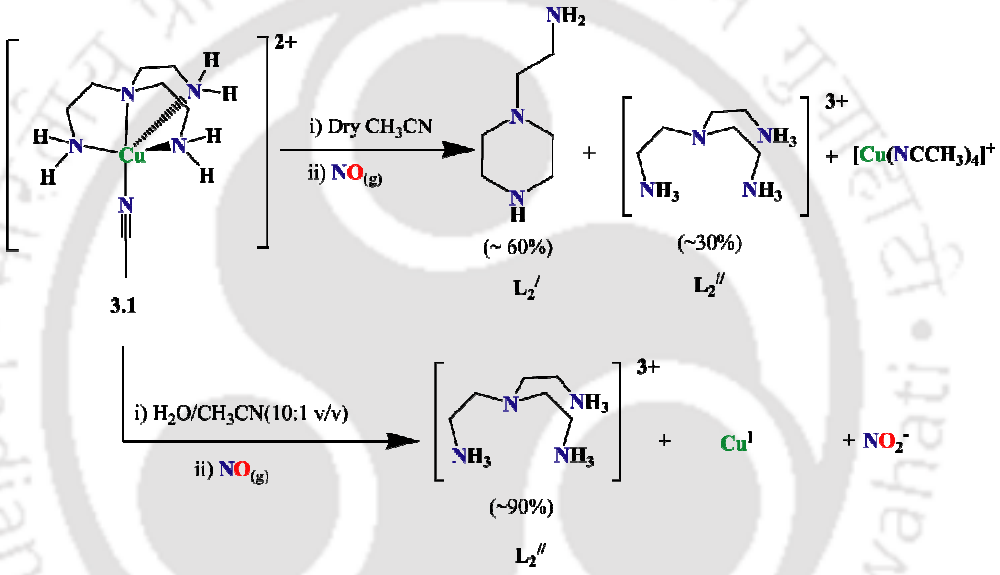

Scheme S.3.1

Chapter 4: ***Nitric oxide reactivity of copper(II) complexes of bidentate amine ligands***

In this chapter, three Cu^{II} complexes **4.1**, **4.2** and **4.3** with bidentate ligands $\mathbf{L_4}$, $\mathbf{L_5}$ and $\mathbf{L_6}$ [$\mathbf{L_4}$, N,N′-dimethyl ethylenediamine; $\mathbf{L_5}$, N,N′-diethylethylenediamine and $\mathbf{L_6}$, N,N′-diisobutylethylenediamine], respectively, were synthesized. The complexes were characterized by various spectroscopic techniques as well as by X-ray single crystal structure determination (Figure S.4.1). The complexes **4.1**, **4.2** and **4.3** exhibited broad *d-d* band having λ_{max} at 563 nm (ε, 100 M^{-1} cm^{-1}), 575 nm (ε, 120 M^{-}

^{1} cm^{-1}) and 582 nm (ε, 124 M^{-1} cm^{-1}), respectively. All the complexes displayed one electron paramagnetism and characteristic signals in X-band EPR spectroscopy.

The NO reactivity of the complexes was studied in acetonitrile solvent. The formation of thermally unstable [Cu^{II}-NO$^{\bullet}$] intermediate on reaction of the complexes with NO in acetonitrile solution was confirmed by UV-visible (Figure S.4.2) and EPR spectroscopic studies. The *d-d* transition for complex **4.1** was shifted from 563 nm to 605 nm immediately after purging NO.

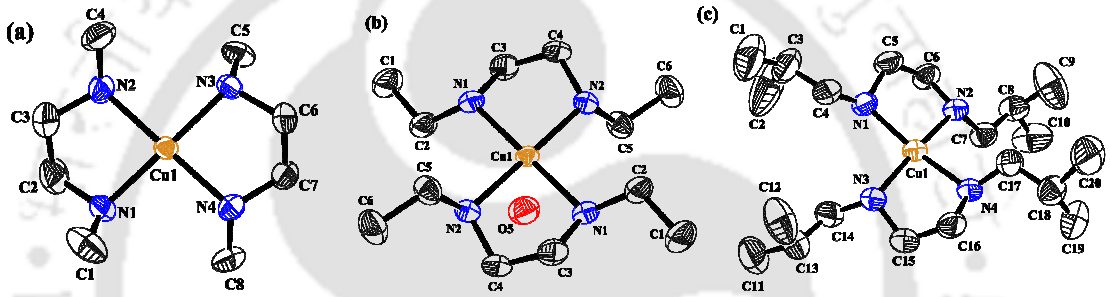

Figure S.4.1: ORTEP diagrams of the complexes (a) **4.1**, (b) **4.2** and (c) **4.3** (50% thermal ellipsoid plot; perchlorates and hydrogen atoms are omitted for clarity).

In cases of complexes **4.2** and **4.3**, it was shifted to 622 nm and 652 nm, respectively. The stability of [Cu^{II}-NO$^{\bullet}$] intermediate was found to decrease as the bulkiness of N-substitution on the ligand framework increases. The reduction was found to result with a simultaneous mono- and di-nitrosation at the amine sites of the ligands. All the nitrosation products were isolated and characterized by using the various spectroscopic analyses. The relative ratio of the yield of mono- and di-nitrosation products was found to be dependent on the N-substitution present in the ligand framework (Scheme S.4.1).

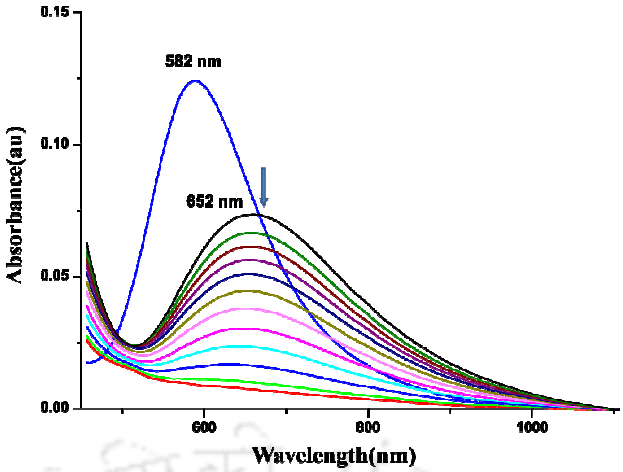

Figure S.4.1: UV-visible spectra of the reaction of complex **4.3** with NO in acetonitrile solvent at room temperature (blue trace represents the Cu^{II}-species, black represents that of the [Cu^{II}-$NO^{\bullet}$] intermediate which gradually decomposed to Cu^{I}).

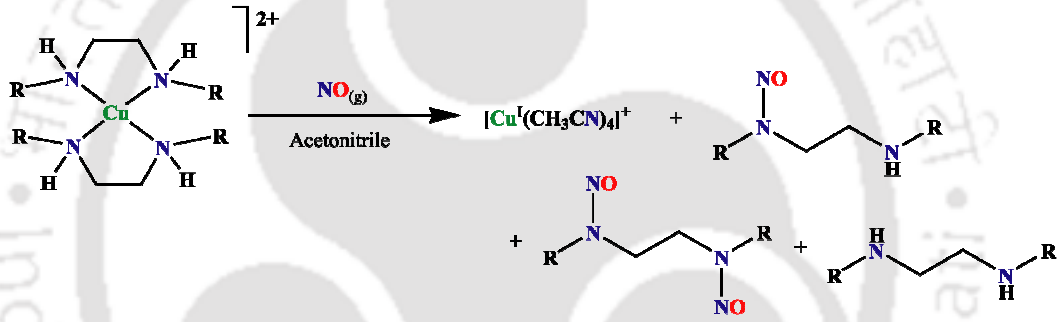

Scheme S.4.2

R	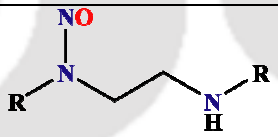	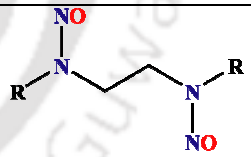
Me	$L_4^{/}$, 16%	$L_4^{//}$, 17%
Et	$L_5^{/}$, 8%	$L_5^{//}$, 24%
^{i}Bu	$L_6^{/}$, 5%	$L_6^{//}$, 30%

Chapter 5: ***Nitric oxide reduction of copper(II) complexes of 2-aminomethyl pyridine and bis-(2-aminoethyl)amine***

In this chapter, two Cu^{II} complexes, **5.1** and **5.2** with L_7 and L_8 [L_7, 2- aminomethyl pyridine; L_8, *bis*-(2-aminoethyl)amine], respectively, were synthesized and

characterized. These complexes, in degassed acetonitrile solvent, on exposure to NO gas, were found to form thermally unstable [Cu^{II}-$NO^{\bullet}$] intermediate which then resulted into the reduction of the Cu^{II} centers. The formation of the [Cu^{II}-$NO^{\bullet}$] intermediate was evidenced by UV-visible, solution FT-IR and EPR spectroscopic studies. The *d-d* transition for complex **5.1** was found to appear at 582 nm which was shifted to 660 nm after reaction with NO. In case of complex **5.2**, it shifted from 575 nm to 595 nm (Figure S.5.1a). The rate of decomposition of the intermediate at 298K were found to be 1.3×10^{-3} sec^{-1} and 2.2×10^{-3} sec^{-1}, for complexes **5.1** and **5.2**, respectively. The solution FT-IR spectra of the acetonitrile solutions of complexes **5.1** and **5.2** after purging NO were recorded. A new intense and sharp band was found to appear at ~1642 cm^{-1} and 1635 cm^{-1} for complexes **5.1** and **5.2**, respectively, corresponding to the vibration of NO coordinated to the Cu^{II} center (Figure S.5.1b). On NO purging to the degassed solution of complexes **5.1** and **5.2**, they became EPR silent. These can be attributed to the formation of [Cu^{II}-$NO^{\bullet}$] intermediates in both the cases.

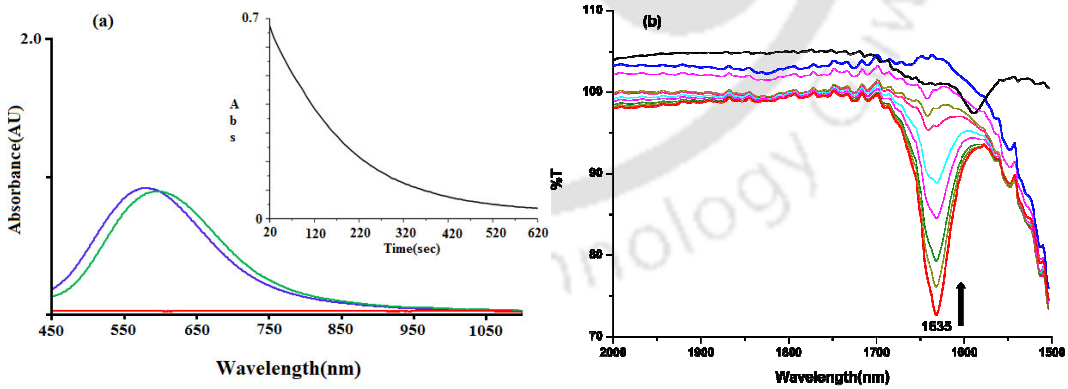

Figure S.5.1: (a) UV-visible spectra of the reaction of complex **5.2** with NO in acetonitrile solvent at room temperature (blue trace represents the Cu^{II} species, green represents that of the [Cu^{II}-$NO^{\bullet}$] intermediate and red trace represents that of the Cu^{I} after complete reduction). **(b)** Solution FT-IR spectra of complex **5.2** in acetonitrile (dark blue colored trace is for complex and the other represent that after addition of NO which disappears with times. Black trace is that of the colorless solution obtained after full reduction).

In the present study, the reduction of the Cu^{II} centers by NO afforded ligand transformation through diazotization at the primary amine coordination site, in both the cases (Scheme S.5.1). The modified ligands, in each case, were isolated and characterized.

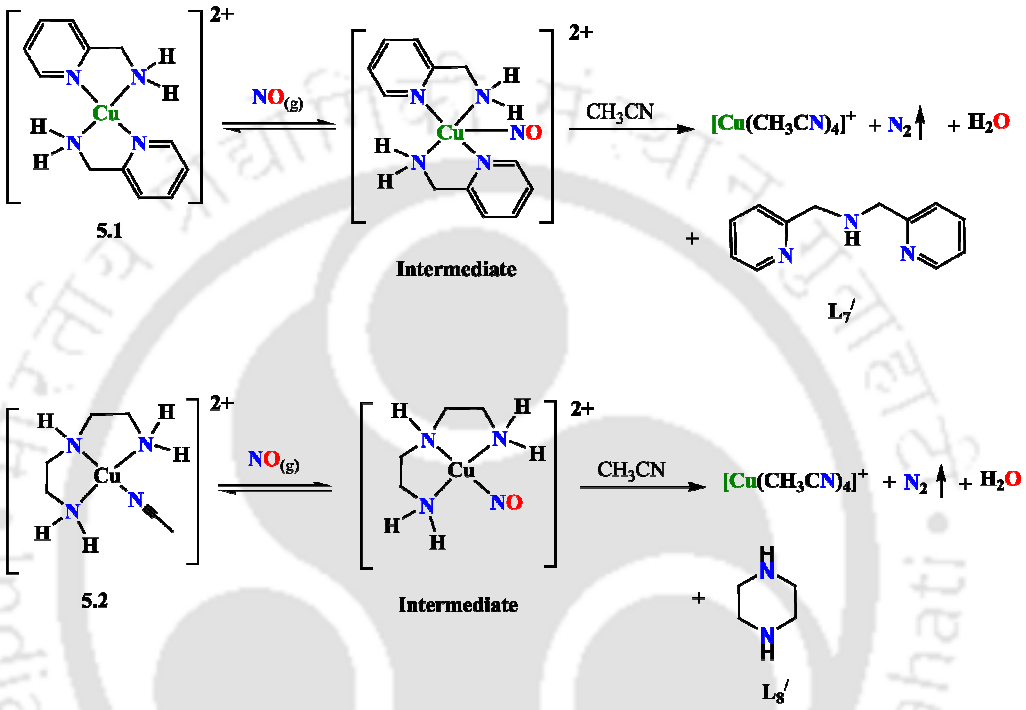

Scheme S.5.1

Chapter 6: ***Nitric oxide reactivity of copper(II) complexes of bidentate amine ligands having aliphatic and aromatic N-donor sites***

In this chapter, two Cu^{II} complexes, **6.1** and **6.2** with $\mathbf{L_9}$ and $\mathbf{L_{10}}$ [$\mathbf{L_9}$, 2-(2-aminoethyl)-pyridine; $\mathbf{L_{10}}$, 2-(N-ethyl-2-aminoethyl)-pyridine], respectively, were prepared. These complexes were characterized by various spectroscopic techniques. The complex **6.1** was reported earlier, also. The complexes **6.1** and **6.2** exhibited broad *d-d* bands at λ_{max} 576 nm (ε, 187 M^{-1} cm^{-1}) and at λ_{max} 598 nm (ε, 210 M^{-1} cm^{-}

^{1}), respectively, in acetonitrile solvent. Both the complexes displayed one electron paramagnetism and characteristic signals in X-band EPR spectroscopy.

These complexes, in degassed acetonitrile solvent, on exposure to NO gas, were found to form thermally unstable [Cu^{II}-$NO^{\bullet}$] intermediate which then resulted into the reduction of the Cu^{II} centers. The formation of the [Cu^{II}-$NO^{\bullet}$] intermediate was evidenced by UV-visible (Figure S.6.1), solution FT-IR and EPR spectroscopic studies. On purging NO gas to a degassed acetonitrile solution of complex **6.1**, the *d-d* transition was shifted to 650 nm. For complex **6.2**, it was shifted from 598 nm to 652 nm. The rate constants of decomposition of [Cu^{II}-$NO^{\bullet}$] intermediates were found to be 1.09×10^{-1} sec^{-1} and 5.40×10^{-2} sec^{-1}, respectively. The reduction of the Cu^{II} centers by NO afforded ligand transformation through diazotization at the primary amine coordination site in case of complex **6.1** and in water it produced alcoholic product (Scheme S.6.1), as expected. In case of complex **6.2,** the reaction of NO afforded nitrosation at the NH- site (Scheme S.6.2). The modified ligands, in each case, were isolated and characterized by various spectroscopic studies.

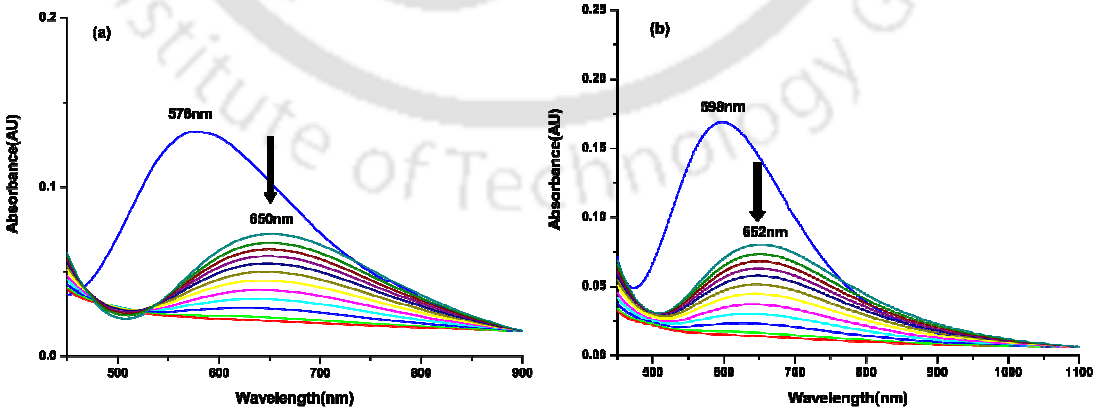

Figure S.6.1: UV-visible spectra of the reaction of complexes **6.1**(a) and **6.2**(b) with NO in acetonitrile solvent at room temperature. (Blue trace represents the Cu^{II}-species, green represents that of the [Cu^{II}-$NO^{\bullet}$] intermediate which gradually reduced to Cu^{I}).

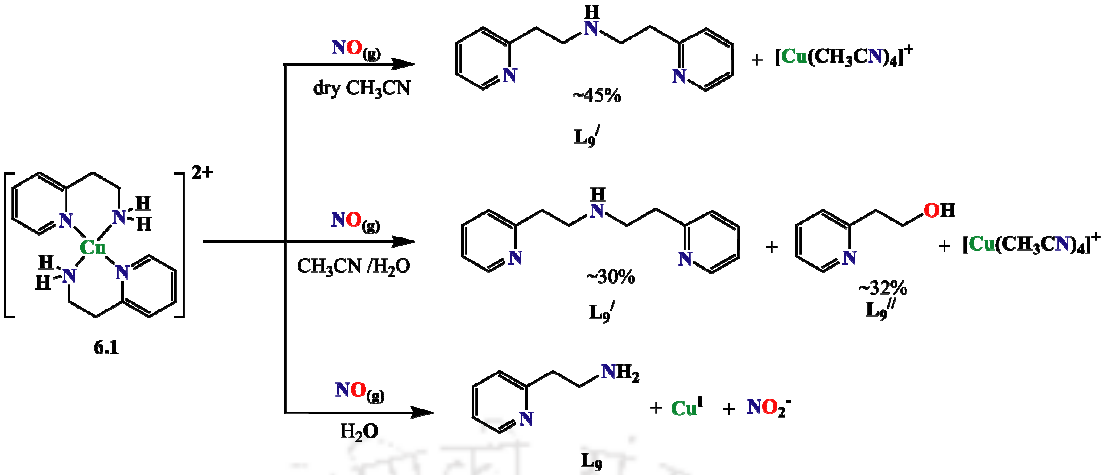

Scheme S.6.1

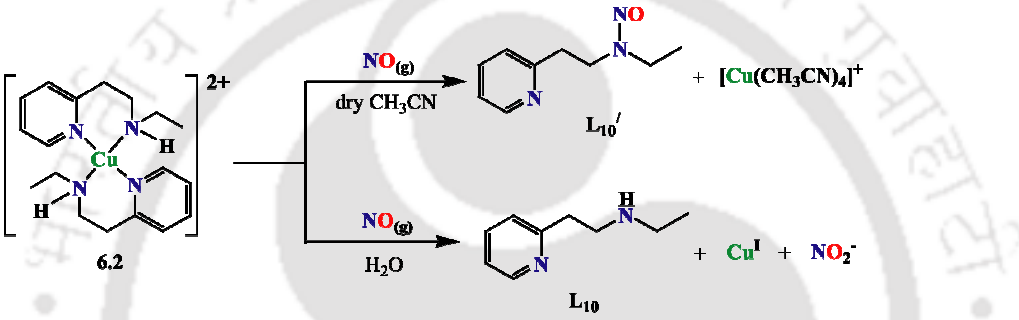

Scheme S.6.2

Chapter 1

Introduction

1.1 General aspects of nitric oxide

Nitric oxide (NO) has attracted enormous research attention from chemists and biochemists since it has been identified as an essential component in many physiological processes in mammals. Furchgott, Ignarro and Murad were awarded Nobel Prize in 1998 for the discovery of the multiple roles played by NO in physiological and pathological functions in human body.[1-4] The physiological functions of NO are various; e.g. it acts as killer of invading microorganisms; primary messenger in regulating blood pressure; neuro-transmitter etc. Dysfunction in NO metabolism, has been identified to associate with a number of diseases, such as arthritis, hypertension, septic shock etc.[1-9] Most of these activities are attributed to the formation of nitrosyl complexes with metallo-proteins, primarily iron or copper-proteins.[10-12] For instance, in soluble guanylyl cyclase (sGC),[13, 14] the formation of a nitrosyl complex with Fe^{II} leads to labilization of a *trans* axial (proximal) histidine ligand in the protein backbone, and the resulting change in the protein conformation is believed to activate the enzyme for catalytic formation of the secondary messenger cyclic-guanylyl monophosphate (cGMP) from guanylyl triphosphate (GTP). The enzymatic formation of cGMP, results into the relaxation of smooth muscle tissue of blood vessels, hence lowering blood pressure. NO is also known as an important biological agent (also referred to as a 'endothelial derived relaxing factor (EDRF)')

whose binding to heme and non-heme proteins provides a basis for both sensing and signalling which leads to vassodialation/muscle relaxation.[15, 16] The reduction of Cu^{II} centres in some proteins, such as cytochrome *c* oxidase and laccase, to Cu^{I} on exposure to NO has also been known for a long time.[10, 17] In cytochrome *c* oxidase, the NO reduction of Cu^{II} to Cu^{I} is believed to regulate the electron transport activity of this protein.[18] It is also known to generate powerful nitrating and/or oxidizing agent peroxynitrite by its reaction with superoxides.[19-21] Thus, a deep knowledge on the interaction/activation of NO with/by transition metal ions is very important to understand its biological roles.

1.2 General features of nitric oxide

Nitric oxide (NO) in gaseous state is a stable free radical and it exists in a monomeric form. It has a boiling point (1 atm) 121K and a melting point 110K.[16] In air, NO reacts spontaneously with O_2 to form nitrogen dioxide (NO_2). NO can combine rapidly with both organic and oxygen-centered radical to yield a variety of highly active intermediates. At low temperature and high pressure, NO dimerises to produce N_2O_2.[16]

NO is a di-atomic stable free radical. It has eleven valence electrons and two possible Lewis structures which are shown bellow.

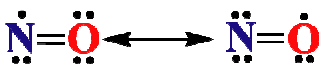

Figure 1.1: Lewis structures of NO.

Both of these structures indicate the presence of a double bond, but the actual N-O bond length is found to 1.154 Å which suggests a higher bond order. It can be

explained by the molecular orbital (MO) diagram of NO (Figure 1.2). It has a $^2\Pi$ ground state with a bond order of 2.5, which is consistent with its bond length between those of N_2 (1.06 Å) and O_2 (1.18 Å).[22] The MO diagram depicts that, the π^* orbital is the singly occupied highest occupied molecular orbital (HOMO), but it is polarized toward nitrogen in a manner opposing the polarization of the lower energy π^b orbital resulting into a relatively nonpolar diatomic molecule having the NO stretch ν_{NO}, at 1875 cm^{-1} in the infrared spectrum.

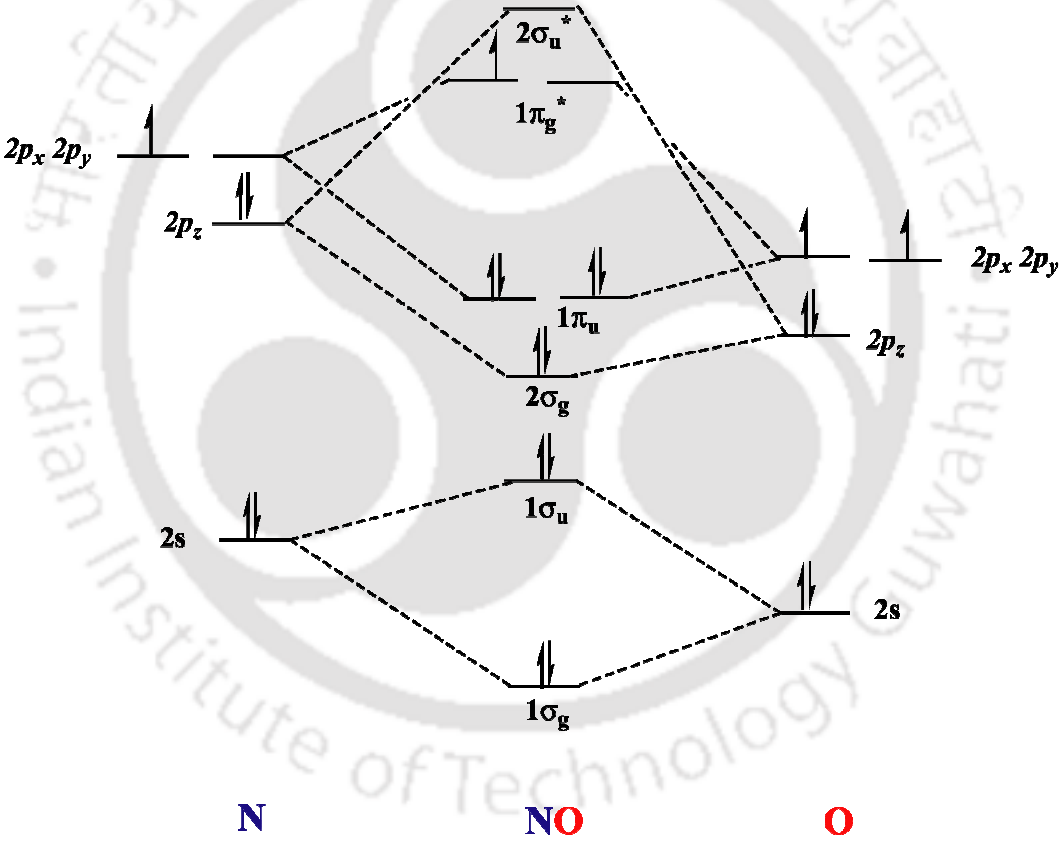

Figure 1.2: Molecular orbital diagram of NO.

The HOMO of NO possesses only nitrogen character as greater electronegativity of the oxygen lowers the energy of O-atom. Hence, NO prefers to bind to the metal

centre *via* N-atom. NO can bind to metal centre by the loss of one electron forming nitrosonium cation, NO^+, or by gaining one electron forming nitroxyl anion, NO^- (Figure 1.3). The nitrosonium cation is isoelectronic to CO, having the lone pair on *sp* hybrid orbital; thus, a linear M-N-O moiety is anticipated with an entity which is formally NO^+. On the other hand, the NO^- is isoelectronic to dioxygen (O_2); N-atom here is sp^2 hybridized for which a M-N-O bond angle of ~120° is expected.[16]

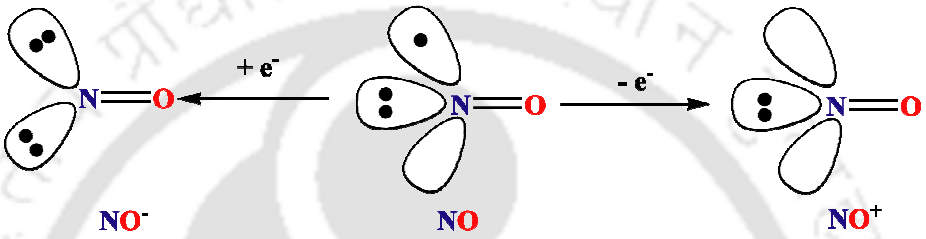

Figure 1.3: Schematic presentation of binding of NO.

Binding modes of NO to metal centres can be of three types: (i) linear end on, (ii) bent end on and (iii) side-on (Figure **1.4**).[23]

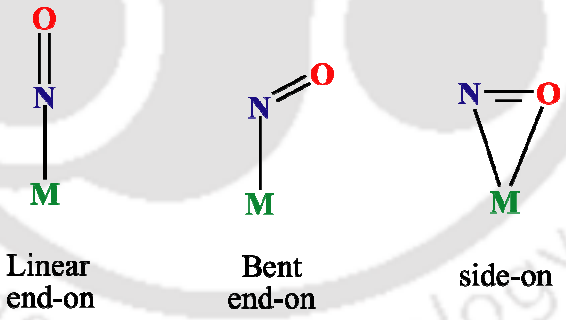

Figure 1.4: Different binding modes of NO to metal centres.

1.3 Literature Survey

1.3.1 Copper(II)-Nitrosyl Complexes

The biological and physiological reactivity of NO are mostly attributed to the formation of nitrosyl complexes of metallo-proteins e.g. iron or copper-proteins. [10-12]

In this direction, the iron-nitrosyls, both in protein and synthetic model systems have been studied extensively and ferriheme proteins are known to undergo reduction in aqueous media on exposure to NO. These reactions are known to proceed through two distinct steps: (i) formation of iron(III)-nitrosyl adduct; (ii) followed by the pH dependent reduction of Fe^{III} to Fe^{II} with a simultaneous attack of hydroxide ion to the activated nitrosonium group [Fe^{III}-NO ↔ Fe^{II}-NO^+] leading to the formation of nitrite.[24-26] NO reductions of Cu^{II} are also known though have not been studied as extensively as iron-nitrosyls, both in proteins and synthetic model systems. Several examples of reduction of Cu^{II} by NO and their use for NO detection are reported in recent years.[27-28] However, there are hardly any example which shows the distinct spectral evidence of formation of [Cu^{II}-$NO^{\bullet}$] intermediate except two reported by Diaz et. al. and Hayton et. al.[29, 30] Furthermore, there is no report on the coordination of NO in aqueous solution though an aqueous solution gives a better approach to in vivo conditions than the studied organic solvents.

In biological systems, the reactivity of Cu^{II} center with NO, is believed to proceed through the formation of [Cu^{II}-$NO^{\bullet}$] intermediate.[31] For instance, the reduction of NO_2^- to NO by copper nitrite reductase (CuNiR) is an important component of the global nitrogen cycle.[32-35] It is believed that a [Cu^{I}-NO^+ ↔ Cu^{II}-$NO^{\bullet}$] intermediate is involved in the conversion of nitrite to NO or, in some cases to N_2O by nitrite reductase e.g. from *Achromobacter cycloclastes* (Scheme 1.1).[36-39] This intermediate can be classified as a $\{CuNO\}^{10}$ (9 metal *d* electrons + 1NO π^* electrons=10 total electrons) complex in the Enemark-Feltham notation.[40]

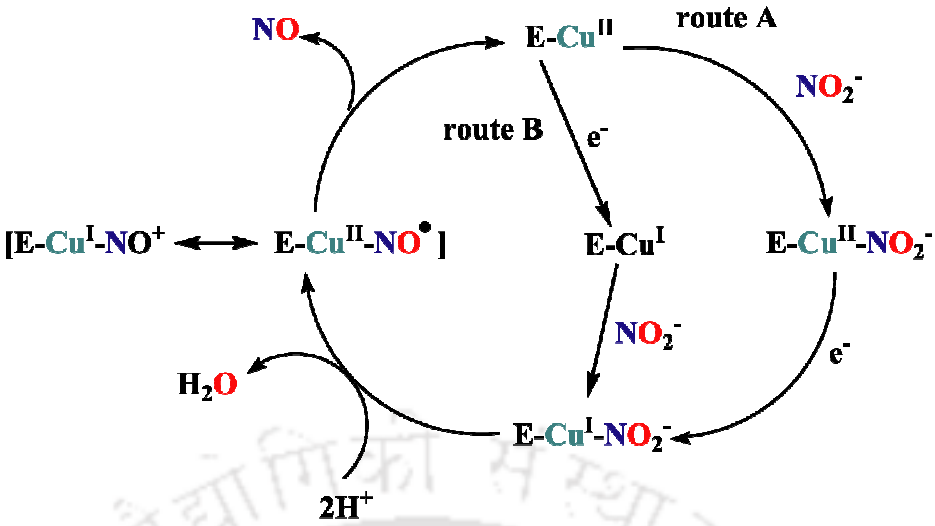

Scheme 1.1: Proposed mechanism for nitrite reduction by Cu-NiR.

Another important aspect of NO interaction with transition metal ion is reductive nitrosylation which has been observed for several ferriheme proteins, for cupric centers in cytochrome *c* oxidase and laccase.[10, 17, 41, 42] Cu^{II} has also been known to promote the nitrosation of various thiolates (forming *S*-nitrosothiols) and Cu^{II} reduction was found to correlate with formation of *S*-nitroso bovine serum albumin (BSA) and *S*-nitroso glutathione. Such observations have been used to fomulate a potential mechanism for the formation of RSNO compounds found in blood.[43, 44] However, Cu^{I} centres are known to participate in side reactions leading to RSNO degradation to reform NO (Equation 1.1).[43, 45] This pathway have received attention as a possible route to β-cys-93 S-nitrosylated hemoglobin which is controversial proposal regarding the NO transport in cardiovascular systems.[46]

$$Cu^{II} + BSA\text{-}SH \underset{+H^+}{\overset{-H^+}{\rightleftharpoons}} [Cu^{II} + BSA\text{-}S^-]^+ \overset{-NO}{\underset{+NO}{\rightleftharpoons}} BSA\text{-}SNO + Cu^{I} \quad \text{----------(1.1)}$$

In this direction, only a few literatures are available that deal with the detail kinetic studies of the Cu^{II}/NO reactions. Tran et al. has reported the reaction of NO with the Cu^{II} complex, $[Cu(dmp)_2(H_2O)]^{2+}$ (dmp, 2,9-dimethyl-1,10-phenanthroline), in methanol leading to the formation of a tetra-coordinated $[Cu(dmp)_2]^{+}$ complex along with methyl nitrite and H_2O (Equation 1.2). They have proposed that this reaction proceeds through the formation of $[Cu^{II}\text{-}NO^{\bullet}]$ species.[47]

$$[Cu(dmp)_2(H_2O)]^{2+} + NO + CH_3OH \longrightarrow [Cu(dmp)_2]^{+} + CH_3ONO + H_2O + H^{+} \quad \text{----------(1.2)}$$

It has been found that the reaction does not occur in CH_2Cl_2 unless methanol is added, and in such solutions the reaction rate is linearly dependent on the concentration of alcohol added.[48]

Ford et. al. has reported another interesting reactivity of NO with the Cu^{II} complex, $[Cu(DAC)]^{2+}$ [DAC, 1,8-bis(9-anthracylmethyl)-derivative of the macrocyclic tetraamine cyclam (1,4,8,11-tetraazacyclotetradecane)].[49] Although the free ligand is fluorescent, the analogous solution of $[Cu(DAC)]^{2+}$ displays no luminescence at room temperature because of its intramolecular quenching by the Cu^{II} center. Introduction of NO to the methanolic solution of $[Cu(DAC)]^{2+}$ restores the fluorescence through the reduction of Cu^{II} to Cu^{I}. The reduction of Cu^{II} center was also found to follow by nitrosation of the ligand and subsequent demetallation (Equation 1.3). The kinetic studies suggest that there was a first-order dependence on concentration of NO and the reaction was accelerated at higher pH.[31, 49]

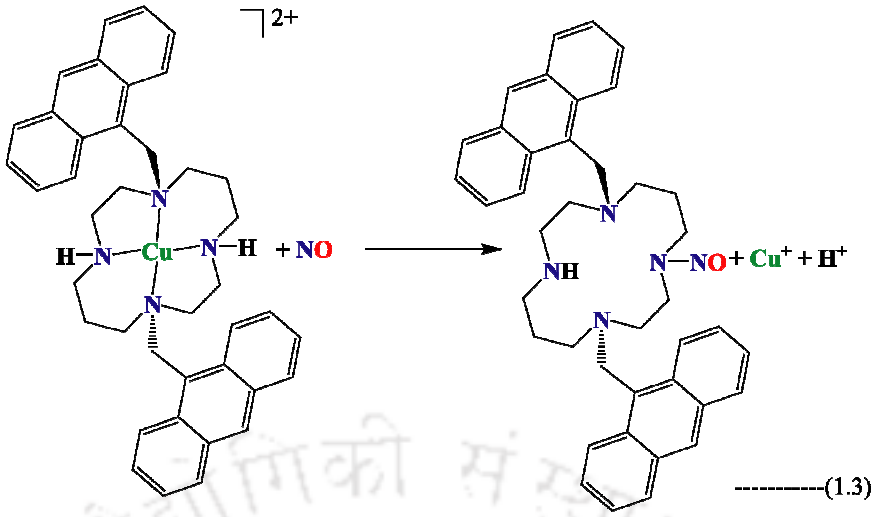

----------(1.3)

A few complexes with a $\{CuNO\}^{10}$ configuration are known. Alcoholic solutions of CuX_2 (X = Cl, Br, F) have been reported to absorb NO, generating deeply colored solutions that exhibit strong ν_{NO} absorptions in their solution IR spectra, but the structures of these materials are not known.[50-52] Another $\{CuNO\}^{10}$ complex reported is $[Cu(NO)(H_2SO_4)_n]^{2+}$, but they are not properly characterized.[53] The lack of structural data for these complexes highlights the need for new copper nitrosyls to be isolated and characterized. Cao and coworkers reported the formation of air-stable copper-nitrosyl and dinitrosyl species in the reaction of copper(II)dithiocarbamates with NO in aqueous solution.[29] This was, perhaps, the first report of formation of air stable copper(II) nitrosyl (Scheme 1.2).

It would be worth mentioning here that Vagliasindi et al has reported a series of the interaction of NO with Cu^{II} complexes of small peptides coming from the N-terminal prion protein octa-repeat region. In aqueous solutions of Cu-Ac-HGGG-NH_2 and Cu-Ac-PHGGGWGQ-NH_2 systems at ~ pH 7.5, reduction of Cu^{II} centers were observed in presence of NO source.[54] Spectral studies suggested that these reductions were

probably mediated by the formation of a labile [Cu^{II}-$NO^{\bullet}$] adduct.[54] However, for an analogous dinuclear system, Cu_2-Ac-$(PHGGGWGQ)_2$-NH_2, the NO interaction

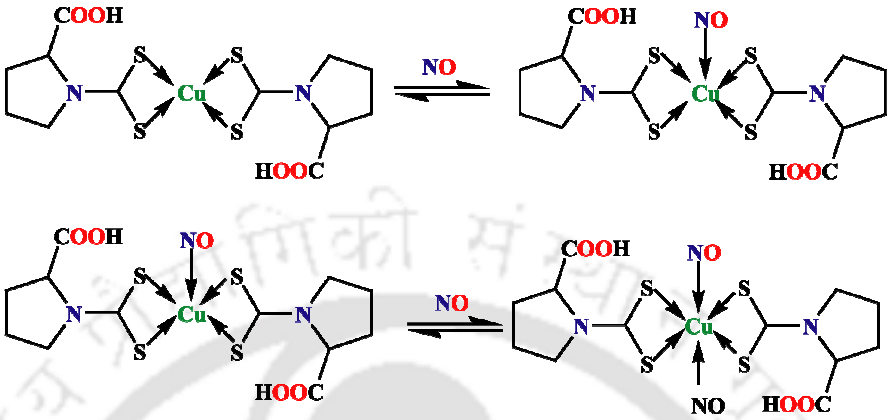

Scheme 1.2

study in aqueous solutions at physiological pH suggested that the reduction of Cu^{II} proceeds through a complicated pathway involving two different intermediate species and a positive cooperativity between two copper centers was observed.[55]

Recently, Hayton et. al. have reported structurally characterised copper(II)-nitrosyl ({CuNO}^{10} configuration) complex, $[Cu(CH_3NO_2)_5(NO)][PF_6]_2$, **1.1**.[30] Here, Cu-N-O angle is found to be 121.0(3)°. This complex shows ν_{NO} at 1933cm^{-1} in FT-IR spectrum. This complex was reported to react with mesitylene to form [mesitylene, NO][PF_6] and [Cu(η^2-1,3,5-$Me_3C_6H_3)_2$][PF_6] by transfer of NO^+ to the mesitylene ring.[30]

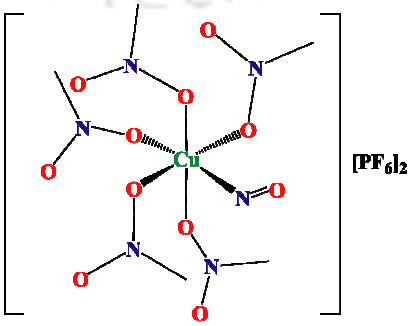

1.1

The process of reductive nitrosylation is used to develop fluorescence-based NO sensors by using Cu^{II} complexes. Lippard's group have reported three strategies for fluorescence based NO detection of transition metals (Scheme 1.3).[56-71]

(a) Fluorescence displacement

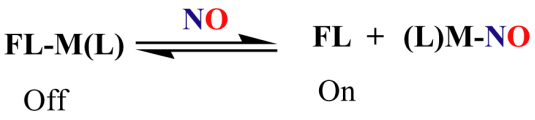

(b) Metal reduction

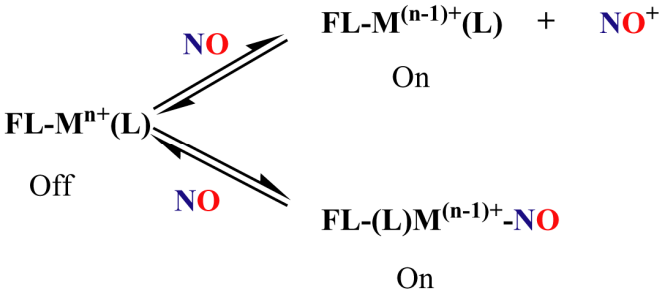

(c) Metal reduction and ligand nitrosation

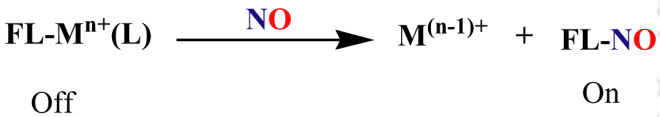

FL=Fluorescent Ligand

Scheme 1.3

For this detection of NO, Lippard et. al. have used various anthracenyl and dansyl flurophore ligands (Figure 1.5).

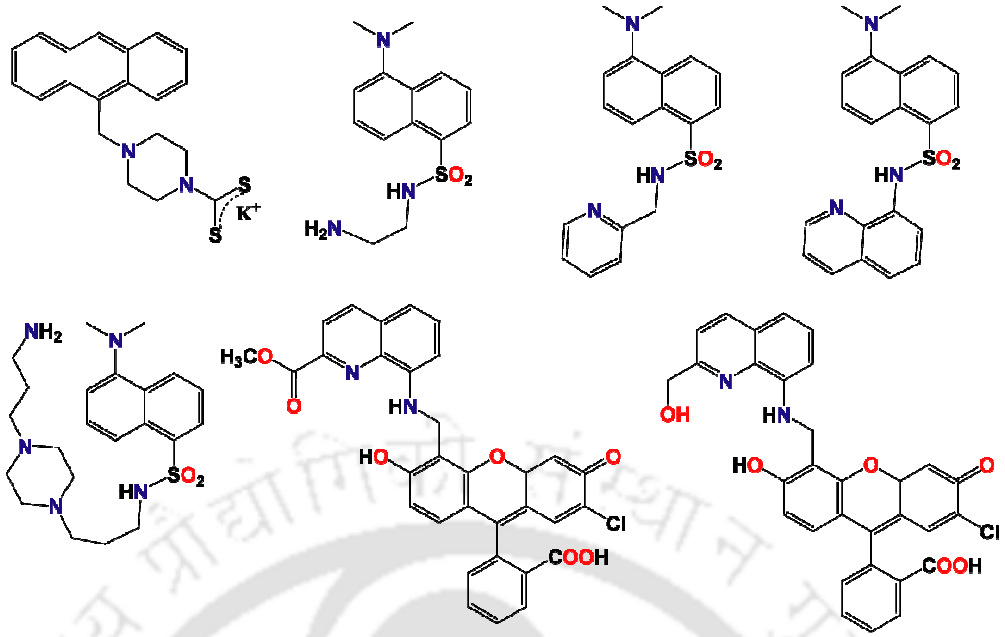

Figure 1.5: Ligands used for fluorescence detection of NO using Cu^{II}-complexes.

1.3.2 Copper(I)-Nitrosyl Complexes

The formation of stable copper(I)nitrosyl compounds at room temperature are exemplified in a few reports.[72, 73] The first Cu(I)-nitrosyl was synthesized in 1983 as a hetero-bimetallic nitrosyl bridging copper-iridium complex, $[IrCl(PPh_3)_2(dppn)(NO)CuCl][PF_6]_2$ [dppn, 3,6-bis(2′-pyridyl)pyridazine] **1.2**.[74] The first homometallic copper(I)-nitrosyl complex, $[Cu_2(XYL\text{-}O^-)(\mu\text{-}NO)](PF_6)_2$, **1.3**, [XYL-O, 2,6-*bis*{*bis*(2-pyridylethyl)aminomethyl}phenolate] was structurally characterized in 1990 by Zubeita et. al.[75] This complex reacts with $[NO_2]^-$ to form the bridging oxo species $[Cu_2(XYL\text{-}O)(\mu\text{-}O)]^+$, N_2O, and O_2.[76] This conversion is important since it is thought to mimic reactivity of nitrite reductase.[77]

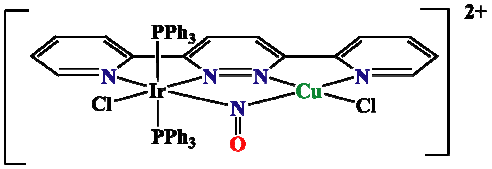

1.2

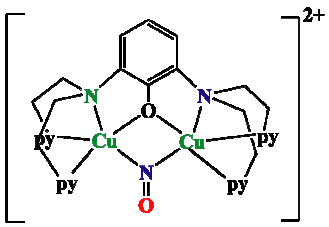

1.3

Further progress in copper(I)-nitrosyl chemistry occurred when the first terminal nitrosyl complex, [Cu{HB(^{t}Bu-pz)$_3$}(NO)], **1.4** was fully characterized by Tolman et. al.[78] This Cu(I)-NO complex have the Cu-N-O angle 163.4^o and exhibits ν_{NO} at 1712 cm^{-1} in FT-IR spectrum. This immediately reacts with O_2 to produce nitrate derivative of **1.4**.[78] Based on electronic spectra, ESR studies, and theoretical calculations, this was believed to have Cu(I)-NO$^{\bullet}$ electronic configuration rather than Cu(II)-NO$^-$ or Cu(0)-NO$^+$. The NO ligand was found to be displaced by MeCN or CO, and it can also be removed by applying vacuum. A series of such type of complexes including **1.5** and their reactivity with carbon monoxide and oxygen have been reported as a model for possible intermediate in nitrite reduction by the copper nitrite reductase (Cu-NiR) from *Achromobacter cycloclastes*.[79]

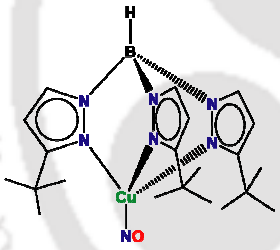

1.4

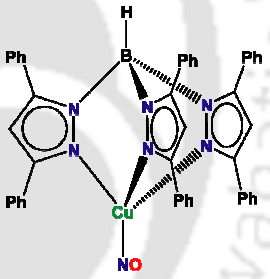

1.5

In continuation, complex **1.6** with *tris*-(3, 5-dimethylpyrazol-1-yl)hydroborate, in the presence of excess NO, was reported to undergo disproportionation to yield N_2O and Cu(HB(Me$_2$-pz)$_3$)(NO$_2$), **1.7**.[80] This disproportionation is proposed to proceed *via* a *cis*-dinitrosyl/hyponitrite intermediate (Scheme 1.4).[80- 82]

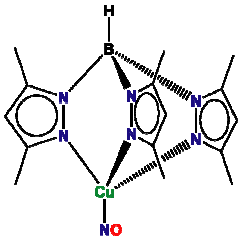

1.6

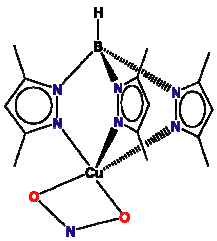

1.7

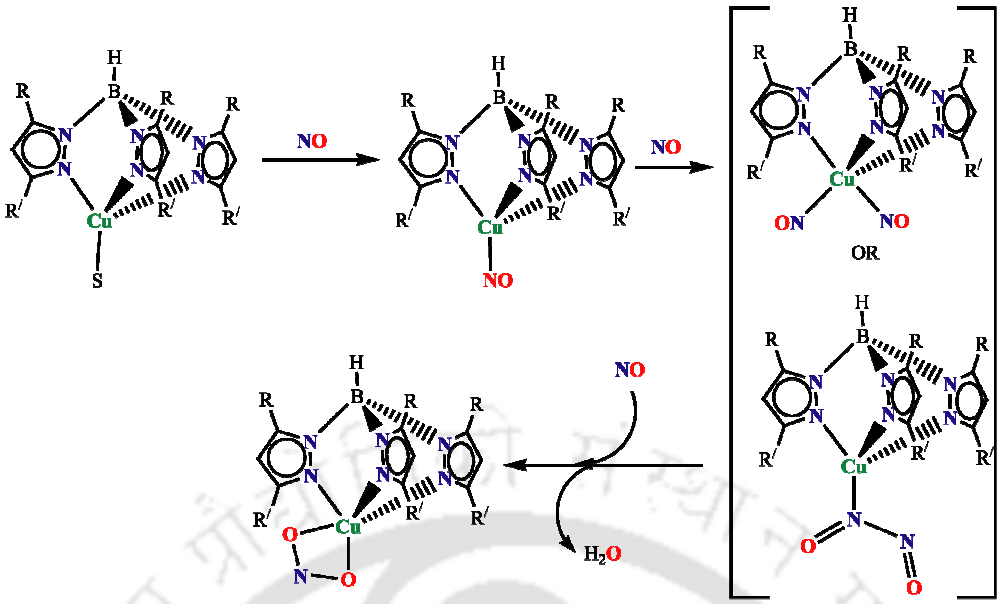

Scheme 1.4

Later on, Tolman's group have reported a new series of copper(I)-nitrosyl complexes, **1.8** and **1.9** with *tris*-(3-(trifluoromethyl)-5-methylpyrazol-1-yl)hydroborate and *tris*-(3-mesitylpyrazol-1-yl)hydroborate, ligands respectively. Crystal structures of these complexes were not reported, but these complexes were well characterized by spectral and chemical studies.[81]

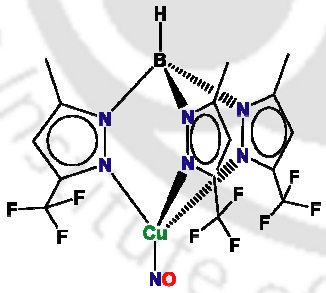

1.8

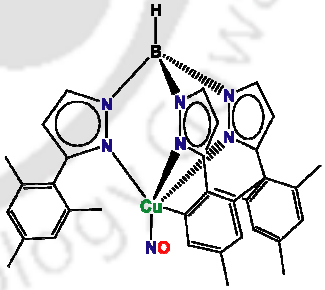

1.9

Fujisawa et. al. has reported another important aspect of copper(I)-nitrosyl compound.[23] They have structurally characterized two mononuclear Cu(I)-nitrosyl complexes, **1.10** and **1.11,** with the related co-ligands hydro *tris*-(3-*tert*-butyl-5-isopropyl-1-pyrazolyl)borate and *tris*-(3-*tert*-butyl-5-isopropyl-1-pyrazolyl)methane

respectively. These complexes exhibit nearly linear nitrosyl ligands and are also considered to have a [Cu^{I}-$NO^{\bullet}$] electronic configuration.[78, 79]

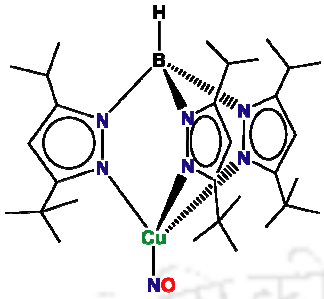

1.10

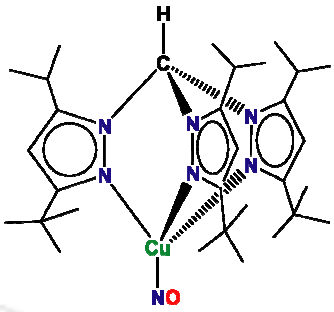

1.11

Interestingly, X-ray crystallographic studies revealed an unusual side-on interaction between NO and the copper center.[75, 83] In a recent study by Murphy and co-workers, a [Cu^{I}-$NO^{\bullet}$] intermediate of Cu-NiR, which was generated by exposing crystals of fully reduced Cu-NiR to NO saturated buffer, has been structurally characterized.[83, 84] This exhibits an unexpected side-on coordination of NO to Cu^{I} which corresponds to a new intermediate in the biological chemistry of NO.

Complex [($^{i}Pr_3$-tacn)Cu(*N*-NO_2)], [$^{i}Pr_3$-tacn, 1,4,7-triisopropyl-1,4,7-tiazacyclononane], in presence of two equivalent of acid (HX) was found to result in the production of one equivalent of NO(g) and concomitant formation of ($^{i}Pr_3$-tacn)Cu$(X)_2$ and H_2O. They proposed that this reaction involve a copper-nitrosyl intermediate.[85, 86]

In addition, copper nitrosyl intermediates were reported in the reactivity studies of peroxynitrite. Peroxynitrite ($^{-}$OON=O) is a reactive agent generated by the near diffusion controlled combination of NO and the superoxide anion ($O_2^{\bullet-}$).[87] In recent times, Karlin and co-workers has reported the formation of new peroxynitrite

complexes from the reaction of [Cu^{I}-$NO^{\bullet}$] complex with dioxygen which affords corresponding copper(II)nitrite on warming at room temperature (Scheme 1.5).[20]

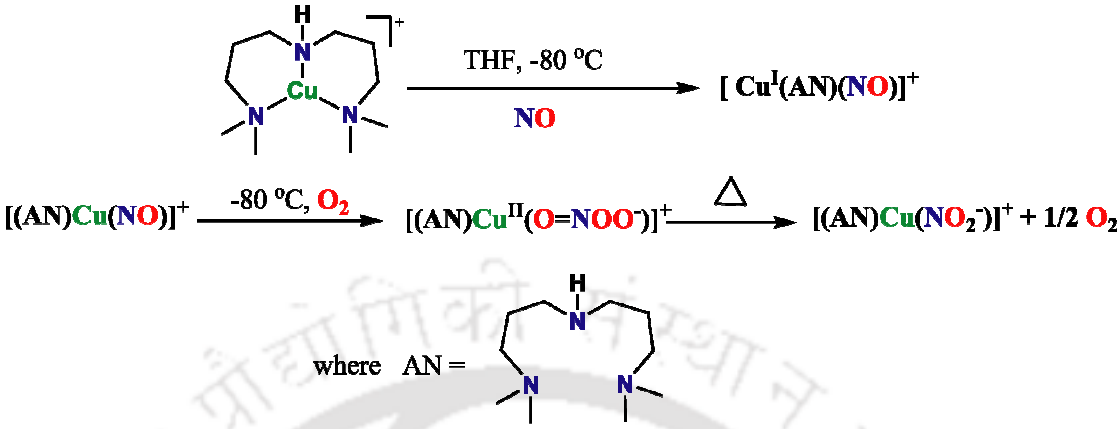

Scheme 1.5

These results essentially instigate us to study the reactivity of NO with Cu^{II} complexes with various ligand frameworks. The works presented in the proceeding chapters of the thesis will preliminary focus on the following aspects:

a) Cu^{II} complex with a tripodal tetradentate ligand, *tris*-[2-(isopropylamino)-ethyl]amine (**L_1**) had been synthesised and it's reactivity with NO in acetonitrile, water and methanol were studied. These studies suggest the formation of a [Cu^{II}-$NO^{\bullet}$] intermediate, {Cu-NO}^{10} complex and also trinitrosation at the amine site was observed.

b) The NO reactivity of Cu^{II} complexes with a tripodal tetradentate ligand, *tris*-[2-aminoethyl]amine (**L_2**) and a bidentate ligand, ethylenediamine (**L_3**) were studied in acetonitrile and water medium. These studies support the formation of NO^{+} in the reaction medium.

c) A series of three Cu^{II} complexes with bidentate N,N$^{/}$-dimethyl ethylenediamine (**L_4**), N,N$^{/}$-diethylethylenediamine (**L_5**) and N,N$^{/}$-diisobutylethylenediamine (**L_6**) were prepared to study their reactivity with NO in acetonitrile. The effect of

substitution at the amine site on the stability of [Cu^{II}-$NO^{\bullet}$] species and also on ligand nitrosation are discussed.

d) Cu^{II} complexes with a bidentate ligand, having one aliphatic and one aromatic N-donor site ligand, 2-aminomethyl pyridine (**L_7**) and a tridentate ligand, *bis*[2-aminoethyl]amine (**L_8**) were synthesised and their reactivity with NO in acetonitrile was studied. These studies also suggested the formation of [Cu^{II}-$NO^{\bullet}$] species**.**

e) The NO reactivity of Cu^{II} complexes with two bidentate ligands, 2-(2-aminoethyl)-pyridine (**L_9**) and 2-(N-ethyl-2-aminoethyl)-pyridine (**L_{10}**) were studied in acetonitrile and water. The effect of chelate ring size on the stability of [Cu^{II}-$NO^{\bullet}$] species have been discussed.

All these chapters will present a brief idea of reactivity of Cu^{II} complexes with NO to result into the formation of transient [Cu^{II}-$NO^{\bullet}$] intermediate as well as ligand nitrosation/modification through diazotisation.

1.4 References

1. Murrad, F. *Angew. Chem., Int. Ed. Engl.* **1999**, *38*, 1856.
2. Ignaro, L. J. *Angew. Chem., Int. Ed. Engl.* **1999**, *38*, 1882.
3. Furchgott, R. F. *Angew. Chem., Int. Ed. Engl.* **1999**, *38*, 1870.
4. Wang, P. G.; Xian, M.; Tang, X.; Wu, X.; Wen, Z.; Cai, T.; Janczuk, A. J., *Chem. Rev*. **2002**, *102*, 1091.
5. *Methods in Nitric Oxide Research*; Feelisch, M.; Stamler, J. S.; Eds.; John Wiley and Sons; Chichester, England, **1996**.
6. Jia, L.; Bonaventura, C.; Bonaventura, J.; Stamler, J. S. *Nature*, **1996**, *380*, 221.

7. Galdwin, M. T.; Lancaster, J. R. Jr.; Freeman, B. A.; Schechter, A. N. *Nat. Med.* **2003**, *9*, 496.

8. Pfeiffer, S.; Mayer, B.; Hemmens, B. *Angew. Chem., Int. Ed. Engl.* **1999**, *38*, 1714.

9. Miranda, K. M.; Nims, R. W.; Thomas, D. D.; Espey, M. G.; Citrin, D.; Bartberger, M. D.; Paolocci, N.; Fukuto, J. M.; Feelisch, M.; Wink, D. A. *J. Inorg. Biochem.* **2003**, *93*, 52.

10. Torres, J.; Svinstunenko, D.; Karlsson, B.; Cooper, C. E.; Wilson, M. T. *J. Am. Chem. Soc.* **2002**, *124*, 963.

11. Ignarro, L. J. *Nitric Oxide: Biology and Pathobiology* Ed.; Academic Press; San Diego, **2000.**

12. Radi, R. *Chem. Res. Toxicol.* **1996**, *9*, 828.

13. Kim, S.; Deinum, G.; Gardner, M. T.; Marletta, M. A.; Babcock, G. T. *J. Am. Chem. Soc.* **1996**, *118*, 8769.

14. Burstyn, J. N.; Yu, A. E.; Dierks, E. A.; Hawkins, B. K.; Dawson, B. K. *Biochemistry*, **1995**, *34*, 5896.

15. *Nitric Oxide: Principles and Actions*, Ignarro, L. J.; Ed.; Lancaster, J.; Academic Press; Inc., New York, **1996**.

16. *Nitrogen monoxide and nitrous oxide binding and reduction*, Lee, D.-H.; Mondal, B.; Karlin, K. D.; in *Activation of small molecules,* Ed. Tollman, W. B.; Wiley-VCH, Germany, **2006**, pp 43-79.

17. Torres, J.; Cooper, C. E.; Wilson, M. T. *J. Biol. Chem*. **1998**, *273*, 8756.

18. Schopfer, M. P.; Mondal, B.; Lee, D.-H.; Sarjeant, A. A. N.; Karlin, K. D. *J. Am. Chem. Soc*. **2009**, *131*, 11304.

19. Maiti, D.; Lee, D.-H.; Sarjeant, A. A. N.; Pau, M. Y. M.; Solomon, E. I.; Gaoutchenova, K.; Sundermeyer, J.; Karlin, K. D. *J. Am. Chem. Soc*. **2008**, *130*, 6700.

20. Park, G. A.; Deepalatha, S.; Simona, C. P.; Lee, D.-H.; Mondal, B.; Sarjeant, A. A. N.; Rio, D. Del: Pau, M. Y. M.; Solomon, E. I.; Karlin, K. D. *J. Biol. Inorg. Chem.* **2009**, 14, 1301.

21. Richter-Addo, G. B.; Legzdins, P. *Metal Nitrosyls*; Oxford University Press, New York, **1992**.

22. Greenwood, N. N.; Earnshaw, A. *Chemistry of the Elements*; Pergamon Press: Oxford, **1993**, pp 508.

23. Fujisawa, K.; Tateda, A.; Miyashita, Y.; Okamoto, K.-i.; Paulat, F.; Praneeth, V. K. K.; Merkle, A.; Lehnert, N. *J. Am. Chem. Soc.* **2008**, *130*, 1205.

24. (a) Fernandez, B. O.; Lorkovic, I. M.; Ford, P. C. *Inorg. Chem.* **2004**, *43*, 5393. (b) Lehnert, N.; Praneeth, V. K. K.; Paulat, F. *J. Comput. Chem.* **2006**, *27*, 1338.

25. (a) Ellison, M. K.; Scheidt, W. R. *J. Am. Chem. Soc.* **1999**, *121*, 5210. (b) Linder, D. P.; Rodgers, K. R.; Banister, J.; Wyllie, G. R. A.; Ellison, M. K.; Scheidt, W. R. *J. Am. Chem. Soc.* **2004**, *126*, 14136.

26. (a) Lim, M. D.; Lorkovic, I. M.; Ford, P. C. *J. Inorg. Biochem.* **2005**, *99*, 151. (b) Shamir, D.; Zilbermann, I.; Maimon, E.; Gellerman, G.; Cohen, H.; Meyerstein, D. *Eur. J. Inorg. Chem.* **2007**, 5029.

27. Kumar, P.; Kalita, A.; Mondal, B. *Dalton Trans.* **2011**, *40*, 8656.

28. Mondal, B.; Kumar, P.; Ghosh, P.; Kalita, A.; Chem. Comm. **2011**, *47*, 2964.

29. Diaz, A.; Ortiz, M.; Sanchez, I.; Cao, R.; Mederos, A.; Sanchiz, J.; Brito, F. *J. Inorg. Biochem.* **2003**, *95*, 283.

30. Wright, A. M.; Wu, G.; Hayton, T. W. *J. Am. Chem. Soc*. **2010**, *132*, 14336.

31. Khin C.; Lim M. D.; Tsuge K.; Iretskii A.; Wu G.; Ford P. C. *Inorg. Chem*. **2007**, *46*, 9323.

32. McQuade, L. E.; Lippard, S. J. *Inorg. Chem.,* **2010**, *49,* 7464.

33. Wasser, I. M.; de Vries, S.; Moenne-Loccoz, P.; Schroder, I.; Karlin, K. D. *Chem. Rev*. **2002**, *102*, 1201.

34. Hulse, C. L.; Tiedje, J. M.; Averill, B. A. *J. Am. Chem. Soc.* **1989**, *111*, 2322.

35. Kujime, M.; Izumi, C.; Tomura, M.; Hada, M.; Fujii, H. *J. Am. Chem. Soc.* **2008**, *103*, 6088.

36. Ferguson, S. J. *Curr. Opin. Chem. Biol.* **1998**, *2*, 182.

37. Richardson, D. J.; Watmough, N. J. *Curr. Opin. Chem. Biol.* **1999**, *3*, 207.

38. Moura, I.; Moura, J. J. G. *Curr. Opin. Chem. Biol.* **2001**, *5*, 168.

39. Ghosh, S.; Dey, A.; Usov, O. M.; Sun, Y.; Grigoryants, V. M.; Scholes, C. P.; Solomon, E. I. *J. Am. Chem. Soc*. **2007**, *129*, 10310.

40. Enemark, J. H.; Feltham, R. D. *Coord. Chem. Rev*. **1974**, *13*, 339.

41. (a) Hoshino, M.; Maeda, M.; Konishi, R.; Seki, H.; Ford, P. C. *J. Am. Chem. Soc.*, **1996**, *118*, 5702. (b) Reichenbach, G.; Sabatini, S.; Palombari, R.; Palmerini, C. A. *Nitric Oxide* **2001**, *5*, 395. (c) Cabail, M. Z.; Pacheco, A. A. *Inorg. Chem*. **2003**, *42*, 270.

42. Fernandez, B. O.; Ford, P. C. *J. Am. Chem. Soc*. **2003**, *125*, 10510.

43. Studbauer, G.; Giuffre, P.; Sarti, P. *J. Biol. Chem.* **1999**, *274*, 28128.

44. (a) Bryan, N. S.; Rassaf, T.; Maloney, R. E.; Rodriguez, C. M.; Saijo, F.; Rodriguez, J. R.; Feelisch, M. *Proc. Natl. Acad. Sci. U.S.A.* **2004**, *101*, 4308. (b) Rassaf, T.; Feelisch, M.; Kelm, M. *Free Radical Biol. Med.* **2004**, *36*, 413. (c) Giustarini, D.; Milzani, A.; Colombo, R.; Dalle-Donne, I.; Rossi, R. *Clin. Chim. Acta* **2003**, *330*, 85.

45. Ford P. C.; Fernandez B. O.; Lim M. D.; *Chem. Rev*. **2005**, *105*, 2439.

46. (a) Luchsinger, B. P.; Rich, E. N.; Gow, A. J.; Williams, E. M.; Stamler, J. S.; Singel, D. J. *Proc. Natl. Acad. Sci. U.S.A.* **2003**, *100*, 461. (b) Moriel, P.; Pereira, I. R. O.; Bertolami, M. C.; Abdalla, D. S. P. *Free Radical Biol. Med.* **2001**, *30*, 318. (c) Inoue, K.; Akaike, T.; Miyamoto, Y.; Okamoto, T.; Sawa, T.; Otagiri, M.; Suzuki, S.; Yoshimura, T.; Maeda, H. *J. Biol. Chem.* **1999**, *274*, 27069.

47. Tran, D.; Ford, P. C. *Inorg. Chem*. **1996**, *35*, 2411.

48. Tran, D.; Skelton, B. W.; White, A. H.; Laverman, L. E.; Ford, P. C. *Inorg. Chem*. **1998**, *37*, 2505.

49. Tsuge, K.; DeRosa, F.; Lim, M. D.; Ford, P. C. *J. Am. Chem. Soc.* **2004**, *126*, 6564.

50. Kohlschu¨tter, V.; Kutscheroff, M. *Chem. Ber.* **1904**, *37*, 3044.

51. Fraser, R. T. M.; Dasent, W. E. *J. Am. Chem. Soc.* **1960**, *82*, 348.

52. Fraser, R. T. M. *J. Inorg. Nucl. Chem.* **1961**, *17*, 265.

53. Tsumore, N.; Xu, Q. *Bull. Chem. Soc. Jpn.* **2002**, 75, 1861.

54. Bonomo, R. P.; Pappalardo, G.; Rizzarelli, E.; Santoro, A. M.; Tabb`I, G.; Vagliasindi, L. I.; *Dalton Trans.,* **2007**, 1400.

55. Bonomo, R. P.; Pappalardo, G.; Rizzarelli, E.; Tabb`ı, G.; Vagliasindi, L. I. *Dalton Trans.* **2008**, 3805.

56. Franz, K. J.; Singh, N.; Lippard, S. J., *Angew. Chem., Int. Ed.* **2000**, *39*, 2120.

57. Franz, K. J.; Singh, N.; Spingler, B.; Lippard, S. J. *Inorg. Chem.* **2000**, *39*, 4081.

58. Hilderbrand, S. A.; Lim, M. H.; Lippard, S. J. *J. Am. Chem. Soc.* **2004**, *126*, 4972.

59. Lim, M. H.; Lippard, S. J. *Inorg. Chem.* **2004**, *43*, 6366.

60. Hilderbrand, S. A.; Lippard, S. J. *Inorg. Chem.* **2004**, *43*, 5294.

61. Franz, K. J.; Singh, N.; Lippard, S. J. *Angew. Chem., Int. Ed.* **2000**, *39*, 2120.

62. Hilderbrand, S. A.; Lippard, S. J. *Inorg. Chem.* **2004**, *43*, 4674.

63. Lim, M. H.; Lippard, S. J. *Inorg. Chem.* **2006**, *45*, 8980.

64. Do, L.; Smith, R. C.; Tennyson, A. G.; Lippard, S. J. *Inorg. Chem.* **2006**, *45*, 8998.

65. Lim, M. H.; Xu, D.; Lippard, S. J. *Nat. Chem. Biol*. **2006**, *2*, 375.

66. Rosenthal, J.; Lippard, S. J. *J. Am. Chem. Soc.* **2010**, *132*, 5536.

67. Lim, M. H.; Lippard, S. J. *Acc. Chem. Res.* **2007**, *40*, 41.

68. Lim, M. H.; Lippard, S. J. *J. Am. Chem. Soc.*, **2005**, *127*, 12170.

69. Lim, M. H.; Lippard, S. J. *Inorg. Chem.,* **2006**, *45,* 8980.

70. Smith, R. C.; Tennyson, A. G.; Won, A. C.; Lippard, S. J. *Inorg. Chem.,* **2006**, *45,* 9367.

71. Lim, M. H.; Wong, B. A.; Pitcock, W. H.; Mokshagundam, D.; Baik, M.-H.; Lippard, S. J. *J. Am. Chem. Soc.*, **2006**, *128*, 14364.

72. Tocheva, E. I.; Rosell, F. I.; Mauk, A. G.; Murphy, M. E. P. *Biochemistry,* **2007**, *46*, 12366.

73. Merkle, A. C.; Lehnert, N. *Inorg. Chem.* **2009**, *48*, 11504.

74. Tiripicchio. A.; Lanfredi. A. M.; Ghedini. M.; Neve. F. *Chem. Commun.* **1983**, 97.

75. Paul, P. P.; Tyeklar, Z.; Farooq, A.; Karlin, K. D.; Liu, S. C.; Zubieta, J. *J. Am. Chem. Soc.* **1990**, *112*, 2430.

76. Paul, P. P.; Karlin, K. D. *J. Am. Chem. Soc.* **1991**, *113*, 6331.

77. Tolman, W. B. *Adv. Chem. Ser.* **1995**, *246*, 195.

78. Carrier, S. M.; Ruggiero, C. E.; Tolman, W. B.; Jameson, G. B. *J. Am. Chem. Soc.* **1992**, *114*, 4407.

79. Ruggiero, C. E.; Carrier, S. M.; Antholine, W. E.; Whittaker, J. W.; Cramer, C. J.; Tolman, W. B. *J. Am. Chem. Soc.* **1993**, *115*, 11285.

80. Ruggiero, C. E.; Carrier, S. M.; Tolman, W. B. *Angew. Chem., Int. Ed. Engl.* **1994**, *33*, 895.

81. Schneider, J. L.; Carrier, S. M.; Ruggiero, C. E.; Young, V. G. Jr.; Tolman W. B. *J. Am. Chem. Soc.* **1998**, *120*, 11408.

82. Hayton, T. W.; Legzdins, P.; Sharp, W. B. *Chem. Rev*. **2002**, *102*, 935.

83. Tocheva, E. I.; Rosell, F. I.; Mauk, A. G.; Murphy, M. E. P. *Science*, **2004**, *304*, 867.

84. Antonyuk, S. V.; Strange, R. W.; Sawers, G.; Eady, R. R.; Hasnain, S. S. *Proc. Natl. Acad. Sci. U.S.A.* **2005**, *102*, 12041.

85. Halfen, J. A.; Tolman, W. B. *J. Am. Chem. Soc.* **1994**, *116*, 5475.

86. Halfen, J. A.; Mahapatra, S.; Wilkinson, E. C.; Gengenbach, A. J.; Young, V. G.; Que, L.; Tolman, W. B. *J. Am. Chem. Soc.* **1996**, *118*, 763.

87. Herold, S.; Koppenol, W. H. *Coord. Chem. Rev.* **2005** , *249*, 499.

Chapter 2

Reduction of copper(II) complex of *tris*-(2-isopropyl aminoethyl)amine by nitric oxide and tri-nitrosation of the ligand

Abstract

Copper(II) complex, **2.1** of a tetradented tripodal ligand, $\mathbf{L_1}$ [$\mathbf{L_1}$, *tris*-(2-isopropylaminoethyl)amine] has been synthesized and characterized. The Cu^{II} center in complex **2.1** in acetonitrile solvent, on exposure to nitric oxide has been found to be reduced to Cu^{I}. This reduction resulted into the concomitant tri-nitrosation of the ligand at terminal amine centers and the release of the modified ligand, $\mathbf{L_1}'$. $\mathbf{L_1}'$ was found to be crystallized out from the reaction mixture as its perchlorate salt. The formation of $\mathbf{L_1}'$-perchlorate was authenticated by FT-IR, ^{1}H-NMR, ^{13}C NMR and X-ray single crystal structure determination. Addition of NO to the methanol solution of complex **2.1** resulted in the reduction of Cu^{II} center with a simultaneous mono- and dinitrosation of the ligand. In water, the reduction of Cu^{II} center by NO was found to afford NO_2^-, but not ligand nitrosation.

2.1 Introduction

Nitric oxide (NO) plays the key roles in mammalian biology such as in vascular regulation, neurotransmission, and immuno-cytotoxicity and some of these activities are attributed to the formation of nitrosyl complexes of metallo-proteins.[1, 2] Hence, the interaction of NO with metal centers has long been of interest to chemists and biochemists.[3] The reduction of Cu^{II} centers in some proteins, such as cytochrome *c* oxidase and laccase, to Cu^{I} on exposure to NO has also been known for a long time.[4] In cytochrome *c* oxidase, the NO reduction of Cu^{II} to Cu^{I} is believed to play the role in regulating the electron transport activity of this protein.[4, 5] In presence of NO, Cu^{II} is also known to facilitate the nitrosation of various thiolates, and this reduction was found to correlate with formation of *S*-nitroso bovine serum albumin and *S*-nitroso glutathione.[6] These observations have been used to suggest a mechanism for the formation of RSNO compounds in blood.[7] Although, the auto-reduction of ferriheme proteins such as methemoglobin and ferricytochrome c (Cyt^{III}) by NO has been studied extensively, the Cu^{II} reduction has not been studied to that extent.[3, 4]

In this context, the NO reactivity of a Cu^{II} complex of a tripodal ligand was studied and the ligand was found to undergo nitrosation to the corresponding N-nitroso amines in the process of reduction of Cu^{II} to Cu^{I} by NO.

2.2 Results and discussions

The complex **2.1** was prepared by the reaction of $[Cu(H_2O)_6](ClO_4)_2$ in acetonitrile solution with equivalent amount of the ligand. It was isolated from the reaction mixture as blue crystalline solid (Scheme 2.1).

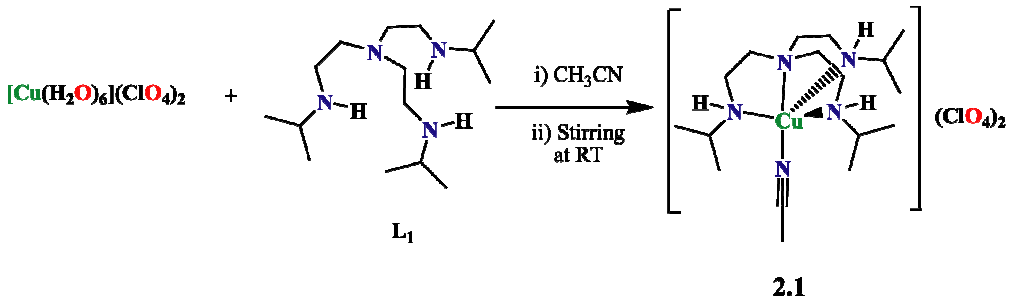

Scheme 2.1

The complex **2.1** exibited satisfactory elemental analyses (experimental section) and it behaved as 1:2 electrolyte [Λ_M ($\Omega^{-1}cm^2mol^{-1}$), 228] in acetonitrile solution. The complex was characterized by various spectroscopic techniques. The single crystal X-ray structure of complex **2.1** was determined. The single crystal structure of **2.1** revealed that Cu^{II} is surrounded by five nitrogen donor atoms (four from $\mathbf{L_1}$ and one from coordinated acetonitrile) in a distorted trigonal bipyramidal geometry (Figure 2.1). The structural index parameter, τ, has been found to be ~ 0.6. The three terminal nitrogen atoms of $\mathbf{L_1}$ occupied the equatorial positions; whereas the central nitrogen of $\mathbf{L_1}$ and the nitrogen from coordinated acetonitrile occupied the axial positions. The crystallographic table and selected bond lengths and angles are given in Appendix I (Table A1.1, A1.2 and A1.3).

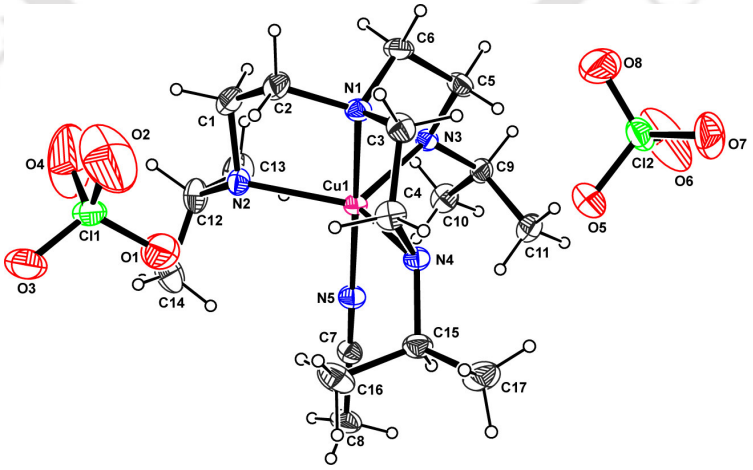

Figure 2.1: ORTEP diagram of complex **2.1**(30% thermal ellipsoid plot).

The complex **2.1**, in acetonitrile solvent, exhibited broad *d-d* band with λ_{max}(ε/ $M^{-1}cm^{-1}$), 826 nm (340), 615 nm (110) (shoulder) (Figure 2.2). In room temperature magnetic moment measurement, it showed one electron paramagnetism ($\mu_{obs.}$, 1.56 BM). It displayed four line X-band EPR at room temperature in acetonitrile (g_{ave}= 2.0845) (Figure 2.3).[8]

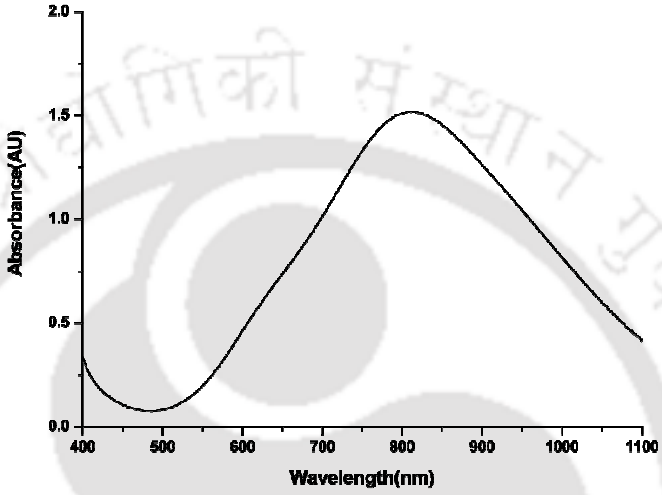

Figure 2.2: UV-visible spectrum of complex **2.1** in acetonitrile.

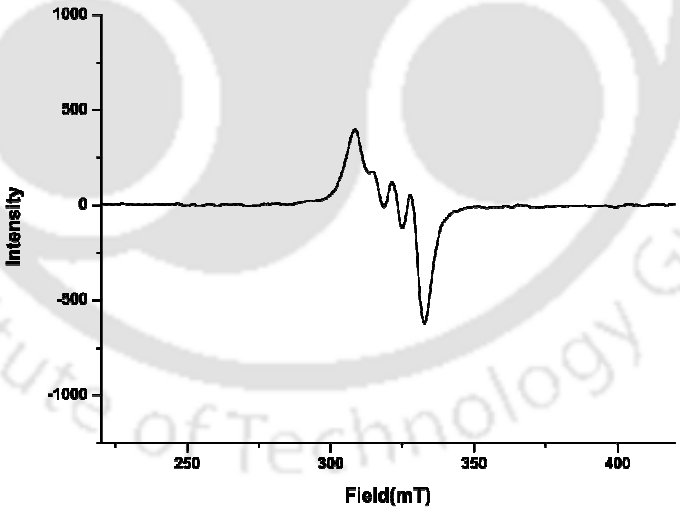

Figure 2.3: X-Band EPR spectrum of complex **2.1** in acetonitrile at room temperature.

2.2.1 Nitric oxide reactivity of complex 2.1 in acetonitrile

The NO reactivity of the complex **2.1** was studied in acetonitrile solution and the spectral changes were monitored by UV-visible and X-Band EPR spectroscopy. The

d-d transition for complex **2.1** was found to appear at 826 nm. On purging NO gas to a degassed acetonitrile solution of complex **2.1**, the position of the *d-d* transition shifted to 640 nm (Figure 2.4). It is presumably because of the formation of the thermally unstable [Cu^{II}-$NO^{\bullet}$] intermediate. This intermediate was found to decompose gradually to afford colorless solution following pseudo first order kinetics and the spectral changes were monitored by UV-visible spectroscopy (Figure 2.4, inset). The rate constant for the decomposition of the intermediate was found to be 5.64×10^{-2} sec^{-1} at 298K.

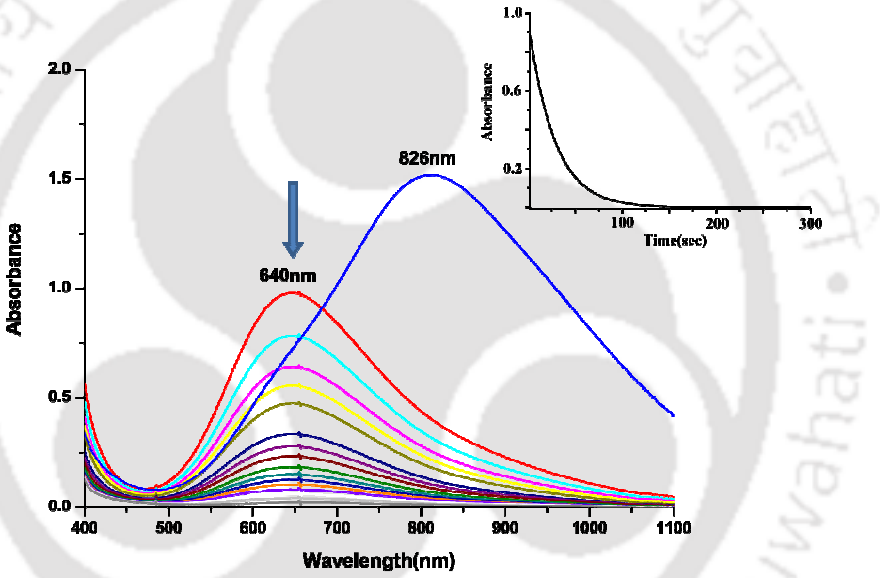

Figure 2.4: UV-visible spectroscopic monitoring of the gradual decay of $[L_1Cu^{II}\text{-}NO]^{2+}$ to Cu^{I} in acetonitrile at 298K. (Blue trace represents the spectrum of the complex **2.1** before the reaction with NO). Inset: Time scan plot of the gradual decay of $[L_1Cu^{II}\text{-}NO]^{2+}$ (λ_{max}, 640 nm) to Cu^{I} in acetonitrile at 298K.

Though, the complex **2.1** in acetonitrile displayed characteristic four line EPR spectrum, the intermediate formed was found to be EPR silent at room temperature (Figure 2.5). It should be noted that the final colorless solution was also observed to be EPR silent owing to the formation of Cu^{I}. This is consistent with the reduction of Cu^{II} to Cu^{I}. In the present case thus, presumably, an unstable [Cu^{II}-$NO^{\bullet}$] intermediate was formed, prior to the reduction of Cu^{II} to Cu^{I}.

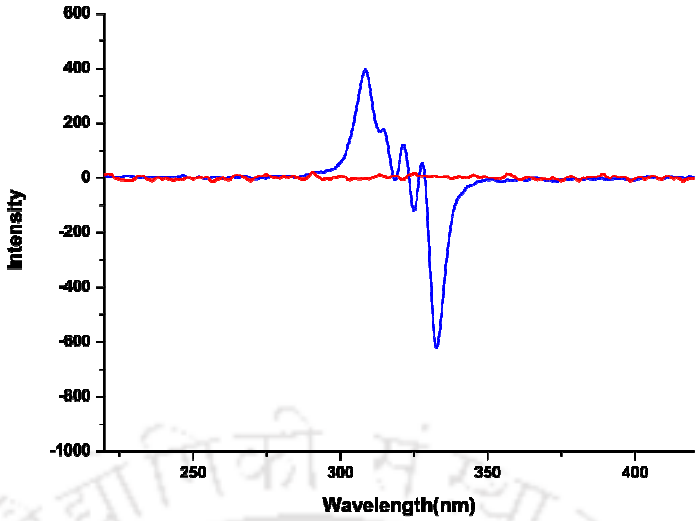

Figure 2.5: X-band EPR spectra of the complex **2.1** (blue trace) and after its reaction with NO (red trace) in acetonitrile at room temperature.

It would be worth mentioning here that Cao et. al. reported the reduction of a series of copper(II) dithiocarbamates with NO in aqueous solution which resulted into the formation of an air-stable copper-nitrosyl and dinitrosyl species.[9] Detailed kinetics studies of the Cu^{II}/NO reactions are not much.[3, 10] In this regard, Tran et. al. studied the NO reduction of the Cu^{II} complex, $[Cu(dmp)_2(H_2O)]^{2+}$ (dmp, 2,9-dimethyl-1,10-phenanthroline), in water and various mixed solvents.[4]

It is interesting to note that the NO reduction of Cu^{II} center in complex **2.1**, in acetonitrile, was accompanied with concomitant nitrosation of the ligand and release of the modified nitrosoamine, $\mathbf{L_1}'$ (yield ~30%)(Scheme 2.2). $\mathbf{L_1}'$ was found to be precipitated out from the reaction mixture as its perchlorate salt. The formation of $\mathbf{L_1}'$-perchlorate was confirmed by its single crystal X-ray structure determination (Figure 2.6) and other spectroscopic studies. The crystallographic table, the tables of selected bond lengths and angles are listed in Appendix I (Table A1.4 and A1.5). The ^{1}H-NMR spectrum of $\mathbf{L_1}'$-perchlorate indicated the terminal amine nitrogen as nitrosation site (Appendix I, Figure A1.1). The ^{13}C-NMR spectrum was also in well agreement

(Appendix I, Figure A1.2). The 1446 cm^{-1} band in FT-IR spectrum of $\mathbf{L_1}'$-perchlorate was consistent with the expected ν_{NO} of nitrosoamine (Appendix I, Figure A1.3).[11] It is important to note that the free ligands did not react with NO at the reaction condition.

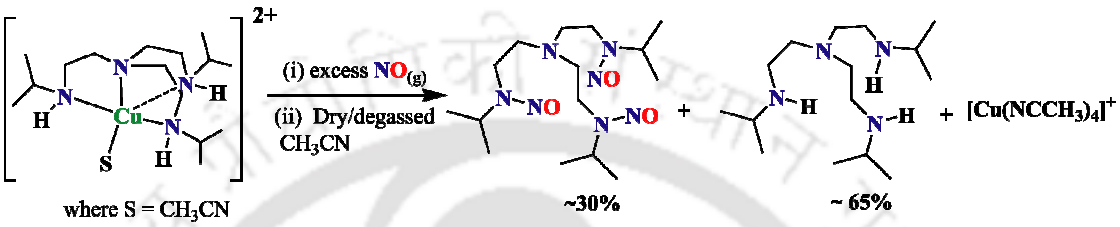

Scheme 2.2

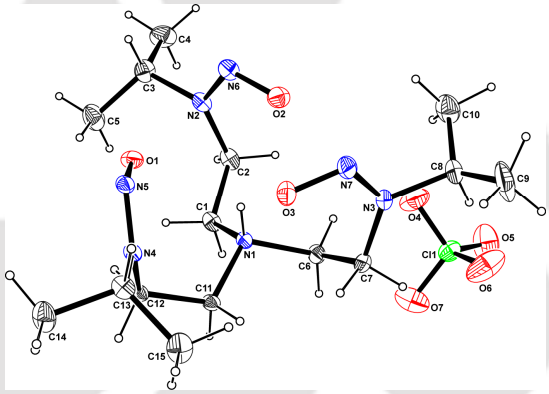

Figure 2.6: ORTEP diagram of $\mathbf{L_1}'$-perchlorate (30% thermal ellipsoid plot).

Ford et. al. reported their observations with $[Cu^{II}(DAC)]^{2+}$ {DAC, 1,8-bis-(9-anthracyl methyl) derivative of the macrocyclic tetraamine cyclam(1,4,8,11-tetraazacyclo tetradecane)} in methanol solution.[12] However, the marked difference to that result is in the present case, the nitrosation took place in all the three terminal nitrogen whereas in DAC ligand, at one nitrogen only.

In case of $[Cu^{II}(DAC)]^{2+}$, after reduction and nitrosation, the release of modified ligand was attributed to the fact that the Cu^{I} favors tetrahedral geometry; whereas the

DAC ligand favors square planer one. At the same time, the nitrosation also weakens the binding ability of the amine nitrogen.[12] Though, in the present case both the Cu^{I} and the ligand favor tetrahedral coordination, the release of $\mathbf{L_1'}$-perchlorate can be attributed to the weakening of amine binding to the Cu^{I} due to nitrosation; this weakening is further enhanced by the protonation of the central nitrogen which results into the $\mathbf{L_1'}$-perchlorate salt.

The mechanism of ligand nitrosation is not very clear. One mechanism could be the attack of NO on the deprotonated amine site followed by electron transfer to the copper center as reported in case of $[Cu^{II}(DAC)]^{2+}$.[12] Alternatively, the key step would be first NO coordination to the copper ion followed by NO^{+} migration to the secondary amine.[12] The observation of the transient intermediates in UV-visible and EPR spectroscopy prior to reduction supports the second possibility. However, the reason for tri-nitrosation in the present case is not very clear. Comparing to the other reported results, one could think of the tri-nitrosation as a result of the combined effect of geometry of the complex, presence of electron donor groups at the terminal amine positions and the difference in mechanistic pathways. However, the presence of some other disproportionation processes facilitated by the metal center can also not be ruled out.

2.2.2 Nitric oxide reactivity of complex 2.1 in methanol

In methanol, NO reactivity of **2.1** was studied and the reduction of Cu^{II} to Cu^{I} was observed. This was confirmed by UV-visible and EPR spectroscopic studies (Appendix I, Figures A1.4, and A1.5). The reduction was found to be accompanied with di- and mono-nitrosation of the ligand; (Scheme 2.3) in contrast, exclusively trinitrosation was observed in acetonitrile.

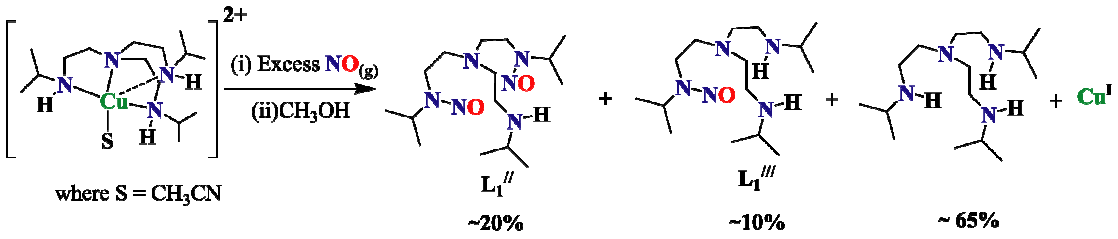

Scheme 2.3

The dinitrosated, $\mathbf{L_1}^{//}$ and mononitrosated, $\mathbf{L_1}^{///}$ ligands were characterized by elemental analysis (experimental section), FT-IR, ^{1}H-NMR, ^{13}C-NMR and ESI-mass spectroscopy (Experimental section, Appendix I, Figures A1.6-A1.13). The $\nu_{N\text{-}NO}$ stretching frequency in $\mathbf{L_1}^{//}$ and $\mathbf{L_1}^{///}$ appeared at 1461 and 1448 cm^{-1} in FT-IR spectrum.

2.2.3 Nitric oxide reactivity of complex 2.1 in water

The reaction of NO with the complex **2.1** was also studied in water medium. In water, Cu^{II} center was observed to undergo reduction to Cu^{I}. This was studied by UV-visible and ^{1}H-NMR spectroscopy (Appendix I, Figures A1.14 and A1.15). Further, the reduction of complex **2.1** in water was confirmed by ^{1}H-NMR studies in D_2O. The complex displayed broad ^{1}H-NMR signal in D_2O due to the presence of paramagnetic Cu^{II} centre (Figure 2.10a). After the reduction of Cu^{II} to Cu^{I}, the solution showed well resolved signals in ^{1}H-NMR spectrum (Figure 2.10b).

In water, the reduction of Cu^{II} centre by NO was not found to afford any ligand nitrosation. On the other hand, the formation of NO_2^- in solution was evidenced by Greiss's test (Scheme 2.4). This can be attributed to the higher reactivity of NO^+ with water than N-H group.

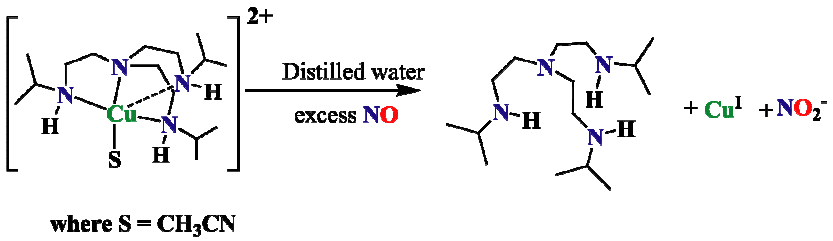

Scheme 2.4

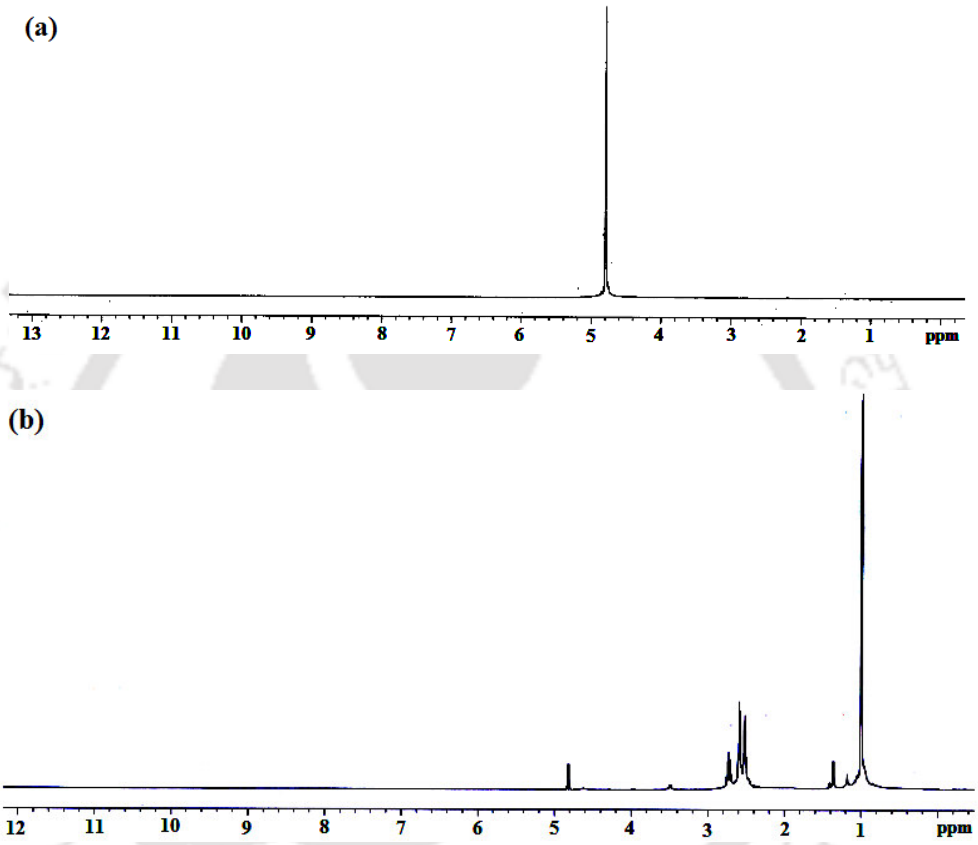

Figure 2.10: ^{1}H-NMR spectra of complex **2.1**(a) before and (b) after the reaction with NO.

2.3 Conclusion

The NO reduction of the Cu^{II} center in complex **2.1** was found proceed through unstable [Cu^{II}-$NO^{\bullet}$] intermediate in acetonitrile. The reduction was resulted into the concomitant tri-nitrosation of the ligand. In methanol, the reduction afforded only mono- and di-nitrosation. In water, it was accompanied with the formation of NO_2^-; but no ligand nitrosation was found.

2.4 Experimental Section

2.4.1 Materials and methods

All reagents and solvents were purchased from commercial sources and were of reagent grade. Ligand, **L_1** was purchased from Sigma-Aldrich and used as received. Acetonitrile was distilled from calcium hydride. Deoxygenation of the solvent and solutions were effected by repeated vacuum/purge cycles or bubbling with nitrogen for 30 minutes. NO gas was purified by passing through KOH and P_2O_5 column. UV-visible spectra were recorded on a Perkin Elmer Lambda 25 UV-visible spectrophotometer. FT-IR spectra of the solid samples were taken on a Perkin Elmer spectrophotometer with samples prepared as KBr pellets. Solution electrical conductivity was checked using a Systronic 305 conductivity bridge. ^{1}H-NMR spectra were obtained with a 400 MHz Varian FT spectrometer. Chemical shifts (ppm) were referenced either with an internal standard (Me_4Si) or to the residual solvent peaks. The X-band Electron Paramagnetic Resonance (EPR) spectra were recorded on a JES-FA200 ESR spectrometer, at room temperature. Elemental analyses were obtained from a Perkin Elmer Series II Analyzer. The magnetic moment of complexes was measured on a Cambridge Magnetic Balance.

Single crystals were grown by slow diffusion followed by slow evaporation technique. The intensity data were collected using a Bruker SMART APEX-II CCD diffractometer, equipped with a fine focus 1.75 kW sealed tube MoK_α radiation (λ = 0.71073 Å) at 273(3) K, with increasing ω (width of 0.3° per frame) at a scan speed of 3 s/frame. The SMART software was used for data acquisition. Data integration and reduction were undertaken with SAINT and XPREP software.[13] Structures were solved by direct methods using SHELXS-97 and refined with full-matrix least squares

on F^2 using SHELXL-97.[14, 15] All non-hydrogen atoms were refined anisotropically. Structural illustrations have been drawn with ORTEP-3 for Windows.[16]

2.4.2 Synthesis of complex 2.1, $[Cu(L_1)(NCCH_3)](ClO_4)_2$

Copper(II)hexahydrate perchlorate, $[Cu(H_2O)_6](ClO_4)_2$ [0.740 g (2.0 mmol)] was dissolved in 10 ml distilled acetonitrile. To this solution, 0.544 g (2.0 mmol) of the ligand $\mathbf{L_1}$ was added slowly with constant stirring. The color of the solution turned into deep blue from light blue. The stirring was continued for 1h at room temperature. The volume of the solution then reduced to ~2 ml. To this, 10 ml of benzene was added to make a layer on it and kept it overnight on freezer. This resulted into blue crystals of complex **2.1**. Yield: 0.975 g (85%). Elemental Analyses: Calcd. for $C_{17}H_{36}N_5O_8Cl_2Cu$: C, 35.60; H, 6.28; N, 12.21. Found (%): C, 35.66; H, 6.29; N, 12.25. Molar conductivity: [$\Lambda_M(\Omega^{-1}cm^2mol^{-1})$, 228]. FT-IR: 2977, 1085, 625 cm^{-1}; magnetic moment, 1.56 BM.

2.4.3 Isolation of L_1'-perchlorate

To 10 ml of degassed acetonitrile solution of complex **2.1** (250 mg), freshly prepared NO was bubbled for 1 minute. The deep blue color of the solution turned colorless. This solution was allowed to stand for 10 minutes at room temperature. Then the excess of NO was removed and 10 ml of degassed benzene was added to this under dinitrogen atmosphere. The reaction mixture was kept in freezer for two days. The $\mathbf{L_1'}$-perchlorate was found to be crystallized out. Yield: 60 mg (~30%). Elemental Analyses: Calcd. for $C_{15}H_{34}N_7O_7Cl$: C, 39.13; H, 7.39; N, 21.30. Found (%): C, 39.17; H, 7.40; N, 21.28. FT-IR: 2946, 1446, 1101, 625 cm^{-1}; ^{1}H-NMR (400 MHz, $CDCl_3$): δ_{ppm}, 4.58(3H) 3.54(6H), 3.08(6H), 1.27(18H). ^{13}C-NMR (100 MHz, $CDCl_3$): δ_{ppm}, 58.12, 54.02, 40.08, 22.07.

2.4.4 Isolation of $L_1^{//}$ and $L_1^{///}$

In a 100 ml Schlenk flask, complex **2.1** (574 mg, 1.0 mmol) was dissolved in 50 ml degassed methanol. To this, NO gas was purged through a needle for one minute and the mixture was then allowed to stand for 10 minutes. The excess NO was then removed from the system by purging vacuum/nitrogen for several cycles. The colorless solution was then open to air and stirred for 1h to ensure complete oxidation of Cu^{I} center to Cu^{II}. The solution was dried in rotavapour. To this, 5 ml saturated aqueous solution of Na_2S was added and stirred for ½ h. The black precipitate of Cu_2S thus obtained was filtered off and the filtrate was diluted with 50 ml of distilled water. The organic part was then extracted from the mixture using $CHCl_3$ (3 portions × 25 ml). The collected organic layer was then dried under reduced pressure and the residual oil was subjected to column chromatography using silica gel to yield $\mathbf{L_1^{//}}$ and $\mathbf{L_1^{///}}$.

$L_1^{//}$: Yield: 66 mg (~20%). Elemental Analyses: Calcd. for $C_{15}H_{34}N_6O_2$: C, 54.52; H, 10.37; N, 25.43. Found (%): C, 54.42; H, 10.40; N, 25.28. FT-IR: 2977, 1466, 1441, 1360, 1111 cm^{-1}; ^{1}H-NMR (400 MHz, $CDCl_3$): δ_{ppm}, 4.68(m, 1H) 3.54(t, 4H), 2.79(m, 1H), 2.68(s, 4H), 2.54(t, 4H), 1.44(d, 12H), 1.07(d, 16 H). ^{13}C-NMR (100 MHz, $CDCl_3$): δ_{ppm}, 55.64, 54.46, 49.86, 49.12, 45.08, 41.25, 22.92, 21.57. ESI-Mass: (m+1)/z, 331.19.

$L_1^{///}$: Yield: 36 mg (~10%). Elemental Analyses: Calcd. for $C_{15}H_{35}N_5O$: C, 59.76; H, 11.70; N, 23.23. Found (%): C, 59.70; H, 11.70; N, 23.28. FT-IR: 2974, 1466, 1440, 1169, 1122 cm^{-1}; ^{1}H-NMR (400 MHz, $CDCl_3$): δ_{ppm}, 4.66(m, 1H) 3.53(m, 2H), 2.78(t, 2H), 2.63(m, 8H), 2.51(t, 2H), 1.41(d, 6H), 1.04(d, 12 H). ^{13}C-NMR (100 MHz,

$CDCl_3$): $\delta_{ppm,}$ 55.61, 54.35, 49.18, 45.22, 41.25, 22.96, 21.68. ESI-Mass: (m+1)/z, 302.23.

2.5 References

1. *Nitric Oxide: Biology and Pathobiology*; Ignarro, L. J., Ed.; Academic Press; San Diego, **2000**.
2. (a) Moncada, S.; Palmer, R. M. J.; Higgs, E. A. *Pharmacol. Rev*. **1991**, *43*, 109. (b) Butler, A. R.; Williams, D. L. *Chem. Soc. Rev*. **1993**, 233. (c) *Methods in Nitric Oxide Research*; Feelisch, M.; Stamler, J. S.; Eds.; John Wiley and Sons; Chichester, England, **1996**. (d) Jia, L.; Bonaventura, C.; Bonaventura, J.; Stamler, J. S. *Nature*, **1996**, *380*, 221. (e) Galdwin, M. T.; Lancaster, J. R. Jr.; Freeman, B. A.; Schechter, A. N. *Nat. Med*. **2003**, *9*, 496.
3. (a) Ford, P. C.; Fernandez, B. O.; Lim, M. D. *Chem. Rev*. **2005**, *105*, 2439. (b) Lim, M. H.; Wong, B. A.; Pitcocok, W. H. Jr.; Mokshagundam, D.; Baik, M-H.; Lippard, S. J. *J. Am. Chem. Soc.* **2006**, *128*, 14364. (c) Lim, M. H.; Lippard, S. J. *Inorg. Chem.* **2006**, *45*, 8980. (d) Lim, M. H.; Lippard, S. J. *J. Am. Chem. Soc.* **2005**, *127*, 12170. (e) Lim, M. H.; Lippard, S. J. *Nat. Chem. Biol.* **2006**, *2*, 375. (f) Shamir, D.; Zilbermann, I.; Maimon, E.; Gellerman, G.; Cohen, H.; Meyerstein, D. *Euro. J. Inorg. Chem.* **2007**, *32*, 5029.
4. (a) Torres, J.; Svistunenko, D.; Karlsson, B.; Cooper, C. E.; Wilson, M. T. *J. Am. Chem. Soc*. **2002**, *124*, 963. (b) Torres, J.; Cooper, C. E.; Wilson, M. T. *J. Biol. Chem*. **1998**, *273*, 8756. (c) Tran, D.; Skelton, B. W.; White, A. H.; Laverman, L. E.; Ford, P. C. *Inorg. Chem*. **1998**, *37*, 2505. (d) Martin, C. T.; Morse, R. H.; Kanne, R. M.; Gray, H. B.; Malmstrom, B. G.; Chan, S. I. *Biochemistry*, **1981**, *20*, 5147.

5. Cooper, C. E.; Torres, J.; Sharpe, M. A.; Wilson, M. T. FEBS *Lett*. **1997**, *414*, 281.

6. Studbauer, G.; Giuffre, P.; Sarti, P. *J. Biol. Chem*. **1999**, *274*, 28128.

7. (a) Bryan, N. S.; Rassaf, T.; Maloney, R. E.; Rodriguez, C. M.; Saijo, F.; Rodriguez, J. R.; Feelisch, M. *Proc. Natl. Acad. Sci*. U. S. A. **2004**, *101*, 4308. (b) Rassaf, T.; Feelisch, M.; Kelm, M. *Free Radical Biol. Med*. **2004**, *36*, 413.

8. (a) Addison, A. W.; Hendriks, H. M. J.; Reedijk, J.; Thompson, L. K. *Inorg. Chem*. **1981**, *20*, 103. (b) Sorrell, T. N.; Jameson, D. L. *Inorg. Chem*. **1982**, *21*, 1014.

9. Diaz, A.; Ortiz, M.; Sanchez, I.; Cao, R.; Mederos, A.; Sanchiz, J.; Brito, F. *J. Inorg. Biochem*. **2003**, *95*, 283.

10. Lei, Y.; Anson, F. C. *Inorg. Chem*. **1994**, *33*, 5003.

11. (a) Lee, J.; Chen, L.; West, A. H.; Richter-Addo, G. B. *Chem. Rev*. **2002**, *102*, 1019. (b) Sousa, A. K. M. H.; Sousa, J. R.; Santiago, M. O.; Longhinotti, E.; Batista, A. A.; Ellena, J.; Castellano, E. E.; Lopes, L. G. F.; Moreira, I. S. *Tetrahedron Lett*. **2005**, *46*, 1889.

12. Tsuge, K.; DeRosa, F.; Lim, M. D.; Ford, P. C. *J. Am. Chem. Soc*. **2004**, *126*, 6564.

13. SMART, SAINT and XPREP, Siemens Analytical X-ray Instruments Inc., Madison, Wisconsin, USA, **1995**.

14. Sheldrick, G. M. SADABS: software for Empirical Absorption Correction, University of Gottingen, Institut fur Anorganische Chemieder Universitat, Tammanstrasse 4, D-3400 Gottingen, Germany, **1999–2003**.

15. Sheldrick, G. M. SHELXS-97, University of Gottingen, Germany, **1997**.

16. Farrugia, L. J. *J. Appl. Crystallogr*. **1997**, *30*, 565.

Chapter 3

Nitric oxide reactivity of copper(II) complexes of *tris*-(2-aminoethyl)amine and ethylenediamine

Abstract

Two copper(II) complexes, **3.1** and **3.2** with $\mathbf{L_2}$ and $\mathbf{L_3}$ [$\mathbf{L_2}$, *tris*-(2-aminoethyl)-amine; $\mathbf{L_3}$, ethylenediamine] respectively, in degassed acetonitrile solvent, on exposure to NO gas, were found to undergo reduction to Cu^{I}. The process of reduction was evidenced by UV-visible and EPR spectroscopic studies. The reduction of the Cu^{II} centers by nitric oxide afforded ligand transformation through diazotization at the primary amine coordination site, in case of both the complexes. This suggests the formation of NO^{+} in the reaction medium which indirectly indicates the formation of [Cu^{II}-$NO^{\bullet}$] intermediate prior to the reduction. The modified ligands, in each case, were isolated and characterized by various spectroscopic studies.

3.1 Introduction

Nitric oxide (NO) is known to play key role in many biochemical processes such as in vascular regulation, neuro transmission and immuno-cytotoxicity and some of these activities are attributed to the formation of nitrosyl complexes of metalloproteins, primarily iron proteins.[1-9] The best characterized example is the ferroheme enzyme, soluble guanylyl cyclase (sGC).[10, 11] Formation of a nitrosyl complex with Fe(II) leads to labilization of a *trans* axial (proximal) histidine ligand in the protein backbone, and the resulting change in the protein conformation is believed to activate the enzyme for catalytic formation of the secondary messenger cyclic-guanylyl monophosphate (cGMP) from guanylyl triphosphate (GTP). The enzymatic formation of cGMP results into the relaxation of smooth muscle tissue of blood vessels, hence lowering blood pressure. On the other hand, the reduction of Cu^{II} centre in cytochrome *c* oxidase and laccase, to Cu^{I} by NO has been known for a long time.[12-15] In cytochrome *c* oxidase, the NO reduction of Cu^{II} to Cu^{I} is believed to play the role in regulating the electron transport activity of this protein.[16] Cu^{II} is also known to facilitate the nitrosation of various thiolates and this reduction was found to correlate with formation of S-nitroso bovine serum albumin and S-nitroso glutathione.[17] These observations can be used to suggest a mechanism for the formation of RSNO compounds in blood. However, to understand the mechanisms of these biochemical/medical processes, a high degree of understanding of the fundamental chemistry of NO with metal centers under the conditions relevant to its biological formation and decay is essential. However, the Cu^{II}/NO chemistry has not been explored yet to that extent.[18]

In continuation, to study the effect of primary amine site on ligand framework, we have chosen the following two primary amine site containing ligands (Figure 3.1) to prepare their Cu^{II} complexes.

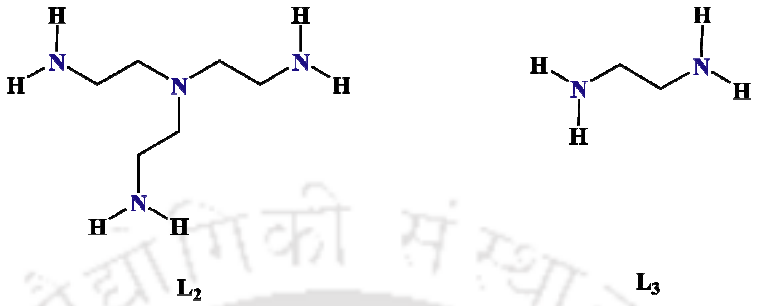

Figure 3.1: List of the ligands used for the present study.

3.2 Results and discussions

The complex **3.1** was prepared by the reaction of an acetonitrile solution of $[Cu(H_2O)_6](ClO_4)_2$ with one equivalent of the ligand, $\mathbf{L_2}$ at room temperature. [19] For complex **3.2**, two equivalents of ligand, $\mathbf{L_3}$ were used (Scheme 3.1) (Experimental section).

The complexes, **3.1** and **3.2** exibited satisfactory elemental analyses (Experiment section) and showed 1:2 conductivity [Λ_M ($\Omega^{-1}cm^2mol^{-1}$), 239 and 229, respectively] in acetonitrile solution. The formation of the complexes **3.1** and **3.2** was further supported by various spectroscopic analyses. The single crystal X-ray structures of both the complexes were determined. The ORTEP diagrams of the complexes are shown in figure 3.2. The crystal structures of complexes **3.1** and **3.2** reported earlier also.[19]

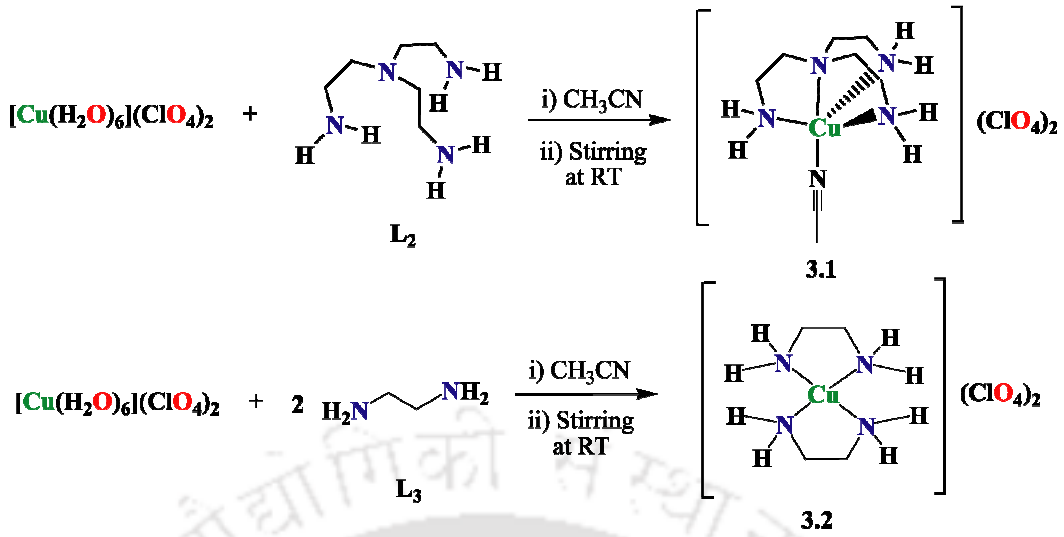

Scheme 3.1

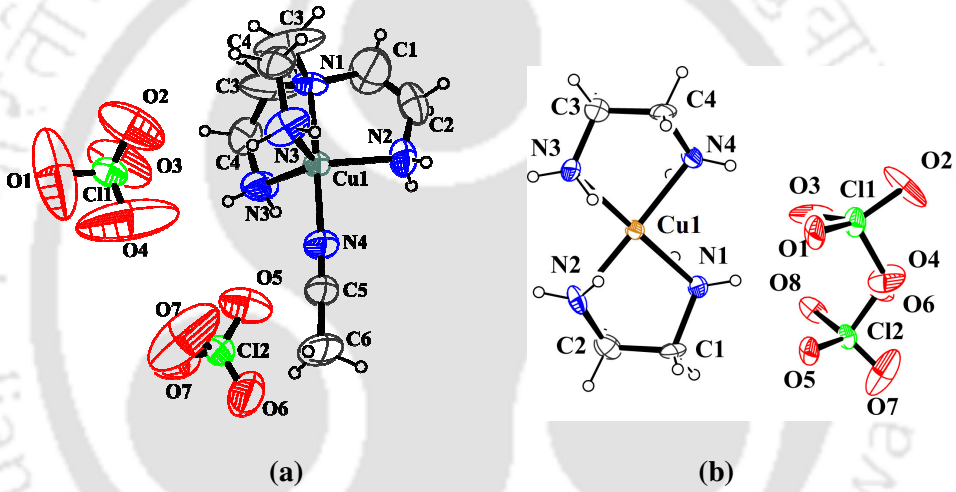

Fugure 3.2: ORTEP diagrams of complexes (a) **3.1** and (b) **3.2** (50% thermal ellipsoid plot).

The room temperature magnetic moment measurement showed one electron paramagnetism for complexes **3.1** and **3.2** (1.69 BM and 1.56 BM, respectively). The complex **3.1**, in acetonitrile solvent, exhibited broad *d-d* bands having λ_{max} at 812 nm (ε, 158 $M^{-1}cm^{-1}$), along with relatively strong intra-ligand absorptions in the UV-region at λ_{max}, 274 nm (ε, 3600 $M^{-1}cm^{-1}$) (Figure 3.3a). For complex **3.2** the *d-d* band appeared with λ_{max} at 550 nm (ε, 187$M^{-1}cm^{-1}$) (Figure 3.3b).

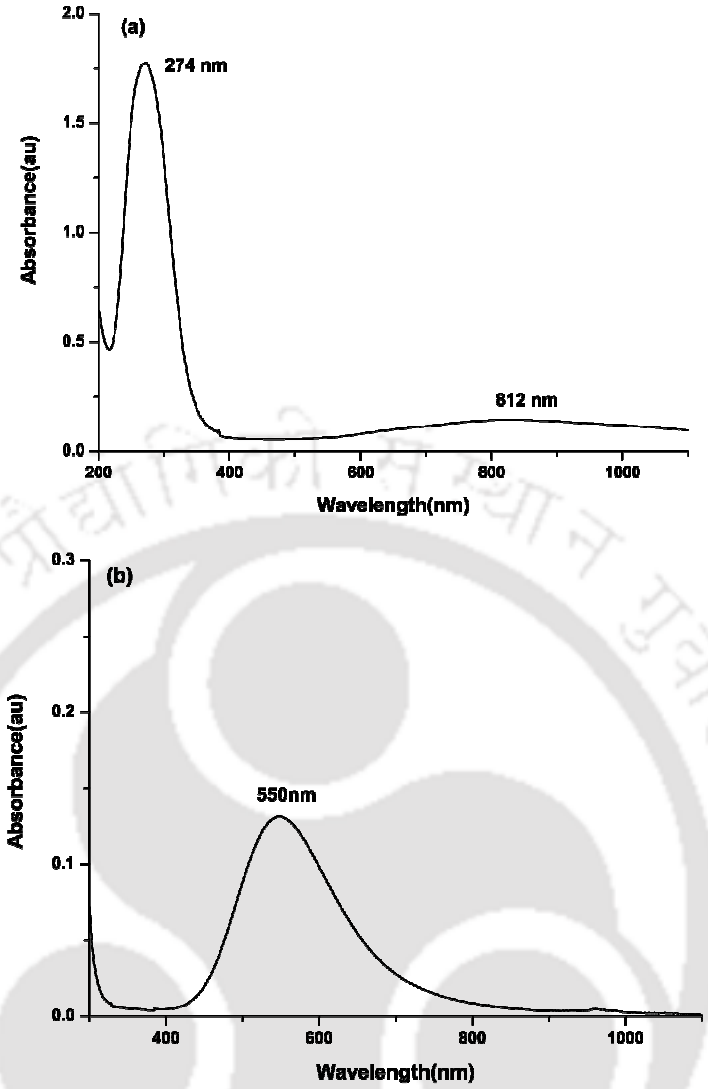

Figure 3.3: UV-visible spectra of complexes (a) **3.1** and (b) **3.2** in acetonitrile.

Both the complexes displayed four line X-band EPR spectra at room temperature in acetonitrile solvent having the g_{ave} values 2.105 and 2.05 (Figure 3.4).

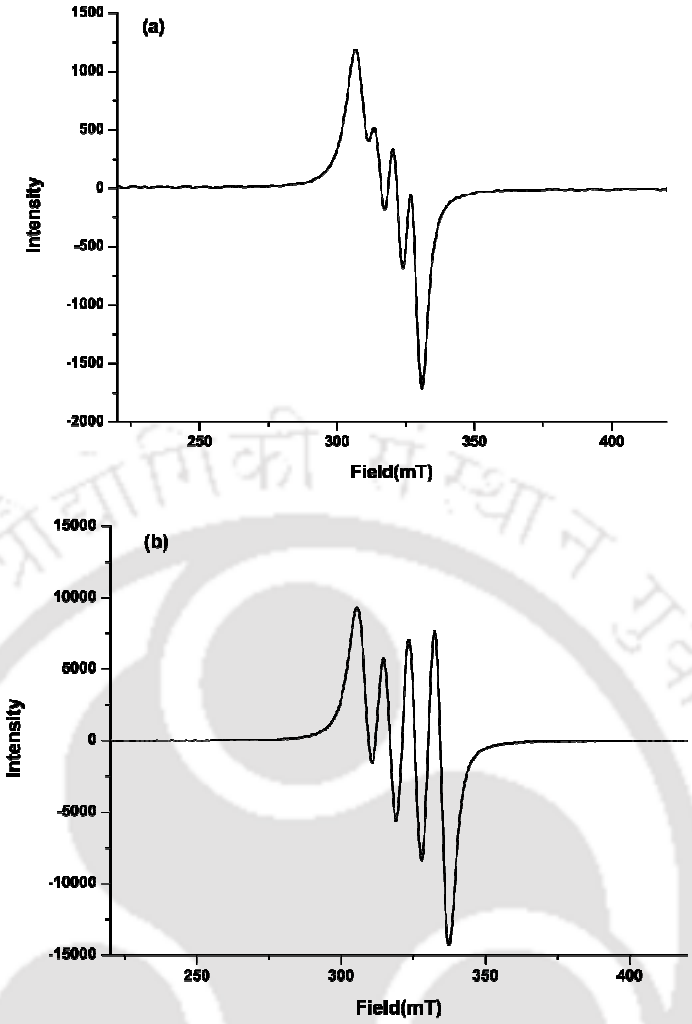

Figure 3.4: X-Band EPR spectra of complexes (a) **3.1** and (b) **3.2** in acetonitrile at room temperature.

3.2.1 Nitric oxide reactivity in acetonitrile

The NO reactivity of the complexes **3.1** and **3.2** were studied in acetonitrile. The spectral changes were monitored by UV-visible and X-Band EPR spectroscopy. In acetonitrile solution, the complexes, **3.1** and **3.2,** exhibited *d-d* transition at λ_{max}, 812 nm and 550 nm respectively. The deep blue solutions of the both the complexes, in dry and degassed acetonitrile, changed into transient green on exposure to NO gas and finally became colorless. The change was monitored by UV-visible spectroscopy (Figure 3.5). It was found that though there were no significant changes in the *d-d* transition band, the higher energy band was shifted from 274 nm to 291 nm

immediately after purging NO to the acetonitrilic solution of complex **3.1.** In case of complex **3.2**, also, there were no significant change in the *d-d* transition band, but change was observed in the UV region, only. The green intermediates were thermally unstable and we were unable to isolate or characterize it properly. This transient intermediate was found to be EPR silent in frozen state at 77 K. In FT-IR spectrum, the green intermediate, in case of **3.1**, exhibited a sharp and strong ν_{NO} frequency at 1650 cm^{-1}, in acetonitrile (Figure 3.6).[20] This frequency was found to diminish gradually and finally disappeared. Presumably, it was a [Cu^{II}-$NO^{\bullet}$] complex which was formed prior to the reduction of Cu^{II}.[12-15, 18]

The intensity of *d-d* band of the green intermediate was found to decrease with time and finally the disappearance of the *d-d* band indicated the complete reduction of Cu^{II} center of complex **3.1** to Cu^{I} by NO (Figure 3.7). The reduction process was monitored with stoichiometric amount of NO and it had been found that the reaction was 1:1 with respect to Cu^{II} and NO (Figure 3.7, inset). In case of complex **3.2**, also, the reduction was confirmed by the disappearance of the *d-d* transition band at 550 nm (Figure 3.8).

The complexes **3.1** and **3.2** showed four line EPR spectra in acetonitrile solution. After NO purging, the signals were found to be disappeared (Figures 3.9a and 3.9b for **3.1** and **3.2,** respectively). This is, again, consistent with the reduction of Cu^{II} to Cu^{I} by NO.[21, 22]

The reduction of Cu^{II} centre had been further authenticated in case of complexes **3.1** and **3.2** by the single crystal structure determination of the reduced complex, $[Cu(CH_3CN)_4]ClO_4$ (Figure 3.10).[§]

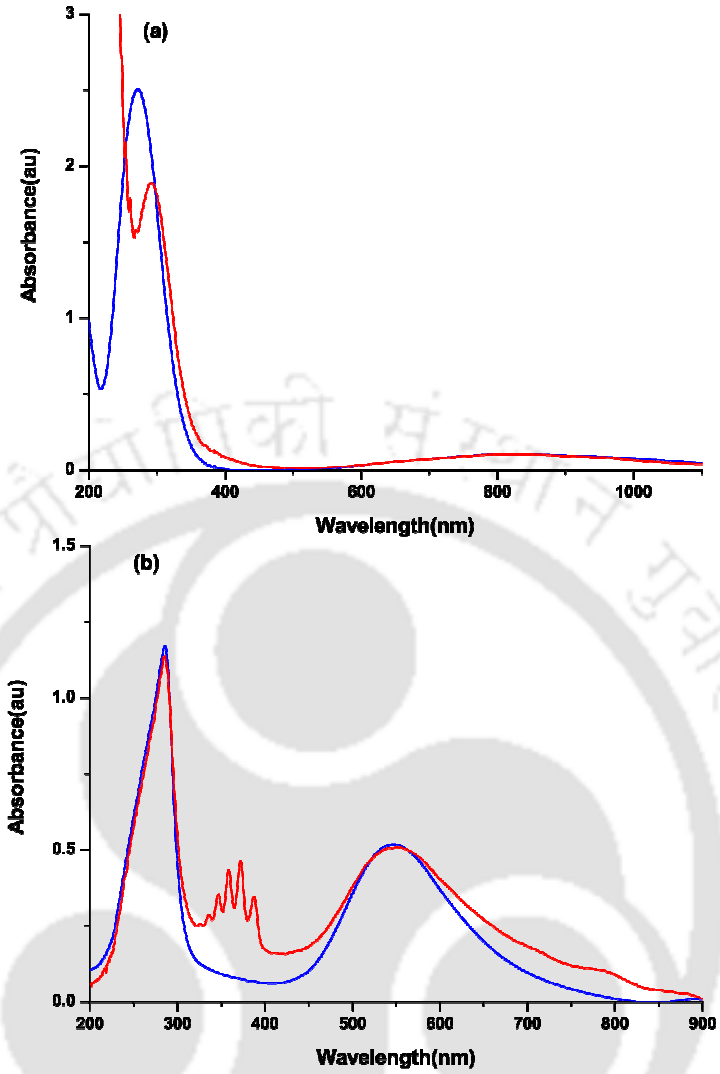

Figure 3.5: UV-visible spectra of complexes (a) **3.1** and (b) **3.2** in acetonitrile. (Blue trace represents the spectrum before purging NO and the red trace represents that immediately after purging NO).

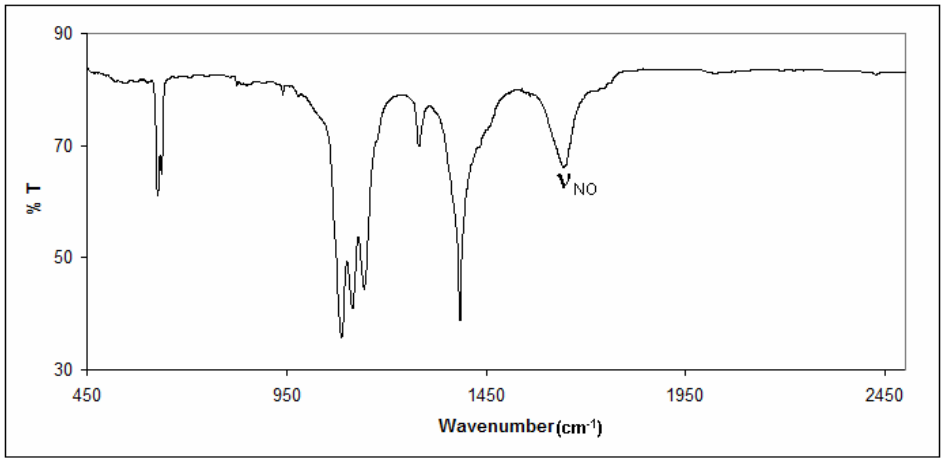

Figure 3.6: Solution FT-IR spectrum of the green intermediate formed in the case of **3.1** in acetonitrile solvent.

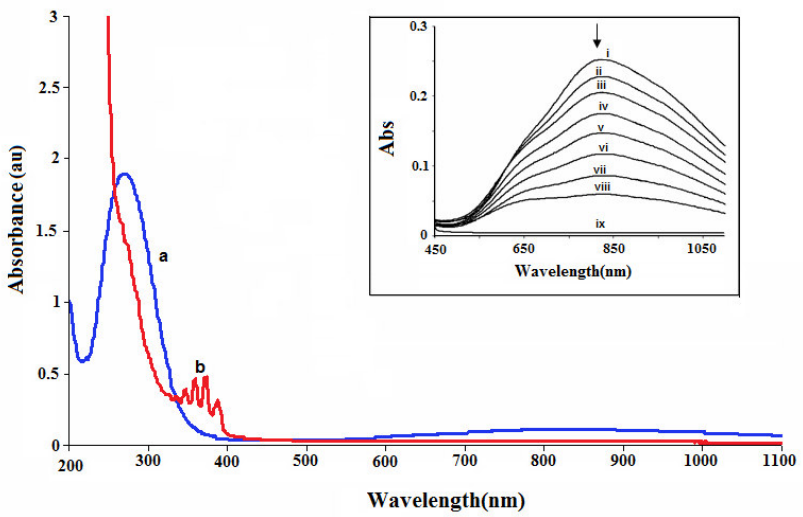

Figure 3.7: UV-visible spectra of (a) complex **3.1** and (b) after reaction with NO in acetonitrile solvent. *Inset*: The enlarged visible region showing the gradual decrease in intensity of the *d-d* band with increasing NO concentration: (i) complex **3.1**; (ii) with 0.1 equivalent; (iii) with 0.2 equivalent; (iv) with 0.3 equivalent; (v) with 0.4 equivalent ; (vi) with 0.5 equivalent; (vii) with 0.6 equivalent; (viii) with 0.7 equivalent and (ix) with 1.1 equivalent NO.

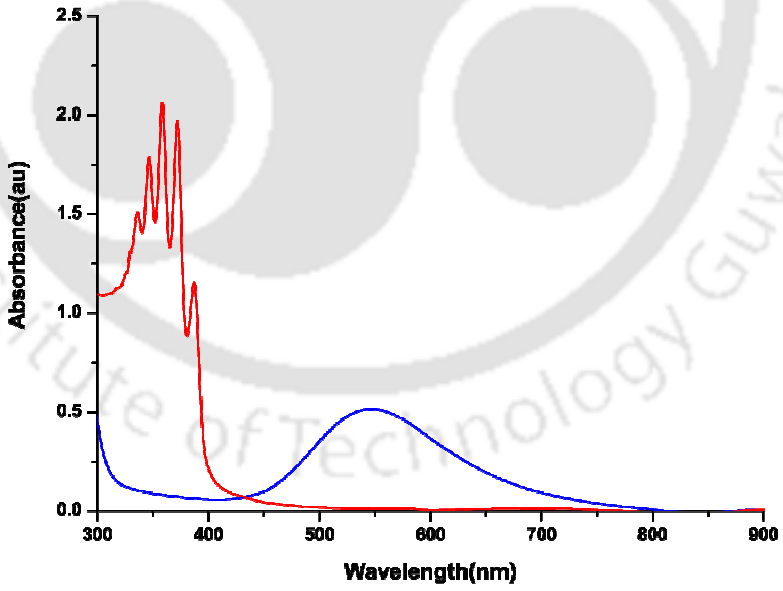

Figure 3.8: UV-visible spectra of complex **3.2** (blue trace) and after purging NO (red trace) showing the reduction of Cu^{II} to Cu^{I}.

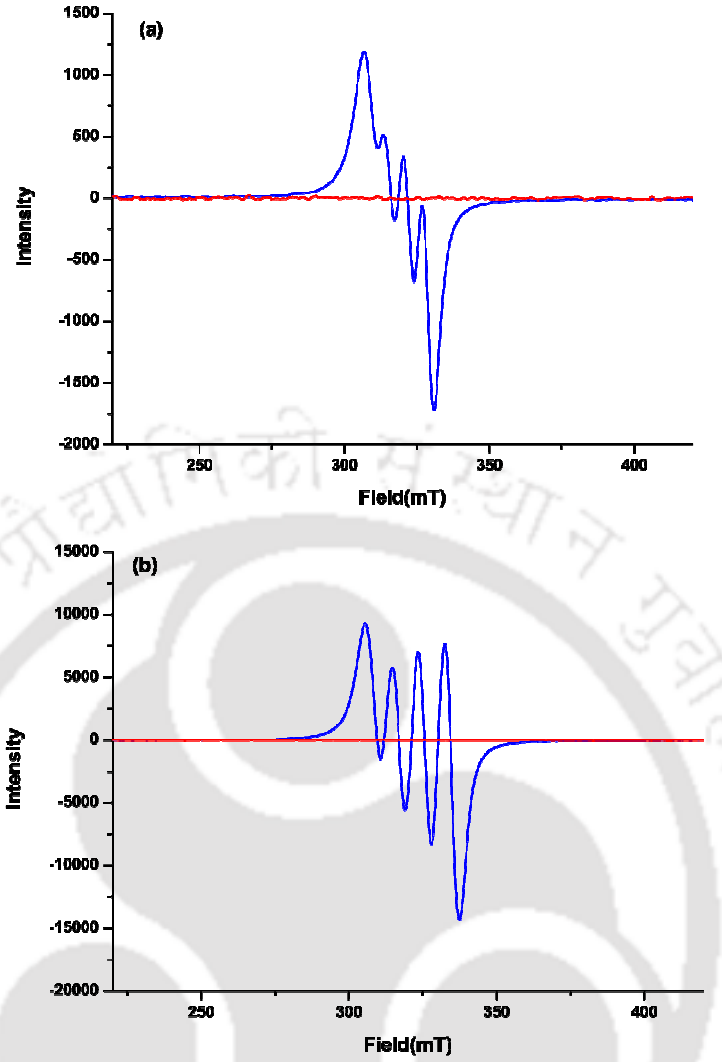

Figure 3.9: X-band EPR spectra of the complexes (a) **3.1** and (b) **3.2** (blue trace represents EPR spectrum of the complex and red trace represents that of the complex after it's reaction with NO).

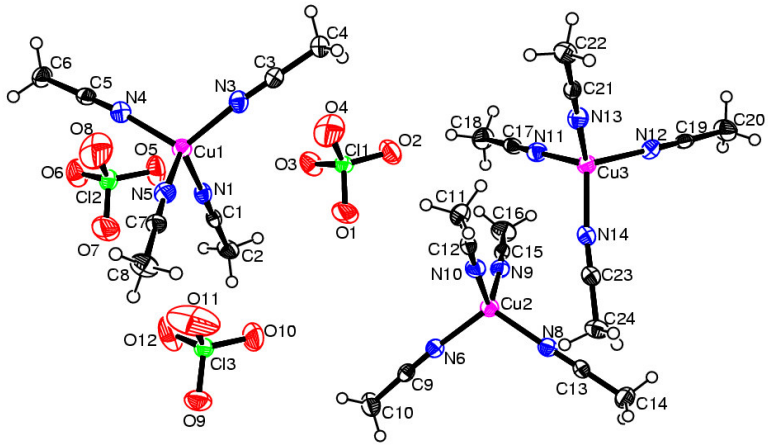

Figure 3.10: ORTEP diagram of $[Cu(CH_3CN)_4]ClO_4$ (50% thermal ellipsoid plot).

Cao et. al. reported the reduction of a series of copper(II) dithiocarbamates with NO in aqueous solution which resulted into the formation of air stable copper nitrosyl and dinitrosyl species.[20] Detailed kinetics studies of the Cu^{II}/NO reactions are not much. [12-15. 18, 23] In this regard, Tran et. al. studied the NO reduction of the Cu^{II} complex, $[Cu(dmp)_2(H_2O)]^{2+}$ (dmp, 2,9-dimethyl-1,10-phenanthroline), in aqueous solution and various mixed solvents.[12-15] In methanol, the product of the $[Cu(dmp)_2(H_2O)]^{2+}$ oxidation of NO was CH_3ONO; in water, it was NO_2^-. The reaction did not occur in CH_2Cl_2 unless methanol was added, and in such solutions the reaction rate was linearly dependent on the concentration of alcohol added.

It is interesting to note that the reduction of Cu^{II} ion in complex **3.1** by NO in dry and degassed acetonitrile was accompanied with a concomitant nitrosation followed by diazotization at the terminal primary amine group of the ligand, $\mathbf{L_2}$ which resulted into the cyclization product, $\mathbf{L_2}'$ along with tri-protonated ligand, $\mathbf{L_2}''$ as its perchlorate salt (Scheme 3.2). This can be attributed to the fact that the NO^+ formed in the reduction process, reacted with the primary amine center of the ligand which resulted into diazotization followed by ring formation.

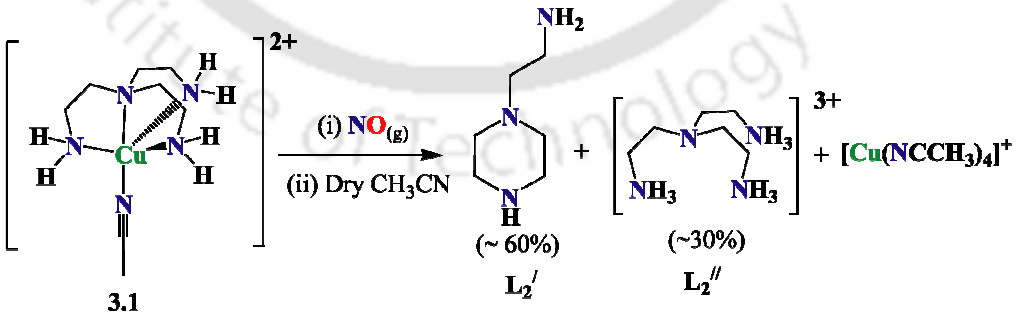

Scheme 3.2

The formation of $\mathbf{L_2}'$ was characterized by its microanalytical data, FT-IR, ^{1}H-NMR, ^{13}C-NMR and ESI-Mass spectroscopy. All the spectroscopic data were in well agreement with its structure (Appendix II, Figure A2.1- A2.4).

The formation of $\mathbf{L_2}''$-perchlorate was further been confirmed by the X-ray single crystal structure determination. The X-ray quality crystals were obtained from the reaction mixture itself on keeping it in freezer for two days. The ORTEP diagram of $\mathbf{L_2}''$-perchlorate is shown in figure 3.11. The crystallographic data is listed in appendix II, table A2.1. In the tri-protonated symmetrical $\mathbf{L_2}''$-perchlorate, central nitrogen is in tetrahedral geometry with a C-N-C bond angle of 109.2(3)° and N1-C1 bond length of 1.476(5) Å. The tables of selected bond angles and distances are given in appendix II (Table A2.2). The formation of $\mathbf{L_2}''$-perchlorate was confirmed by various spectroscopic studies, also (Appendix II, Figure A2.5- A2.7).

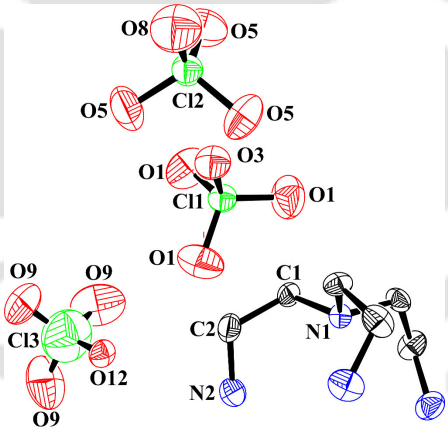

Figure 3.11: ORTEP diagram of $\mathbf{L_2}''$-perchlorate (50% thermal ellipsoid plot, hydrogen atoms are removed for clarity).

In case of complex **3.2**, the reaction of NO afforded similar diazotization at the amine site resulting into the formation of product, $\mathbf{L_3}'$ (Scheme 3.3).

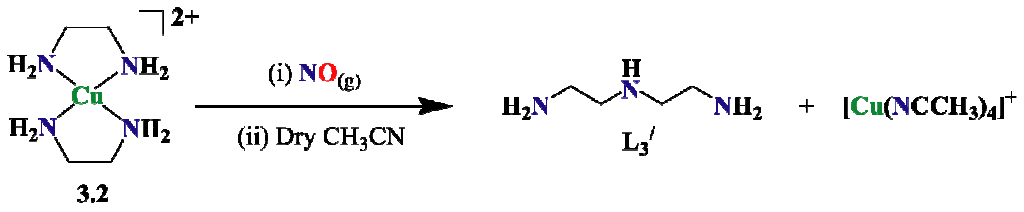

Scheme 3.3

The formation of $\mathbf{L_3}'$ was confirmed by the FT-IR, ^{1}H-NMR, ^{13}C-NMR, and ESI-Mass spectra (Appendix II, Figure A2.8- A2.11).

3.2.2 Nitric oxide reactivity in water

The reactivity study of complexes **3.1** and **3.2** with NO was also studied in water. The reduction process was studied by UV-visible and ^{1}H-NMR spectroscopy. In water, *d-d* transition band of **3.1** appeared with λ_{max} at 860 nm. In presence of NO, this *d-d* transition was found to decrease with time owing to reduction of Cu^{II} to Cu^{I} (Figure 3.12).

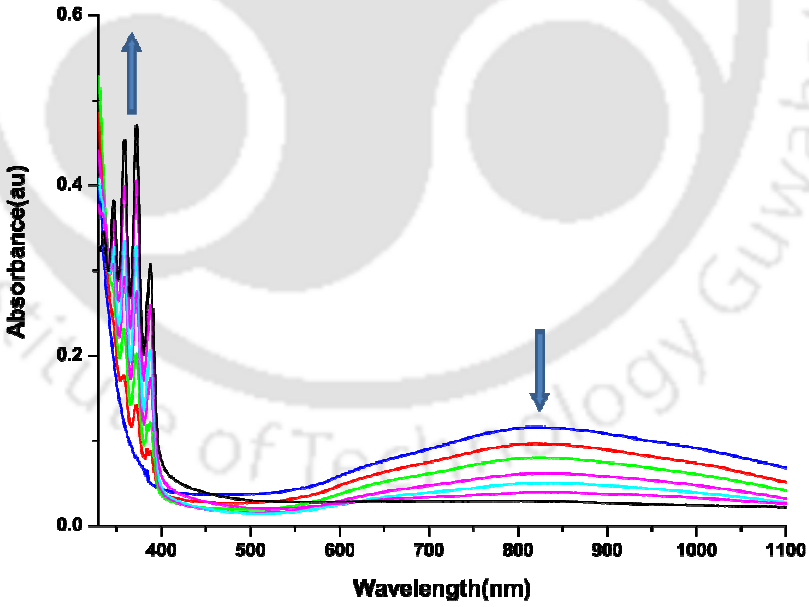

Figure 3.12: UV-visible spectra of the reaction of complex **3.1** with NO in water at room temperature. (Blue trace represents the Cu^{II}-complex which gradually reduced to Cu^{I} represented by down headed arrow).

The reduction process was also characterized by ^{1}H-NMR study. The complex **3.1** did not show well resolved ^{1}H-NMR spectrum as expected due to its paramagnetic nature (Figure 3.13a); but after reaction with NO, it showed well resolved ^{1}H-NMR spectrum (Figure 3.13b)

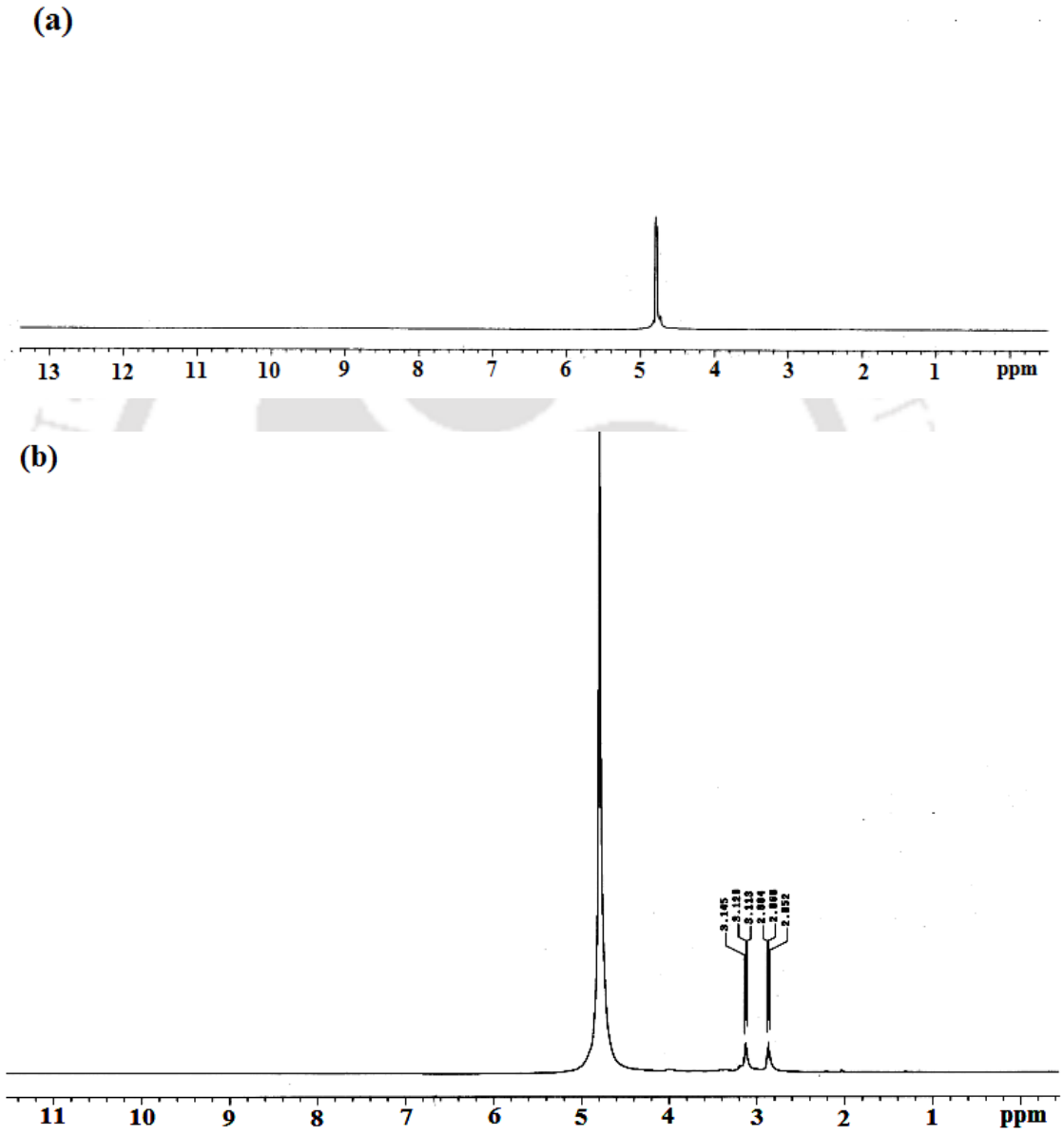

Figure 3.13: ^{1}H-NMR spectra of complex **3.1** (a) before and (b) after reaction with NO in D_2O.

Along with the reduction of the Cu^{II} center in complex **3.1**, the formation of $\mathbf{L_2}^{//}$-perchlorate was obseved. This was attributed to the higher reactivity of NO^{+} with

water to result into NO_2^- and H^+ (Scheme 3.4). The formation of NO_2^- was confirmed by the Greiss's test.

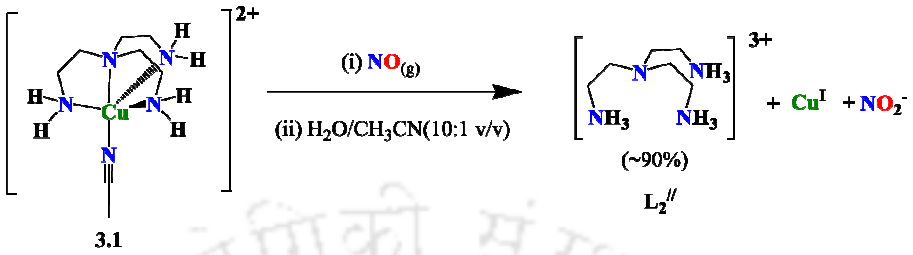

Scheme 3.4

In case of complex **3.2**, also, the reduction process was confirmed by UV-visible and ^{1}H-NMR studies. The intensity of the *d-d* transition band with λ_{max} at 555 nm in water was found to diminish immediately after purging NO gas to result into colorless solution suggesting the formation of Cu^I (Figure 3.14).

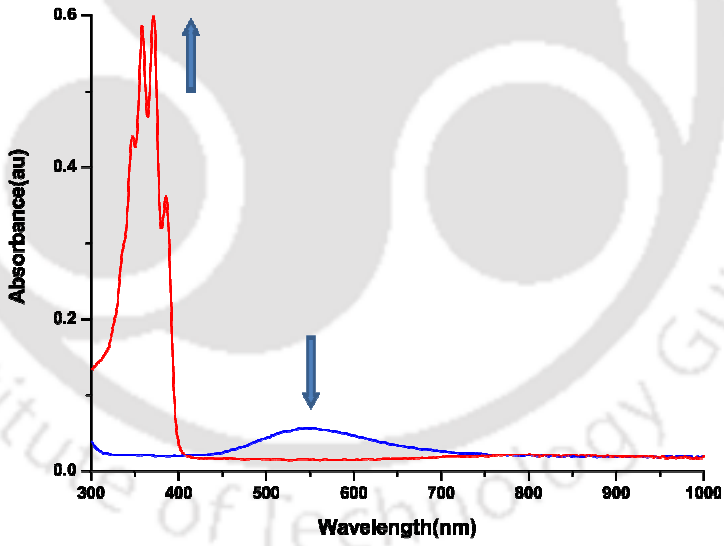

Figure 3.14: UV-visible spectra of the reaction of complex **3.2** with NO in water at room temperature. (Blue trace represents the Cu^{II} complex which gradually reduced to Cu^I, represented by the red trace).

The complex **3.2** displayed broad signals in ^{1}H-NMR spectrum as expected due to the presence of paramagnetic center (Figure 3.15a); however, after the reaction with NO, it exhibited well resolved ^{1}H-NMR spectrum (Figure 3.15b).

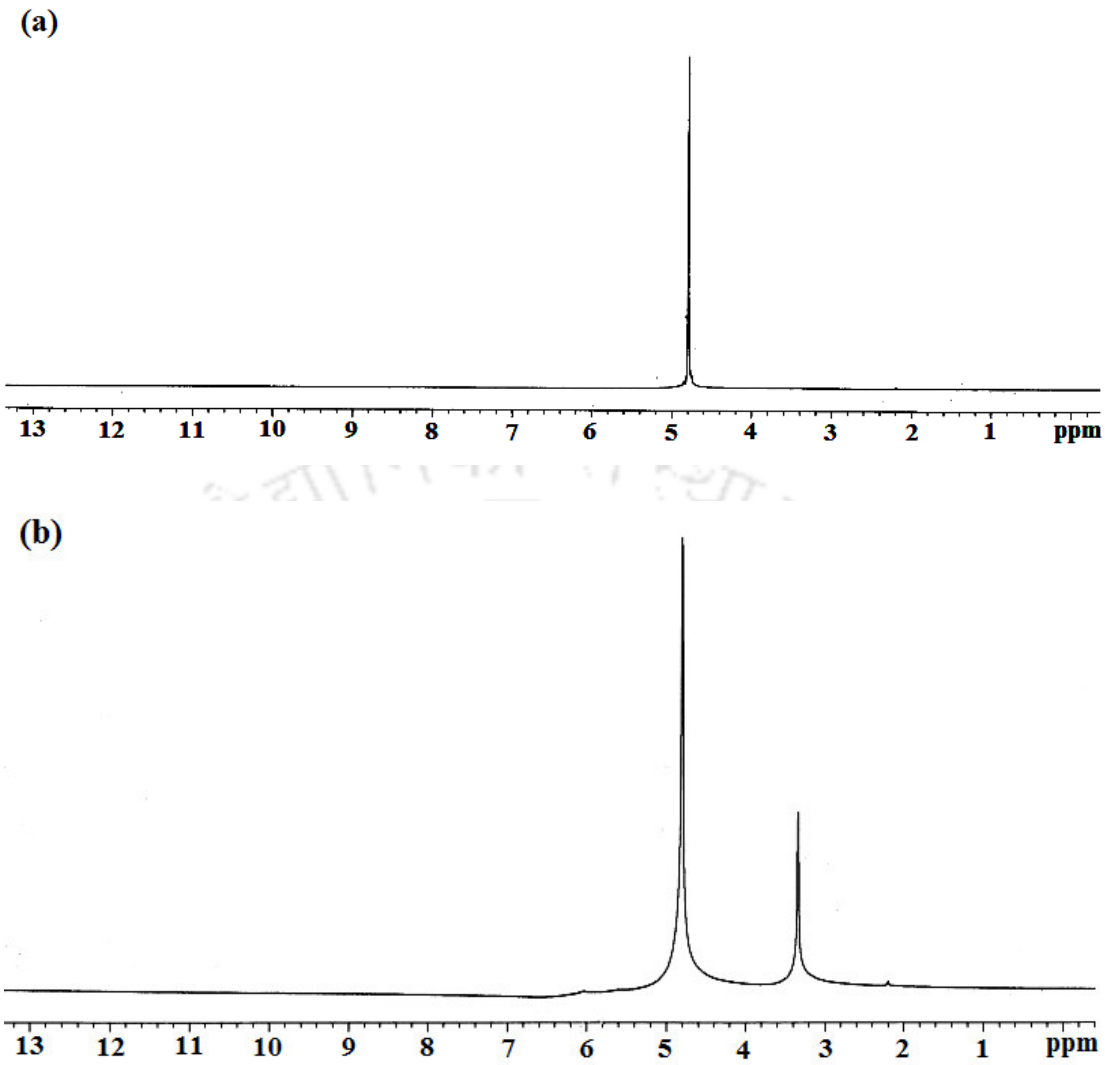

Figure 3.15: ^{1}H-NMR spectra of complex **3.2** (a) before and (b) after reaction of NO in D_2O.

In water, complex **3.2** undergo reduction with simultaneous formation of $\mathbf{L_3}''$ (Scheme 3.5)

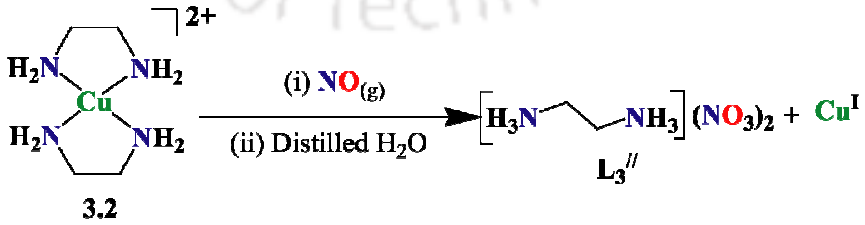

Scheme 3.5

The formation of the ligand $\mathbf{L_3}''$ was confirmed by various spectroscopic studies e.g. FT-IR, ^{1}H-NMR and ^{13}C-NMR (Appendix II, Figure A2.12- A2.14). $\mathbf{L_3}''$ was also

characterized by its X-ray single crystal structure (Figure 3.16). The crystallographic data and tables for selected bond angles and distances are listed in appendix II (Tables A2.3 and A2.4).

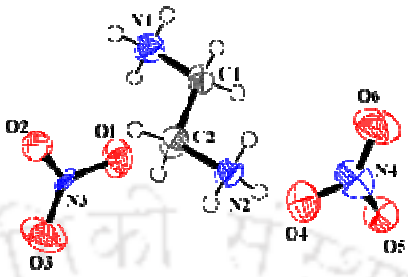

Figure 3.16: ORTEP diagram of $\mathbf{L_3''}$ (50% thermal ellipsoid plot).

3.3 Conclusion

In conclusion, the present work demonstrated the examples of the reactivity of NO with Cu^{II} centers in organic solvent as well as in water. In this regard, Cu^{II} complexes, **3.1** and **3.2** with well-known tripodal ligand, $\mathbf{L_2}$ and bidentate ligand $\mathbf{L_3}$ have been prepared. The Cu^{II} centers in **3.1** and **3.2**, in acetonitrile solution, have been found to undergo reduction to Cu^{I} in presence of NO. This reduction has been supported by UV-visible, ^{1}H-NMR and X-band EPR techniques. The formation of unstable [Cu^{II}-$NO^{\bullet}$] intermediate was observed prior to the reduction of Cu^{II} to Cu^{I} in acetonitrile solution, in both cases. The reduction has been found to be accompanied with a concomitant diazotization of the terminal amine group of ligand which results into the modified ligands $\mathbf{L_2'}$ and $\mathbf{L_2''}$-perchlorate in case of **3.1** and $\mathbf{L_3'}$ and $\mathbf{L_3''}$ in case of **3.2**, respectively.

3.4 Experimental Section

3.4.1 Materials and methods

All reagents and solvents were purchased from commercial sources and were of reagent grade. Acetonitrile was distilled from calcium hydride. Deoxygenation of the

solvent and solutions were effected by repeated vacuum/purge cycles or bubbling with nitrogen for 30 minutes. NO gas was purified by passing through KOH and P_2O_5 column. UV-visible spectra were recorded on a Perkin Elmer Lambda-25 spectrophotometer. FT-IR spectra of the solid samples were taken on a Perkin Elmer spectrophotometer with samples prepared as KBr pellets and for solutions, Varian 660-IR FT-IR spectrometer and NaCl cell of 2 mm path length were used and the spectra shown are the solvent subtracted ones. Solution electrical conductivity was checked using a Systronic 305 conductivity bridge. ^{1}H- NMR spectra were obtained with a 400 MHz Varian FT spectrometer. Chemical shifts (ppm) were referenced with residual solvent peaks. The X-Band Electron Paramagnetic Resonance (EPR) spectra of complexes and of the reaction mixture were recorded on a JES-FA 200 ESR spectrometer, at room temperature. Elemental analyses were obtained from a Perkin Elmer Series II Analyzer. The magnetic moment of complexes is measured on a Cambridge Magnetic Balance.

Single crystals were grown by slow diffusion followed by slow evaporation technique. The intensity data were collected using a Bruker SMART APEX-II CCD diffractometer, equipped with a fine focus 1.75 kW sealed tube MoK_α radiation (λ = 0.71073 Å) at 273K, with increasing ω (width of 0.3° per frame) at a scan speed of 3 s/frame. The SMART software was used for data acquisition. Data integration and reduction were undertaken with SAINT and XPREP software.[24] Structures were solved by direct methods using SHELXS-97 and refined with full-matrix least squares on F^2 using SHELXL-97.[25, 26] All non-hydrogen atoms were refined anisotropically. Structural illustrations have been drawn with ORTEP-3 for Windows.[27]

3.4.2 Synthesis of complex 3.1, $[Cu(L_2)(NCCH_3)](ClO_4)_2$

$[Cu(H_2O)_6](ClO_4)_2$, 0.740 g (2.0 mmol) was dissolved in 10 ml distilled acetonitrile. To this solution, 0.292 g (2.0 mmol) of **L_2** was added slowly with constant stirring. The color of the solution turned into deep blue from light blue. The stirring was continued for 1h at room temperature. The volume of the solution then reduced to ~2 ml. To this, 10 ml of benzene was added to make a layer on it and kept it overnight on freezer. This resulted into blue color crystals of complex **3.1**. Yield: 0.765 g (83%). Elemental Analyses: Calcd. for $C_8H_{21}N_5O_8Cl_2Cu$: C, 21.37; H, 4.71; N, 15.57. Found (%): C, 21.26; H, 4.64; N, 15.25. Molar conductivity: [$\Lambda_M(\Omega^{-1}cm^2mol^{-1})$, 239]. FT-IR: 3253, 1081, 625cm^{-1}; magnetic moment, 1.69 BM.

3.4.3 Synthesis of complex 3.2, $[Cu(L_3)_2](ClO_4)_2$

$[Cu(H_2O)_6](ClO_4)_2$, 0.740 g (2.0 mmol) was dissolved in 10 ml distilled acetonitrile. To this solution, 0.240 g (4.0 mmol) of **L_3** was added slowly with constant stirring. The color of the solution turned into violet from light blue. The stirring was continued for 1h at room temperature. The volume of the solution then reduced to ~2 ml. To this, 10 ml of benzene was added to make a layer on it and kept it overnight on freezer. This resulted into violet color crystals of complex **3.2**. Yield: 0.645 g (84%). Elemental Analyses: Calcd. for $C_4H_{16}N_4O_8Cl_2Cu$: C, 12.56; H, 4.21; N, 14.64. Found (%): C, 12.46; H, 4.29; N, 14.55. Molar conductivity: [$\Lambda_M(\Omega^{-1}cm^2mol^{-1})$, 229]. FT-IR: 2964, 1583, 1089, 1041, 625 cm^{-1}; magnetic moment, 1.56 BM.

3.4.4 Isolation of $[Cu^I(CH_3CN)_4]ClO_4$

The isolation of $[Cu(CH_3CN)_4]ClO_4$ from the reaction of the respective complexes with NO has been done using the same general procedure. The detail is given for complex **3.1**.

In a 50 ml Schlenk flask, complex **3.1** (224 mg, 0.5 mmol) was dissolved in 10 ml degassed acetonitrile. To this deep blue solution, NO gas was purged through a needle for one minute and allowed to stand for 10 minutes. To the resulting colorless solution, 15 ml of degassed benzene was added through a syringe to make a layer. The layered solution was then kept overnight in freezer. The white crystals of $[Cu(CH_3CN)_4]ClO_4$ were filtered out from the colorless solution under nitrogen atmosphere using a Schlenk frit. Yield, 105 mg, ~55%.

Same procedure was followed to isolate the $[Cu(CH_3CN)_4]ClO_4$ from the reaction of complex **3.2** (190 mg, 0.5 mmol) with NO in acetonitrile solution. Yield: 118 mg, ~62%.

3.4.5 Isolation of L_2'

In a 50 ml Schlenk flask, complex **3.1** (449 mg, 1.0 mmol) was dissolved in 30 ml degassed acetonitrile. To this, NO gas was purged through a needle for one minute and the mixture was then allowed to stand for 10 minutes. To the colorless solution, thus obtained, 20 ml of degassed benzene was added through a syringe to make a layer. The layered solution was then kept overnight in freezer. The white crystals of $[Cu(CH_3CN)_4]ClO_4$ were filtered out from the colorless solution under nitrogen atmosphere using a Schlenk frit. The volume of the filtrate was then reduced to 5 ml and stirred for 1h in open air in order to allow the residual Cu^{I} center to oxidise to Cu^{II}. To this, 5 ml saturated aqueous solution of Na_2S was added and stirred for ½ h. The black precipitate of Na_2S, thus obtained was filtered off and the filtrate was diluted with 50 ml of distilled water. The organic part was then extracted from the mixture using $CHCl_3$ (3 portions × 25 ml). The collected organic layer was then dried under reduced pressure and the residual oil was subjected to column chromatography

using silica gel to yield $\mathbf{L_2}'$. Yield, 78 mg (~ 60%). Elemental Analyses: Calcd.(%) for $C_6H_{15}N_3$: C, 55.78; H, 11.70; N, 32.52. Found (%) C, 55.67; H, 11.47; N, 32.82. ^{1}H-NMR(400 MHz, $CDCl_3$), δ_{ppm}, 2.80(t, 4H), 2.70 (t, 2H), 2.31(m, 6H), 1.41(NH). ^{13}C-NMR(100 MHz, $CDCl_3$), δ_{ppm}, 61.93, 54.80, 46.25, 38.75. FT-IR in KBr pellet: 2938(m), 1384 (s), 1369(s). ESI-Mass: (m+1)/z, 130.14.

3.4.6 Isolation of $\mathbf{L_2}''$-perchlorate

To 10 ml of degassed acetonitrile solution of complex **3.1** (449 mg, 1.0 mmol), freshly prepared NO was bubbled for 1 minute. The deep blue color of the solution turned colorless. This solution was allowed to stir for 10 minutes at room temperature. Then the excess of NO was removed and 10 ml of degassed benzene was added to this under dinitrogen atmosphere. The reaction mixture was kept in freezer for two days. The $\mathbf{L_2}'$-perchlorate was found to be crystallized out. Yield: 134 mg (30%). Elemental Analyses: Calcd. for $C_6H_{21}N_4O_{12}Cl_3$: C, 16.10; H, 4.73; N, 12.52. Found (%): C, 16.17; H, 4.70; N, 12.52. FT-IR: 2949, 1590, 1508, 1079, 625 cm^{-1}; ^{1}H-NMR (400 MHz, $CDCl_3$): δ_{ppm}, 3.12(t, 6H) 2.86(t, 6H). ^{13}C-NMR (100 MHz, $CDCl_3$): δ_{ppm}, 49.23, 35.82.

3.4.7 Isolation of $\mathbf{L_3}'$

Same procedure (as in case of $\mathbf{L_2}'$ of complex **3.1**) was adopted for the isolation of $\mathbf{L_3}'$. Yield, 72 mg (~ 70%). Elemental Analyses: Calcd.(%) for $C_4H_{13}N_3$: C, 46.57; H, 12.70; N, 40.73. Found (%) C, 46.60; H, 12.67; N, 40.89. ^{1}H-NMR(400 MHz, $CDCl_3$), δ_{ppm}, 2.01(t, 4H), 1.89 (t, 4H). ^{13}C-NMR(100 MHz, $CDCl_3$), δ_{ppm}, 51.85, 44.09. FT-IR in KBr pellet: 1556(s), 1472 (m), 1310(m) cm^{-1}. ESI-Mass: (m+1)/z, 104.17.

3.4.8 Isolation of $L_3^{//}$

Same procedure (as in case of $L_2^{//}$-perchlorate of complex **3.1**) was adopted for the isolation of $L_3^{//}$. Yield, 61 mg (~32%). Elemental Analyses: Calcd.(%) for $C_2H_{13}N_4O_6$: C, 12.91; H, 5.42; N, 51.58. Found (%) C, 12.90; H, 5.41; N, 50.89. ^{1}H-NMR(400 MHz, $CDCl_3$), δ_{ppm}, 3.36 (t, 4H). ^{13}C-NMR(100 MHz, $CDCl_3$), δ_{ppm}, 55.98. FT-IR in KBr pellet: 3193(m), 2928(m), 1509(m), 1384 (s), 1033(m) cm^{-1}.

3.5 References

1. Moncada, S.; Palmer, R. M. J.; Higgs, E. A. *Pharmacol. Rev.* **1991**, *43*, 109.
2. Feldman, P. L.; Griffith, O. W.; Stuehr, D. J. *Chem. Eng. News*, **1993**, *71*, 26.
3. Butler, A. R.; Williams, D. L. *Chem. Soc. Rev.* **1993**, *233*.
4. Feelisch, M.; Stamler, J. S.; *Methods in Nitric Oxide Research.* Eds.; John Wiley and Sons: Chichester, England, **1996** and references therein.
5. Wink, D. A.; Hanbauer, I.; Grisham, M. B.; Laval, F.; Nims, J. R.W.; Laval, J. Cook, Pacelli, R.; Liebmann, J.; Krishna, M.; Ford, P. C.; Mitchell, J. B. *Curr. Top. Cell. Regul.* **1996**, *34*, 159.
6. Ignarro, L. J.; *Nitric Oxide: Biology and Pathobiology*; Ed.; Academic Press: San Diego **2000**.
7. Schwartz, S. E.; White, W. H. *Trace Atmospheric Constitutents. Properties, Transformation and Fates*, J. Wiley & Sons: New York **1983**.
8. Traylor, T. G.; Sharma, V. S. *Biochemistry*, **1992**, *31*, 2847.
9. Radi, R. *Chem. Res. Toxicol.* **1996**, *9*, 828.
10. Kim, S.; Deinum, G.; Gardner, M. T.; Marletta, M. A.; Babcock, G. T. *J. Am. Chem. Soc.* **1996**, *118*, 8769.

11. Burstyn, J. N.; Yu, A. E.; Dierks, E. A.; Hawkins, B. K.; Dawson, B. K. *Biochemistry.* **1995**, *34*, 5896.

12. Torres, J.; Svistunenko, D.; Karlsson, B.; Cooper, C. E.; Wilson, M. T. *J. Am. Chem. Soc.* **2002**, *124*, 963

13. Torres, J.; Cooper, C. E.; Wilson, M. T.; *J. Biol. Chem.* **1998**, *273,* 8756.

14. Tran, D.; Skelton, B. W.; White, A. H.; Laverman, L. E.; Ford, P. C. *Inorg. Chem.* **1998**, *37*, 2505.

15. Martin, C. T.; Morse, R. H.; Kanne R. M.; Gray, H. B.; Malmstrom, B. G.; Chan, S. I. *Biochemistry*, **1981**, *20*, 5147.

16. Cooper, C. E.; Torres, J.; Sharpe, M. A.; Wilson, M. T. *FEBS Lett*. **1997**, *414*, 281.

17. Studbauer, G.; Giuffre, P.; Sarti, P. *J. Biol. Chem.* **1999**, *274*, 28128.

18. Ford, P. C.; Fernandez, B. O.; Lim, M. D. *Chem. Rev*. **2005**, *105*, 2439.

19. (a) Scott, M. J.; Lee, S. C.; Holm, R. H. *Inorg. Chem.* **1994**, *33*, 4561. (b) Pasquali, M.; Floriani, C.; Gaetani-Manfredotti, A. *Inorg. Chem.* **1980**, *19*, 1191.

20. Diaz, A.; Ortiz, M.; Sanchez, I.; Cao, R.; Mederos, A.; Sanchiz, J.; Brito, F. *J. Inorg. Biochem.* **2003**, *95*, 283.

21. Addison, A. W.; Hendriks, H. M. J.; Reedijk, J.; Thompson, L. K., *Inorg. Chem.* **1981**, *20*, 103.

22. Sorrell, T. N.; Jameson, D. L. *Inorg. Chem.* **1982**, *21*, 1014.

23. Tsuge, K.; DeRosa, F.; Lim, M. D.; Ford, P. C. *J. Am. Chem. Soc.* **2004**, *126*, 6564.

24. SMART, SAINT and XPREP, Siemens Analytical X-ray Instruments Inc., Madison, Wisconsin, USA, **1995**.

25. Sheldrick, G. M. SADABS: software for Empirical Absorption Correction, University of Gottingen, Institut fur Anorganische Chemieder Universitat, Tammanstrasse 4, D-3400 Gottingen, Germany, **1999–2003**.
26. Sheldrick, G. M. SHELXS-97, University of Gottingen, Germany, **1997**.
27. Farrugia, L. J. *J. Appl. Crystallogr*. **1997**, *30*, 565.

[§]The crystal structure of $[Cu(CH_3CN)_4]ClO_4$ is already known. We were sucessful to grow the crystals for this compound which supports the reduction of complex **3.1** by nitric oxide unambiguishly. However, the crystal quality is not very good. Since this was already reported, we have not tried again to grow good quality crystals.

Chapter 4

Nitric oxide reactivity of copper(II) complexes of bidentate amine ligands

Abstract

Three copper(II) complexes, **4.1**, **4.2** and **4.3** with bidentate ligands, $\mathbf{L_4}$, $\mathbf{L_5}$ and $\mathbf{L_6}$ [$\mathbf{L_4}$, N,N$^{/}$-dimethyl ethylenediamine; $\mathbf{L_5}$, N,N$^{/}$-diethylethylenediamine and $\mathbf{L_6}$, N,N$^{/}$-diisobutylethylenediamine], respectively, were synthesized as their perchlorate salts. The single crystal structures for all the complexes were determined. The nitric oxide reactivity of the complexes was studied in acetonitrile solvent. The formation of thermally unstable [Cu^{II}-$NO^{\bullet}$] intermediate on reaction of the complexes with nitric oxide in acetonitrile solution was observed prior to the reduction of Cu^{II} centre to Cu^{I}. The reduction was found to result with a simultaneous mono- and di-nitrosation at the secondary amine sites of the ligands. All the nitrosation products were isolated and characterized. The ratio of the yield of mono- and di-nitrosation products was found to be dependent on the N-substitution present in the ligand framework.

4.1 Introduction

The interaction of nitric oxide (NO) with metallo-proteins leading to the formation of their nitrosyls are believed to be the key step for most of the biochemical activities of nitric oxide in mammalian biology.[1-6] Thus, the NO reactivity of the metal ions, specially iron and copper, are of immense interest for the chemists and biochemists. NO induced reduction Cu^{II} centers to Cu^{I} in some metallo-proteins has been reported long back.[7] This reduction is known to facilitate the nitrosation of various thiolates to form S-nitrosothiols, e.g. S-nitroso bovine serum albumin and S-nitroso glutathione.[8-10] Hence, in small molecules, the interaction of Cu^{II} center with NO is also an emerging field of research.[11-14] In this direction, Ford's group have reported the detail studies of N-nitrosation during the reduction of Cu^{II} by NO.[15] Recently, in our laboratory, we have observed tri-nitrosation of the ligand during the reduction of Cu^{II} to Cu^{I} by NO in the cases of $[Cu(tiaea)(CH_3CN)]^{2+}$ and $[Cu(teaea)(CH_3CN)]^{2+}$ [tiaea, *tris*-(2-isopropylaminoethyl)amine and teaea, *tris*-(2-ethylaminoethyl)amine].[16] In continuation, to study the role of the ligand framework and denticity to control the degree of N-nitrosation of the ligand, we have chosen the following three bidentate secondary amine ligands (Figure 4.1) to prepare their Cu^{II} complexes and studied their reactivity with NO.

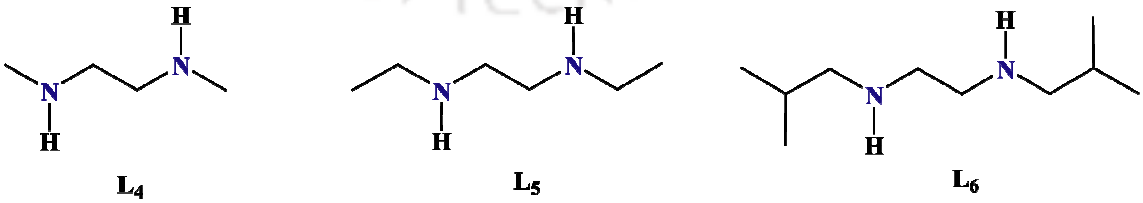

Figure 4.1: List of the ligands used for the present study.

4.2 Results and discussions

Ligands $\mathbf{L_5}$ and $\mathbf{L_6}$ were synthesized following the general procedure for mono-alkylation of primary amines (Apendix III).[17] The elemental analyses of the synthesized ligands were found to be in good agreement with the expected values (Apendix III). They were characterized by FT-IR, ^{1}H-NMR, ^{13}C-NMR, Mass spectroscopy (Apendix III). All the complexes were synthesized by the reaction of hexaaquacopper(II) perchlorate with the respective ligands (Scheme 4.1) and isolated

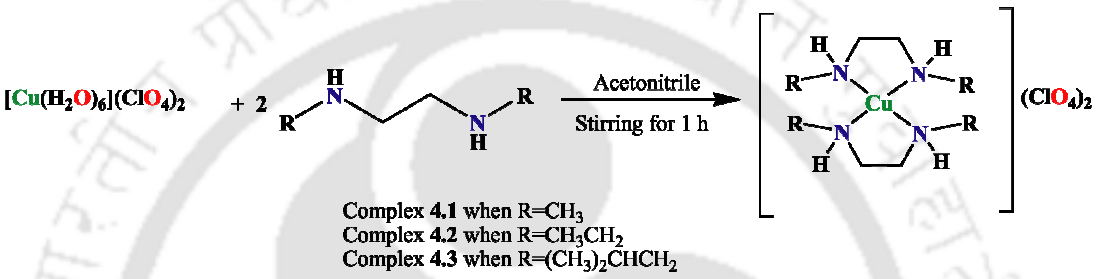

Scheme 4.1

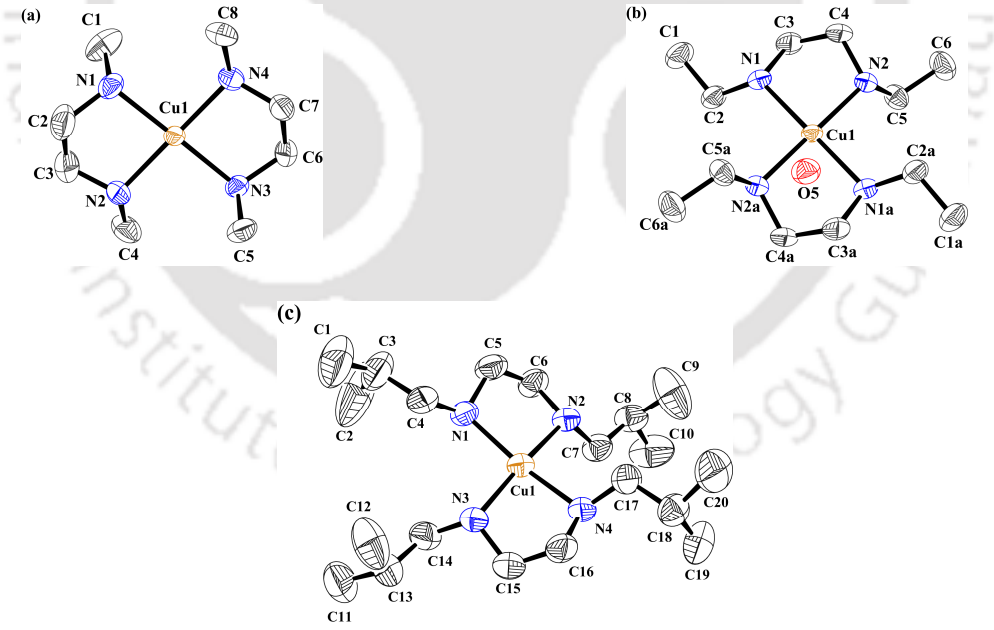

Figure 4.2: ORTEP diagram of complexes (a) **4.1**, (b) **4.2** [a (2-x, 2-y, 2-z) symmetry transformation is implied by each additional atom level] and (c) **4.3**. (50% Thermal ellipsoid plot; Hydrogen and perchlorate are removed for clarity).

as solid. All the complexes displayed satisfactory elemental analyses (experimental section). They were characterized by various spectroscopic methods (experimental

section) as well as by single crystal X-ray structure determination. It should be noted that the crystal structure of complex **4.1** was reported earlier with slightly different parameters.[18] The perspective ORTEP view of complexes **4.1**, **4.2** and **4.3** are shown in figure 4.2. It should be noted that complex **4.2** had crystallographically imposed inversion symmetry with Cu1 on an inversion centre. The crystallographic data and important bond angles and distances are listed in tables A3.2, A3.3 and A3.4 respectively in appendix III. The central metal ions Cu^{II}, in all the complexes were coordinated with four N-donor atoms in a distorted square planar geometry. The average Cu-N distances were within the range observed in other reported analogous complexes.[19]

The *d-d* transition for complexes **4.1**, **4.2** and **4.3** appeared at 563, 575 and 582 nm, respectively, in acetonitrile solvent (Figure 4.3). This shift in λ_{max} attributed to the increasing order of covalent character of the σ-bond on moving from methyl to ethyl to isobutyl group at the N-substitution.[20] All the complexes displayed axial EPR spectra at 77 K characteristic for the square planar Cu^{II} complexes having d_x^2-y^2

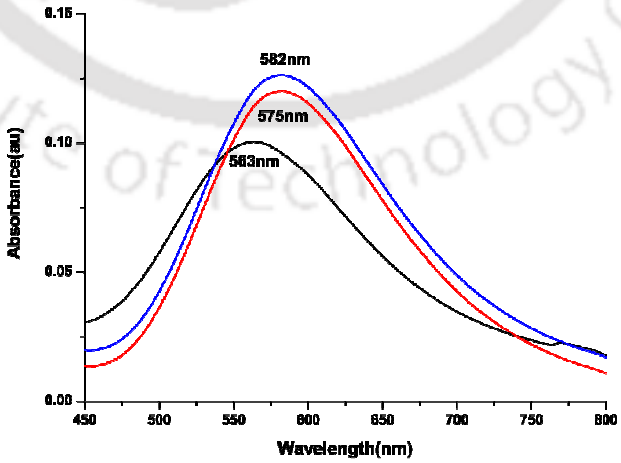

Figure 4.3: UV-visible spectra of **4.1** (black trace), **4.2** (red trace), **4.3** (blue trace) in acetonitrile solution.

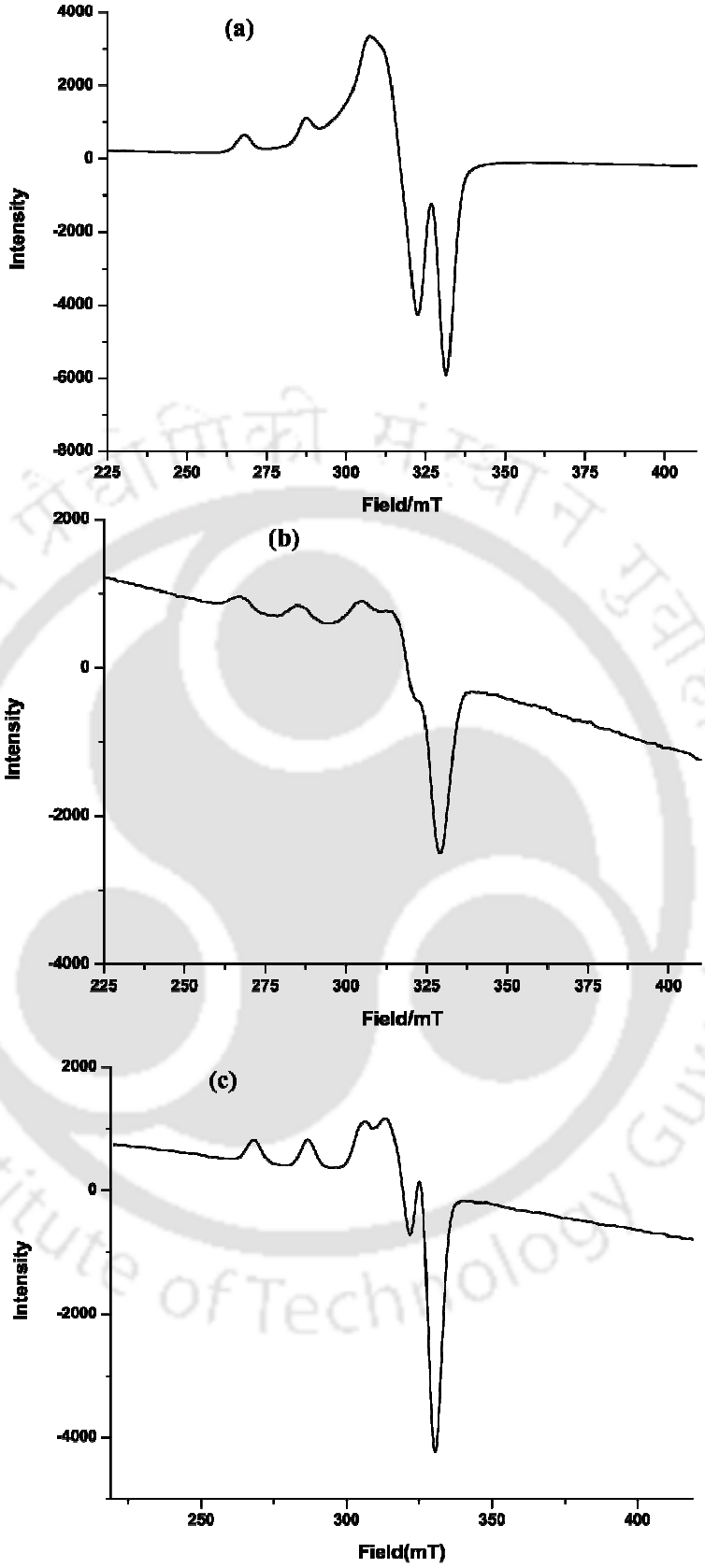

Figure 4.4: X-band EPR spectra of (a) **4.**1, (b) **4.2** and (c) **4.3** in CH_3CN/CH_3OH (50%) at 77K.

ground state. [21] The calculated values $g_{\parallel} > g_{\perp}$; $A_{\parallel}$ were in the range of other reported analogous Cu^{II} complexes (Figure 4.4).[21] The complexes were found to exhibit one electron paramagnetism at room temperature. They behaved as 1:2 electrolytes in acetonitrile solvent (experimental section).

4.2.1 Nitric oxide reactivity in acetonitrile

In acetonitrile solvent, in presence of NO, the Cu^{II} center of all the complexes were found to undergo reduction to Cu^{I} and it was studied by UV-visible, EPR and solution FT-IR spectroscopy. In case of complex **4.1**, the *d-d* transition band at 563 nm shifted to 605 nm immediately after purging NO owing to the formation of thermally unstable green [Cu^{II}-$NO^{\bullet}$] intermediate complex (Figure 4.5a). [Cu^{II}-$NO^{\bullet}$] intermediates were observed to form in the reaction of $[Cu(tiaea)(CH_3CN)]^{2+}$ and $[Cu(teaea)(CH_3CN)]^{2+}$ [tiaea, *tris*-(2-isopropylaminoethyl)amine and teaea, *tris*-(2-ethylaminoethyl)amine], with NO and were reported to exhibit the *d-d* transition at 640 nm and 605 nm, respectively.[16] The intensity of the band corresponding to the [Cu^{II}-$NO^{\bullet}$] intermediate were observed to decrease with time indicating the formation of the Cu^{I} species following pseudo-first order kinetics (Figure 4.5a, inset). The rate constant was calculated to be 4.48 x 10^{-1} min^{-1} at 298 K. Similarly, the *d-d* band for complexes **4.2** and **4.3** were observed to be shifted from 575 and 582 nm to 622 and 652 nm, respectively, on purging NO in acetonitrile solution indicating the formation of [Cu^{II}-$NO^{\bullet}$] intermediates (Figures 4.5b and 4.5c). The decomposition rate constants were found to be 9.30 x 10^{-1} min^{-1} and 36.67 x 10^{-1} min^{-1} at 298 K, in cases of complexes **4.2** and **4.3**, respectively. Thus, the order of the rate of decomposition of the [Cu^{II}-$NO^{\bullet}$] intermediate in cases of the complexes **4.1**, **4.2** and **4.3** was **4.3 > 4.2 > 4.1**. This can be attributed to the effect of bulk of alkyl substitution on the ligand

framework. For $[Cu(tiaea)(CH_3CN)]^{2+}$ and $[Cu(teaea)(CH_3CN)]^{2+}$ also, the order of rate constants was $[Cu(tiaea)(CH_3CN)]^{2+} > [Cu(teaea)(CH_3CN)]^{2+}$ at 298 K indicating the effect of bulk of N-alkyl group on the ligand framework.

Though complexes **4.1**, **4.2** and **4.3** were found to be EPR active in acetonitrile solvent, the green intermediates obtained after their reaction with NO were found to be EPR silent at 298 K (Figures 4.6a, 4.6b and 4.6c). This can be attributed to the formation of diamagnetic $[Cu^{II}\text{-}NO^{\bullet}]$ intermediate in all the cases. It should be noted that the complete reduction of Cu^{II} center by NO would also result into EPR silent Cu^{I} species. However, in the present cases, the presence of the *d-d* band of the intermediate complexes clearly indicates the existence of $[Cu^{II}\text{-}NO^{\bullet}]$ rather than Cu^{I}. Similar observations were reported for $[Cu(tiaea)(CH_3CN)]^{2+}$ and $[Cu(teaea)(CH_3CN)]^{2+}$.[16] It would be worth mentioning here that the structurally characterized $[Cu^{II}\text{-}NO^{\bullet}]$ complex, $[Cu(CH_3NO_2)_5(NO)][PF_6]_2$, was also found to be EPR silent owing to the antiferromagnetic coupling between the paramagnetic centers present in the molecule.[22]

In solution FT-IR spectroscopic studies of the acetonitrile solutions of the complexes after purging NO, a new band was found to appear at 1632, 1630 and 1634 cm^{-1} in cases of complexes **4.1**, **4.2** and **4.3**, respectively, corresponding to the vibration of NO coordinated to the Cu^{II} center (Figures 4.7a, 4.7b and 4.7c). These ν_{NO} of $[Cu^{II}\text{-}NO^{\bullet}]$ were found to disappear with time indicating the unstable nature of the intermediates. Thus, the appearance of the band at ~1632 cm^{-1}, supports the formation of the $[Cu^{II}\text{-}NO^{\bullet}]$ prior to the reduction of Cu^{II} centers in the present cases. In case of

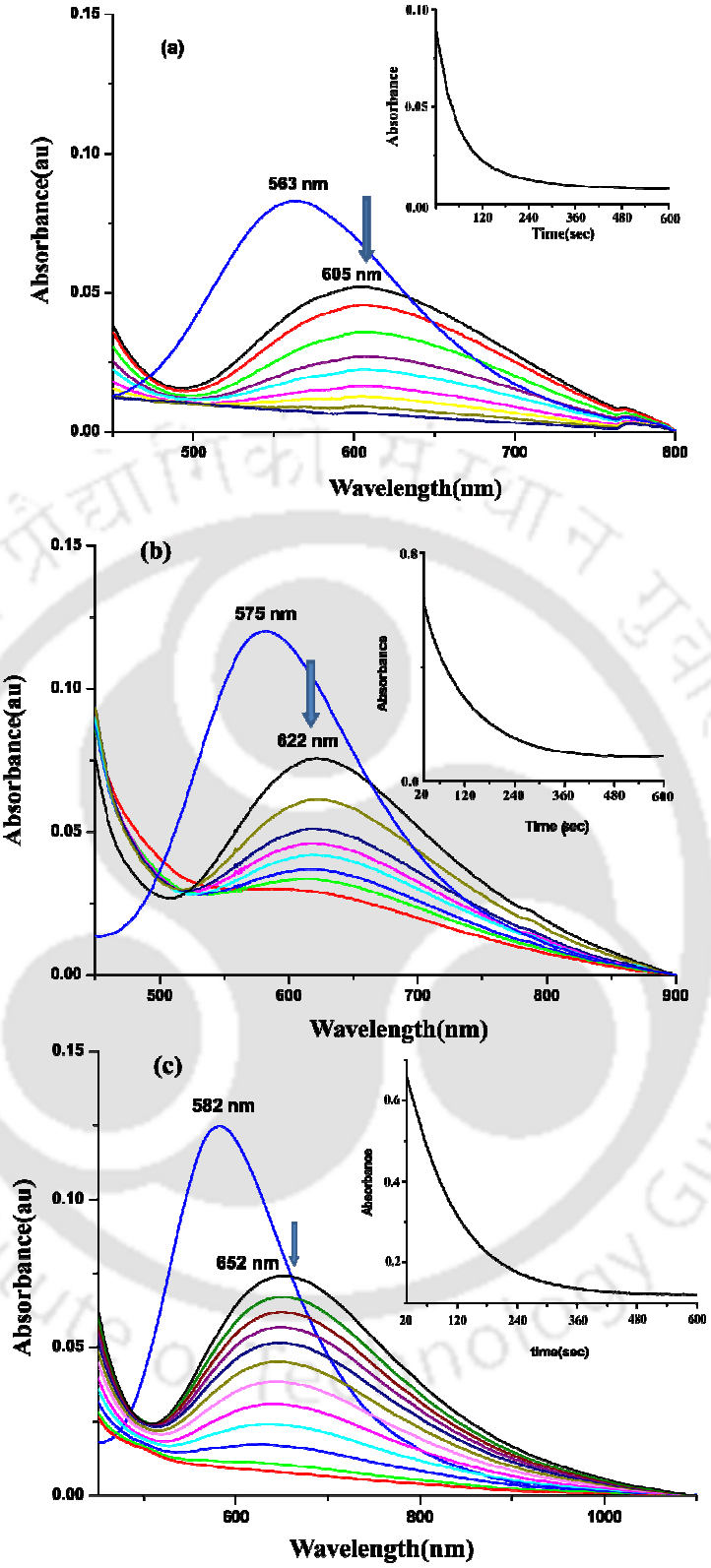

Figure 4.5: UV-visible spectra of the reaction of complexes, (a) **4.1**, (b) **4.2** and (c) **4.3** with NO in acetonitrile solvent at room temperature. (Blue trace represents the Cu^{II}-species, black represents that of the [Cu^{II}-$NO^{\bullet}$] intermediate which gradually reduced to Cu^{I}-species represented by down headed arrow). Inset: Time-scan plot for the decomposition of [Cu^{II}-$NO^{\bullet}$] at room temperature.

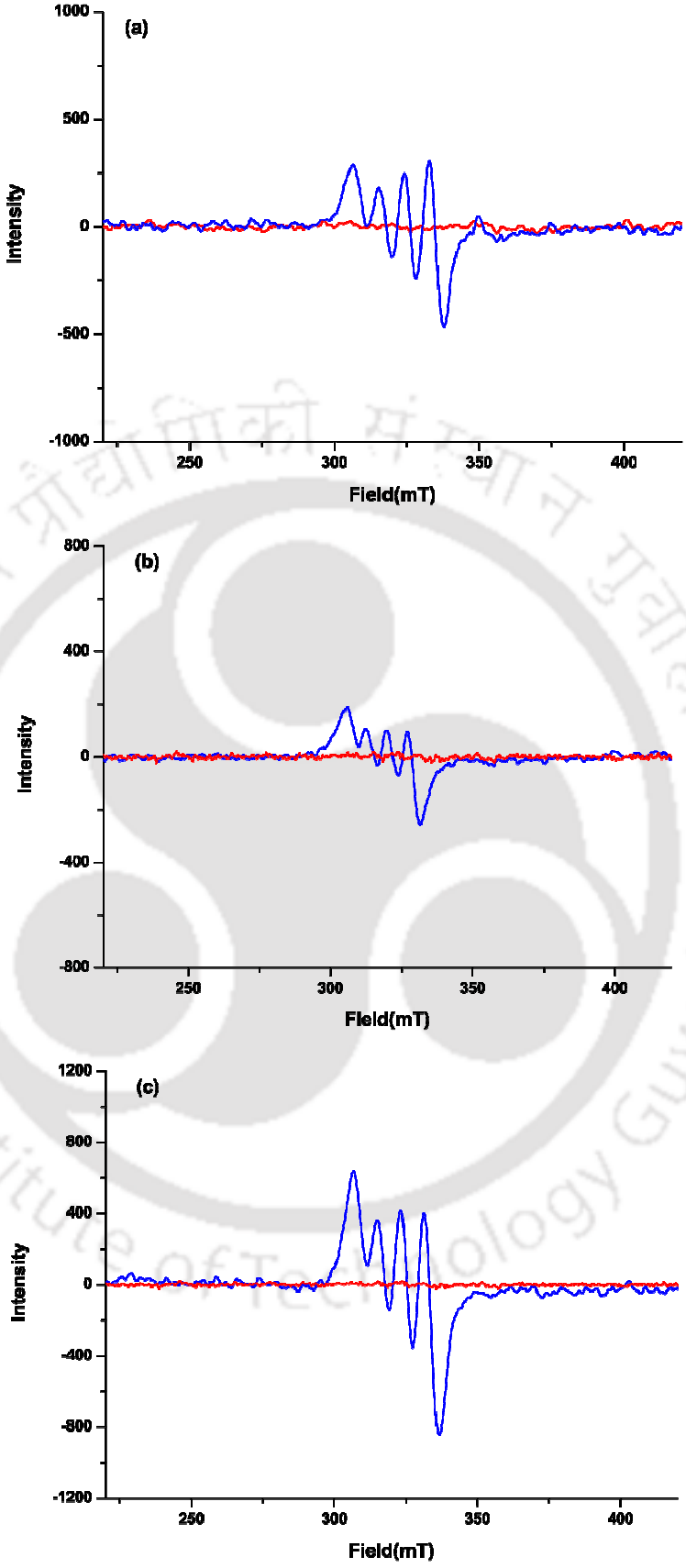

Figure 4.6: X-Band EPR spectra of complexes (a) **4.1** (b) **4.2** and (c) **4.3** in acetonitrile before (blue trace) and immediately after (red trace) purging NO at room temperature.

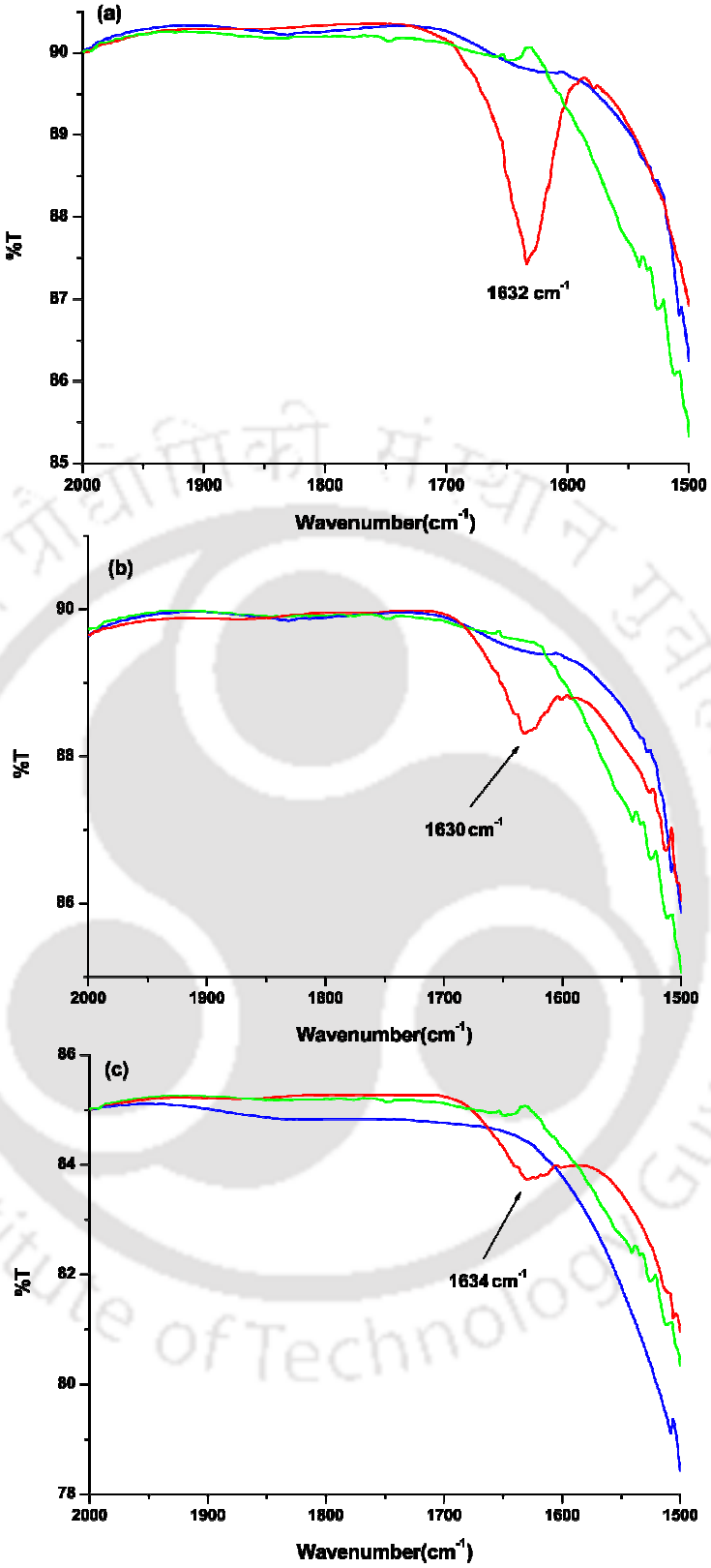

Figure 4.7: Solution FT-IR spectra complexes(a) **4.1** (b) **4.2** and (c) **4.3** in acetonitrile (blue trace represents IR spectra of complexes, red represents that immediately after purging NO which shows sharp peak at~1630 cm^{-1} and green represents that after 5 minutes).

$[Cu(tren)(CH_3CN)]^{2+}$, the ν_{NO} of $[Cu^{II}\text{-}NO^{\bullet}]$ was found to appeared at 1650 cm^{-1} in acetonitrile.[16] It should be noted that for the air-stable solid copper-nitrosyl of copper(II)-dithiocarbamate, the ν_{NO} for the NO coordinated to copper appears at 1682 cm^{-1}.[23] In contrary, for $[Cu(CH_3NO_2)_5(NO)][PF_6]_2$, the ν_{NO} frequency was reported to appear at 1933 cm^{-1} in nujol mull. The higher ν_{NO} frequency in case of $[Cu(CH_3NO_2)_5(NO)][PF_6]_2$ might be resulted from the bent geometry [Cu1-N1-O1) 121.0(3)°] of the nitrosyl ligand at an equatorial site.[22]

The reduction of Cu^{II} centers in the present study was further authenticated by the isolation of the reduced complex, $[Cu(CH_3CN)_4]ClO_4$. Since the crystal structure of $[Cu(CH_3CN)_4]ClO_4$ had already been reported by Soregh et. al., attempt was not made to determine the single crystal structure of $[Cu(CH_3CN)_4](ClO_4)$.[24]

It would be worth mentioning here that Vagliasindi et. al. has reported a series of the interaction of NO with Cu^{II} complexes of small peptides coming from the N-terminal prion protein octa-repeat region. In aqueous solutions of Cu-Ac-HGGG-NH_2 and Cu-Ac-PHGGGWGQ-NH_2 systems at ~ pH 7.5, the reduction of Cu^{II} centers were observed in presence of NO source.[25] Spectral studies suggested that these reductions were probably mediated by the formation of a labile Cu(II)-NO adduct.[25] However, for an analogous dinuclear system, Cu_2-Ac-$(PHGGGWGQ)_2$-NH_2, the NO interaction study in aqueous solutions at physiological pH suggested that the reduction of Cu^{II} proceeds through a complicated pathway involving two different intermediate species and a positive cooperativity between two copper centers was observed.[26]

The reduction of the Cu^{II} centers, by NO, in the present set of complexes was found to be accompanied with N-nitrosation at the ligand frameworks. Ford et. al. reported

earlier that the Cu^{II} center in $[Cu^{II}(DAC)]^{2+}$ {DAC = 1,8-bis(9-anthracylmethyl) derivative of the macrocyclic tetraamine cyclam (1,4,8,11-tetraazacyclotetradecane)} in methanol solution, in presence of a base, undergo reduction by NO with concomitant mono-N-nitrosation of the ligand. Similar observations were reported for $[Cu(Ds\text{-}AMP)_2]$ and $[Cu(Ds\text{-}en)_2]$ [where Ds-en and Ds-AMP are the conjugate bases of dansylethylenediamine (Ds-Hen) and dansyl aminomethylpyridine (Ds-HAMP), respectively] which gave mono-N-nitrosation of the DS-en and DS-AMP ligands.[27] On the other hand, the reaction of $[Cu(tiaea)(CH_3CN)]^{2+}$ and $[Cu(teaea)(CH_3CN)]^{2+}$ with NO were found to afford tri-N-nitrosation of the ligand.[16] From detail quantitative and theoretical studies of $[Cu^{II}(DAC)]^{2+}$, it has been established that the reaction proceeds through a pathway analogous to the inner-sphere mechanism for electron transfer between two metal centers through a bridging ligand. In this case, NO behaves as the reductant, Cu^{II}, the oxidant and the coordinated amido anion behaves as the bridging ligand. The preference of Cu^{I} for tetrahedral coordination and the decreased donor ability of the nitrosated ligand resulted in the demetallation of the macrocyclic ring after the reduction. An example of such a mechanism was found in the reaction of $[Ru(NH_3)_6]^{3+}$ with NO in alkaline solution to yield the Ru(II)-dinitrogen complex, $[Ru(NH_3)_5(N_2)]^{2+}$.[28]

In contrary, with $[Cu(tiaea)(CH_3CN)]^{2+}$ and $[Cu(teaea)(CH_3CN)]^{2+}$, the reduction was found to proceed through the formation of a thermally unstable $[Cu^{II}\text{-}NO^{\bullet}]$ intermediate and tri-nitrosation at the ligand was observed.[16] This mechanism, in fact, is more close to that of ferriheme reduction, where the nitrosation would be the one involving the initial NO coordination to the Cu^{II} center to form $[Cu^{II}\text{-}NO^{\bullet} \leftrightarrow Cu^{I}\text{-}NO^{+}]$ followed by amine deprotonation and migration of NO^{+} to the coordinated

amide to result into the nitrosoamine.[29-35] Subsequently, demetallation from the ligand will take place. This, indeed, has been suggested earlier by Wayland and others.[36] In the present cases also, the formation of the thermally unstable [Cu^{II}-$NO^{\bullet}$] was observed spectroscopically prior to the reduction.

It is interesting to note that though in cases of $[Cu(tiaea)(CH_3CN)]^{2+}$ and $[Cu(teaea)(CH_3CN)]^{2+}$, exclusively tri-nitrosation of the ligand was observed; in the present study, both the mono- and di-nitrosation of the ligand were found with almost 65% of unreacted ligand in each cases (Scheme 4.2). All the nitrosation products were isolated and characterized completely [Experimental section and Appendix III, Figures A3.21- A3.43]. The formation of di-nitrosation product ($\mathbf{L_4''}$) in case of complex **4.1** was further confirmed by its X-ray single crystal structure determination. The ORTEP diagram of $\mathbf{L_4''}$ is shown in figure 4.8. It has crystallographically imposed two fold symmetry. Crystalographic parameters, selected bond lengths and selected bond angles are shown in table A3.5 and A3.6 in appendix III. It should be noted that the free ligands did not react with NO in the experimental condition to afford the N-nitrosation products.

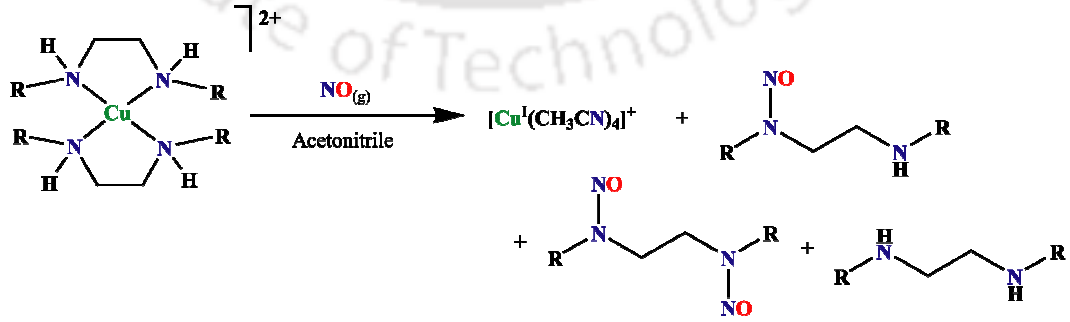

Scheme 4.2

R	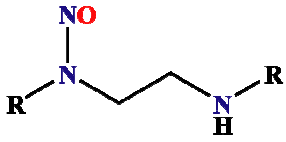	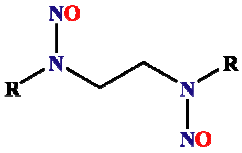
Me	L_4', 16%	L_4'', 17%
Et	L_5', 8%	L_5'', 24%
^{i}Bu	L_6', 5%	L_6'', 30%

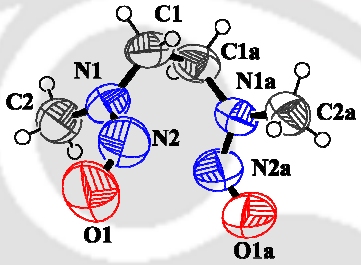

Figure 4.8: ORTEP diagram of ligand L_4'' [a (-x, y, 1/2-z) symmetry transformation is implied by each additional atom level] (50% thermal ellipsoid plot).

It is interesting to note that the yield of mono and di-nitrosation products obtained in cases of complexes **4.1**, **4.2** and **4.3** were in the order of **4.1** > **4.2** ≈ **4.3** and **4.3** > **4.2** > **4.1**, respectively. Hence, it is evident that the yield of di-nitrosation product increases on moving from methyl, ethyl to isobutyl group on N-substitution of the ligand. Perhaps, the better electron donor ability of the group at N-substitution, facilitates more than one nitrosation at the secondary amine centers of the ligand. The formation of the [Cu^{II}-$NO^{\bullet}$] intermediate prior to the reduction of Cu^{II} to Cu^{I} might also have some role to control the degree of nitrosation.

4.3 Conclusion

The NO reactivity of three Cu^{II} complexes of bidentate amine ligands was studied in acetonitrile solvent. All the complexes afforded thermally unstable [Cu^{II}-$NO^{\bullet}$]

intermediate on reaction with NO in acetonitrile solution followed by the reduction of Cu^{II} centers to Cu^{I}. The reduction was resulted with a simultaneous mono- and di-nitrosation at the secondary amine sites of the ligand. Similar N-nitrosation was observed with $[Cu(tiaea)(CH_3CN)]^{2+}$ and $[Cu(teaea)(CH_3CN)]^{2+}$; however, in those cases exclusive tri-nitrosation was observed. On the other hand, in cases of $[Cu^{II}(DAC)]^{2+}$, $Cu(Ds\text{-}AMP)_2$ and $Cu(Ds\text{-}en)_2$, where the reduction took place through deprotonation in presence of base, exclusive mono-nitrosation was found. The ratio of the yield of mono- and di-nitrosation product, in the present case, is found to be dependent on the N-substitution present in the ligand framework.

4.4 Experimental Section

4.4.1 Materials and methods

All reagents and solvents were purchased from commercial sources and were of reagent grade. Ligand, **L_4** was purchased from Sigma-Aldrich and used as received. Acetonitrile was distilled from calcium hydride. Deoxygenation of the solvent and solutions were effected by repeated vacuum/purge cycles or bubbling with nitrogen for 30 minutes. NO gas was purified by passing through KOH and P_2O_5 column. UV-visible spectra were recorded on a Perkin Elmer Lambda-25 UV-visible spectrophotometer. FT-IR spectra of the solid samples were taken on a Perkin Elmer spectrophotometer with samples prepared as KBr pellets and for solutions, Varian 660-IR FT-IR spectrometer and NaCl cell of 2 mm path length were used and the spectra shown are the solvent subtracted ones. Solution electrical conductivity was checked using a Systronic 305 conductivity bridge. ^{1}H-NMR spectra were obtained with a 400 MHz Varian FT spectrometer. Chemical shifts (ppm) were referenced either with an internal standard (Me_4Si) or to the residual solvent peaks. The X-band

Electron Paramagnetic Resonance (EPR) spectra were recorded on a JES-FA200 ESR spectrometer, at room temperature and 77K with microwave power, 0.998 mW; microwave frequency, 9.14 GHz and modulation amplitude, 2. Elemental analyses were obtained from a Perkin Elmer Series II Analyzer. The magnetic moment of complexes was measured on a Cambridge Magnetic Balance.

Single crystals were grown by slow diffusion followed by slow evaporation technique. The intensity data were collected using a Bruker SMART APEX-II CCD diffractometer, equipped with a fine focus 1.75 kW sealed tube MoK_α radiation (λ = 0.71073 Å) at 273(3) K, with increasing ω (width of 0.3° per frame) at a scan speed of 3 s/frame. The SMART software was used for data acquisition. Data integration and reduction were undertaken with SAINT and XPREP software and structures were solved by direct methods using SHELXS-97 and refined with full-matrix least squares on F^2 using SHELXL-97.[37-39] All non-hydrogen atoms were refined anisotropically. Structural illustrations have been drawn with ORTEP-3 for Windows.[40]

4.4.2 Synthesis of the complexes

All the complexes were synthesized using a general procedure of the reaction of hexaaquacopper(II) perchlorate with respective ligands. The details are given for complex **4.1**.

Complex 4.1, $[Cu(L_4)_2](ClO_4)_2$

Copper(II) perchlorate hexahydrate, $[Cu(H_2O)_6](ClO_4)_2$ (370 mg, 1.0 mmol) was dissolved in 10 ml of freshly distilled acetonitrile and to this light blue solution, the ligand $\mathbf{L_4}$, N,N′-dimethyl ethylenediamine (176 mg, 2.0 mmol), was added drop wise. The color of the solution changed to violet. The resulting mixture was stirred for 1 h. Then the volume of the solution was reduced to ~2 ml and layered with benzene.

Storage of this at ~ -20 °C overnight resulted in the precipitation of blue crystalline compound. Yield: 385 mg (~87%). Elemental Analyses: Calcd.(%) for $C_8H_{24}N_4O_8Cl_2Cu$: C, 21.90; H, 5.51; N, 12.77. Found (%) C, 21.94; H, 5.52; N, 12.71. UV-vis. (acetonitrile): λ_{max}, 563 nm (ε, 100 M^{-1} cm^{-1}). FT-IR (KBr pellet): υ_{ClO4}^-, 1113, 1088, 625 cm^{-1}. X-band EPR data: $g_{\|}$, 2.280; $g_{\perp}$, 2.096; $A_{\|}$, 91×10^{-4} cm^{-1}. Molar conductance: Λ_M ($\Omega^{-1}cm^2mol^{-1}$), 247 in acetonitrile. μ_{eff} : 1.76 BM.

Complex 4.2, $[Cu(L_5)_2](ClO_4)_2$

Yield: 421 mg (~ 85%). Elemental Analyses: Calcd.(%) for $C_{12}H_{32}N_4O_8Cl_2Cu$: C, 29.12; H, 6.51; N, 11.32. Found (%) C, 29.07; H, 6.50; N, 11.26. UV-vis. (acetonitrile): λ_{max}, 575 nm (ε, 120 M^{-1} cm^{-1}). FT-IR (KBr pellet): υ_{ClO4}^-, 1111, 1089, 627 cm^{-1}. X-band EPR data: $g_{\|}$, 2.262; $g_{\perp}$, 2.082; $A_{\|}$, 90×10^{-4} cm^{-1}. Molar conductance: Λ_M ($\Omega^{-1}cm^2mol^{-1}$), 232 in acetonitrile. μ_{eff}: 1.69 BM.

Complex 4.3, $[Cu(L_6)_2](ClO_4)_2$

Yield: 519 mg (~ 86%). Elemental Analyses: Calcd.(%) for $C_{20}H_{48}N_4O_8Cl_2Cu$: C, 39.56; H, 7.97; N, 9.22. Found (%) C, 39.50; H, 7.98; N, 9.14. UV-vis. (acetonitrile): λ_{max}, 582 nm (ε, 124 M^{-1} cm^{-1}). FT-IR (KBr pellet): υ_{ClO4}^-, 1111, 1089, 625 cm^{-1}. X-band EPR data $g_{\|}$, 2.282; $g_{\perp}$, 2.098; $A_{\|}$, 92×10^{-4} cm^{-1}. Molar conductance: Λ_M ($\Omega^{-1}cm^2mol^{-1}$), 241 in acetonitrile. μ_{eff} : 1.65 BM.

4.4.3 Isolation of $[Cu^I(CH_3CN)_4]ClO_4$

The isolation of $[Cu(CH_3CN)_4]ClO_4$ from the reaction of the respective complexes with NO were done using the same general procedure. The detail is given for complex **4.1**.

In a 50 ml Schlenk flask, complex **4.1** (219 mg, 0.5 mmol) was dissolved in 10 ml degassed acetonitrile. To this solution, NO gas was purged through a needle for one minute and allowed to stand for 10 minutes. To the resulting colorless solution, 15 ml of degassed benzene was added through a syringe to make a layer. The layered solution was then kept overnight in freezer. The white crystals of $[Cu(CH_3CN)_4]ClO_4$ were filtered out from the colorless solution under nitrogen atmosphere using a Schlenk frit. Yield, 110 mg, ~65%.

Same procedure was followed to isolate the $[Cu(CH_3CN)_4]ClO_4$ from the reaction of complex **4.2** (247 mg, 0.5 mmol) and complex **4.3** (303 mg, 0.5 mmol) with NO in acetonitrile solution. Yield: 118 mg, ~72% (Complex **4.2**) and 105 mg ~ 64% (Complex **4.3**).

4.4.4 Isolation of L_4' and L_4''

In a 50 ml Schlenk flask, complex **4.1** (438 mg, 1.0 mmol) was dissolved in 30 ml degassed acetonitrile. To this, NO gas was purged through a needle for one minute and the mixture was then allowed to stand for 10 minutes. To the colorless solution, thus obtained, 20 ml of degassed benzene was added through a syringe to make a layer. The layered solution was then kept overnight in freezer. The white crystals of $[Cu(CH_3CN)_4]ClO_4$ were filtered out from the colorless solution under nitrogen atmosphere using a Schlenk frit. The volume of the filtrate was then reduced to 5 ml and stirred for 1 h in open air in order to allow the residual Cu^{I} center to oxidise to Cu^{II}. To this, 5 ml saturated aqueous solution of Na_2S was added and stirred for ½ h. The black precipitate thus obtained was filtered off and the filtrate was diluted with 50 ml of distilled water. The organic part was then extracted from the mixture using $CHCl_3$ (3 portions × 25 ml). The collected organic layer was then dried under reduced

pressure and the residual oil was subjected to column chromatography using silica gel to yield $\mathbf{L_4'}$ and $\mathbf{L_4''}$.

For $\mathbf{L_4'}$: Yield, 20 mg (~ 16%). Elemental Analyses: Calcd.(%) for $C_4H_{11}N_3O$: C, 41.01; H, 9.46; N, 35.87. Found (%) C, 41.07; H, 9.47; N, 35.82. ^{1}H-NMR(400 MHz, $CDCl_3$), δ_{ppm}, 2.42(s, 3H), 2.70 (t, 2H), 3.04(s, 3H), 4.20(t, 2H). ^{13}C-NMR(100 MHz, $CDCl_3$), δ_{ppm}, 53.17, 49.37, 36.00, 31.98. FT-IR in KBr pellet: 1456(s), 1384 (s), 1329(s), 1049(m) cm^{-1}. ESI-Mass: (m+1)/z, Calcd. 118.15; Found, 118.14.

For $\mathbf{L_4''}$: Yield, 25 mg (~ 17%). Elemental Analyses: Calcd.(%) for $C_4H_{10}N_4O_2$: C, 32.87; H, 6.90; N, 38.34. Found (%) C, 32.83; H, 6.92; N, 38.30. ^{1}H-NMR(400 MHz, $CDCl_3$), δ_{ppm}, 3.00(s, 3H), 3.03 (s, 6H), 3.67(s, 4H), 3.72(s, 6H), 3.76(s, 3H), 3.93(t, 2H,), 4.24(t, 2H,), 4.51(s, 4H). ^{13}C-NMR(100 MHz, $CDCl_3$), δ_{ppm}, 51.08, 49.31, 42.59, 41.27, 39.78, 39.38, 32.06, 31.62. The presence of extra signals in ^{1}H- and ^{13}C-NMR spectra are due to isomeric impurities.[41] FT-IR in KBr pellet: 1449(s), 1421 (s), 1316(s), 1050(s), 1027(s) cm^{-1}. ESI-Mass: (m+1)/z, Calcd. 147.15; Found, 147.20.

4.4.5 Isolation of $\mathbf{L_5'}$ and $\mathbf{L_5''}$

Same procedure (as in case of complex **4.1**) was adopted for the isolation of $\mathbf{L_5'}$ and $\mathbf{L_5''}$.

For $\mathbf{L_5'}$: Yield, 24 mg (~ 8%). Elemental Analyses: Calcd.(%) for $C_6H_{15}N_3O$: C, 49.63; H, 10.41; N, 28.94. Found (%) C, 49.60; H, 10.41; N, 28.89. ^{1}H-NMR(400 MHz, $CDCl_3$), δ_{ppm}, 1.03(m, 6H), 1.34 (t, 2H), 3.59(q, 2H), 3.63(t, 2H), 4.14(m, 2H).^{13}C-NMR(100 MHz, $CDCl_3$), δ_{ppm}, 51.85, 47.61, 43.94, 39.49, 14.13, 11.31. FT-IR in KBr pellet: 1456(s), 1382 (m), 1233(m) cm^{-1}. ESI-Mass: (m+1)/z, Calcd. 146.20; Found, 146.12.

For $L_5^{//}$: Yield, 88 mg (~ 24%). Elemental Analyses: Calcd.(%) for $C_6H_{14}N_4O_2$: C, 41.37; H, 8.10; N, 32.16. Found (%) C, 41.33; H, 8.11; N, 32.10. ^{1}H-NMR(400 MHz, $CDCl_3$), δ_{ppm}, 1.06 (m, 6H), 1.22(s, 3H), 1.39(m, 8H), 2.14(s, 2H), 3.59(m, 8H), 3.89(t, 4H), 4.13(m, 8H), 4.46(s, 2H). ^{13}C-NMR(100 MHz, $CDCl_3$), δ_{ppm}, 49.78, 48.41, 48.10, 47.35, 42.53, 40.44, 39.67, 39.31, 29.87, 14.19, 14.13, 11.34. The presence of extra signals in ^{1}H- and ^{13}C- NMR spectra are due to isomeric impurities .[41] FT-IR in KBr pellet: 1456(s), 1375 (s), 1309(s), 1071(s), 1027(s) cm^{-1}. ESI-Mass: $(m+Na^+)/z$, Calcd. 197.20; Found, 197.19.

4.4.6 Isolation of $L_6^{/}$ and $L_6^{//}$

Same procedure (as in case of complex **4.1**) was adopted for the isolation of $L_6^{/}$ and $L_6^{//}$.

For $L_6^{/}$: Yield, 21 mg (~ 5%). Elemental Analyses: Calcd.(%) for $C_{10}H_{23}N_3O$: C, 59.66; H, 11.52; N, 20.87. Found (%) C, 59.63; H, 11.51; N, 20.84. ^{1}H-NMR(400 MHz, $CDCl_3$), δ_{ppm}, 4.15(t), 3.92 (d), 3.63 (t), 3.43(d), 2.97(t), 2.68(t), 2.42(d), 2.36(d), 2.36(d), 2.09(m), 1.99(m), 1.65(m), 1.22(s), 0.94(d), 0.87(d),0.86(d), 0.83(d). ^{13}C-NMR(100 MHz, $CDCl_3$), δ_{ppm}, 60.45, 57.85, 57.72, 52.71, 51.29, 49.72, 48.12, 45.99, 44.60, 29.84, 28.52, 27.35, 26.58. The presence of extra signals in ^{1}H- and ^{13}C-NMR spectra are due to isomeric impurities.[41] FT-IR in KBr pellet: 1960, 2962, 2858, 1465, 1375, 1096, 669 cm^{-1}. ESI-Mass: (m+1)/z, Calcd. 202.31; Found, 202.16.

For $L_6^{//}$: Yield, 140 mg (~ 30%). Elemental Analyses: Calcd.(%) for $C_{10}H_{22}N_4O_2$: C, 52.15; H, 9.63; N, 24.33. Found (%) C, 52.12; H, 9.63; N, 24.29. ^{1}H-NMR(400 MHz, $CDCl_3$), δ_{ppm}, 4.46(s), 4.14(t), 3.90(d), 3.87(d), 3.57(s), 3.38(t), 2.07(m), 1.95(m), 1.22(s), 0.95(s), 0.93(d), 0.84(s), 0.82(d). ^{13}C-NMR(100 MHz, $CDCl_3$), δ_{ppm}, 60.61,

40.87, 27.44, 20.05. FT-IR in KBr pellet: 2962, 2927, 1458, 1374, 1290, 1025, 657 cm^{-1}. ESI-Mass: $(m+Na^{+})/z$, Calcd. 253.31; Found, 253.17.

4.5 References

1. Richter-Addo, G. B.; Legzdins, P. *Metal Nitrosyls*; Oxford University Press, New York, **1992**.
2. (a) Studbauer, G.; Giuffre, P.; Sarti, P. *J. Biol. Chem.* **1999**, *274*, 28128. (b) Moncada, S.; Palmer, R. M. J.; Higgs, E. A. *Pharmacol. Rev.* **1991**, *43*, 109. (c) Butler, A. R.; Williams, D. L. *Chem. Soc. Rev*. **1993**, 233.
3. (a) Feelisch, M.; Stamler, J. S. *Methods in Nitric Oxide Research*; John Wiley and Sons; Chichester, England, **1996**. (b) Jia, L.; Bonaventura, C.; Bonaventura, J.; Stamler, J. S. *Nature*, **1996**, *380*, 221. (c) Galdwin, M. T.; Lancaster Jr. J. R.; Freeman, B. A.; Schechter, A. N. *Nat. Med*. **2003**, *9*, 496.
4. (a) Ye, R. W.; Toro-Suarez, I.; Tiedje, J. M.; Averill, B. A. *J. Biol. Chem.* **1991**, *266*, 12848. (b) Hulse, C. L.; Averill, B. A.; Tiedje, J. M. *J. Am. Chem. Soc.* **1989**, *111*, 2322. (c) Jackson, M. A.; Tiedje, J. M.; Averill, B. A. *FEBS Lett.* **1991**, *291*, 41.
5. (a) Godden, J. W.; Turley, S.; Teller, D. C.; Adman, E. T.; Liu, M.Y.; Liu, W.; Payne, J.; LeGall, J. *Science*, **1991**, *153*, 438. (b) Adman, E. T.; Turley, S. in *Bioinorganic Chemistry of Copper;* Karlin, K. D.; Tyekllr, Z. Eds., Chapman & Hall, Inc.: New York, **1993**; pp 397. (c) Ferguson, S. J. *Curr. Opin. Chem. Biol.* **1998**, *2*, 182.
6. (a) Richardson, D. J.; Watmough, N. J. *Curr. Opin. Chem. Biol.* **1999**, *3*, 207. (b) Moura, I.; Moura, J. J. G. *Curr. Opin. Chem. Biol.* **2001**, *5*, 168. (c) Tocheva, E. I.; Rosell, F. I.; Mauk, A. G.; Murphy, M. E. P. *Biochem.* **2007**, *46*, 12366. (d) Torres, J.; Cooper, C. E.; Wilson, M. *J. Biol. Chem.*, **1998**, *273*, 8756. (e) Zhou,

X.; Espey, M. G.; Chen, J. X.; Hofseth, L. J.; Miranda, K. M.; Hussain, S. P.; Winks, D. A.; Harris, C. C. *J. Biol. Chem.*, **2000**, *275*, 21241.

7. (a) Torres, J.; Svistunenko, D.; Karlsson, B.; Cooper, C. E.; Wilson, M. T.; *J. Am. Chem. Soc.* **2002**, *124*, 963. (b) Torres, J.; Cooper, C. E.; Wilson, M. T. *J. Biol. Chem.* **1998**, *273*, 8756. (c) Tran, D.; Skelton, B. W.; White, A. H.; Laverman, L. E; Ford, P. C. *Inorg. Chem.* **1998**, *37*, 2505. (d) Martin, C. T.; Morse, R. H.; Kanne, R. M.; Gray, H. B.; Malmstrom, B. G.; Chan, S. I. *Biochem.* **1981**, *20*, 5147.
8. (a) Stamler, J. S.; Singel, D. J.; Loscalzo, J. *Science*, **1992**, *258*, 1898. (b) Williams, R. J. P. *Chem. Soc. Rev.* **1996**, 77. (c) Drapier, J.-C.; Bouton, C. *Bioessays,* **1996**, *18*, 549.
9. (a) Stamler, J. S. *Cell*, **1994**, *78*, 931. (b) Feelisch, M. S.; Rassaf, T.; Mnaimneh, S.; Singh, N.; Byran, N. S.; Jourd'Heuil, D.; Kelm, M. *FASEB J.* **2002**, *16*, 1775.
10. (a) Bryan, N. S.; Rassaf, T.; Maloney, R. E.; Rodriguez, C. M.; Saijo, F.; Rodriguez, J. R.; Feelisch, M. *Proc. Natl. Acad. Sci. U. S. A.* **2004**, *101*, 4308. (b) Luchsinger, B. P.; Rich, E. N.; Gow, A. J.; Williams, E. M.; Stamler, J. S.; Singel, D. J. *Proc. Natl. Acad. Sci. U. S. A.* **2003**, *100*, 461.
11. (a) Martin, C. T.; Morse, R. H.; Kanne, R. M.; Gray, H. B.; Malmstrom, B. G.; Chan, S. I. *Biochem.* **1981**, *20*, 5147. (b) Gorren, A. C. F.; de Boer, E.; Wever, R. *Biochem. Biophys. Acta* **1987**, *916*, 38. (c) Cooper, C. E.; Torres, J.; Sharpe, M. A.; Wilson, M. T. *FEBS Lett.* **1997**, *414*, 281.
12. Torres, J.; Cooper, C. E.; Wilson, M. T. *J. Biol. Chem.* **1998**, *273*, 8756. (b) Torres, J.; Svistunenko, D.; Karlsson, B.; Cooper, C. E.; Wilson, M. T. *J. Am. Chem. Soc.* **2002**, *124*, 963.

13. (a) Tran, D.; Ford, P. C. *Inorg. Chem.* 1**996**, *35*, 2411. (b) Lim, M. D.; Capps, K. B.; Karpishin, T. B.; Ford, P. C. *Nitric Oxide, Biol. Chem.* **2005**, *12*, 244.

14. (a) Brown, G. C. *Biochim. Biophys. Acta* **2001**, *1504*, 46. (b) Torres, J.; Sharpe, M. A.; Rosquist, A.; Cooper, C. E.; Wilson, M. T. *FEBS Lett.* **2000**, *475*, 263. (c) Wijma, H. J.; Canters, G. W.; de Vries, S.; Verbeet, M. P. *Biochem.* **2004**, *43*, 10467.

15. (a) Tsuge, K.; DeRosa, F.; Lim, M. D.; Ford, P. C. *J. Am. Chem. Soc*. **2004**, *126*, 6564. (b) Khin, C.; Lim, M. D.; Tsuge, K.; Iretskii, A.; Wu, G.; Ford, P. C. *Inorg. Chem*. **2007**, *46*, 9323.

16. Sarma, M.; Kalita, A.; Kumar, P.; Singh, A.; Mondal, B. *J. Am. Chem. Soc.* **2010**, *132*, 7846.

17. Kurosawa, W.; Kan, T; Fukuyama, T. *Org. Syn*. **2002**, *79*, 186.

18. (a) Nasamen, R.; Virtano, I.; Mvllvmaki, H. *Suom. Kemistil*. **1966**, *B39*, 200. (b) Andino, M. M.; Curet, J. D.; Muir, M. M.; Ryan, R. C. *Acta Cryst*. **1976**, *B32*, 3185.

19. (a) DeBord, J. R. D.; Haushalter, R. C.; Meyer, L. M.; Rose, D. J.; Zapf, P. J.; Zubieta, J. *Inorg. Chim. Acta,* **1997**, *256*, 165. (b) Chiari, B.; Cinti, A.; Piovesana, O.; Zanazzi, P. F. *Inorg. Chem.* **1995**, *34*, 2652. (c) Tzavellas, L. C.; Pachini, S.; Tsiamis, C.; Hatzidimitriou, A. G. *Polyhedron*, **2007**, *26*, 1404. (d) Bodoki, A.; Hangan, A.; Oprean, L.; Alzuet, G.; Castiñeiras, A.; Borrás, J. *Polyhedron*, **2009**, *28*, 2537. (e) Choy, J. H.; Kim, D.-K.; Park, J.-C.; Choi, S.-N.; Kim, Y.-J. *Inorg. Chem.* **1997**, *36,* 189.

20. Hiroshi, Y.; Taro, I. *Bull. Chem. Soc. Jap.* **1969**, *42*, 2187.

21. (a) Hathaway, B. J.; Tomlinson, A. A. G. *Coord. Chem. Rev.* **1970**, *5*, 1. (b) Hathway, B. J.; Billing, D. E.; Nicols, P.; Procter, I. M. *J. Chem. Soc. A*, **1969**,

312. (c) Hathway, B. J. in *Comprehensive Coordination Chemistry*, eds. G. Wilkinson, R. D.; Gillard, J. A. McCleverty, Pergamon, Oxford, **1987**, Vol 5, pp 533. (d) Patra, A. K.; Ray, R.; Mukherjee, M. *Dalton Trans*. **1999**, 2461.

22. Wright, A. M.; Wu, G.; Hayton, T. W. *J. Am. Chem. Soc*. **2010**, *132*, 14336.
23. Diaz, A.; Ortiz, M.; Sanchez, I.; Cao, R.; Mederos, A.; Sanchiz, J.; Brito, F.; *J. Inorg. Biochem.* **2003**, *95*, 283.
24. Soregh, C.; Kierkegaard, P.; Norrestam, R. *Acta Crystallogr*. Sect. B **1975**, *31*, 314.
25. Bonomo, R. P.; Pappalardo, G.; Rizzarelli, E.; Santoro, A. M.; Tabb`I, G.; Vagliasindi, L. I. *Dalton Trans.,* **2007**, 1400.
26. Bonomo, R. P.; Pappalardo, G.; Rizzarelli, E.; Tabb`I, G.; Vagliasindi, L. I. *Dalton Trans.* **2008**, 3805.
27. Lim, M. H.; Lippard, S. J. *J. Am. Chem. Soc*., **2005**, *127*, 12170.
28. Pell, S. D.; Armor, J. N. *J. Am. Chem. Soc.* **1973***, 95,* 7625.
29. (a) Chien, J. C. W.; *J. Am. Chem. Soc.* **1969**, *91*, 2166. (b) Wayland, B. B.; Olson, L. W.; *J. Am. Chem. Soc.* **1974**, *96*, 6037. (c) Trofimova, N. S.; Safronov, A. Y.; Ikeda, O. *Inorg. Chem.* **2003**, *42*, 1945.
30. (a) Walker, F. A. *J. Inorg. Biochem.* **2005**, *99*, 216. (b) Rousseau, D. L.; Li, D.; Couture, M.; Yeh, S. R. *J. Inorg. Biochem.* **2005**, *99*, 306. (c) George, S. J.; Allen, J. W. A.; Ferguson, S. J.; Thorneley, R. N. F. *J. Biol. Chem.* **2000**, *275*, 33231.
31. (a) Pinakoulaki, E.; Gemeinhardt, S.; Saraste, M.; Varotsis, C. *J. Biol. Chem.* **2002**, *277*, 23407. (b) Praneeth, V. K. K.; Paulat, F.; Berto, T. C.; DeBeer George, S.; Nather, C.; Sulok, C. D.; Lehnert, N. *J. Am. Chem. Soc.* **2008**, *130*, 15288.

32. (a) Soldatova, A. V.; Ibrahim, M.; Olson, J. S.; Czernuszewicz, R. S.; Spiro, T. G. *J. Am. Chem. Soc.* **2010**, *132*, 4614. (b) Wasser, I. M.; de Vries, S.; Moe¨nne-Loccoz, P.; Schro¨der, I.; Karlin, K. D. *Chem. Rev.* **2002**, *102*, 1201.

33. (a) Fernandez, B. O.; Lorkovic, I. M.; Ford, P. C. *Inorg. Chem.* **2004**, *43*, 5393. (b) Lehnert, N.; Praneeth, V. K. K.; Paulat, F. *J. Comput. Chem.* **2006**, *27*, 1338.

34. (a) Ellison, M. K.; Scheidt, W. R. *J. Am. Chem. Soc.* **1999**, *121*, 5210. (b) Linder, D. P.; Rodgers, K. R.; Banister, J.; Wyllie, G. R. A.; Ellison, M. K.; Scheidt, W. R. *J. Am. Chem. Soc.* **2004**, *126*, 14136.

35. (a) Lim, M. D.; Lorkovic, I. M.; Ford, P. C. *J. Inorg. Biochem.* **2005**, *99*, 151. (b) Shamir, D.; Zilbermann, I.; Maimon, E.; Gellerman, G.; Cohen, H.; Meyerstein, D. *Eur. J. Inorg. Chem.* **2007**, 5029.

36. Hoshino, M.; Maeda, M.; Konishi, R.; Seki, H.; Ford, P. C. *J. Am. Chem. Soc.* **1996**, *118*, 5702.

37. SMART, SAINT and XPREP, Siemens Analytical X-ray Instruments Inc., Madison, Wisconsin, USA, **1995**.

38. Sheldrick, G. M. SADABS: software for Empirical Absorption Correction, University of Gottingen, Institut fur Anorganische Chemieder Universitat, Tammanstrasse 4, D-3400 Gottingen, Germany, **1999–2003**.

39. Sheldrick, G. M. SHELXS-97, University of Gottingen, Germany, **1997**.

40. Farrugia, L. J. J. *Appl. Crystallogr.* **1997**, *30*, 565.

41. Harris, R. K.; Spragg, R. A. *J. Mol. Spect.* **1969**, *30*, 77.

Chapter 5

Nitric oxide reduction of copper(II) complexes of 2-aminomethyl pyridine and *bis*-(2-aminoethyl)amine

Abstract

Two copper(II) complexes, **5.1** and **5.2** with $\mathbf{L_7}$ and $\mathbf{L_8}$ [$\mathbf{L_7}$, 2-aminomethyl pyridine; $\mathbf{L_8}$, *bis*-(2-aminoethyl)amine], respectively, in degassed acetonitrile solvent, on exposure to NO gas, were found to form thermally unstable [Cu^{II}-$NO^{\bullet}$] intermediate which then resulted into the reduction of the Cu^{II} center. The formation of the [Cu^{II}-$NO^{\bullet}$] intermediate was evidenced by UV-visible, solution FT-IR, EPR spectroscopic studies. The reduction of the Cu^{II} centers by nitric oxide afforded ligand transformation through diazotization at the primary amine coordination site, in both the cases. The modified ligands, in each case, were isolated and characterized.

5.1 Introduction

The coordination of nitric oxide (NO) to the transition metal ions and its activation have attracted the chemists attention as various biological and physiological reactivity of NO are attributed to the formation of nitrosyl complexes of metallo-proteins, mostly iron or copper-proteins. [1-3] For instance, it is believed that a [Cu^{I}-NO^{+} ↔ Cu^{II}-$NO^{\bullet}$] intermediate is involved in the conversion of nitrite to NO or, in some cases to N_2O by nitrite reductase e.g. from *Achromobacter cycloclastes*.[4-6] Here, nitrite binding and dehydration to form the nitrosyl intermediate is believed to take place at a copper site in the protein which is coordinated to three histidines and a water (or hydroxide) as ligand in a pseudo tetrahedral geometry.[7] On the other hand, metal-nitrosyl adducts presumably play important roles in nitrosation reactions of various thiols to give S-nitrosothiols which are proposed as important carriers of NO equivalents in cellular systems.[8-10] In this direction, the iron-nitrosyls, both in protein and synthetic model systems have been studied extensively and ferriheme proteins are known to undergo reduction in aqueous media in the presence of NO.[11-14] These reactions proceed through two distinct steps: (i) formation of iron(III)-nitrosyl adduct; (ii) followed by the pH dependent reduction of Fe^{III} to Fe^{II} with a simultaneous attack of hydroxide ion to the activated nitrosonium group [Fe^{III}-NO ↔ Fe^{II}-NO^{+}] leading to the formation of nitrite.[15-17] NO reduction of Cu^{II} are also known though have not been studied as extensively as iron-nitrosyls, both in proteins and synthetic model systems.[18-21] The groups of Lippard and Ford have reported several examples of reduction of Cu^{II} by NO and their use for NO detection.[22-28] Ford group has reported the detailed studies on ligand nitrosation observed during the reduction processes.[29] However, there are hardly any example which shows the distinct spectral evidence of

formation of [Cu^{II}-$NO^{\bullet}$] intermediate except the very recent ones.[30] In this context, here we report the interaction of NO with Cu^{II} complexes of two N-donor ligands (Figure 5.1) in acetonitrile solvent.

L_7 L_8

Figure 5.1: List of the ligands used for the present study.

5.2 Results and discussions

The complex **5.1** was prepared by the reaction of an acetonitrile solution of $[Cu(H_2O)_6](ClO_4)_2$ with two equivalents of the ligand, L_7 at room temperature for 1 h (experimental section).[31] On cooling, blue crystals of the complex were obtained from the mixture (Scheme 5.1). The complex **5.2** was synthesized following the same procedure except only one equivalent of the ligand, L_8 was used (experimental section).

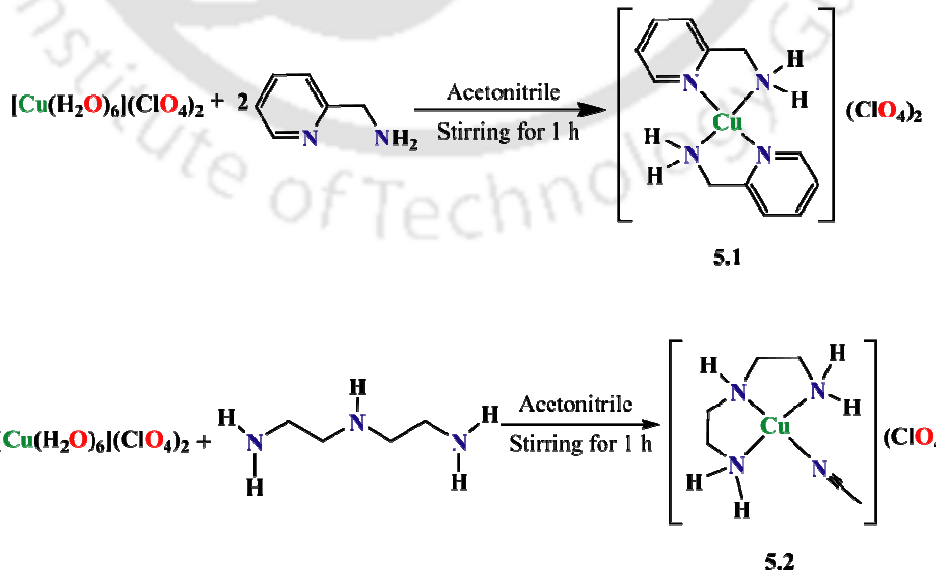

Scheme 5.1

All the complexes exhibited satisfactory elemental analyses (experimental section). The formation of the complex **5.1** had been further supported by X-ray single crystal structure (Figure 5.2) and various spectroscopic analyses such as UV-visible (Figure 5.3), FT-IR (Appendix IV, Figure A4.1) and EPR (Figure 5.4) spectroscopy.[32] Both the complexes showed vibrational bands at 1081 cm^{-1} and 625 cm^{-1} which confirmed the presence of perchlorate anions. The crystallographic table and the table for bond lengths and bond angles are given in Appendix IV (Table A4.1and A4.2). The room temperature magnetic moment measurement showed one electron paramagnetism for both the complexes (1.77 and 1.56 BM for complexes **5.1** and **5.2**, respectively). The complexes **5.1** and **5.2** displayed characteristic spectra in X-band EPR at room temperature in acetonitrile (g_{ave}, 2.07 and 2.14 for complexes **5.1** and **5.2**, respectively).[33] Both the complexes were found to behave as 1:2 electrolyte in acetonitrile solution [Λ_M ($\Omega^{-1}cm^2mol^{-1}$), 247 and 259 for complexes **5.1** and **5.2**, respectively].[34]

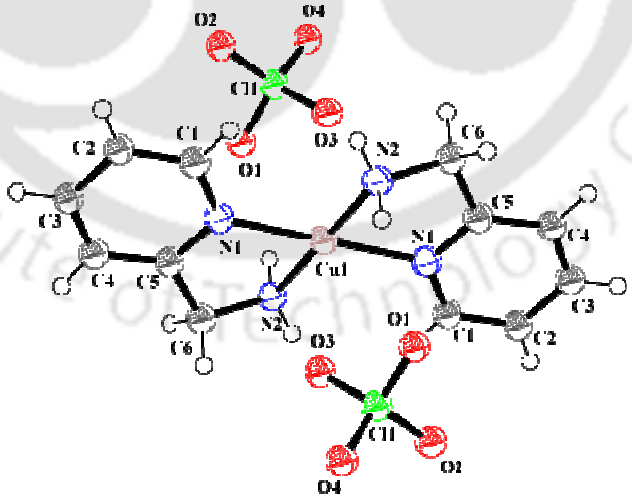

Figure 5.2: ORTEP diagram of complex **5.1**[a (-x, -y, -z) symmetry transformation is implied by each additional atom level] (50% Thermal ellipsoid plot).

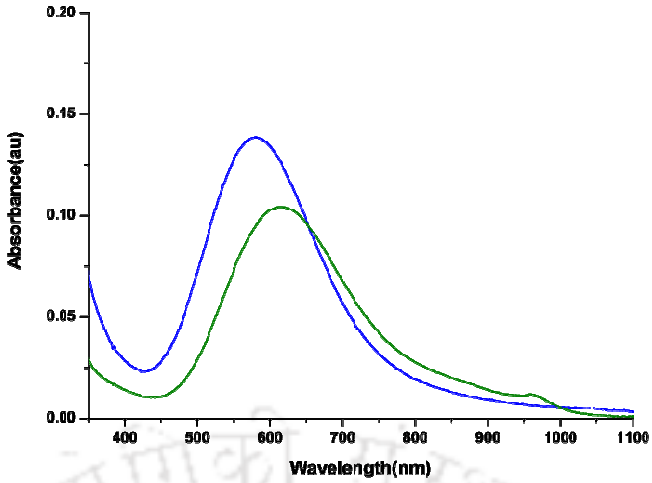

Figure 5.3: UV-visible spectra of complexes **5.1** (blue trace) and **5.2** (green trace) in acetonitrile solution.

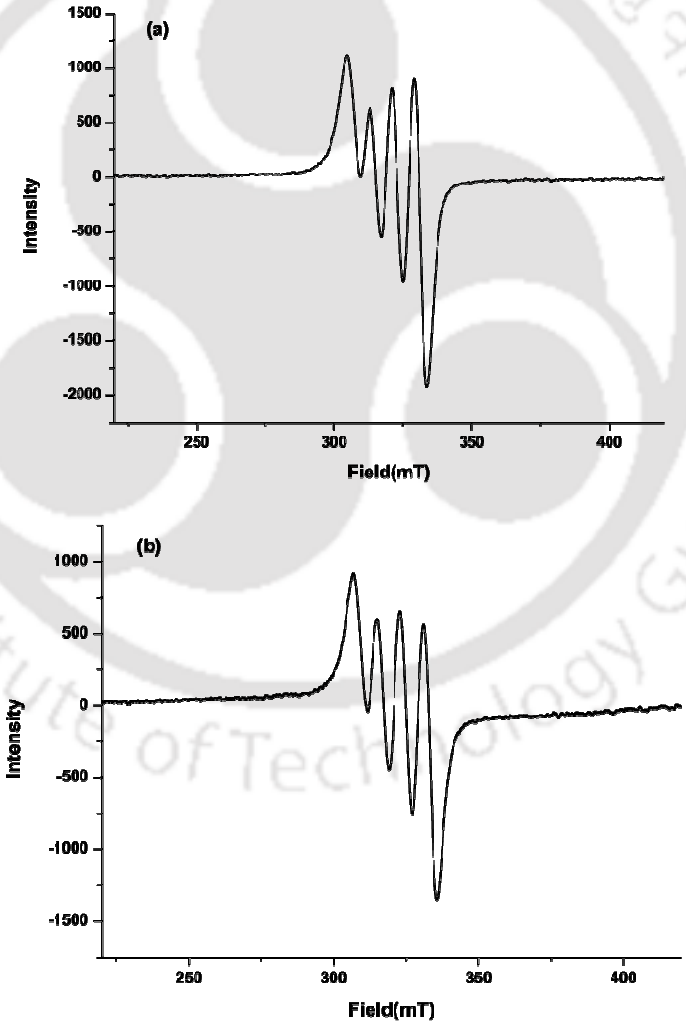

Figure 5.4: X-band EPR spectra of complexes (a) **5.1** and (b) **5.2** in acetonitrile solution at room temperature.

5.2.1 Nitric oxide reactivity in acetonitrile

The nitric oxide (NO) reactivity of both the complexes was studied in acetonitrile solution and the spectral changes were monitored by UV-visible spectroscopy. The *d-d* transition for complex **5.1** was found to appear at λ_{max}, 582 nm. On purging nitric oxide gas to a degassed acetonitrile solution of complex **5.1**, the position of the *d-d* transition shifted to 660 nm (Figure 5.5a). [Cu^{II}-$NO^{\bullet}$] intermediates observed in the reaction of [Cu(tiaea)(CH_3CN)]$^{2+}$ and [Cu(teaea)(CH_3CN)]$^{2+}$ [tiaea, *tris*-(2-isopropyl-

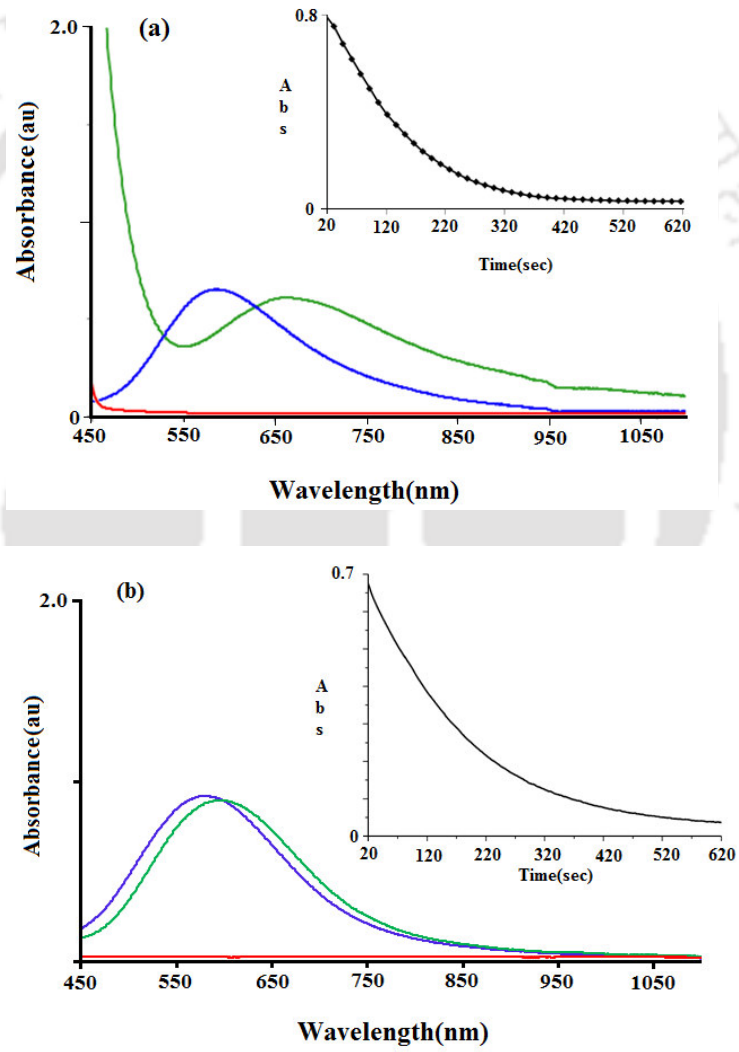

Figure 5.5: UV-visible spectra of the reaction of complexes (a) **5.1** and (b) **5.2** with NO in acetonitrile solvent at room temperature. (Blue trace represents the Cu^{II}-species, green represents that of the [Cu^{II}-$NO^{\bullet}$] intermediate and red trace represents the spectrum of fully reduced Cu^{I}-species){Insets are the corresponding time scan plots at 660 and 595 nm, for complexes **5.1** and **5.2**, respectively}.

aminoethyl)amine and teaea, *tris*-(2-ethylaminoethyl)amine], with NO were reported to display the *d-d* transition at 640 and 605 nm, respectively.[35] The intensity of the transition at 660 nm was found to diminish gradually with time indicating the reduction of Cu^{II} center to Cu^{I} (Figure 5.5a). It is presumably because of the formation of the thermally unstable [Cu^{II}-$NO^{\bullet}$] intermediate prior to reduction of Cu^{II} center. The same reduction was observed with complex **5.2**, also. The *d-d* transition for complex **5.2** at 575 nm, was found to shift to 595 nm immediately after purging NO gas and found to disappear with time (Figure 5.5b) following a pseudo first order rate law with respect to complex concentration. The calculated rate constants at 298 K were 1.3×10^{-3} sec^{-1} and 2.2×10^{-3} sec^{-1} for complexes **5.1** and **5.2**, respectively.

On purging NO to the degassed acetonitrile solution of complexes **5.1** and **5.2**, they became EPR silent. This can be attributed to the formation of [Cu^{II}-$NO^{\bullet}$] intermediates (Figure 5.6).[30] With $[Cu(tiaea)(CH_3CN)]^{2+}$ and $[Cu(teaea)(CH_3CN)]^{2+}$ complexes, also, the [Cu^{II}-$NO^{\bullet}$] species were observed to be EPR silent.[35]

The solution FT-IR spectra in acetonitrile solutions of complexes **5.1** and **5.2** after purging NO were recorded. A new intense and sharp band was found to appear at ~1642 cm^{-1} and 1635 cm^{-1} for complexes **5.1** and **5.2**, respectively, corresponding to the vibration of NO coordinated to the Cu^{II} center (Figure 5.7).[36] It would be worth mentioning here that the addition of nitrosyl perchlorate to acetonitrile solution of the free ligands did not give rise to these vibrations which, in turn, supports their assignment. These ν_{NO} of [Cu^{II}-$NO^{\bullet}$] were found to disappear with time indicating the unstable nature of the intermediate (Figure 5.7). Hence, the appearance of the band at ~1642 cm^{-1} and 1635 cm^{-1} for complexes **5.1** and **5.2**, respectively, supports the

formation of the [Cu^{II}-$NO^{\bullet}$] prior to the reduction of Cu^{II} centers in both the cases. In case of $[Cu(tren)(CH_3CN)]^{2+}$ [tren = N,N-*bis*-(2-aminoethyl)ethane-1,2-diamine] complex, the ν_{NO} of [Cu^{II}-$NO^{\bullet}$] was found to appear at1650 cm^{-1}.[36] It would be worth mentioning here that for the air-stable solid copper-nitrosyl of copper(II) dithiocarbamate, the ν_{NO} for the NO coordinated to copper appears at 1682 cm^{-1}.[30] Recently, Hayton et. al. reported the appearance of ν_{NO} band at 1933 cm^{-1} for structurally characterized copper(II)-nitrosyl.[30]

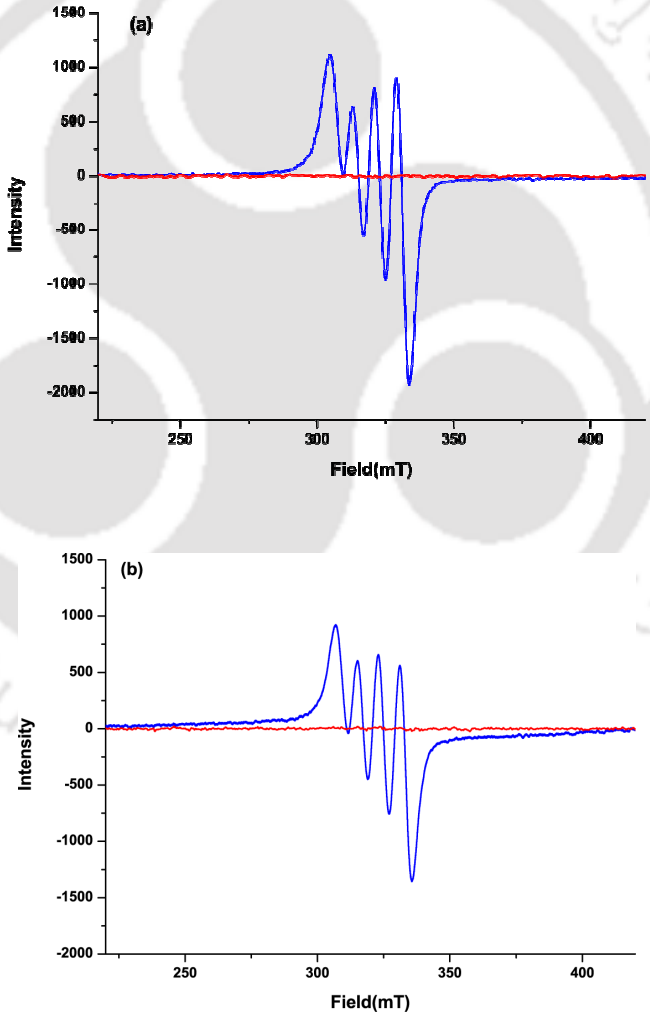

Figure 5.6: X-band EPR spectra of complexes (a) **5.1** and (b) **5.2** after reaction with NO in acetonitrile solvent at room temperature. (Black traces correspond to the respective complexes and red traces represent the spectra of [Cu^{II}-$NO^{\bullet}$] intermediates).

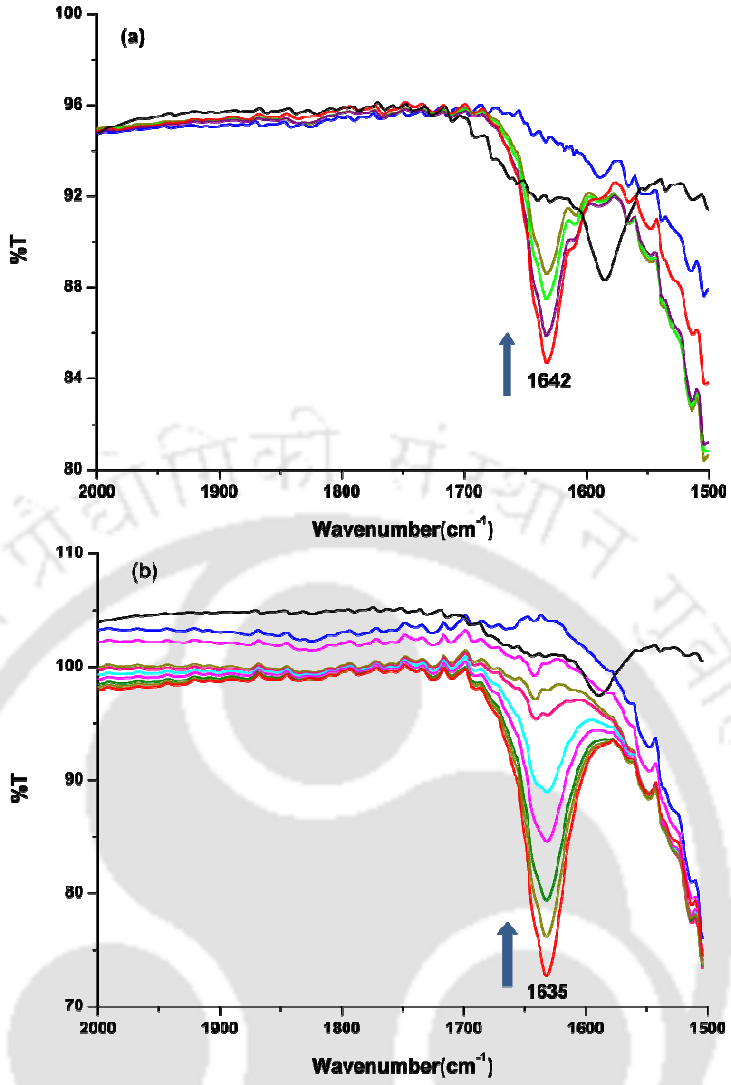

Figure 5.7: The solvent subtracted FT-IR spectra obtained from the reaction of complexes (a) **5.1** and (b) **5.2** with NO in acetonitrile at room temperature. The top blue trace represents the spectra of complexes befor purging NO in acetonitrile; red trace represents the spectra of [Cu^{II}-$NO^{\bullet}$] intermediate after the reaction of complexes with NO and black trace represents the spectra of the colorless species obtained after complete reduction.

The reduction of Cu^{II} centre was further authenticated in case of complex **5.2** by the single crystal structure determination of the reduced complex, $[Cu(CH_3CN)_4]ClO_4$. Since the crystal structure of $[Cu(CH_3CN)_4]ClO_4$ has already been reported by Soregh

et. al., attempt were not made to grow better quality crystals of $[Cu(CH_3CN)_4](ClO_4)$.[37]

There are not much report on the detailed studies of the Cu^{II}/NO reactions. Tran et. al. studied the NO reduction of the Cu^{II} complex, $[Cu(dmp)_2(H_2O)]^{2+}$ (dmp, 2,9-dimethyl-1,10-phenanthroline), in aqueous solution and in various mixed solvents.[38] In methanol, the product of the $[Cu(dmp)_2(H_2O)]^{2+}$ oxidation of NO is CH_3ONO; in water, it is NO_2^-. They observed that the reaction did not occur in pure acetonitrile or CH_2Cl_2 unless a protic reactant such as methanol or water was added, and in such solutions the reaction rate was linearly dependent on the concentration of alcohol/water added.[38] In comparison, complexes **5.1** and **5.2** exhibited facile reduction of Cu^{II} center in neat acetonitrile without the presence of any protic solvent.

In the present cases, on the basis of spectral evidence of formation of the $[Cu^{II}\text{-}NO^{\bullet}]$ intermediate, the NO reduction process can be rationalized in terms of an inner sphere mechanism as illustrated in scheme 5.2. It is believed that in the first step NO coordinates to the Cu^{II} center to form an inner sphere complex, $[Cu^{II}\text{-}NO^{\bullet}]$, which is susceptible toward nucleophilic attack by the amine center of the ligands owing to charge transfer from NO to the metal center $[Cu^{II}\text{-}NO^{\bullet} \leftrightarrow Cu^{I}\text{-}NO^{+}]$. The presence of terminal primary amine groups in the ligand frameworks might provide a facile site for the attack of the generated NO^+ resulting into the ligand modification through diazotization. The dissociation of the modified ligand from the metal center would be rapid step owing to higher stability of $[Cu^{I}(CH_3CN)_4]^+$ and preferential tetrahedral coordination. It would be worth mentioning here that in case of $[Cu(dmp)_2(H_2O)]^{2+}$, reported by Tran et. al., though a putative inner sphere complex, $[Cu(dmp)_2(NO)]^{2+}$ was proposed to form, no spectral evidence was observed.[38] Even in the early stage of

spectral changes when the reactive aqueous solutions were mixed in the stopped-flow kinetics spectrophotometer, there was no obvious indication of the formation of the $[Cu^{II}\text{-}NO^{\bullet}]$ intermediate, in case of $[Cu(dmp)_2(NO)]^{2+}$.[38]

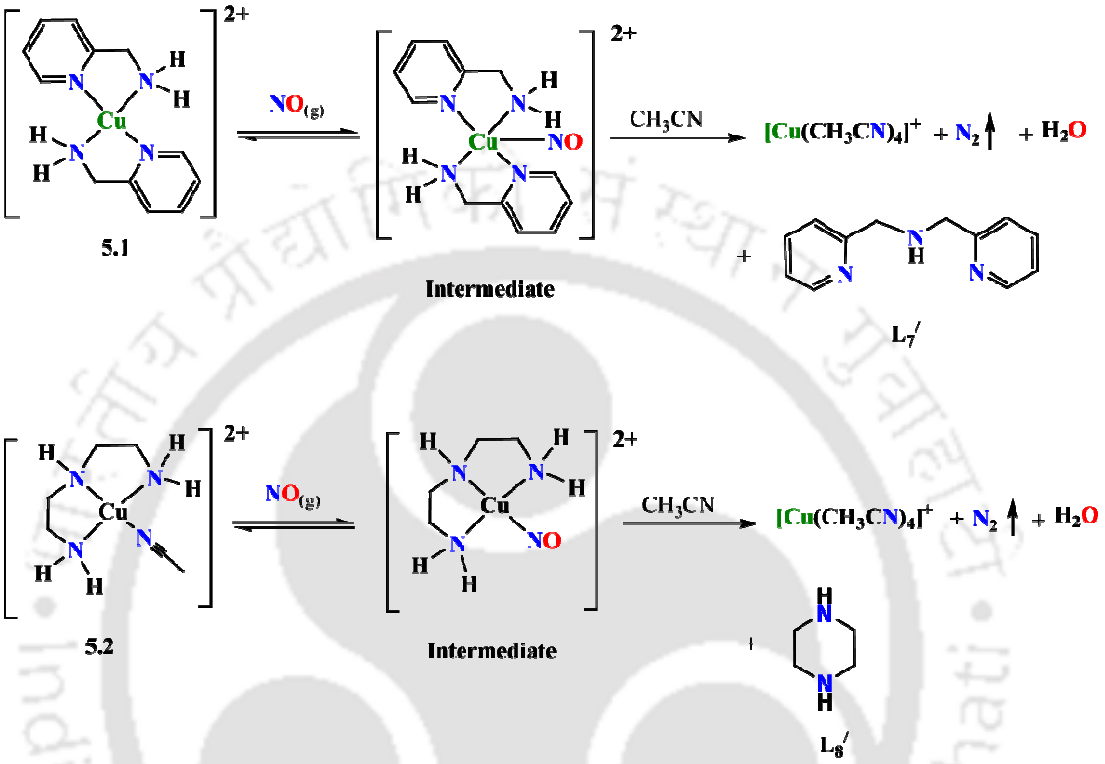

Scheme 5.2

To evaluate the viability of both the two potential mechanisms, Ford et. al. studied the NO reduction of $[Cu(dpp)_2]^{2+}$ (dpp, 2,9-diphenyl-1,10-phenanthroline) in methanol solution.[38] Since $[Cu(dpp)_2]^{2+}$ has higher reduction potential compared to $[Cu(dmp)_2(H_2O)]^{2+}$ and 2, 9-di-phenyl groups in dpp are more bulky than methyl groups in the same site in dmp, it is expected that $[Cu(dpp)_2]^{2+}$ would be more reactive compared to $[Cu(dmp)_2(H_2O)]^{2+}$ *via* outer sphere mechanism but less so *via* inner sphere one. It has been found that the latter one appears to be the case. However, there were no direct spectral evidence of formation of the $[Cu^{II}\text{-}NO^{\bullet}]$ intermediate complex. This inner sphere mechanism scheme involving the NO

coordination to the metal center before reduction, is consistent for the reductive nitrosylation of various ferrihemes and ferrihemoproteins reported by Wayland and Hoshino et al.[15, 39, 40] It would be worth mentioning here that for the reduction of Cu^{II} center by NO in $[Cu(DAC)_2]^{2+}$ (DAC, 1,8-bis(9-anthracylmethyl)-derivative of the macrocyclic tetraamine cyclam), a somewhat different mechanism have been proposed.[22] The initial step is proposed to be the reversible deprotonation of the coordinated secondary amine followed by the addition of NO at the amide site with a simultaneous electron transfer to reduce the Cu^{II} center.

The reduction of Cu^{II} ion by NO in the present set of complexes were accompanied with concomitant diazotization of the primary amine center of the ligands which resulted into the modification of the respective ligand frameworks (Scheme 5.2) and a putative mechanism of the formation of $\mathbf{L_7'}$ is illustrated in scheme 5.3. The diazotization of primary amines by copper-nitrosyls has been observed earlier also.[40]

In case of $[Cu(tren)(CH_3CN)]^{2+}$ (Complex **3.1**, Chapter 3), in pure acetonitrile, the formation of 2-piperazin-1-ylethanamine was reported to be because of the diazotization of the primary amine center of tren by the in-situ generated NO^+ from the reduction of Cu^{II} center by NO.[36] However, the same reaction, in acetonitrile:water (10:1) mixture, did not found to result the diazotization product. This is because of the higher reactivity of NO^+ towards water to afford NO_2^-.[36] On the other hand, $[Cu(tiaea)(CH_3CN)]^{2+}$ and $[Cu(teaea)(CH_3CN)]^{2+}$ were reported to afford tri-N-nitrosoamine concomitant to the reduction of Cu^{II} center.[35]

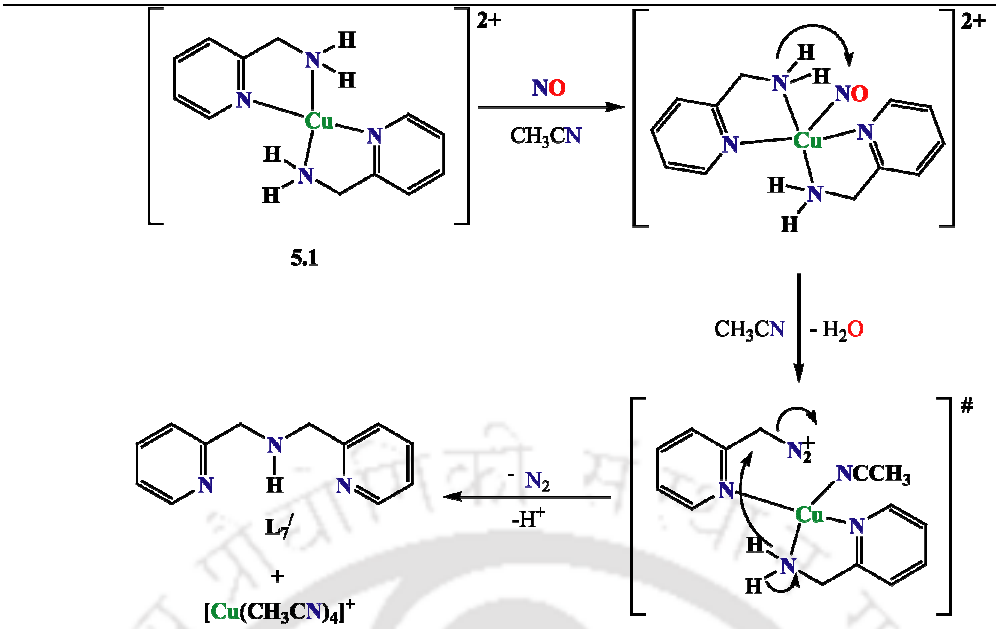

Scheme 5.3

Ford et. al. reported that the reduction of Cu^{II} center by NO in $[Cu^{II}(DAC)]^{2+}$ complex in methanol solution was accompanied by N-nitrosation of the ligand.[22b] In case of $[Cu^{II}(DAC)]^{2+}$, after reduction and nitrosation, the release of modified ligand was attributed to the fact that the Cu^{I} favors tetrahedral geometry; whereas the DAC ligand favors square planar one. At the same time the nitrosation also weakens the binding ability of the amine nitrogen.[22b] In the present case, the release of $\mathbf{L_7}'$ and $\mathbf{L_8}'$ can be attributed to the weakening of amine binding to the Cu^{I} due to the planar structure of the modified ligand in case of complex **5.1** and the ring structure in case of complex **5.2**.

The modified ligand, $\mathbf{L_7}'$ was characterized by various spectroscopic techniques (Experimental section and Appendix IV, Figures A4.2-A4.5). The formation of $\mathbf{L_8}'$ was confirmed by comparing its spectral data such as ^{1}H NMR, ^{13}C-NMR, FT-IR and ESI-mass spectra with that of the authentic sample of piperazine (Experimental section and Appendix IV, Figures A4.6-A4.9). It was observed that the free ligands, in

degassed acetonitrile, on bubbling with NO did not result into the same ligand transformation.

5.3 Conclusion

The reduction of Cu^{II} centres in complexes, **5.1** and **5.2**, by NO was studied in acetonitrile. Both the complexes resulted into the formation of thermally unstable [Cu^{II}-$NO^{\bullet}$] intermediate prior to the reduction. The intermediate has been characterized by UV-visible, solution FT-IR and EPR spectroscopy. The decomposition of the intermediate resulting in the completely reduced [$Cu^{I}(CH_3CN)_4$] was found to follow the pseudo-first order kinetics. A detailed study of the NO reduction kinetics of $[Cu^{II}(dmp)_2(H_2O)]^{2+}$ and $[Cu(dpp)_2]^{2+}$ were reported earlier where the involvement of the [Cu^{II}-$NO^{\bullet}$] intermediate was speculated without any spectral evidence. A completely different mechanism was proposed for the similar reduction of Cu^{II} center by NO in $[Cu(DAC)_2]^{2+}$. The present study, demonstrates the formation of well characterized [Cu^{II}-$NO^{\bullet}$] intermediate as seen in case of reductive nitrosylation of ferriheme proteins. The reduction of Cu^{II} centers in complexes **5.1** and **5.2**, were observed to result in the ligand modification. The modified ligands were isolated and completely characterized.

5.4 Experimental Section

5.4.1 Materials and methods

All reagents and solvents were purchased from commercial sources and were of reagent grade. Acetonitrile was distilled from calcium hydride. Deoxygenation of the solvent and solutions were effected by repeated vacuum/purge cycles or bubbling with nitrogen for 30 minutes. NO gas was purified by passing through KOH and P_2O_5

column. UV-visible spectra were recorded on a Perkin Elmer Lambda-25, UV-visible spectrophotometer. FT-IR spectra of the solid samples were taken on a Perkin Elmer spectrophotometer with samples prepared as KBr pellets and for solutions, Varian 660-IR FT-IR spectrometer and NaCl cell of 2 mm path length were used and the spectra shown are the solvent subtracted ones. Solution electrical conductivity was checked using a Systronic 305 conductivity bridge. ^{1}H-NMR spectra were obtained with a 400 MHz Varian FT spectrometer. Chemical shifts (ppm) were referenced either with an internal standard (Me_4Si) or to the residual solvent peaks. The X-band Electron Paramagnetic Resonance (EPR) spectra were recorded on a JES-FA200 ESR spectrometer, at room temperature. Elemental analyses were obtained from a Perkin Elmer Series II Analyzer. The magnetic moment of complexes is measured on a Cambridge Magnetic Balance.

Single crystals were grown by slow diffusion followed by slow evaporation technique. The intensity data were collected using a Bruker SMART APEX-II CCD diffractometer, equipped with a fine focus 1.75 kW sealed tube MoK_α radiation (λ = 0.71073 Å) at 273(3) K, with increasing ω (width of 0.3° per frame) at a scan speed of 3 s/frame. The SMART software was used for data acquisition. Data integration and reduction were undertaken with SAINT and XPREP software.[41, 42] Structures were solved by direct methods using SHELXS-97 and refined with full-matrix least squares on F^2 using SHELXL-97.[43] All non-hydrogen atoms were refined anisotropically. Structural illustrations have been drawn with ORTEP-3 for Windows.[44]

5.4.2 Synthesis of complex 5.1, $[Cu(L_7)_2](ClO_4)_2$

Copper(II) perchlorate hexahydrate, $[Cu(H_2O)_6](ClO_4)_2$ (370 mg, 1.0 mmol) was dissolved in 10 ml of freshly distilled acetonitrile and to this blue solution, the ligand

L_7 , 2-aminomethyl pyridine (216 mg, 2.0 mmol), was added drop wise. The color of the solution changed to violet. The resulting mixture was stirred for 1 h. Then the volume of the solution was reduced to ~2 ml and layered with benzene. Storage of this at ~ -20°C overnight resulted in the precipitation of blue crystalline compound. Yield: 410 mg (~ 85%). Elemental Analyses: Calcd.(%) for $C_{14}H_{16}N_4O_8Cl_2Cu$: C, 21.36; H, 4.67; N, 15.57. Found (%) C, 21.33; H, 4.67; N, 15.55. UV-vis. (acetonitrile): λ_{max}, 582 nm (ε, 138 M^{-1} cm^{-1}) and 302 nm (ε, 4120 M^{-1} cm^{-1}). FT-IR (KBr pellet): υ_{ClO4^-}, 1081 cm^{-1}, 625 cm^{-1}. X-band EPR data: g_{av}, 2.07. Molar conductance: Λ_M ($\Omega^{-1}cm^2mol^{-1}$), 247 in acetonitrile. μ_{eff} : 1.77 BM.

5.4.3 Synthesis of complex 5.2, $[Cu(L_8)(CH_3CN)](ClO_4)_2$

$[Cu^{II}(H_2O)_6](ClO_4)_2$ (370 mg, 1.0 mmol) was dissolved in 10 ml freshly distilled acetonitrile. To this solution, 103 mg (1.0 mmol) of the ligand **L_8**, *bis*-(2-aminoethyl)amine was added slowly with constant stirring. The color of the solution turned into deep blue. The stirring was continued for 1h at room temperature. The volume of the solution then reduced to ~2 ml. Benzene (5 ml) was layered onto this solution and storage at ~ -20 °C overnight resulted in the precipitation of blue microcrystals of complex **5.2**. Yield: 0.350 g (85%). Elemental Analyses: Calcd.(%) for $C_6H_{16}N_4O_8Cl_2Cu$: C, 19.20; H, 5.24; N, 16.79. Found (%): C, 19.22; H, 5.25; N, 16.75. UV-vis. (acetonitrile): λ_{max}, 575 nm (ε, 140 M^{-1} cm^{-1}). FT-IR (KBr pellet): υ_{ClO4^-}, 1095 cm^{-1}, 627 cm^{-1}. The X-band EPR data: g_{av}, 2.14. Molar conductance: Λ_M ($\Omega^{-1}cm^2mol^{-1}$), 259 in acetonitrile. μ_{eff} : 1.56 BM.

5.4.4 Isolation of $[Cu^{I}(CH_3CN)_4]ClO_4$

In a 50 ml Schlenk flask, complex **5.1** (240 mg, 0.5 mmol) was dissolved in 10 ml degassed acetonitrile. To this solution, NO gas was purged through a needle for one minute and allowed to stand for 10 minutes. To the resulting colorless solution, 15 ml of degassed benzene was added through a syringe to make a layer. The layered solution was then kept overnight in freezer. The white crystals of $[Cu(CH_3CN)_4]ClO_4$ were filtered out from the colorless solution under nitrogen atmosphere using a Schlenk frit. Yield, 115 mg, ~70%.

Same procedure was followed to isolate the $[Cu(CH_3CN)_4]ClO_4$ from the reaction of complex **5.2** (204 mg, 0.5 mmol) and NO in acetonitrile solution. Yield: 100 mg, ~60%.

5.4.5 Isolation of L_7'

In a 50 ml Schlenk flask, complex **5.1** (240 mg, 0.5 mmol) was dissolved in 15 ml degassed acetonitrile. To this, NO gas was purged through a needle for one minute and the mixture was then allowed to stand for 10 minutes. To the colorless solution, thus obtained, 20 ml of degassed benzene was added through a syringe to make a layer. The layered solution was then kept overnight in freezer. The white crystals of $[Cu(CH_3CN)_4]ClO_4$ were filtered out from the colorless solution under nitrogen atmosphere using a Schlenk frit. The volume of the filtrate was then reduced to 5 ml and stirred for 1 h in open air in order to allow the residual Cu^{I} center to oxidise to Cu^{II}. To this, 5 ml saturated aqueous solution of Na_2S was added and stirred for ½ h. The black precipitate thus obtained was filtered off and the filtrate was diluted with 50 ml of distilled water. The organic part was then extracted from the mixture using $CHCl_3$ (3 portions × 25 ml). The collected organic layer was then dried under reduced

pressure and the residual oil was subjected to column chromatography using silica gel to yield $\mathbf{L_7'}$ (60 mg, ~ 60%). ^{1}H-NMR(400 MHz, $CDCl_3$), δ_{ppm}, 1.54 (s, 4H), 7.00 (t, 2H), 7.41(t, 2H), 7.94(d, 2H), 8.36(d, 2H). ^{13}C-NMR(100 MHz, $CDCl_3$), δ_{ppm}, 158.92, 149.01, 136.32, 124.66, 120.51, 49.02. FT-IR in KBr pellet: 1035(m), 1069 (s), 1241(s), 1262(m), 1361(s), 1430(w), 1498(w), 1540(w), 1635(w) cm^{-1}. ESI-Mass: (m+1)/z, 200.02.

5.4.6 Isolation of $\mathbf{L_8'}$

$\mathbf{L_8'}$ was isolated from the reaction of complex **5.2** with NO in acetonitrile following the same procedure for $\mathbf{L_8'}$. Yield: 30 mg, ~ 70%. ^{1}H-NMR(400 MHz, $CDCl_3$), δ_{ppm}, 2.79 (CH_2), 1.90 (NH). ^{13}C-NMR(100 MHz, $CDCl_3$), δ_{ppm}, 47.64. FT-IR in KBr pellet, 1551(s), 1434(s), 1274(s), 1129(w), 1000(m), 854(w) cm^{-1}. ESI-Mass: (m+1)/z, 87.08. All data are found to be in agreement with that of piperazine.

5.5 References

1. Richter-Addo, G. B.; Legzdins, P. *Metal Nitrosyls*; Oxford University Press, New York, **1992**.
2. (a) Studbauer, G.; Giuffre, P.; Sarti, P.; *J. Biol. Chem.* **1999**, *274*, 28128. (b) Moncada, S.; Palmer, R. M. J.; Higgs, E. A. *Pharmacol. Rev.* **1991**, *43*, 109. (c) Butler, A. R.; Williams, D. L.; *Chem. Soc. Rev*. **1993**, 233.
3. (a) Feelisch, M.; Stamler, J. S. *Methods in Nitric Oxide Research*; John Wiley and Sons; Chichester, England, **1996**. (b) Jia, L.; Bonaventura, C.; Bonaventura, J.; Stamler, J. S. *Nature*, **1996**, *380*, 221. (c) Galdwin, M. T.; Lancaster, J. R. Jr.; Freeman, B. A.; Schechter, A. N. *Nat. Med*. **2003**, *9*, 496.
4. (a) Ye, R. W.; Toro-Suarez, I.; Tiedje, J. M.; Averill, B. A. *J. Biol. Chem.* **1991**, *266*, 12848. (b) Hulse, C. L.; Averill, B. A.; Tiedje, J. M. *J. Am. Chem. Soc.*

1989, *111*, 2322. (c) Jackson, M. A.; Tiedje, J. M.; Averill, B. A. *FEBS Lett.* **1991**, *291*, 41.

5. (a) Godden, J. W.; Turley, S.; Teller, D. C.; Adman, E. T.; Liu, M. Y.; Payne, W. J.; LeGall, J. *Science,* **1991**, *153*, 438. (b) Adman, E. T.; Turley, S. In *Bioinorganic Chemistry of Copper;* Karlin, K. D., Tyekllr, Z., Eds.; Chapman & Hall, Inc.: New York, **1993**; pp 397. (c) Ferguson, S. J. *Curr. Opin. Chem. Biol.* **1998**, *2*, 182.
6. (a) Richardson, D. J.; Watmough, N. J. *Curr. Opin. Chem. Biol.* **1999**, *3*, 207. (b) Moura, I.; Moura, J. J. G. *Curr. Opin. Chem. Biol.* **2001**, *5*, 168. (c) Tocheva, E. I.; Rosell, F. I.; Mauk, A. G.; Murphy, M. E. P. *Biochem.* **2007**, *46*, 12366. (d) Ghosh, S.; Dey, A.; Usov, O. M.; Sun, Y.; Grigoryants, V. M.; Scholes, C. P.; Solomon, E. I. *J. Am. Chem. Soc*. **2007**, *129*, 10310.
7. Libby, E.; Averill, B. A. *Biochem. Biophys. Res. Commun.* **1992**, *187*, 1529.
8. (a) Stamler, J. S.; Singel, D. J.; Loscalzo, J. *Science*, **1992**, *258*, 1898. (b) Williams, R. J. P. *Chem. Soc. Rev.* **1996**, 77. (c) Drapier, J.-C.; Bouton, C. *Bioessays* **1996**, *18*, 549.
9. (a) Stamler, J. S. *Cell*, **1994**, *78*, 931. (b) Feelisch, M. S.; Rassaf, T.; Mnaimneh, S.; Singh, N.; Byran, N. S.; Jourd'Heuil, D.; Kelm, M. *FASEB J.* **2002**, *16*, 1775.
10. (a) Bryan, N. S.; Rassaf, T.; Maloney, R. E.; Rodriguez, C. M.; Saijo, F.; Rodriguez, J. R.; Feelisch, M. *Proc. Natl. Acad. Sci. U. S. A.* **2004**, *101*, 4308. (b) Luchsinger, B. P.; Rich, E. N.; Gow, A. J.; Williams, E. M.; Stamler, J. S.; Singel, D. J. *Proc. Natl. Acad. Sci. U. S. A.* **2003**, *100*, 461.
11. (a) Chien, J. C. W. *J. Am. Chem. Soc.* **1969**, *91*, 2166. (b) Wayland, B. B.; Olson, L. W. *J. Am. Chem. Soc.* **1974**, *96*, 6037. (c) Trofimova, N. S.; Safronov, A. Y.; Ikeda, O. *Inorg. Chem.* **2003**, *42*, 1945.

12. (a) Walker, F. A. *J. Inorg. Biochem.* **2005**, *99*, 216. (b) Rousseau, D. L.; Li, D.; Couture, M.; Yeh, S. R. *J. Inorg. Biochem.* **2005**, *99*, 306. (c) George, S. J.; Allen, J. W. A.; Ferguson, S. J.; Thorneley, R. N. F. *J. Biol. Chem.* **2000**, *275*, 33231.

13. (a) Pinakoulaki, E.; Gemeinhardt, S.; Saraste, M.; Varotsis, C. *J. Biol. Chem.* **2002**, *277*, 23407. (b) Praneeth, V. K. K.; Paulat, F.; Berto, T. C.; DeBeer George, S.; Nather, C.; Sulok, C.; Lehnert, N. *J. Am. Chem. Soc.* **2008**, *130*, 15288.

14. (a) Soldatova, A. V.; Ibrahim, M.; Olson, J. S.; Czernuszewicz, R. S.; Spiro, T. G. *J. Am. Chem. Soc.* **2010**, *132*, 4614. (b) Wasser, I. M.; de Vries, S.; Moe¨nne-Loccoz, P.; Schro¨der, I.; Karlin, K. D. *Chem. Rev.* **2002**, *102*, 1201.

15. (a) Hoshino, M.; Maeda, M.; Konishi, R.; Seki, H.; Ford, P. C. *J. Am. Chem. Soc.* **1996**, *118*, 5702. (b) Fernandez, B. O.; Lorkovic, I. M.; Ford, P. C. *Inorg. Chem.* **2004**, *43*, 5393. (c) Lehnert, N.; Praneeth, V. K. K.; Paulat, F. *J. Comput. Chem.* **2006**, *27*, 1338.

16. (a) Ellison, M. K.; Scheidt, W. R. *J. Am. Chem. Soc.* **1999**, *121*, 5210. (b) Linder, D. P.; Rodgers, K. R.; Banister, J.; Wyllie, G. R. A.; Ellison, M. K.; Scheidt, W. R. *J. Am. Chem. Soc.* **2004**, *126*, 14136.

17. (a) Lim, M. D.; Lorkovic, I. M.; Ford, P. C. *J. Inorg. Biochem.* **2005**, *99*, 151. (b) Shamir, D.; Zilbermann, I.; maimon, E.; Gellerman, G.; Cohen, H.; Meyerstein, D. *Eur. J. Inorg. Chem.* **2007**, 5029.

18. (a) Martin, C. T.; Morse, R. H.; Kanne, R. M.; Gray, H. B.; Malmstrom, B. G.; Chan, S. I. *Biochem.* **1981**, *20*, 5147. (b) Gorren, A. C. F.; de Boer, E.; Wever, R. *Biochem. Biophys. Acta* **1987**, *916*, 38. (c) Cooper, C. E.; Torres, J.; Sharpe, M. A.; Wilson, M. T. *FEBS Lett.* **1997**, *414*, 281.

19. (a) Torres, J.; Cooper, C. E.; Wilson, M. T. *J. Biol. Chem*. **1998**, *273*, 8756. (b) Torres, J.; Svistunenko, D.; Karlsson, B.; Cooper, C. E.; Wilson, M. T. *J. Am. Chem. Soc*. **2002**, *124*, 963.

20. (a) Tran, D.; Ford, P. C. *Inorg. Chem.* **1996**, *35,* 2411. (b) Lim, M. D.; Capps, K. B.; Karpishin, T. B.; Ford, P. C. *Nitric Oxide, Biol. Chem.* **2005**, *12*, 244.

21. (a) Brown, G. C. *Biochim. Biophys. Acta* **2001**, *1504*, 46. (b) Torres, J.; Sharpe, M. A.; Rosquist, A.; Cooper, C. E.; Wilson, M. T. *FEBS Lett.* **2000**, *475*, 263. (c) Wijma, H. J.; Canters, G. W.; de Vries, S.; Verbeet, M. P. *Biochem.* **2004**, *43*, 10467.

22. (a) Ford, P. C.; Fernandez, B. O.; Lim, M. D. *Chem. Rev*. **2005**, *105*, 2439. (b) Tsuge, K.; DeRosa, F.; Lim, M. D.; Ford, P. C. *J. Am. Chem. Soc*. **2004**, *126*, 6564. (c) Lim, M. H.; Wong, B. A.; Pitcock, W. H. Jr.; Mokshagundam, D.; Baik, M-H.; Lippard, S. J. *J. Am. Chem. Soc*. **2006**, *128*, 14364.

23. (a) Lim, M. H.; Lippard, S. J. *Inorg. Chem*. **2006**, *45*, 8980. (b) Lim, M. H.; Lippard, S. J. *J. Am. Chem. Soc.* **2005**, *127*, 12170. (c) Lim, M. H.; Xu, D.; Lippard, S. J. *Nat. Chem. Biol*. **2006**, *2*, 375.

24. (a) Franz, K. J.; Singh, N.; Lippard, S. J. *Angew. Chem., Int. Ed.* **2000**, *39*, 2120. (b) Franz, K. J.; Singh, N.; Spingler, B.; Lippard, S. J. *Inorg. Chem.* **2000**, *39*, 4081.

25. (a) Hilderbrand, S. A.; Lippard, S. J. *Inorg. Chem.* **2004**, *43*, 4674. (b) Lim, M. H.; Lippard, S. J. *Inorg. Chem.* **2004**, *43*, 6366.

26. (a) Franz, K. J.; Singh, N.; Lippard, S. J. *Angew. Chem., Int. Ed.* **2000**, *39*, 2120. (b) Hilderbrand, S. A.; Lippard, S. J. *Inorg. Chem.* **2004**, *43*, 5294.

27. (a) Hilderbrand, S. A.; Lim, M. H.; Lippard, S. J. *J. Am. Chem. Soc.* **2004**, *126*, 4972. (b) Do, L.; Smith, R. C.; Tennyson, A. G.; Lippard, S. J. *Inorg. Chem.* **2006**, *45*, 8998.

28. (a) Rosenthal, J.; Lippard, S. J. *J. Am. Chem. Soc.* **2010**, *132*, 5536. (b) Lim, M. H.; Lippard, S. J. *Acc. Chem. Res.* **2007**, *40*, 41.

29. (a) Khin, C.; Lim, M. D.; Tsuge, K.; Iretskii, A.; Wu, G.; Ford, P. C. *Inorg. Chem*. **2007**, *46*, 9323.

30. (a) Tsumore, N.; Xu, Q. *Bull. Chem. Soc. Jpn.* **2002**, *75*, 1861. (b) Diaz, A.; Ortiz, M.; Sanchez, I. ; Cao, R.; Mederos, A.; Sanchiz, J.; Brito, F. *J. Inorg. Biochem.* **2003**, *95*, 283. (c) Wright, A. M.; Wu, G.; Hayton, T. W. *J. Am. Chem. Soc.* **2010**, *132*, 14336.

31. Ramadan A. M.; El-Naggar, M. M. *J. Inorg. Biochem*. **1996**, *63*, 143.

32. (a) Hu, H.-M.; Long, D.-L.; Zeng, H.-Y.; Cheng, W.-D.; Huang, J.-S. *Acta Crystallographica, Sec. C: Crystal Structure Commun.* **1999**, C55(5). (b) O'Connor, C. J.; Eduok, E. E.; Owens, J. W.; Stevens, E. D.; Klein, C. L. *Inorg. Chim. Acta* **1986**, *117*, 175.

33. (a) Addison, A. W.; Hendriks, H. M. J.; Reedijk, J.; Thompson, L. K. *Inorg. Chem.* **1981**, *20*, 103. (b) Sorrell, T. N.; Jameson, D. L. *Inorg. Chem*. **1982**, *21*, 1014.

34. Mondal, B.; Puranik, V. G.; Lahiri, G. K. *Inorg. Chem.* **2002**, *41*, 5831.

35. Sarma, M.; Kalita, A.; Kumar, P.; Singh, A.; Mondal, B. *J. Am. Chem. Soc.* **2010**, *132*, 7846.

36. (a) Fujishima, A.; Iwase, T.; Honda, K. *J. Am. Chem. Soc*. **1976**, *98*, 1627. (b) Sarma, M.; Singh, A.; Mondal, B. *Inorg. Chim. Acta*, **2010**, *363*, 63.

37. Soregh, C.; Kierkegaard, P.; Norrestam, R. *Acta Cryst.*, *Sect. B.* **1975**, *31*, 314.

38. Tran, D.; Skelton, B. W.; White, A. H.; Laverman, L. E.; Ford, P. C. *Inorg. Chem.* **1998**, *37*, 2505.

39. (a) Gwost, D.; Caulton, K. G., *Chem. Commun*, **1973**, 64. (b) Gwost, D.; Caulton, K. G. *Inorg. Chem.* **1973**, *12*, 2095.

40. (a) Wayland, B. B., Olson, L. W. *Chem. Commun*, **1973**, 897. (b) Hoshino, M.; Maeda, M.; Konishi, R.; Seki, H.; Ford, P. C. *J. Am. Chem. Soc.*, **1996**, *118*, 5702.

41. SMART, SAINT and XPREP, Siemens Analytical X-ray Instruments Inc., Madison, Wisconsin, USA, **1995**.

42. Sheldrick, G. M. SADABS: software for Empirical Absorption Correction, University of Gottingen, Institut fur Anorganische Chemieder Universitat, Tammanstrasse 4, D-3400 Gottingen, Germany, **1999–2003**.

43. Sheldrick, G. M. SHELXS-97, University of Gottingen, Germany, **1997**.

44. Farrugia, L. J. *J. Appl. Crystallogr.* **1997**, *30*, 565.

Chapter 6

Nitric oxide reactivity of copper(II) complexes of bidentate amine ligands having aliphatic and aromatic N-donor sites

Abstract

Two copper(II) complexes, **6.1** and **6.2** with $\mathbf{L_9}$ and $\mathbf{L_{10}}$ [$\mathbf{L_9}$, 2-(2-aminoethyl)-pyridine; $\mathbf{L_{10}}$, 2-(N-ethyl-2-aminoethyl)-pyridine], respectively, were synthesized and characterized. Addition of nitric oxide gas to the degassed acetonitrile solution of the complexes were found to result in unstable [Cu^{II}-$NO^{\bullet}$] intermediates followed by the reduction of the Cu^{II} center to Cu^{I}. The formation of the [Cu^{II}-$NO^{\bullet}$] intermediate was evidenced by UV-visible, solution FT-IR and X-band EPR spectroscopic studies. The reduction of Cu^{II} centers to Cu^{I} was monitored by various spectroscopic techniques. In case of complex **6.1**, the reduction of the Cu^{II} center by NO afforded ligand transformation through diazotization at the primary amine site in acetonitrile solution; whereas, in acetonitrile-water mixture, it resulted in 2-(pyridine-2-yl)ethanol. On the other hand, reduction of Cu^{II} center by NO in complex **6.2** was found to yield N-nitrosation at the secondary amine site in the ligand framework. The final organic products, in each case, were isolated and characterized by various spectroscopic studies.

6.1. Introduction

Activation of NO by transition metal ions has been a subject of interest for chemists and biochemists since its discovery as signaling agent in mammalian biology.[1-3] It has also been found to be responsible for immuno-cytotoxicity in mammals.[3] Some of these activities are attributed to the formation of nitrosyl complexes of metallo-proteins, mostly of iron and copper.[4] Iron-nitrosyls, both in protein and synthetic model systems, thus, have been studied extensively.[4-8] The reduction of Cu^{II} centres in some proteins, such as cytochrome *c* oxidase and laccase, to Cu^{I} by NO is known for a long time, has not been studied as extensively as iron.[6, 7] In recent years, however, this has been exemplified by a number of model Cu^{II} complexes. For instance, Cu^{II} centers in $[Cu(dmp)_2(X)]^{2+}$ (dmp = 2,9-dimethyl-1,10-phenanthroline, X = solvent) and analogous complexes were reported to undergo reduction by NO. From the detailed mechanistic study, reduction was proposed to proceed through a inner-sphere pathway though the formation of $[Cu^{II}\text{-}NO^{\bullet}]$ was not observed even in the early stage of reaction.[9, 10] It was observed that the reduction was accompanied by the nitrosation of the solvent resulting into methylnitrite or NO_2^- in case of methanol or water respectively (Equation 6.1).[9, 10]

$$[Cu(dmp)_2(X)]^{2+} + NO + CH_3OH \longrightarrow [Cu(dmp)_2]^{+} + CH_3ONO + H^{+} \quad \text{-----(6.1)}$$

In methanol solution, the Cu^{II} center of $[Cu^{II}(DAC)]^{2+}$ {DAC, 1,8-bis(9-anthracylmethyl) derivative of the macrocyclic tetraamine cyclam (1,4,8,11-tetraazacyclotetradecane)} was reported to be reduced by NO accompanied with a concomitant nitrosation of the ligand.[11, 12] Detail quantitative and theoretical studies suggested that the reaction proceeds through a pathway analogous to the inner-sphere mechanism for electron transfer between two metal centers through a bridging ligand

where NO is the reductant, Cu^{II}, the oxidant and the coordinated amido anion behaves as the bridging ligand. Coordination preference of Cu^{I} and the decreased donor ability of the nitrosated ligand resulted in the demetallation of the macrocyclic ring after the reduction. Similar mechanistic pathway was reported by Armor et al. in the reaction of $[Ru(NH_3)_6]^{3+}$ with NO in alkaline solution resulting into the Ru(II)-dinitrogen complex, $[Ru(NH_3)_5(N_2)]^{2+}$.[13] Nitrosation of a coordinated amide ligand with the concomitant reduction of Ru^{III} to Ru^{II} leads to the formation of a coordinated nitroso amine, which on subsequent dehydration results in the coordinated dinitrogen complex.

Wayland and others suggested an alternative mechanism, more close to that of ferriheme reduction, which involves the initial NO coordination to the Cu^{II} center to form $[Cu^{II}\text{-}NO \leftrightarrow Cu^{I}\text{-}NO^{+}]$.[14] It was proposed that in the successive steps, amine deprotonation and migration of NO^{+} to the coordinated amide would result into the nitrosoamine. Subsequently, demetalation from the ligand may occur.

In our recent studies, with $[Cu^{II}(tren)(CH_3CN)]^{2+}$, $[Cu^{II}(taea)(CH_3CN)]^{2+}$, $[Cu^{II}(tieae)(CH_3CN)]^{2+}$, $[Cu(pymea)_2]^{2+}$ and $[Cu(baea)(CH_3CN)]^{2+}$ [tren, *tris*-(2-aminoethyl)amine; taea, *tris*-(2-ethylaminoethyl)amine; tieae, *tris*-(2-isopropyl aminoethyl)amine; pymea, pyridine-2-methylamine and baea, *bis*-(2-aminoethyl)amine], the reduction was found to proceed through the formation of a thermally unstable $[Cu^{II}\text{-}NO^{\bullet}]$ intermediate.[15-17] It should be noted that in case of Cu^{II} complexes of ppmea and mimpea [ppmea, 2-(pyridin-2-yl)-N-((pyridin-2-yl)methyl)ethaneamine; mimpea, N-((methyl-1H-imidazol-2-yl)methyl)-2-(pyridine-2-yl)ethanamine], any indication of the formation of an $[Cu^{II}\text{-}NO^{\bullet}]$ inner-sphere complex have not been observed prior to the reduction.[18] This is attributed to the much lower values of the equilibrium constants, K_{NO}. This difference in mechanistic pathway is,

mostly, because of the difference in ligand environment. This has been exemplified in cases of $[Cu(mtad)]^{2+}$ and $[Cu(tmd)_2]^{2+}$ [mtad, 5,5,7,12,12,14-hexamethyl-1,4,8,11-tetraazacyclotetradecane; tmd, 5,5,7-trimethyl-[1,4]-diazepane].[19] It was found that in case of $[Cu(mtad)]^{2+}$, the reduction takes place in methanol medium in presence of sodium methoxide through a deprotonation pathway as reported earlier in case of $[Cu(DAC)]^{2+}$. On the other hand, the reduction was observed to be very facile in dry acetonitrile in case of $[Cu(mtd)_2]^{2+}$ and proceeds through a $[Cu^{II}\text{-}NO^{\bullet}]$ intermediate. Thus, it was noticed that though the macrocyclic ligands prefer deprotonation pathway, non-macrocyclic one prefers $[Cu^{II}\text{-}NO^{\bullet}]$ intermediate pathway which is similar to that observed in the ferriheme reduction. DFT calculations also suggested the facile formation of $[Cu^{II}\text{-}NO^{\bullet}]$ intermediate for $[Cu(mtad)]^{2+}$. Hence, it is logical to believe that the ligand frameworks have a significant role to control the mechanistic pathway for the reduction of Cu^{II}.

In this direction, as a continuation of our earlier work, two Cu^{II} complexes with ligands **L_9** and **L_{10}** [**L_9**, 2-(2-aminoethyl)-pyridine; **L_{10}**, 2-(N-ethyl-2-aminoethyl)-pyridine] (Figure 6.1) were prepared and their NO reactivity were studied.

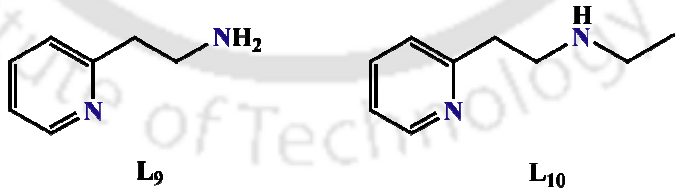

L_9 **L_{10}**

Figure 6.1: Ligands used for the present study.

6.2 Results and discussions

Ligand, **L_{10}** was synthesized following general procedure for the mono-alkylation of primary amines (Appendix V).[20] The elemental analyses of the synthesized ligand was

found to be in good agreement with the calculated values. It was further characterized by FT-IR, ^{1}H-NMR, ^{13}C-NMR and ESI-Mass spectroscopy (Appendix V, Figures A5.1-A5.12). The complexes **6.1** and **6.2** were synthesized by the reaction of hexaaquacopper(II)perchlorate with the respective ligands in 1:2 molar equivalence and isolated as solid (Scheme 6.1).

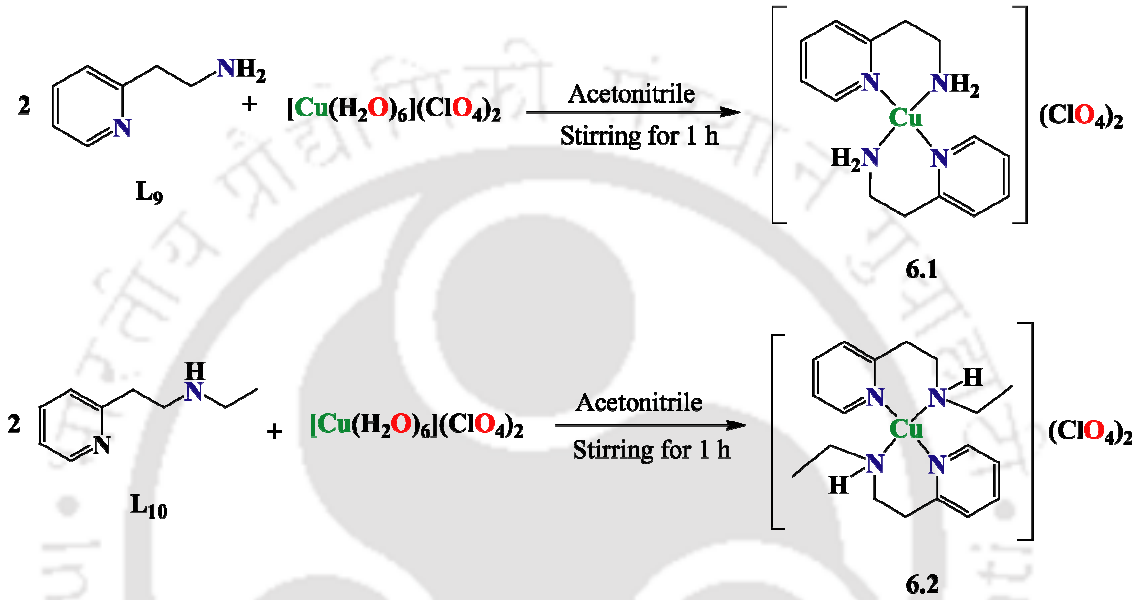

Scheme 6.1

All the complexes displayed satisfactory elemental analyses (experimental section). The formation of complex **6.1** was further confirmed by its X-ray single crystal structure determination. The crystal structure of complex **6.1** was reported earlier.[21] The crystallographic data was given in appendix V (Table A5.1). The ORTEP diagram of complex **6.1** is shown in figure 6.2.

The *d-d* transition for complexes **6.1** and **6.2** appears at 576 and 596 nm, respectively, in acetonitrile solvent (Figure 6.3). This shift in λ_{max} can be attributed to the increasing order of covalent character of the σ-bond on moving from H to ethyl group at the N-substitution.[22]

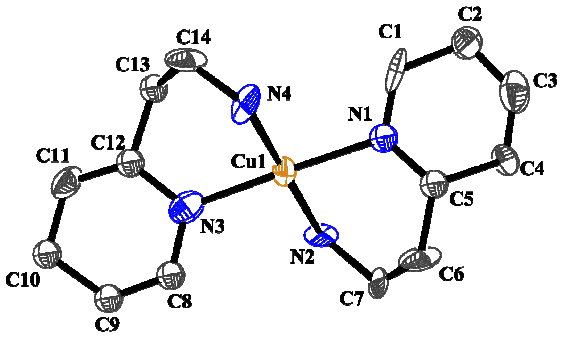

Figure 6.2: ORTEP diagram of complex **6.1** (50% thermal ellipsoid plot).

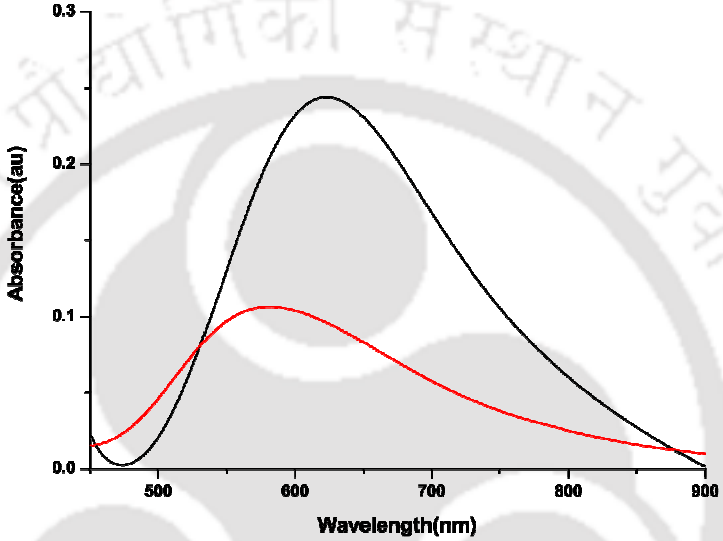

Figure 6.3: UV-visible spectra of complexes **6.1** (red trace) and **6.2** (black trace) in acetonitrile solution.

Both the complexes displayed axial EPR spectra at 77 K characteristic for the square planar Cu^{II} complexes having d_x^2-y^2 ground state (Experimental section and Figure 6.4). The complexes were found to exhibit one electron paramagnetism at room temperature. They behaved as 1:2 electrolytes in acetonitrile solvent (Experimental section).

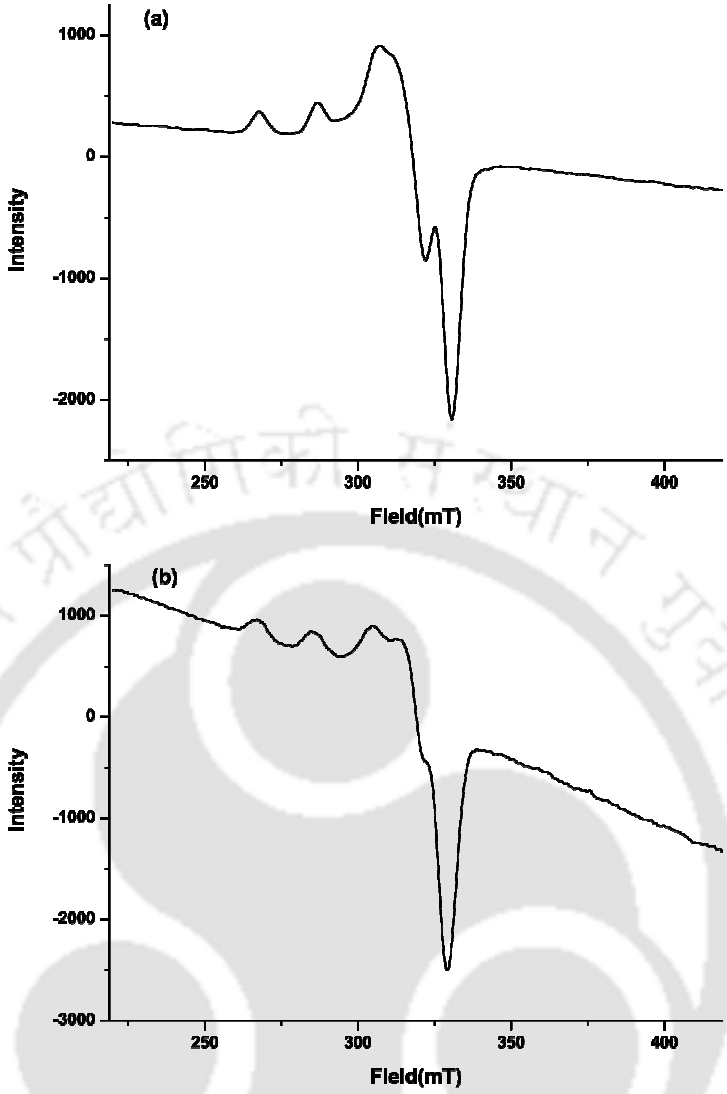

Figure 6.4: X-Band EPR spectra of complexes **6.1** (a) and **6.2** (b) in acetonitrile solution at 77K.

6.2.1 Nitric oxide reactivity in acetonitrile and water

Addition of NO gas to a dry and degassed acetonitrile solution of complex **6.1** resulted into the formation of an unstable green intermediate which has been formulated as the [Cu^{II}-$NO^{\bullet}$] complex. This had been studied by UV-visible, EPR and solution FT-IR spectroscopy. In UV-visible spectrum, the *d-d* transition band of complex **6.1** at 576 nm was shifted to 650 nm immediately after purging NO owing to the formation of [Cu^{II}-$NO^{\bullet}$] intermediate (Figure 6.5a). Similar [Cu^{II}-$NO^{\bullet}$] intermediates were reported to form in the reaction of $[Cu(tiaea)(CH_3CN)]^{2+}$ and $[Cu(teaea)(CH_3CN)]^{2+}$ [tiaea, *tris*-(2-

isopropylaminoethyl)amine and teaea, *tris*-(2-ethylaminoethyl)amine], with NO and they displayed the *d-d* transition at 640 nm and 605 nm, respectively.[16] The *d-d* transitions for the [Cu^{II}-$NO^{\bullet}$] intermediates were reported to appear at 660 nm and 595 nm in cases of $[Cu(amepy)_2]^{2+}$ and $[Cu(aeta)_2]^{2+}$ [amepy, 2-aminomethyl pyridine; aeta, *bis*-(2-aminoethyl)amine], respectively.[17] The intensity of the band corresponding to the [Cu^{II}-$NO^{\bullet}$] intermediate was found to diminish with time suggesting the reduction of Cu^{II} center to Cu^{I} following pseudo-first order kinetics (Figure 6.5a, inset). The rate constant was calculated to be 5.40×10^{-2} sec^{-1} at 298 K. The *d-d* transition of the complex **6.2** was shifted from 596 nm to 652 nm in presence of NO in acetonitrile solvent indicating the formation of [Cu^{II}-$NO^{\bullet}$] intermediate (Figure 6.5b). The rate constant for the reduction of Cu^{II} to Cu^{I} in this case was 1.09×10^{-1} sec^{-1} at 298 K (Figure 6.5b, inset). Thus, the order of the rate of decomposition of the [Cu^{II}-$NO^{\bullet}$] intermediate in case of complex **6.2** is found to be greater than that of complex **6.1**. This can be attributed to the effect of the ethyl substitution on the ligand framework in case of complex **6.2**. For $[Cu(tiaea)(CH_3CN)]^{2+}$ and $[Cu(teaea)(CH_3CN)]^{2+}$, the order of rate constants was $[Cu(tiaea)(CH_3CN)]^{2+} > [Cu(teaea)(CH_3CN)]^{2+}$ at 298 K indicating the effect of bulk of N-alkyl group on the ligand framework.[16] It should be noted that *d-d* transition for $[Cu(amepy)_2]^{2+}$ appears at 582 nm; whereas the corresponding [Cu^{II}-$NO^{\bullet}$] absorbs in the visible region at 660 nm.[17] In this case, the calculated rate constant for the decay of [Cu^{II}-$NO^{\bullet}$] to Cu^{I} was 1.3×10^{-3} s^{-1} at 298 K. The difference in absorption band in the visible region and the rate constant for the decomposition of [Cu^{II}-$NO^{\bullet}$] for complex **6.1** compared to $[Cu(amepy)_2]^{2+}$ is, presumably, because of the greater chelate ring size in case of complex **6.1**. It is evident that in the present case, the increase in the chelate ring from five to six membered one, destabilizes the [Cu^{II}-$NO^{\bullet}$] intermediate. It

would be worth mentioning here that for complex with cyclic amine ligands, $[Cu(tmd)_2]^{2+}$, the decomposition of $[Cu^{II}\text{-}NO^{\bullet}]$ was found to follow a pseudo-first order kinetics with a rate constant of 8.45×10^{-3} s^{-1}.[19]

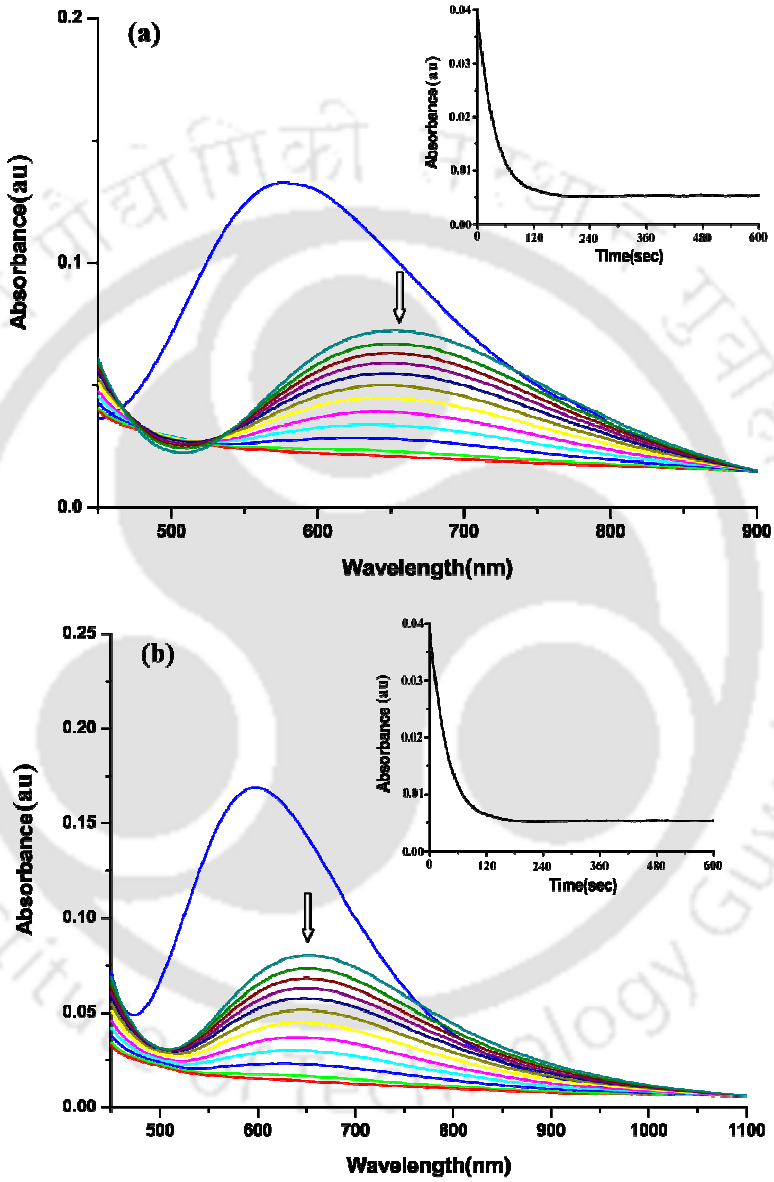

Figure 6.5: UV-visible spectra of the reaction of complexes (a) **6.1** and (b) **6.2** with NO in acetonitrile solvent at room temperature. (Blue trace represents the Cu^{II}-species, green represents that of the $[Cu^{II}\text{-}NO^{\bullet}]$ intermediate which gradually reduced to Cu^{I} represented by down headed arrow). Inset: Time-scan plot for the decomposition of $[Cu^{II}\text{-}NO^{\bullet}]$ at room temperature.

Complexes **6.1** and **6.2** were found to exhibit characteristic EPR signals in acetonitrile solvent; whereas, the respective green intermediates obtained after their reaction with NO were found to be EPR silent at 298 K (Figures 6.6a and 6.6b). This is attributed to the anti-ferromagnetic coupling of the paramagnetic Cu^{II} centers with NO, in both the cases. The complete reduction of Cu^{II} center by NO to the diamagnetic Cu^{I} would also result into EPR silent solution. The presence of the *d-d* band of the intermediates, however, indicates the existence of $[Cu^{II}\text{-}NO^{\bullet}]$ rather than Cu^{I}. In earlier reports of $[Cu(tiaea)(CH_3CN)]^{2+}$, $[Cu(teaea)(CH_3CN)]^{2+}$, $[Cu(amepy)_2]^{2+}$ and $[Cu(aeta)_2]^{2+}$, the

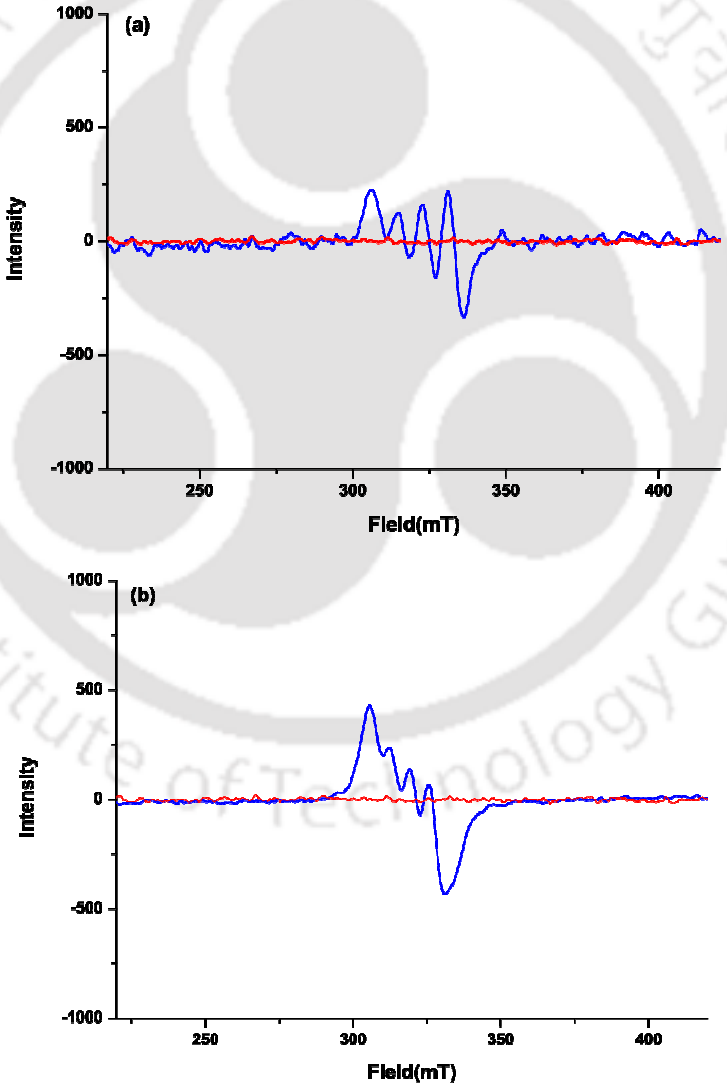

Figure 6.6: X-Band EPR spectrum of complexes (a) **6.1** and (b) **6.2** in acetonitrile before (blue trace) and after (red trace) purging NO at room temperature.

[Cu^{II}-$NO^{\bullet}$] intermediates also were found to be EPR silent.[16, 17] Structurally characterized [$Cu(CH_3NO_2)_5(NO)][PF_6]_2$ complex was reported as EPR silent.[23]

In solution FT-IR spectrum of the acetonitrile solutions of the complexes **6.1** and **6.2,** after purging NO, a new band was found to appear at ~1630 and 1634 cm^{-1} respectively and were found to disappear with time indicating unstable nature of the intermediates (Figures 6.7a and 6.7b, respectively). These are attributed to the vibration of NO

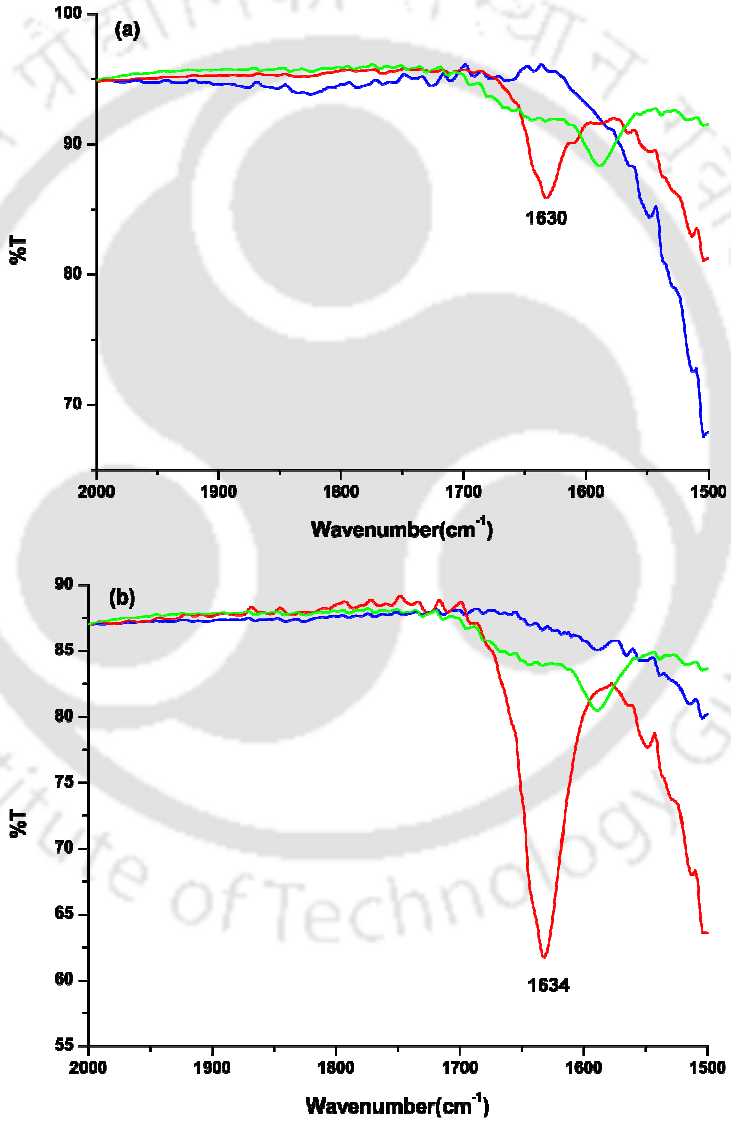

Figure 6.7: Solution FT-IR spectra complexes (a) **6.1** and (b) **6.2** in acetonitrile (blue trace represents solution IR of complexes, red represents that immediately after purging NO which shows sharp peak at ~ 1630 cm^{-1} and green represents that after 5 minutes).

coordinated to the Cu^{II} center. Thus the appearance of these bands essentially supports the formation of the [Cu^{II}- $NO^{\bullet}$] prior to the reduction of Cu^{II} centers. For $[Cu(tren)(CH_3CN)]^{2+}$ this vibration was found to appear at 1650 cm^{-1} in acetonitrile.[16] On the other hand, the ν_{NO} frequency appears at 1642 and 1635 cm^{-1} in the cases of $[Cu(amepy)_2]^{2+}$ and $[Cu(aeta)_2]^{2+}$, respectively, in acetonitrile.[17]. It was reported to appear at 1682 cm^{-1} for the air-stable solid copper-nitrosyl of copper(II)-dithiocarbamate.[24] However, for $[Cu(CH_3NO_2)_5(NO)][PF_6]_2$, it appears at 1933 cm^{-1} in nujol mull. This higher ν_{NO} frequency in case of $[Cu(CH_3NO_2)_5(NO)][PF_6]_2$ can be attribute to the bent geometry [Cu1-N1-O1) 121.0(3)°] of the nitrosyl ligand at an equatorial site.[23]

To authenticate the reduction of Cu^{II} centers in the present cases, the reduced complex, $[Cu(CH_3CN)_4]ClO_4$ was isolated and characterized by its X-ray single crystal structure determination. Since the crystal structure of $[Cu(CH_3CN)_4]ClO_4$ was reported earlier by Soregh et. al., it is not been included.[25]

The NO reactivity of complexes **6.1** and **6.2** were also studied in water. In water the *d-d* band of the complexes **6.1** and **6.2** appears at λ_{max} 600 and 645 nm respectively. Immediately after purging NO, the band sifted to ~650 nm in both the cases and finaly diminished due to reduction of Cu^{II} to Cu^{I} (Figure 6.8a and 6.8b, respectively).

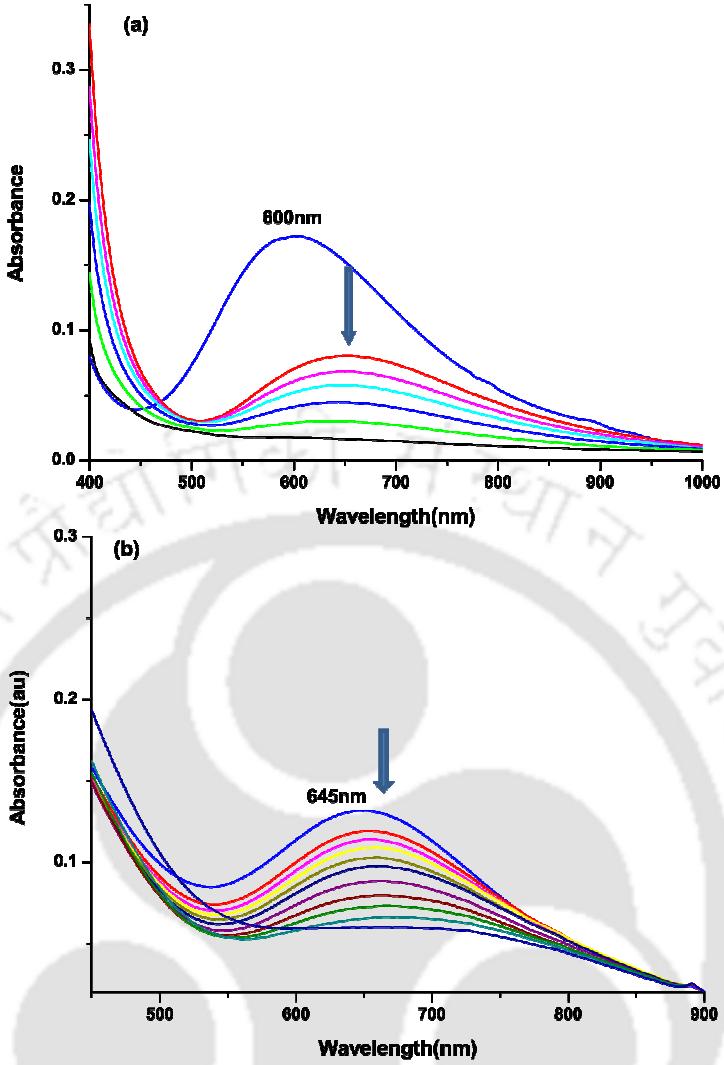

Figure 6.8: UV-visible spectra of the reaction of complexes (a) **6.1** and (b) **6.2** with NO in water at room temperature (blue trace represents that of the un-reacted complexes, red represents that immediately after purging NO which which decreases with time).

Further, the reduction of complexes, **6.1** and **6.2** in water, were confirmed by ^{1}H NMR studies in D_2O. The complexes did not show well resolved ^{1}H-NMR in D_2O due to the paramagnetic nature of Cu^{II} center (Figure 6.9a and 6.9b for complexes **6.1** and **6.2** respectively).

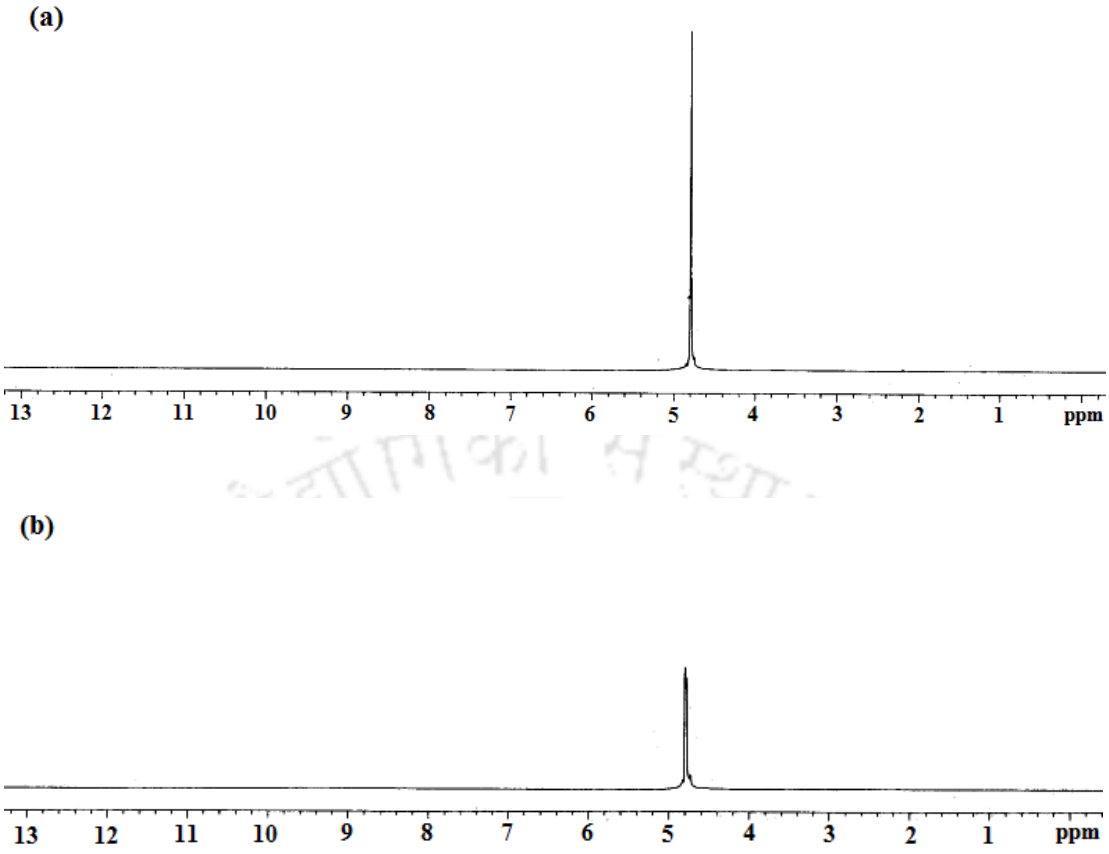

Figure 6.9: ^{1}H-NMR spectra of complexes (a) **6.1** and (b) **6.2** in D_2O.

As NO reacts with the complexes, the reduction of Cu^{II} to Cu^{I} takes place because of which the complexes shows well resolved ^{1}H-NMR spectra (Figures 6.10a and 6.10b). This proves the reduction process.

In case of complex **6.1**, in dry and distilled acetonitrile solution, the reduction was found to accompany with concomitant diazotization of the primary amine centers of the ligands which resulted into the modification of the ligand framework, $\mathbf{L_9'}$ (Scheme 6.2). It is interesting to note that in acetonitrile:water (9:1) mixture, the reduction afforded $\mathbf{L_9'}$ along with the alcoholic derivative, $\mathbf{L_9''}$. However, in water medium, no ligand modification was observed owing to the higher reactivity of NO^{+} (formed during the reduction of Cu^{II} to Cu^{I}) with water (Scheme 6.2). This, rather, resulted into the formation of NO_2^{-} which was confirmed qualitatively by Greiss's test.

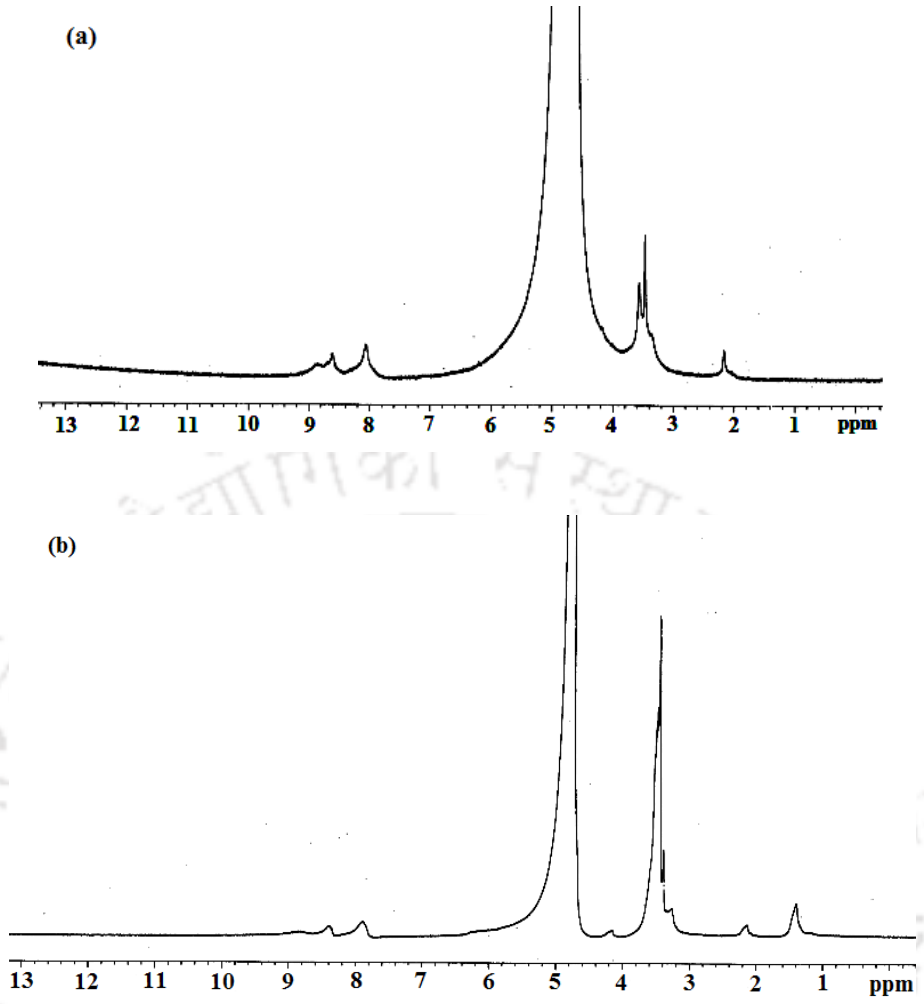

Figure 6.10: ^{1}H-NMR spectra of complexes (a) **6.1** and (b) **6.2** in D_2O after the reaction with NO.

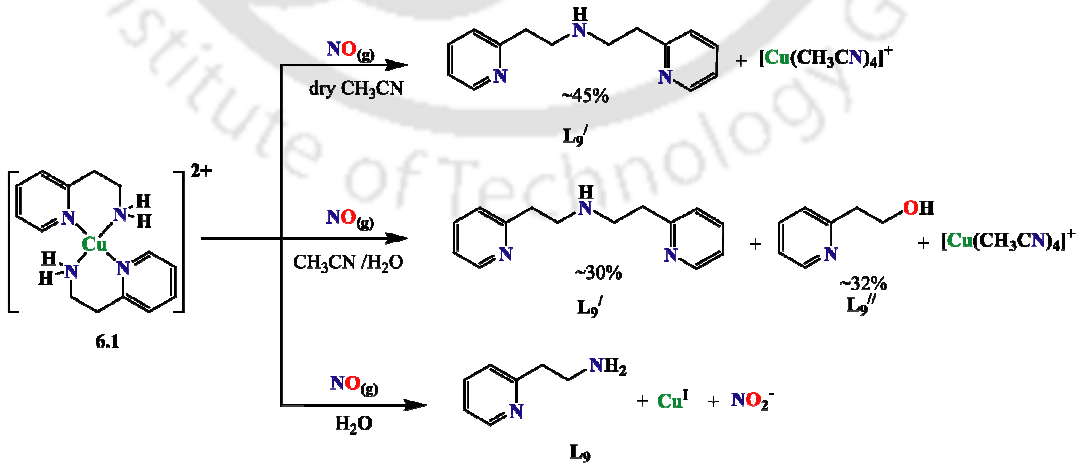

Scheme 6.2

In case of complex **6.2**, along with the reduction of the Cu^{II} centre, N-nitrosation at the ligand framework was observed in acetonitrile solution (Scheme 6.3). However, in water, the reduction resulted into the formation of NO_2^-, only.

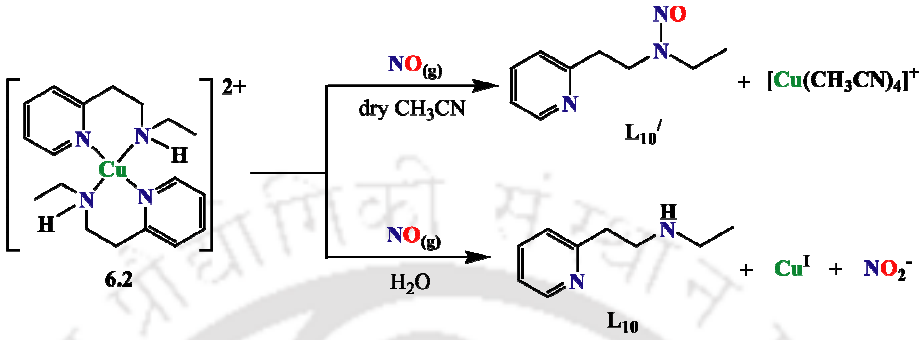

Scheme 6.3

All these organic products, $\mathbf{L_9'}$, $\mathbf{L_9''}$ and $\mathbf{L_{10}'}$ were characterized by FT-IR, ^{1}H-NMR, ^{13}C-MNR and ESI-Mass spectroscopy (Experimental section, Appendix V, Figures A5.13-A5.24).

6.3 Conclusion

In conclusion, the present work demonstrates a set of examples of the reactivity of NO with Cu^{II} centers in acetonitrile and in water media. Both the complexes afforded unstable [Cu^{II}-$NO^{\bullet}$] intermediate on reaction with NO, in acetonitrile solution, followed by the reduction of Cu^{II} centers to Cu^{I}. In water, though NO results in the reduction of Cu^{II} to Cu^{I} the formation of [Cu^{II}-$NO^{\bullet}$] was not observed. The stability of the [Cu^{II}-$NO^{\bullet}$] intermediate formed was found to be dependent on the chelate ring size and substituents present in the ligand frameworks. The reduction resulted into modification of the ligand through diazotization of the primary amine site or N-nitrosation at the secondary amine site of the ligand frameworks.

6.4 Experimental Section

6.4.1 Materials and methods

All reagents and solvents were purchased from commercial sources and were of reagent grade. Acetonitrile was distilled from calcium hydride. Deoxygenation of the solvent and solutions were effected by repeated vacuum/purge cycles or bubbling with nitrogen for 30 minutes. NO gas was purified by passing through KOH and P_2O_5 column. UV-visible spectra were recorded on a Perkin Elmer Lambda 25 spectrophotometer. FT-IR spectra of the solid samples were taken on a Perkin Elmer spectrophotometer with samples prepared as KBr pellets and for solutions, Varian 660-IR FT-IR spectrometer and NaCl cell of 2 mm path length were used and the spectra shown are the solvent subtracted ones. Solution electrical conductivity was checked using a Systronic 305 conductivity bridge. ^{1}H- NMR spectra were obtained with a 400 MHz Varian FT spectrometer. Chemical shifts (ppm) were referenced with residual solvent peaks. The X-Band Electron Paramagnetic Resonance (EPR) spectra of complexes and of the reaction mixture were recorded on a JES-FA 200 ESR spectrometer, at room temperature. Elemental analyses were obtained from a Perkin Elmer Series II Analyzer. The magnetic moment of complexes is measured on a Cambridge Magnetic Balance.

Single crystals were grown by slow diffusion followed by slow evaporation technique. The intensity data were collected using a Bruker SMART APEX-II CCD diffractometer, equipped with a fine focus 1.75 kW sealed tube MoK_α radiation (λ = 0.71073 Å) at 273K, with increasing ω (width of 0.3° per frame) at a scan speed of 3 s/frame. The SMART software was used for data acquisition. Data integration and reduction were undertaken with SAINT and XPREP software.[23] Multi-scan empirical absorption corrections were applied to the data using the program SADABS.[26]

Structures were solved by direct methods using SHELXS-97 and refined with full-matrix least squares on F^2 using SHELXL-97.[27, 28] All non-hydrogen atoms were refined anisotropically. Structural illustrations have been drawn with ORTEP-3 for Windows.[29]

6.4.2 Synthesis of complex 6.1, $[Cu(L_9)_2][(ClO_4)_2$

$[Cu(H_2O)_6](ClO_4)_2$, 0.740 g (2.0 mmol) was dissolved in 10 ml distilled acetonitrile. To this solution, 0.488 g (4.0 mmol) of the ligand **L_9** was added slowly with constant stirring. The color of the solution turned dark blue from light blue. The stirring was continued for 1h at room temperature. The volume of the solution was then reduced to ~2 ml. To this, 10 ml of benzene was added to make a layer on it and kept it overnight on freezer. This resulted into dark crystals of complex **6.1**. Yield: 0.880 g (85%). Elemental Analyses: Calcd. for $C_{14}H_{20}N_4O_8Cl_2Cu$: C, 33.18; H, 3.98; N, 11.06; Found (%): C, 33.14; H, 3.97; N, 10.99. Molar conductivity: [$\Lambda_M(\Omega^{-1}cm^2mol^{-1})$, 230]. FT-IR: 3232, 2936, 1614, 1079, 625 cm^{-1}; magnetic moment, 1.62 BM. EPR data: $g_{\parallel}$, 2.268, $g_{\perp}$, 2.015 and A, 174.56 cm^{-1}.

6.4.3 Synthesis of complex 6.2, $[Cu(L_{10})_2](ClO_4)_2$

The complex **6.2** was synthesised following the similar procedure as complex **6.1** except for the use of **L_{10}** in place of **L_9**. Yield: 0.950 g (85%). Elemental Analyses: Calcd. for $C_{18}H_{28}N_4O_8Cl_2Cu$: C, 38.41; H, 5.01; N, 9.95; Found (%): C, 38.46; H, 5.01; N, 9.92. Molar conductivity: [$\Lambda_M(\Omega^{-1}cm^2mol^{-1})$, 217]. FT-IR: 2969, 2019, 1610, 1449, 1085 cm^{-1}; magnetic moment, 1.67 BM. EPR data: $g_{\parallel}$, 2.257, $g_{\perp}$, 2.026 and A, 174.59 cm^{-1}.

6.4.4 Isolation of $[Cu^{I}(CH_3CN)_4]ClO_4$

The isolation of $[Cu(CH_3CN)_4]ClO_4$ from the reactions of the respective complexes with NO has been done using the same general procedure. The detail is given for complex **6.1**.

In a 100 ml Schlenk flask, complex **6.1** (253 mg, 0.5 mmol) was dissolved in 50 ml degassed acetonitrile. To this deep blue solution, NO gas was purged through a needle for one minute and allowed to stand for 10 minutes. To the resulting colorless solution, 15 ml of degassed benzene was added through a syringe to make a layer. The layered solution was then kept overnight in freezer. The white crystals of $[Cu(CH_3CN)_4]ClO_4$ were filtered out from the colourless solution under nitrogen atmosphere using a Schlenk frit. Yield, 115 mg, ~61%.

Same procedure was followed to isolate the $[Cu(CH_3CN)_4]ClO_4$ from the reaction of complex **6.2** (281 mg, 0.5 mmol) with NO in acetonitrile solution. Yield: 105 mg, ~56%.

6.4.5 Isolation of L_9' and L_9''

In a 100 ml Schlenk flask, complex **6.1** (506 mg, 1.0 mmol) was dissolved in 50 ml degassed acetonitrile. To this, NO gas was purged through a needle for one minute and the mixture was then allowed to stand for 10 minutes. To the colorless solution, thus obtained, 20 ml of degassed benzene was added through a syringe to make a layer. The layered solution was then kept overnight in freezer. The white crystals of $[Cu(CH_3CN)_4]ClO_4$ were filtered out from the colorless solution under nitrogen atmosphere using a Schlenk frit. The volume of the filtrate was then reduced to 5 ml and stirred for 1 h in open air in order to allow the residual Cu^{I} center to oxidise to Cu^{II}. To this, 5 ml saturated aqueous solution of Na_2S was added and stirred for ½ h. The black

precipitate of Cu_2S thus obtained was filtered off and the filtrate was diluted with 50 ml of water. The organic part was then extracted from the mixture using $CHCl_3$ (3 portions × 25 ml). The collected organic layer was then dried under reduced pressure and the residual oil was subjected to column chromatography using silica gel to yield $\mathbf{L_9'}$ and $\mathbf{L_9''}$. In case of dry and distilled acetonitrile, we are yield up with only $\mathbf{L_9'}$.

For $\mathbf{L_9'}$: Yield, 190 mg (~ 84%). Elemental Analyses: Calcd.(%) for $C_{14}H_{17}N_3$: C, 73.98; H, 7.54; N, 18.49. Found (%) C, 73.57; H, 7.44; N, 18.29. ^{1}H-NMR(400 MHz, $CDCl_3$), δ_{ppm}, 8.48(d, 2H), 7.58(t, 2H), 7.12(m, 4H), 3.61(t, 4H), 2.94(t, 4H). ^{13}C-NMR(100 MHz, $CDCl_3$), δ_{ppm}, 160.87, 149.22, 136.87, 123.64, 121.76, 38.95, 37.84. FT-IR in KBr pellet: 2927(m), 1644 (s), 1566(s), 1384(s), 1053(m). ESI-Mass: (m+23)/z, Calcd. 250.14; Found, 250.01.

For $\mathbf{L_9''}$: Yield, 39 mg (~ 32%). Elemental Analyses: Calcd.(%) for C_7H_9NO: C, 68.27; H, 7.37; N, 11.37. Found (%) C, 68.83; H, 6.92; N, 11.30. ^{1}H-NMR(400 MHz, $CDCl_3$), δ_{ppm}, 8.45(d, 1H), 7.59(t, 1H), 7.12(m, 2H), 3.98(t, 2H), 2.98(t, 2H). ^{13}C-NMR(100 MHz, $CDCl_3$), δ_{ppm}, 161.95, 148.34, 136.89, 129.63, 121.76, 61.95,39.24. FT-IR in KBr pellet: 2923(m), 1636(m), 1384(s), 1053(s) cm^{-1}. ESI-Mass: (m+23)/z, Calcd. 146.07; Found, 146.04.

6.4.6 Isolation of $\mathbf{L_{10}'}$

Same procedure (as in case of complex **6.1**) was adopted for the isolation of $\mathbf{L_{10}'}$.

Yield, 128 mg(71%). Elemental Analyses: Calcd.(%) for $C_9H_{13}N_3O$: C, 60.32; H, 7.31; N, 23.45. Found (%) C, 60.07; H, 7.47; N, 23.12. ^{1}H-NMR(400 MHz, $CDCl_3$), δ_{ppm}, 8.51(t), 7.58(m), 7.13(m), 4.46(t), 3.97(q), 3.90(q), 3.54(q), 3.22(t), 2.94(t), 1.27(t), 1.05(t). ^{13}C-NMR(100 MHz, $CDCl_3$), δ_{ppm}, 157.87, 157.40, 149.36, 149.22, 136.63,

123.43, 121.82, 121.73, 51.26, 47.71, 43.54, 39.12, 37.10, 34.03, 13.77, 10.97. FT-IR in KBr pellet: 2940(m), 1594 (m), 1148(m), 1436(s), 1071(m), 771(m) cm^{-1}. ESI-Mass: (m+23)/z, Calcd. 202.11; Found, 202.09.

6.5 References

1. Koshland, Jr, D. E. *Science*, **1992**, *253*, 1861.
2. Tran D., Skelton, A. H., White, A. H., Laverman L. H., Ford. P. C. *Inorg. Chem.* **1998**, *37*, 2505.
3. Ignarro, L. J.; *Nitric Oxide: Biology and Pathobiology* Ed.; Academic Press; San Diego, **2000.**
4. (a) Moncada, S.; Palmer, R. M. J.; Higgs, E. A. *Pharmacol. Rev*. **1991**, *43*, 109. (b) Butler, A.R.; Williams, D. L. *Chem. Soc. Rev*. **1993**, 233. (c) *Methods in Nitric Oxide Research*; Feelisch, M.; Stamler, J. S.; Eds.; John Wiley and Sons; Chichester, England, **1996**. (d) Jia, L.; Bonaventura, C.; Bonaventura, J.; Stamler, J. S. *Nature*, **1996**, *380*, 221.
5. Ford P. C.; Fernandez B. O.; Lim M. D.; *Chem. Rev*. **2005**, *105*, 2439.
6. Torres, J.; Svistunenko, D.; Karlsson, B.; Cooper, C. E.; Wilson, M. T. *J. Am. Chem. Soc*. **2002**, *124*, 963.
7. Torres, J.; Cooper, C. E.; Wilson, M. T. *J. Biol. Chem*. **1998**, *273*, 8756.
8. Luchsinger, B. P.; Rich, E. N.; Gow, A. J.; Williams, E. M.; Stamler, J. S.; Singel, D. J. *Proc. Natl. Acad. Sci. U.S.A.* **2003**, *100*, 461.
9. Tran, D.; Ford, P. C. *Inorg. Chem*. **1996**, *35*, 2411.
10. Tran, D.; Skelton, B. W.; White, A. H.; Laverman, L. E.; Ford, P. C. *Inorg. Chem.* **1998**, *37*, 2505.
11. Tsuge, K.; DeRosa, F.; Lim, M. D.; Ford, P. C. *J. Am. Chem. Soc.* **2004**, *126*, 6564.

12. Khin C.; Lim M. D.; Tsuge K.; Iretskii A.; Wu G.; Ford P. C. *Inorg. Chem*. **2007**, *46*, 9323.

13. Pell, S. D.; Armor, J. N. *J. Am. Chem. Soc.* **1973**, *95*, 7625.

14. (a) Wayland, B. B.; Olson, L. W. *J. Am. Chem. Soc.* **1974**, *96*, 6037. (b) Wayland, B. B., Olson, L. W. *Chem. Commun*, **1973**, 897.

15. Sarma, M.; Singh, A.; Mondal, B. *Inorg. Chim. Acta*, **2010**, *363*, 63.

16. Sarma, M.; Kalita, A.; Kumar, P.; Singh, A.; Mondal, B. *J. Am. Chem. Soc.* **2010**, *132*, 7846.

17. Sarma, M.; Mondal, B. *Inorg. Chem*. **2011**, *50*, 3206.

18. Kumar, P.; Kalita, A.; Mondal, B. *Dalton Trans.* **2011**, *40*, 8656.

19. Kalita, A.; Kumar, P.; Deka, R. C.; Mondal, B. *Inorg. Chem.* **2011**, *50*, 11868.

20. Kurosawa, W.; Kan, T; Fukuyama, T. *Org. Syn*. **2002**, *79*, 186.

21. Copeland, V. C.; Halfield, W. E.; Hodgson, D. J. *Inorg. Chem*. **1973**, *12*, 1340.

22. Hiroshi, Y.; Taro, I. *Bull. Chem. Soc. Jap.* **1969**, *42*, 2187

23. Wright, A. M.; Wu, G.; Hayton, T. W. *J. Am. Chem. Soc*. **2010**, *132*, 14336.

24. Diaz, A.; Ortiz, M.; Sanchez, I.; Cao, R.; Mederos, A.; Sanchiz, J.; Brito, F. *J. Inorg. Biochem.* **2003**, *95*, 283.

25. Soregh, C.; Kierkegaard, P.; Norrestam, R. *Acta Crystallogr. Sec. B.* **1975**, *31*, 314.

26. SMART, SAINT and XPREP, Siemens Analytical X-ray Instruments Inc., Madison, Wisconsin, USA, **1995**.

27. Sheldrick, G. M. SADABS: software for Empirical Absorption Correction, University of Gottingen, Institut fur Anorganische Chemieder Universitat, Tammanstrasse 4, D-3400 Gottingen, Germany, **1999–2003**.

28. Sheldrick, G. M. SHELXS-97, University of Gottingen, Germany, **1997**.

29. Farrugia, L. J. *J. Appl. Crystallogr*. **1997**, *30*, 565.

Appendix I

Table A1.1. Crystallographic data for complex **2.1**

	Complex **2.1**
Formulae	C_{17} H_{36} C_{l2} Cu N_5 O_8
Mol. wt.	572.95
Crystal system	Monoclinic
Space group	P2(1)/n
Temperature /K	296(2)
Wavelength /Å	0.71073
a /Å	10.0634(2)
b /Å	16.7202(3)
c /Å	15.7994(3)
α/°	90.00
β/°	91.7180(10)
γ/°	90.00
V/ Å^3	2657.24(9)
Z	4
Density/Mgm^{-3}	1.432
Abs. Coeff. /mm^{-1}	1.071
Abs. correction	None
F(000)	1200
Total no.of reflections	9865
Reflections, $I > 2\sigma(I)$	2257
Max. 2θ/°	28.27
Ranges (h, k, l)	-13 <= h <=13 -20 <= k <=22 -18 <= l <= 21
Complete to 2θ (%)	95.4%
Refinement method	Full-matrix least-squares on F^2
Goof (F^2)	1.089
R indices [$I > 2\sigma(I)$]	0.0532
R indices (all data)	0.0725

Table A1.2: Selected bond lengths (Å) for complex **2.1**.

	Complex **2.1**
Cu(1)-N(1)	2.040(2)
Cu(1)-N(2)	2.040(2)
Cu(1)-N(3)	2.179(2
Cu(1)-N4)	2.113(2)
Cu(1)-N(5)	1.984(3)
N(1)-C(2)	1.496(4)

N(1)-C(3)	1.493(4)
N(1)-C(6)	1.488(4)
N(2)-C(1)	1.495(5)
N(2)-C(12)	1.501(4)
N(3)-C(5)	1.476(4)
N(3)-C(9)	1.493(4)
N(4)-C(4)	1.496(4)
N(4)-C(15)	1.493(4)
N(5)-C(7)	1.139(4)

Table A1.3. Selected bond angles (°) for complex **2.1.**

	Complex **2.1**
N(1)-Cu(1)-N(2)	84.82(10)
N(1)-Cu(1)-N(3)	84.43(10)
N(1)-Cu(1)-N(4)	83.73(10)
N(2)-Cu(1)-N(3)	116.39(10)
N(4)-Cu(1)-N(2)	128.37(10
N(4)-Cu(1)-N(3)	112.31(9)
N(5)-Cu(1)-N(1)	175.61(10)
N(5)-Cu(1)-N(2)	95.42(11)
N(5)-Cu(1)-N(3)	99.35(10)
N(5)-Cu(1)-N(4)	92.72(11
C(7)-N(5)-Cu(1)	173.3(3)

Table A1.4. Crystallographic data for $\mathbf{L_1'}$-perchlorate.

	$\mathbf{L_1'\text{-}ClO_4}$
Formulae	$C_{15}\,H_{34}\,N_7\,O_7\,Cl$
Mol. wt.	459.94
Crystal system	Orthorhombic
Space group	Pna2(1)
Temperature /K	296(2)
Wavelength /Å	0.71073
a /Å	11.6744(3)
b /Å	18.4324(4)
c /Å	10.8887(2)
α/°	90.00
β/°	90.00
γ/°	90.00
V/ $Å^3$	2343.11(9)
Z	4
Density/Mgm^{-3}	1.304

Abs. Coeff. /mm^{-1}	0.211
Abs. correction	None
F(000)	984
Total no.of reflections	9410
Reflections, $I > 2\sigma(I)$	2149
Max. 2θ/°	28.34
Ranges (h, k, l)	-15 <= h <=15 -21 <= k <=24 -14 <= l <= 14
Complete to 2θ (%)	99.8%
Refinement method	Full-matrix least-squares on F^2
Goof (F^2)	1.042
R indices [$I > 2\sigma(I)$]	0.0537
R indices (all data)	0.0692

Table A1.5: Selected bond lengths(Å) and bond angles(°) for **L_1'**-perchlorate.

Bond length(Å)		**Bond angles (°)**	
N(1)-C(1)	1.508(4)	N(1)-C(1)-C(2)	115.6(2)
N(1)-C(6)	1.517(3)	N(2)-C(2)-C(1)	115.5(2)
N(1)-C(11)	1.522(3)	N(2)-C(3)-C(4)	109.9(3)
N(2)-C(3)	1.481(5)	N(2)-C(3)-C(5)	111.4(4)
N(2)-C(6)	1.314(4)	N(3)-C(7)-C(6)	116.0(2)
N(3)-C(7)	1.285(4)	N(4)-C(12)-C(11)	115.32(19)
N(4)-C(5)	1.301(3)	N(4)-C(13)-C(15)	111.2(3)
N(4)-C(13)	1.479(4)	C(1)-N(1)-C(11)	110.6(2)
N(2)-N(6)	1.314(4)	C(2)-N(2)-C(3)	123.2(3)
N(3)-N(7)	1.285(4)	C(6)-N(1)-C(11)	109.5(2)
N(4)-N(5)	1.301(3)	C(7)-N(3)-C(8)	119.8(3)
C(2)-N(2)	1.463(4)	N(5)-N(4)-C(12)	121.3(2)
C(7)-N(3)	1.453(4)	N(5)-N(4)-C(13)	115.3(2)
C(8)-N(3)	1.497(4)	N(7)-N(3)-C(7)	123.1(2
C(12)-N(4)	1.461(3)	O(1)-N(5)-N(4)	115.7(2)
N(5)-O(1)	1.232(3)	O(2)-N(6)-N(2)	113.7(3)
N(6)-O(2)	1.235(4)	O(3)-N(5)-N(4)	114.8(3)
N(7)-O(3)	1.256(3)		

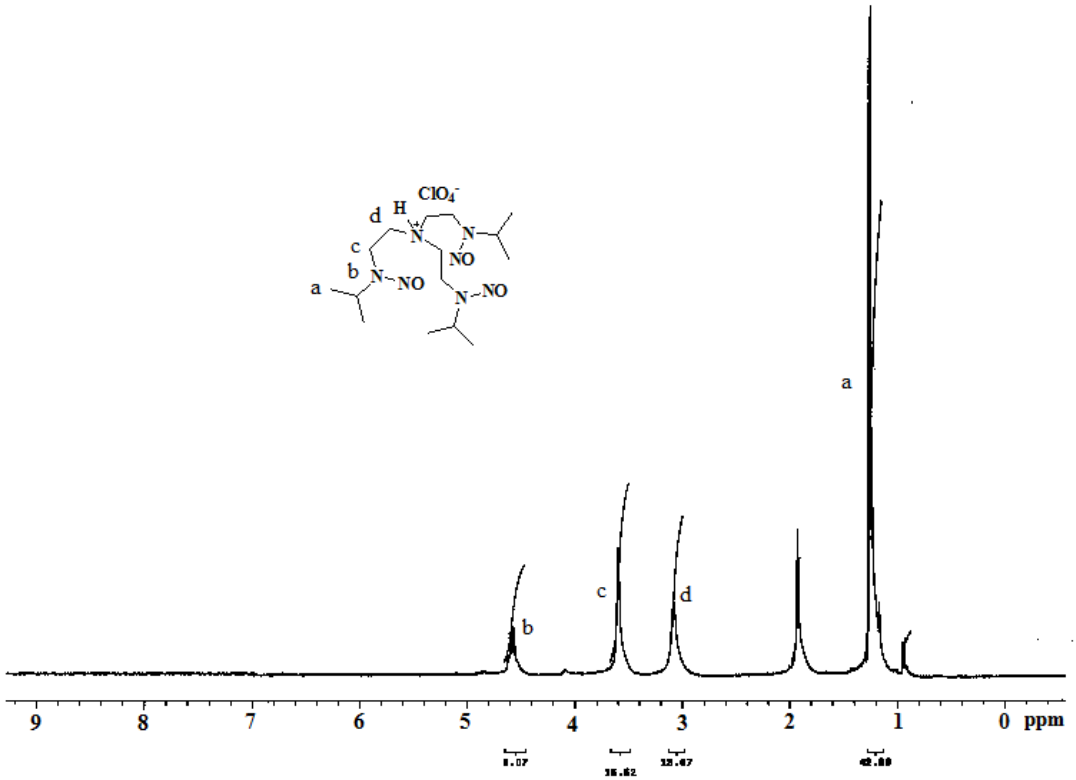

Figure A1.1: ^{1}H-NMR spectrum of $\mathbf{L_1}'$-perchlorate in CD_3CN at room temperature.

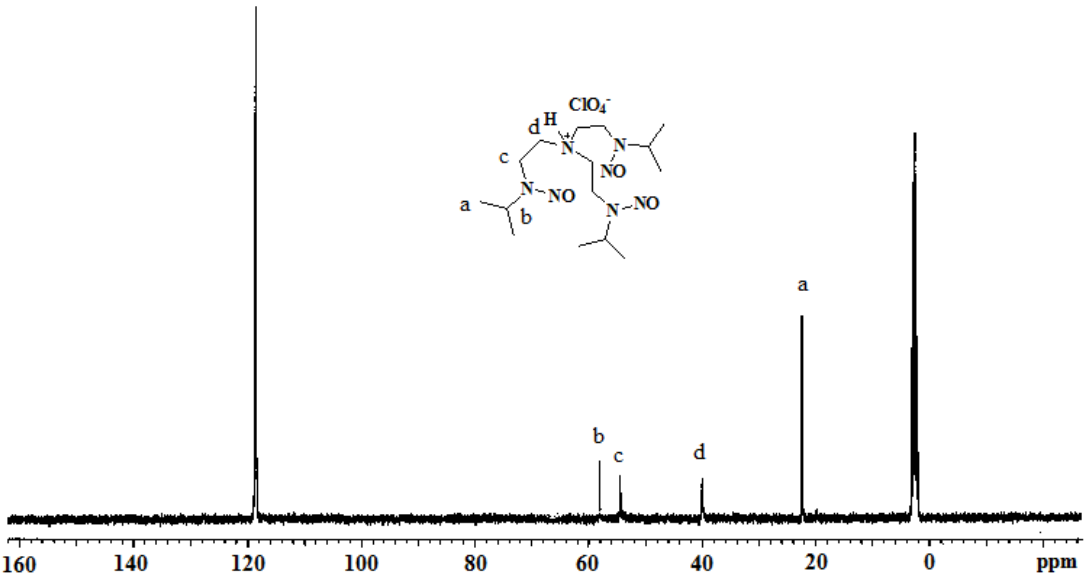

Figure A1.2: ^{13}C-NMR spectrum of $\mathbf{L_1}'$-perchlorate in CD_3CN at room temperature.

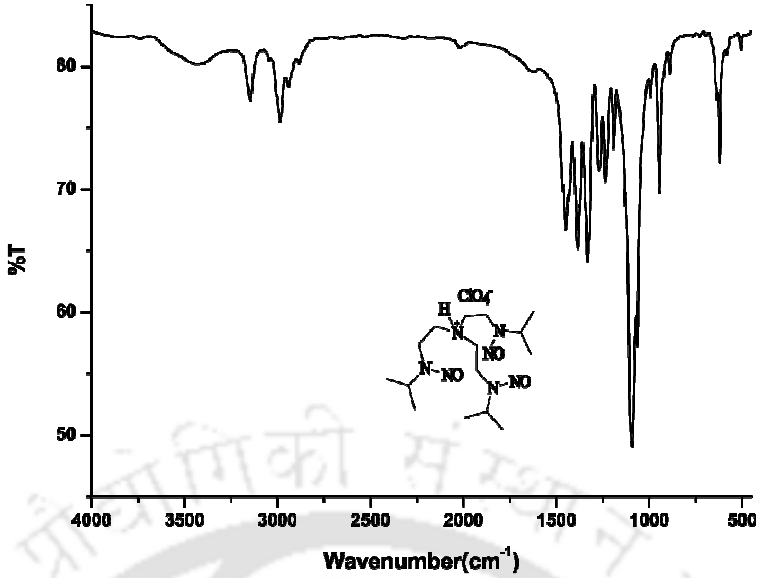

Figure A1.3: FT-IR spectrum of L_1'-perchlorate in KBr pellete.

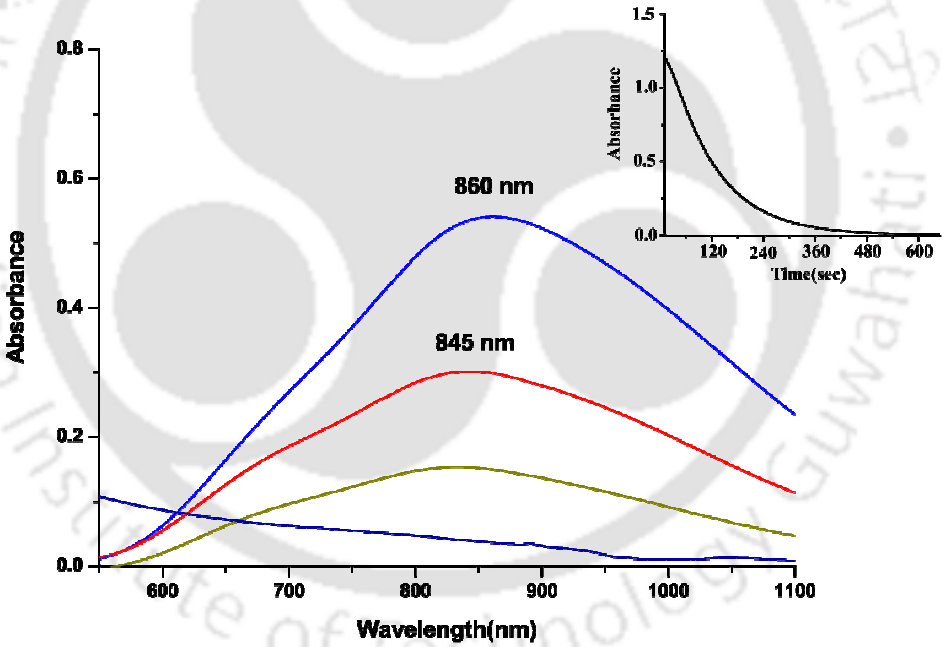

Figure A1.4: UV-visible spectra of complex **2.1** in methanol (blue trace is for complex **2.1** before and red represents that after addition of NO. Bottom most dark trace represents the spectrum of colorless solution). Inset: Time scan plot of the gradual decay of $[L_1Cu^{II}\text{-}NO]^{2+}$ (λ_{max}, 845 nm) to Cu^{I} in methanol at 298K.

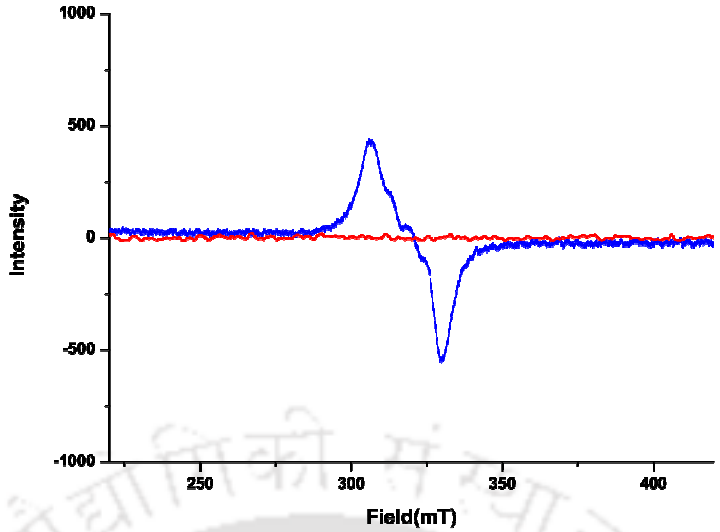

Figure A1.5: X-band EPR spectra of the complex **2.1** (blue trace) and immediately after its reaction with NO (red trace) in methanol at room temperature.

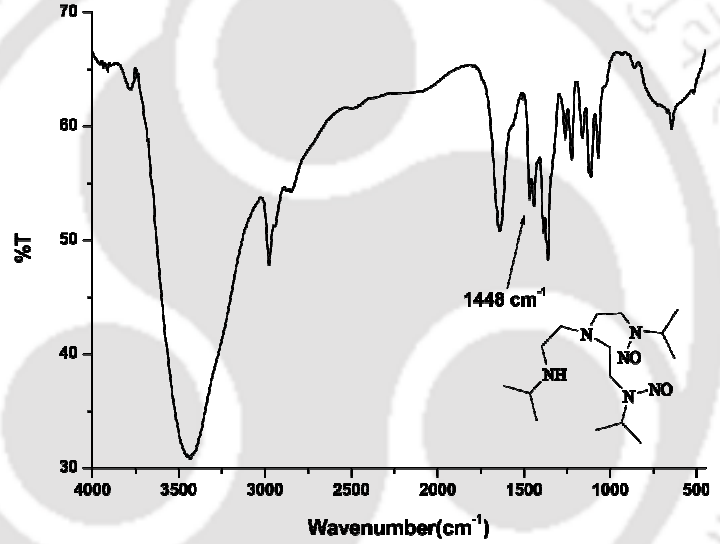

Figure A1.6: FT-IR spectrum of $L_1^{//}$ in KBr pellet.

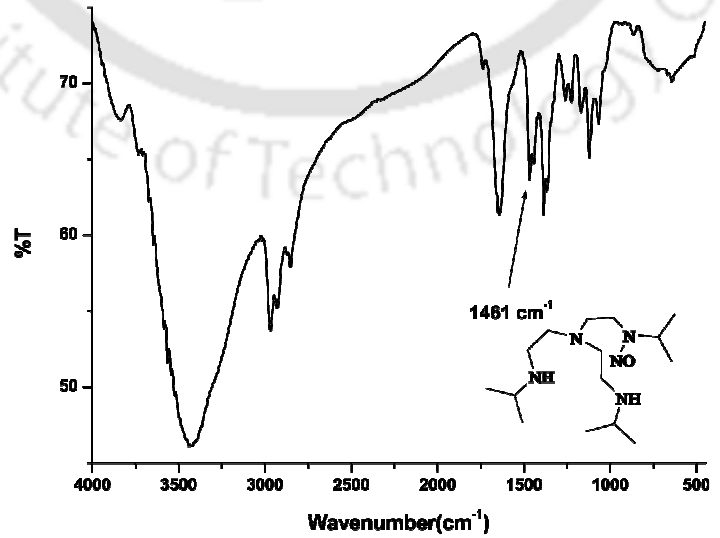

Figure A1.7: FT-IR spectrum of $L_1^{///}$ in KBr pellet.

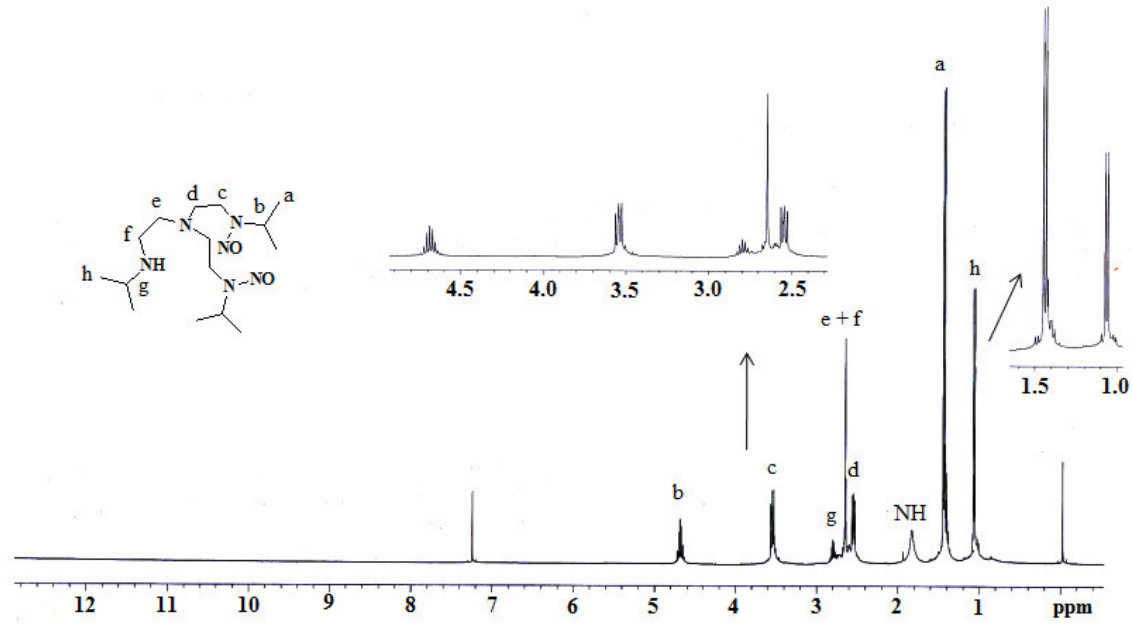

Figure A1.8: ^{1}H-NMR spectrum of $\mathbf{L_1''}$ in CD_3Cl.

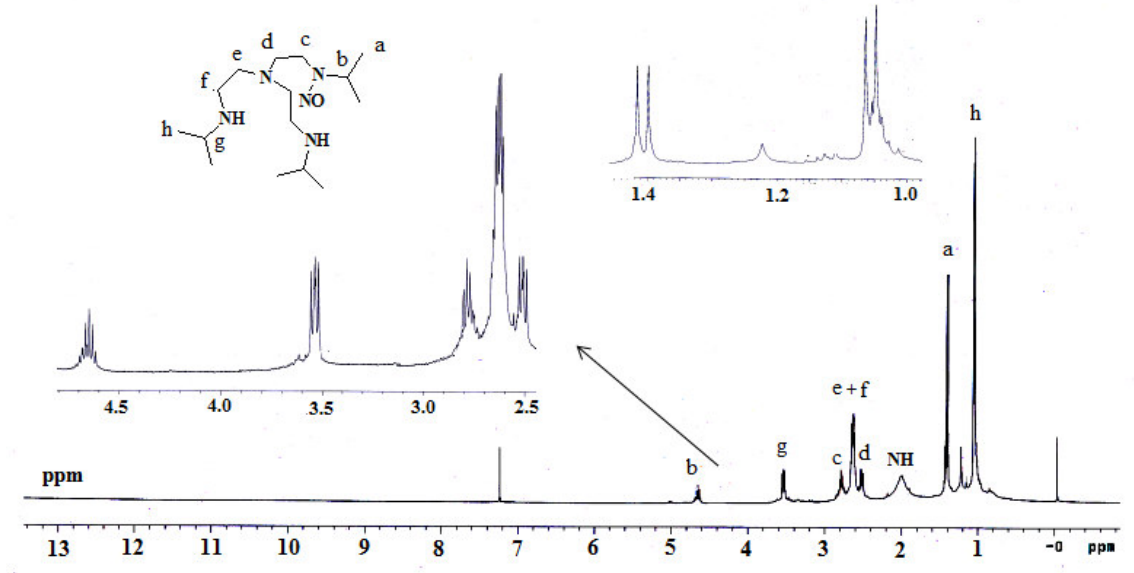

Figure A1.9: ^{1}H-NMR spectrum of $\mathbf{L_1'''}$ in CD_3Cl.

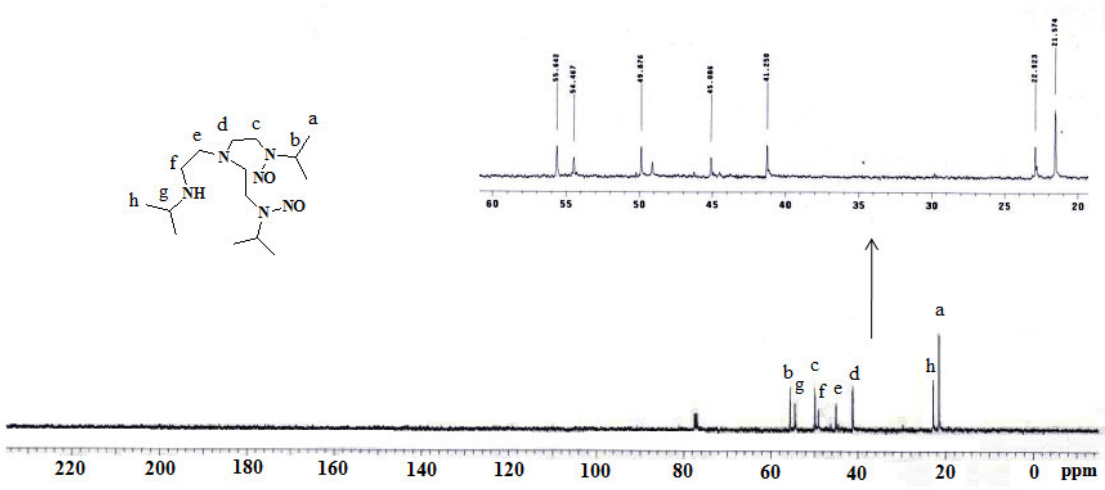

Figure A1.10: ^{13}C-NMR spectrum of $\mathbf{L_1}''$ in CD_3Cl.

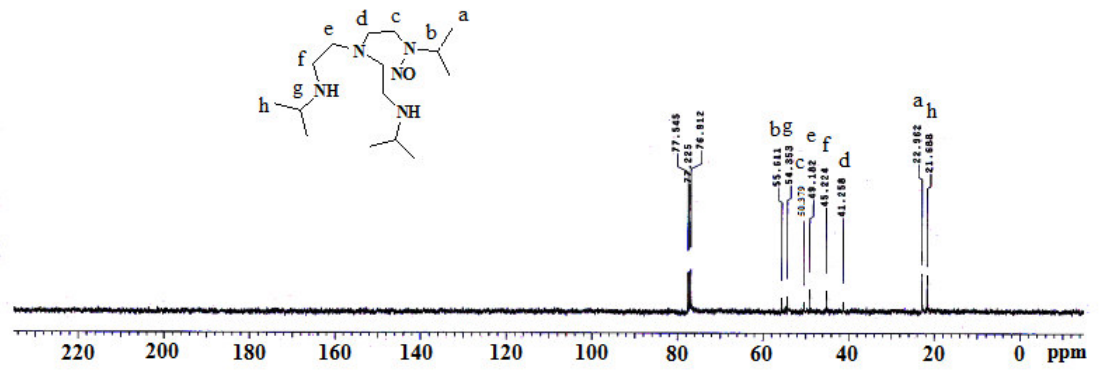

Figure A1.11: ^{13}C-NMR spectrum of $\mathbf{L_1}'''$ in CD_3Cl.

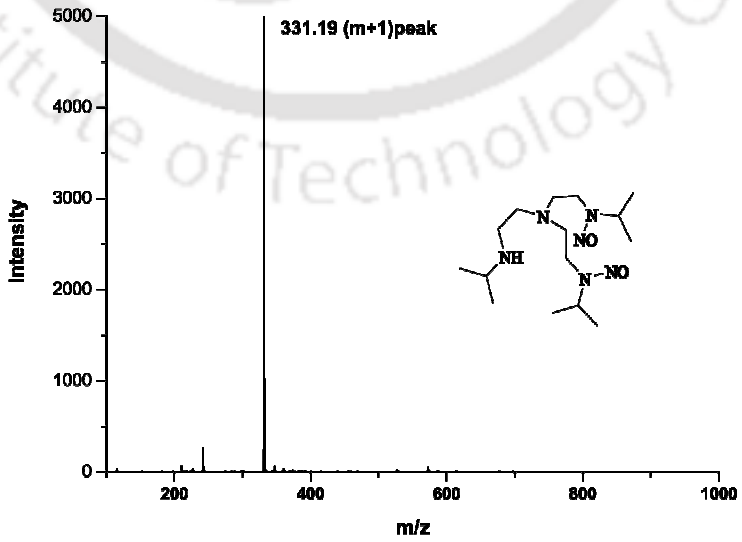

Figure A1.12: ESI-Mass spectrum of $\mathbf{L_1}''$ in methanol.

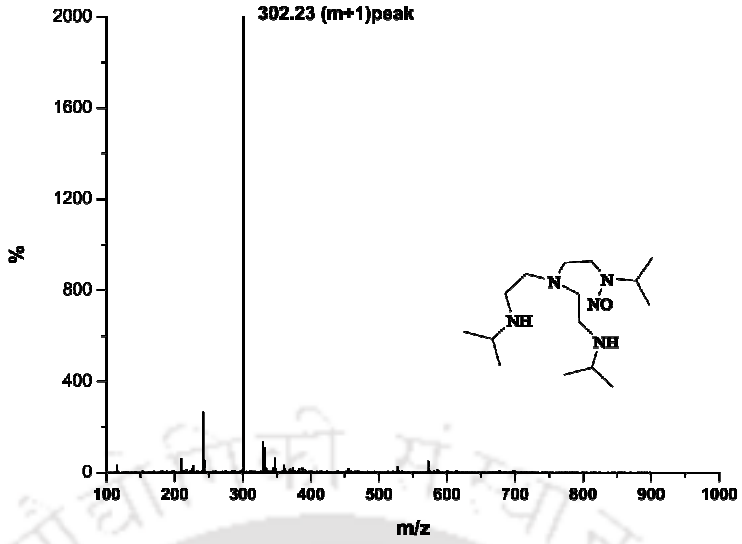

Figure A1.13: ESI-Mass spectrum of $\mathbf{L_1}^{///}$ in methanol.

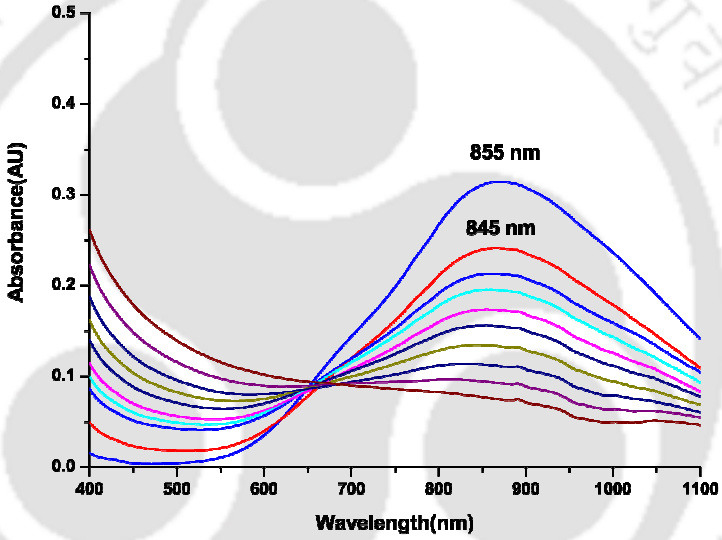

Figure A1.14: UV-visible spectra of the reaction of complex **2.1** with NO in water at room temperature. (Blue trace represents the Cu^{II} complex, red represents that of the $[Cu^{II}\text{-}NO^{\bullet}]$ intermediate which gradually reduced to Cu^{I}).

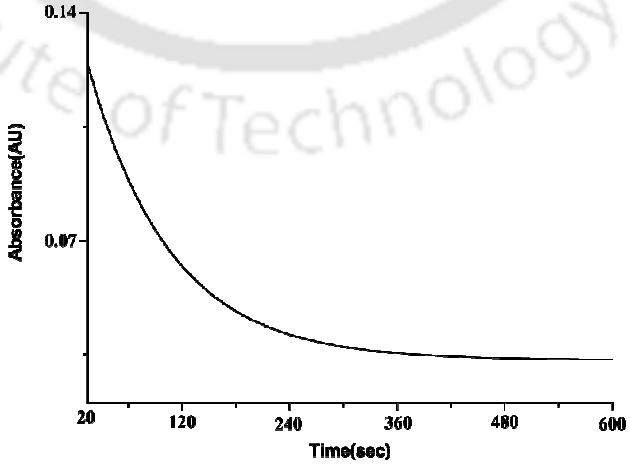

Figure A1.15: Time scan plot of the gradual decay of $[L_1Cu^{II}\text{-}NO]^{2+}$ (λ_{max}, 845 nm) to Cu^{I} in water at 298K.

Appendix II

Table A2.1. Crystallographic Data for $\mathbf{L_2''}$-perchlorate

Formulae	$C_6 H_{12} Cl_3 N_4 O_{12}$
Mol. wt.	447.62
Crystal system	Cubic
Space group	P213
Temperature /K	293(2)
Wavelength /Å	0.71073
a /Å	11.7511(12)
b /Å	11.7511(0)
c /Å	11.7511(0)
α/°	90.000(0)
β/°	90.000(0)
γ/°	90.000(0)
V/ Å^3	1622.69(10)
Z	4
F(000)	928
Total no.of reflections	16288
Reflections, $I > 2\sigma(I)$	3462
Max. 2θ/°	28.25
Ranges (h, k, l)	-15 <= h <=15 -15 <= k <=14 -15 <= l <= 15
Complete to 2θ (%)	100%
Refinement method	Full-matrix least-squares on F^2
Goof (F^2)	1.168
R indices [$I > 2\sigma(I)$]	0.0813
R indices (all data)	0.0849

Table A2.2. Selected bond lengths (Å) and bond angles (°) of $\mathbf{L_2''}$-perchlorate

Bond length (Å)		**Bond angle (°)**	
N(1)-C(1)	1.476(5)	N(1)-C(1)-C(2)	111.1(4)
N(2)-C(2)	1.485(8)	N(2)-C(2)-C(1)	111.4(5)
C(1)-C(2)	1.526(8)	C(1)-N(1)-C(1)	109.2(3)

Table A2.3. Crystallographic Data for $\mathbf{L_3''}$

Formulae	$C_4\ H_{10}\ N_4\ O_6$
Mol. wt.	186.14
Crystal system	Triclinic
Space group	P1
Temperature /K	296(2)
Wavelength /Å	0.71073
a /Å	5.046(4)
b /Å	5.521(4)
c /Å	7.207(5)
α/°	105.11(5)
β/°	90.12(6)
γ/°	93.74(6)
V/ Å^3	193.4(3)
Z	1
F(000)	98
Total no.of reflections	1284
Reflections, $I > 2\sigma(I)$	897
Max. 2θ/°	28.28
Ranges (h, k, l)	-6 <= h <=6 -6 <= k <=7 -9 <= l <= 9
Complete to 2θ (%)	83.20%
Refinement method	Full-matrix least-squares on F^2
Goof (F^2)	1.038
R indices [$I > 2\sigma(I)$]	0.0449
R indices (all data)	0.0746

Table A2.4. Selected bond lengths (Å) and bond angles (°) of $\mathbf{L_3''}$

Bond length (Å)		**Bond angle (°)**	
N(1)-C(1)	1.478(9)	N(1)-C(1)-C(2)	109.5(6)
N(2)-C(2)	1.476(9)	N(2)-C(2)-C(1)	112.2(6)
C(1)-C(2)	1.512(9)	-	-

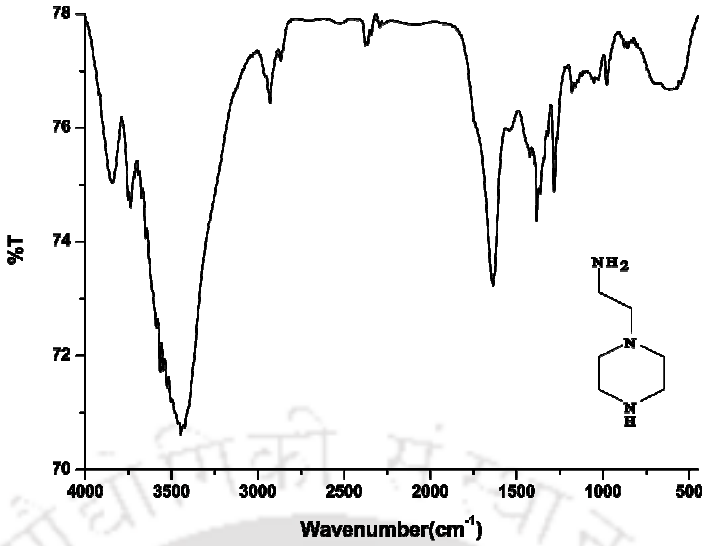

Figure A2.1: FT-IR spectrum of $\mathbf{L_2'}$ in KBr pellet.

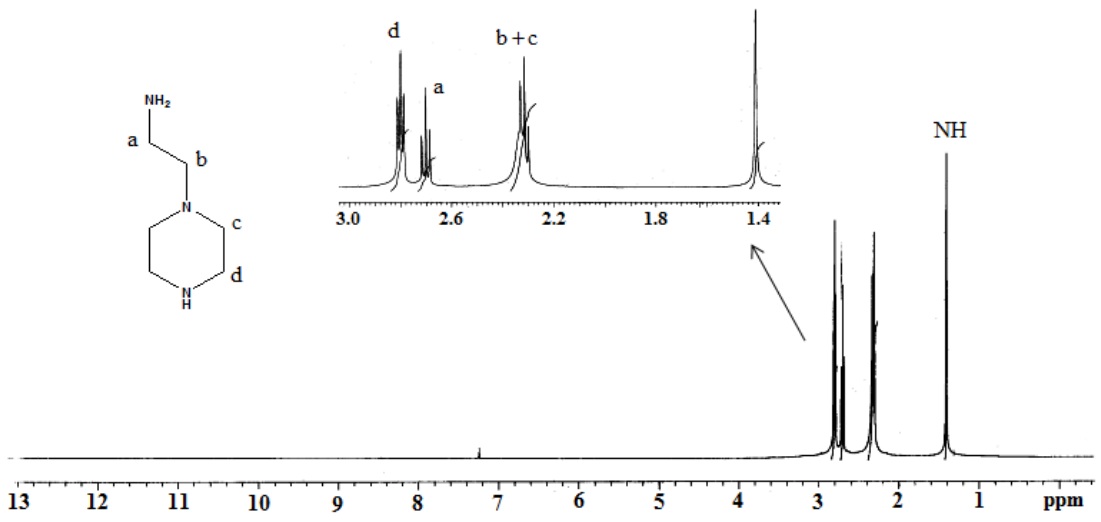

Figure A2.2: ^{1}H-NMR spectrum of $\mathbf{L_2'}$ in $CDCl_3$.

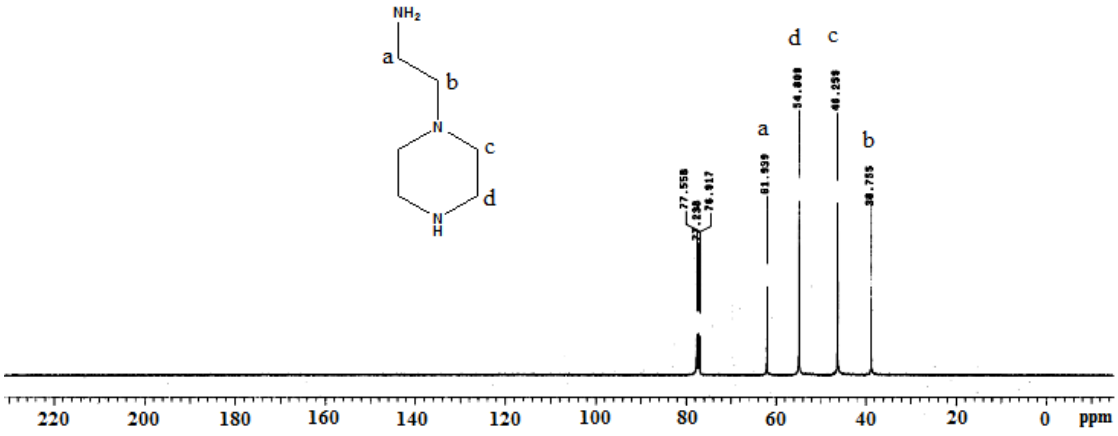

Figure A2.3: ^{13}C-NMR spectrum of $\mathbf{L_2'}$ in $CDCl_3$.

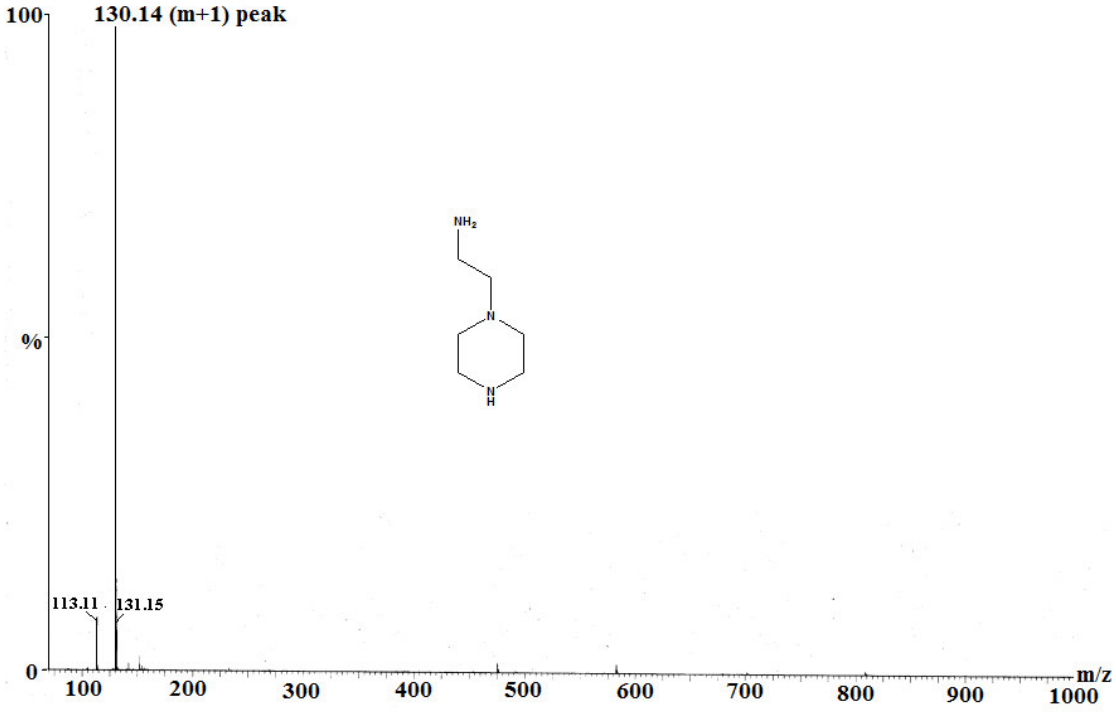

Figure A2.4: ESI-Mass spectrum of L_2' in methanol.

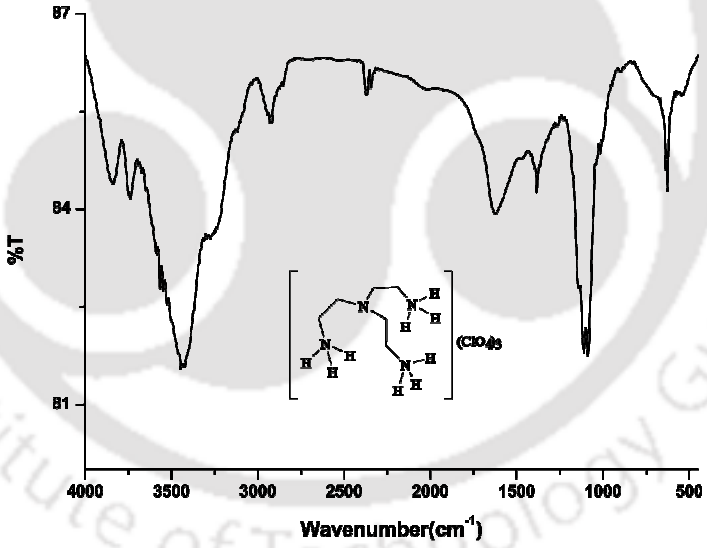

Figure A2.5: FT-IR spectrum of L_2''-perchlorate in KBr pellet.

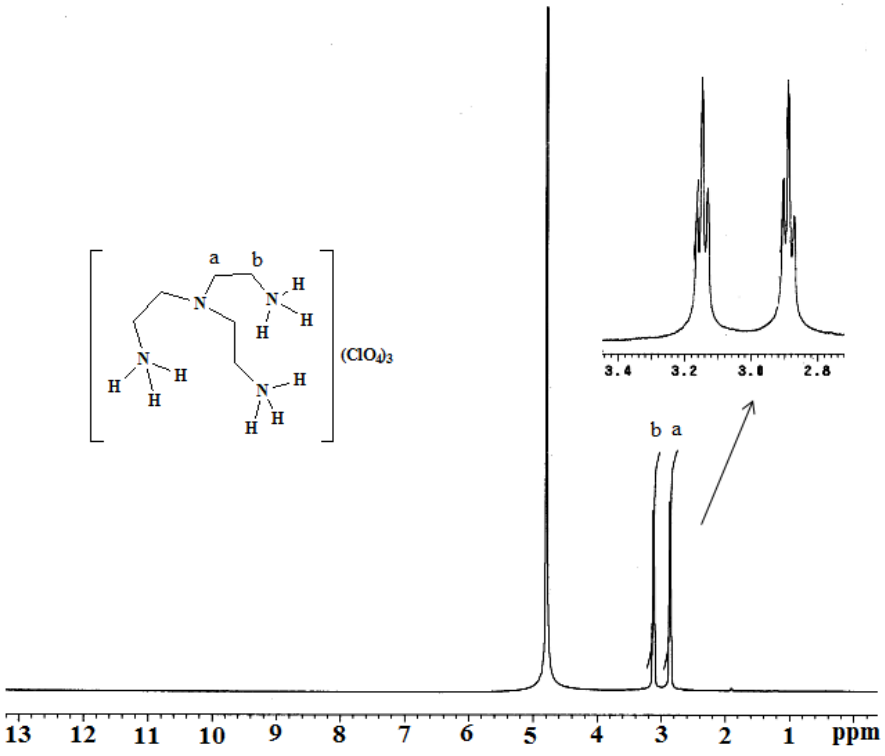

Figure A2.6: ^{1}H-NMR spectrum of $\mathbf{L_2''}$-perchlorate in D_2O.

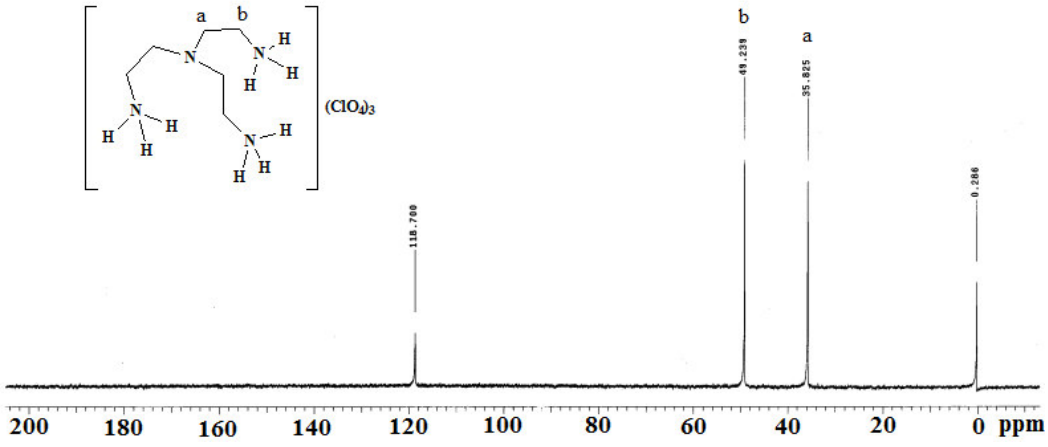

Figure A2.7: ^{13}C-NMR spectrum of $\mathbf{L_2''}$-perchlorate in D_2O (a drop of CD_3CN is added as standard).

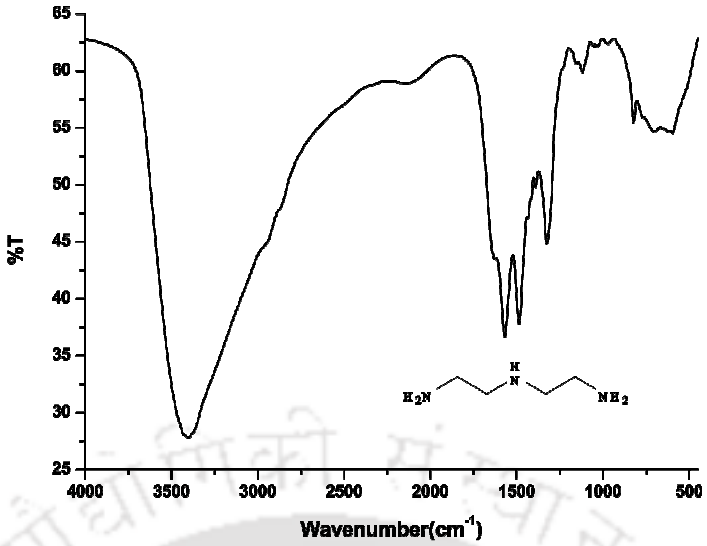

Figure A2.8: FT-IR spectrum of $\mathbf{L_3}'$ in KBr pellet.

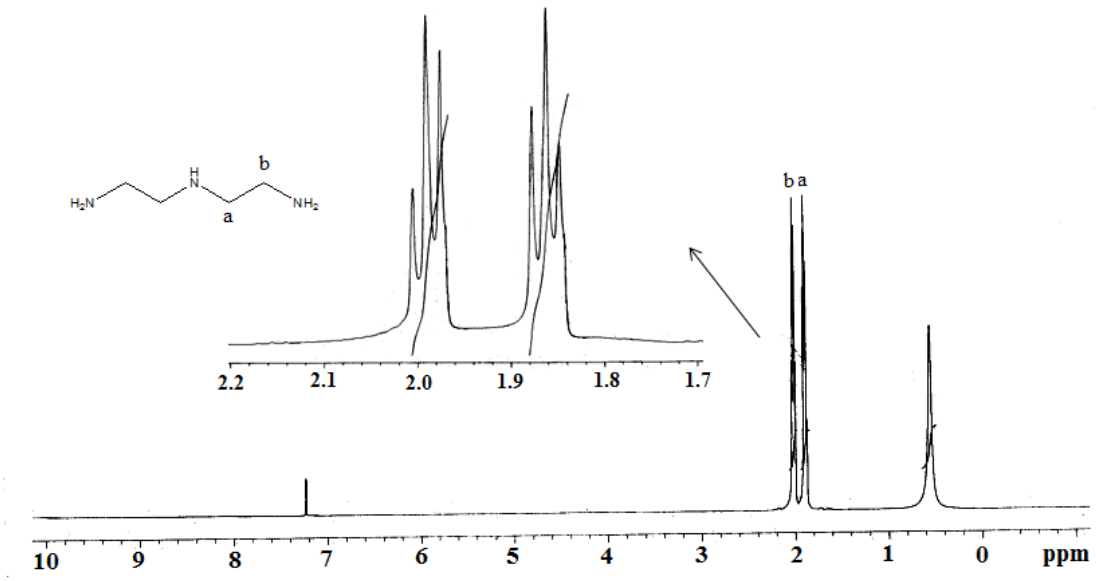

Figure A2.9: ^{1}H-NMR spectrum of $\mathbf{L_3}'$ in $CDCl_3$.

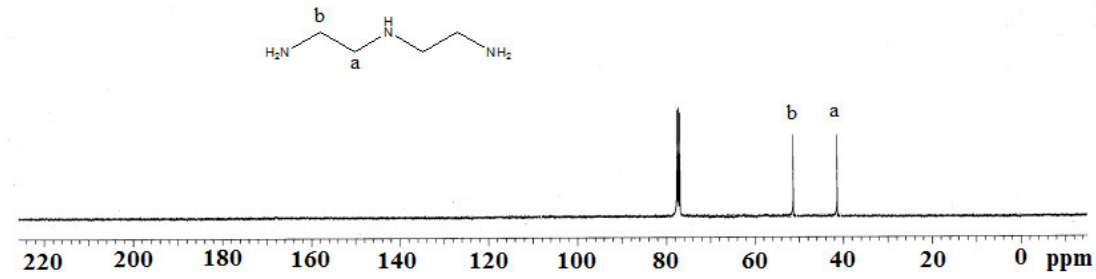

Figure A2.10: ^{13}C-NMR spectrum of $\mathbf{L_3}'$ in $CDCl_3$.

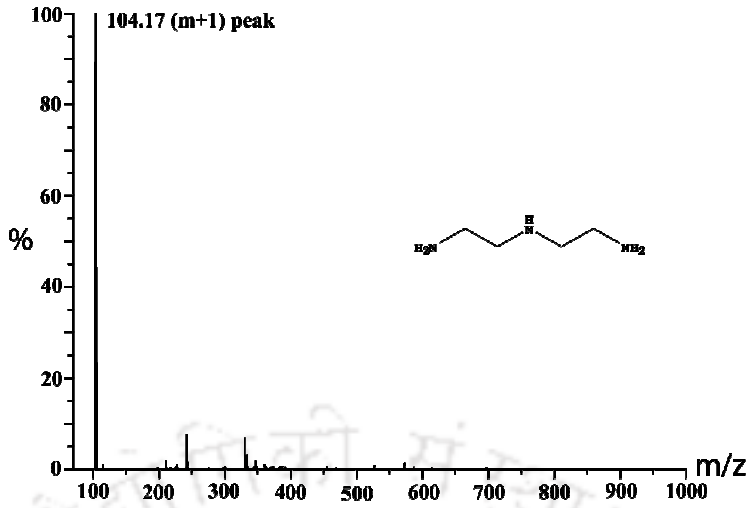

Figure A2.11: ESI-Mass spectrum of $\mathbf{L_3}'$ in methanol.

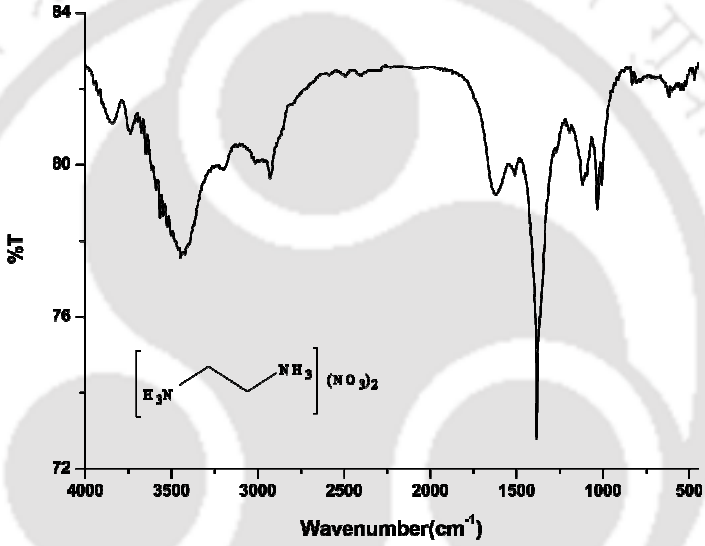

Figure A2.12: FT-IR spectrum of $\mathbf{L_3}''$ in KBr pellet.

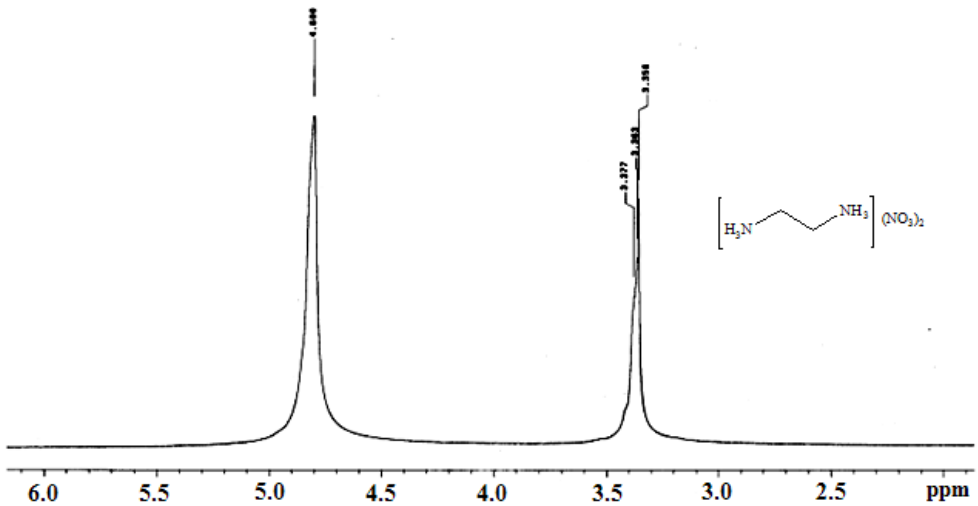

Figure A2.13: ^{1}H-NMR spectrum of $\mathbf{L_3}''$ in D_2O.

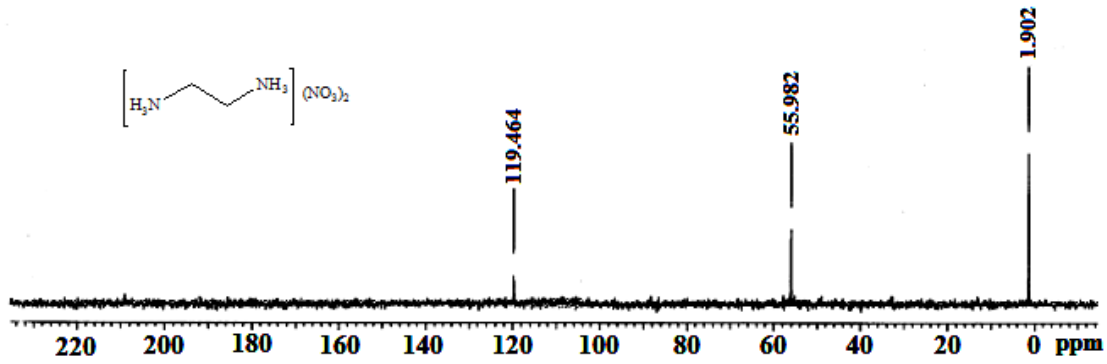

Figure A2.14: ^{13}C-NMR spectra of $\mathbf{L_3''}$ in D_2O (one drop of CD_3CN is added as standard).

Appendix III

The ligands $\mathbf{L_5}$ and $\mathbf{L_6}$ were synthesized in the laboratory from ethylenediamine. The detail procedure of synthesis of the ligands and their characterizations are shown in this section.

Synthesis of ligands L_5

Ligand $\mathbf{L_5}$ was synthesized in three steps (Scheme A3.1):

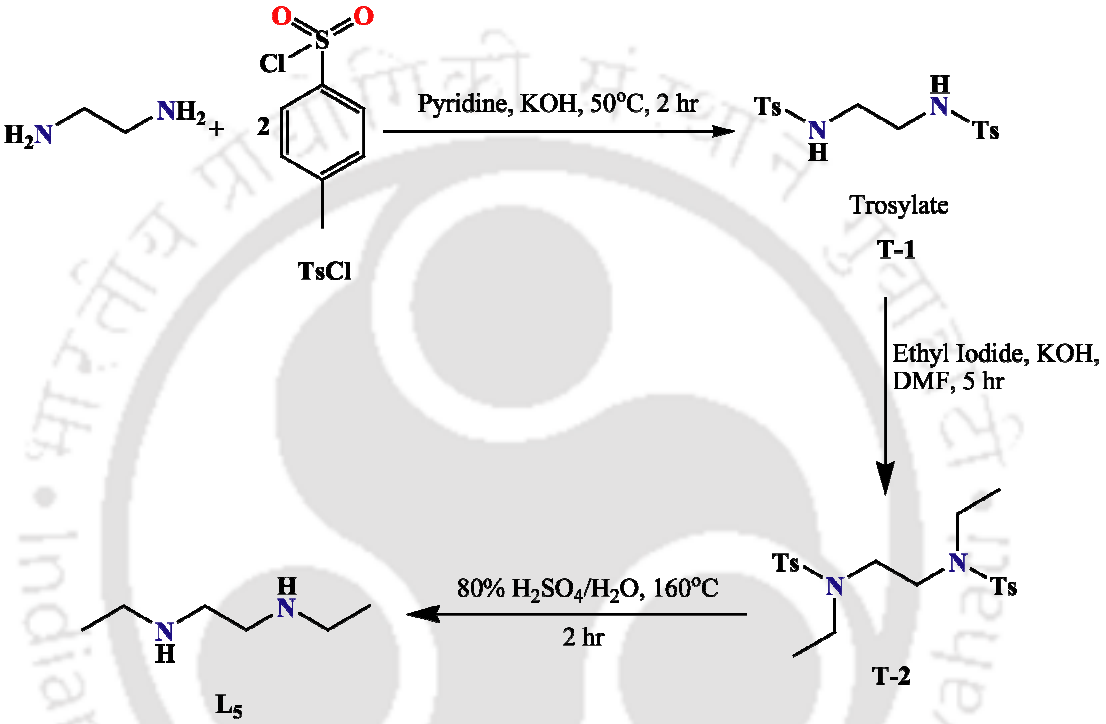

Scheme A3.1

Step I. Tosylation of ethylenediamine:

A 250-ml two-necked round-bottomed flask equipped with a magnetic stirring bar, reflux condenser and a rubber septum was charged with ethylenediamine (0.360 g; 6.0 mmol), pyridine (20 ml) and potassium hydroxide (1.01 g; 18.0 mmol). The mixture was stirred and cooled in an ice bath while 3.43 g (18.0 mmol) of tosyl chloride was added over a period of 5 min. After 5 min, the ice bath was removed and the reaction mixture was heated to 50 °C in an oil bath for 2 h with constant stirring. The reaction mixture was allowed to cool to room temperature was then poured into 20 ml ice-cold water. The crude tosylated product was obtained as whitish precipitate. The precipitate was purified by column chromatography using hexane to give 1.9 g (~ 85%) of N, N$^{/}$-*p*-methylbenzenesulfonamide ethylenediamine(**T-1**). FT-IR: 1408, 1335, 1158 cm^{-1}. ^{1}H-NMR (400 MHz, $CDCl_3$): δ_{ppm}, 7.69(d, 4H) 7.28(d, 4H),

3.02(t, 4H), 2.40(s, 6H). ^{13}C-NMR (100 MHz, $CDCl_3$): δ_{ppm}, 140.09, 137.58, 127.63, 125.67, 49.01, 21.80. (m+1)/z: 369.21.

Step II: Ethylation of T-1:

A 250-ml two-necked round-bottomed flask equipped with a magnetic stirring bar, reflux condenser and a rubber septum was charged with 1.1 g (3.0 mmol) of **T-1**, 1.1 g (21.0 mmol) of potassium hydroxide, and 20 ml of anhydrous dimethylformamide (DMF). To this 2 g (12.0 mmol) ethyl iodide was added over a period of 5 min and the resulting mixture was heated at 60 °C in an oil bath for 4h. The reaction mixture was then allowed to cool to room temperature, diluted with 250 ml of water, and extracted with $CHCl_3$ (100 ml X 3 portions). The combined organic extracts were washed with brine (100 ml), dried over anhydrous sodium sulphate and concentrated under reduced pressure to give pale yellow oil. The oil was purified by column chromatography on neutral alumina to give 0.85 g (~65%) of **T-2** as a viscous pale yellow liquid FT-IR: 1408, 1335, 1158 cm^{-1}. ^{1}H-NMR (400 MHz, $CDCl_3$): δ_{ppm}, 7.66(d, 4H) 7.29(d, 4H), 3.25(s, 4H). 3.20(q, 4H), 2.40(s, 6H), 1.143(s, 6H). ^{13}C-NMR (100 MHz, $CDCl_3$): δ_{ppm}, 143.62, 136.34, 129.96, 127.32, 48.21, 44.76, 21.69, 14.31. (m+1)/z: 425.71.

Step III. Hydrolysis of T-2:

A 100-ml two-necked round-bottomed flask equipped with a magnetic stirring bar, reflux condenser, and a rubber septum was charged with 4.24 (10.0 mmol) of **T-2**, 17 ml of 80% H_2SO_4, and the resulting mixture was heated at 160 °C in an oil bath with constant stirring till solid goes into solution. The reaction mixture was then allowed to cool to room temperature, diluted with 30 ml of water and neutralized with 20% NaOH solution. The resulting amine was then extracted with 3 X 50 ml portions of dichloromethane. The combined organic extracts were washed with brine (100 ml), dried over anhydrous sodium sulphate and concentrated under reduced pressure. The residue was purified by column chromatography on neutral alumina to give 0.75 g (~65%) of the desired amine $\mathbf{L_5}$. FT-IR: 1561, 1484, 1307, 1121, 719 cm^{-1}. ^{1}H-NMR (400 MHz, $CDCl_3$): δ_{ppm}, 2.70 (s, 4H), 2.63 (q, 4H), 1.60(s, 1H), 1.08(t, 6H). ^{13}C-NMR (100 MHz, CDCl3): δ_{ppm}, 49.26, 44.23, 15.30; (m+1)/z: 117.21.

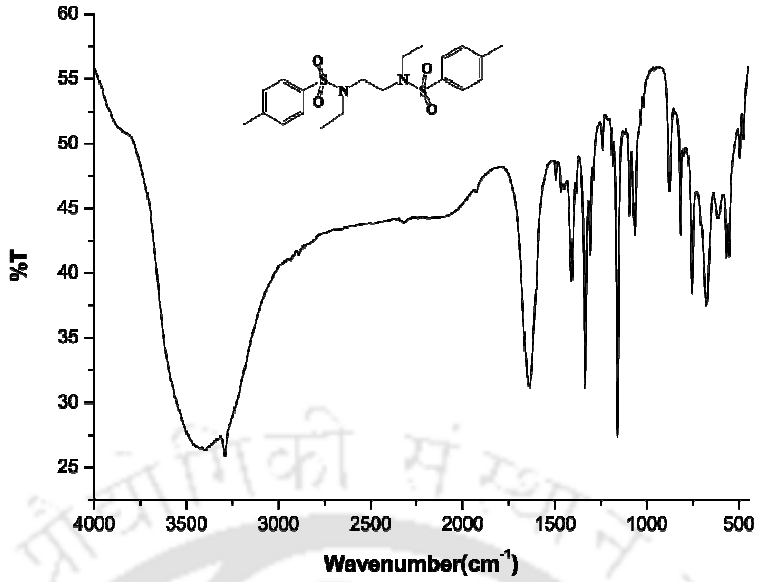

Figure A3.1: FT-IR spectrum of **T-1** in KBr pellet.

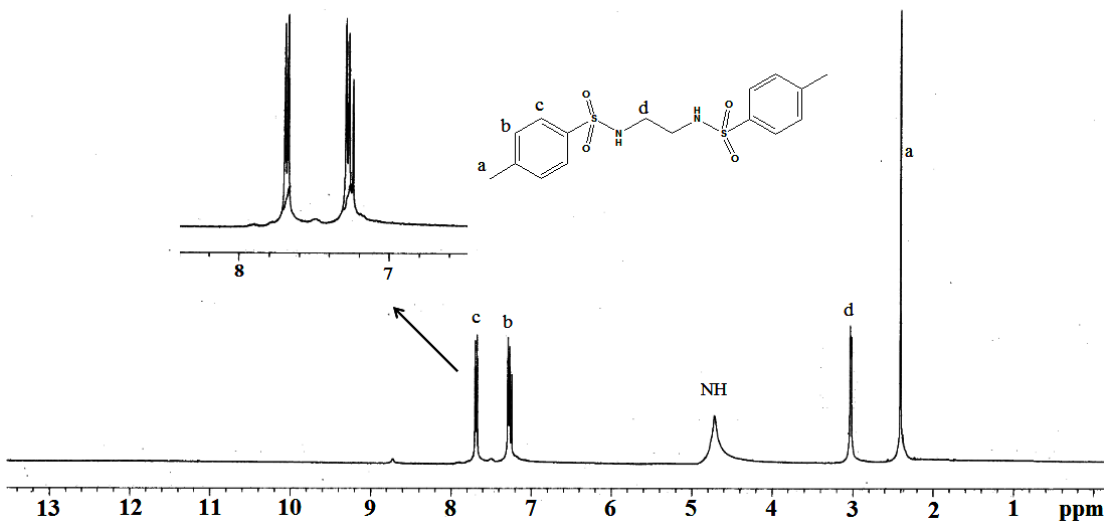

Figure A3.2: ^{1}H-NMR spectrum of **T-1** in $CDCl_3$.

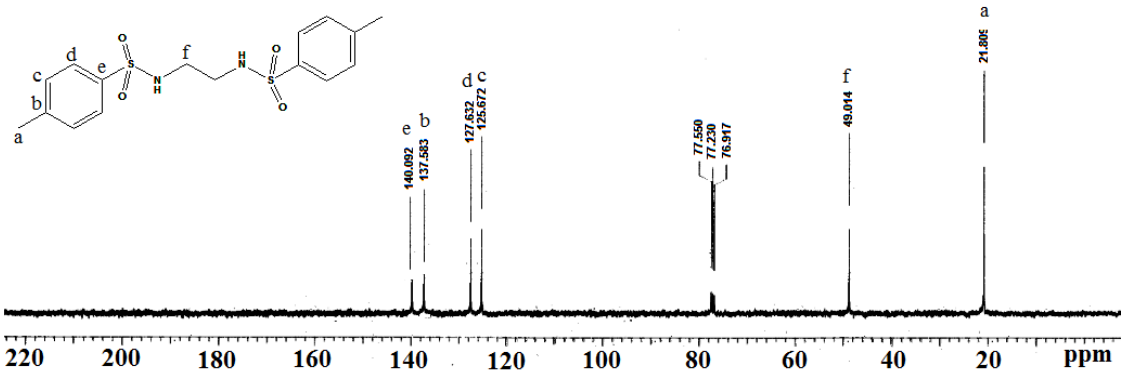

Figure A3.3: ^{13}C-NMR spectrum of **T-1** in $CDCl_3$.

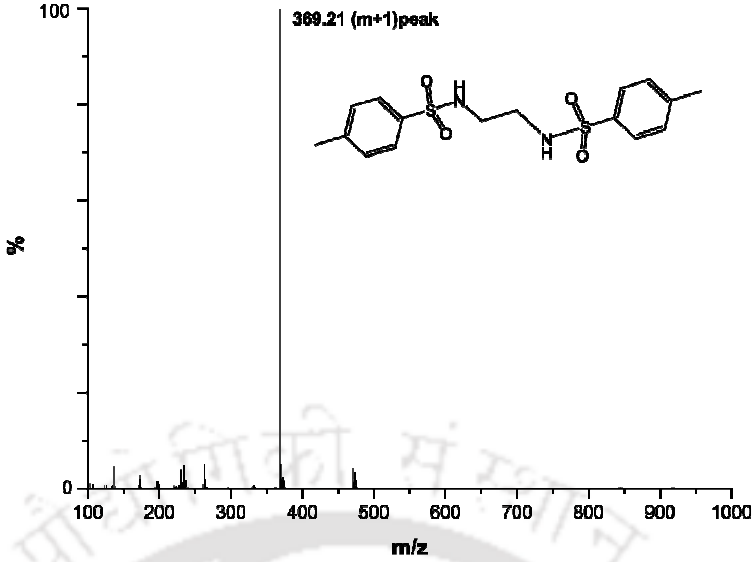

Figure A3.4: ESI-Mass spectrum of **T-1** in methanol.

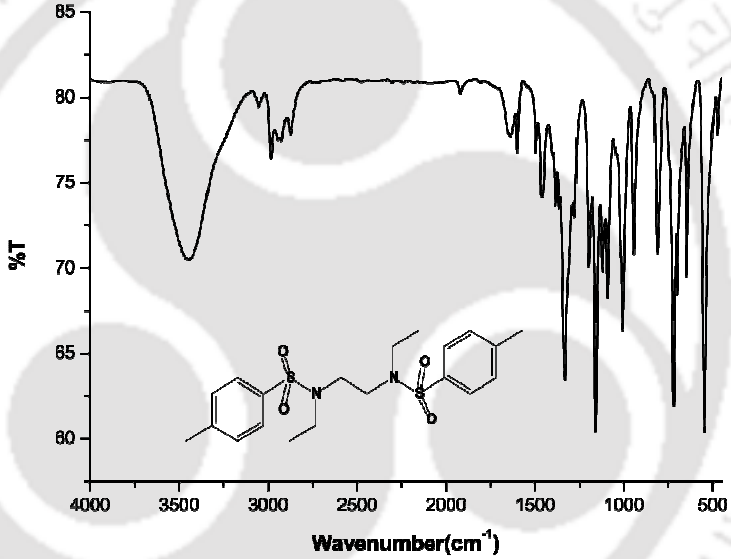

Figure A3.5: FT-IR spectrum of **T-2** in KBr pellet.

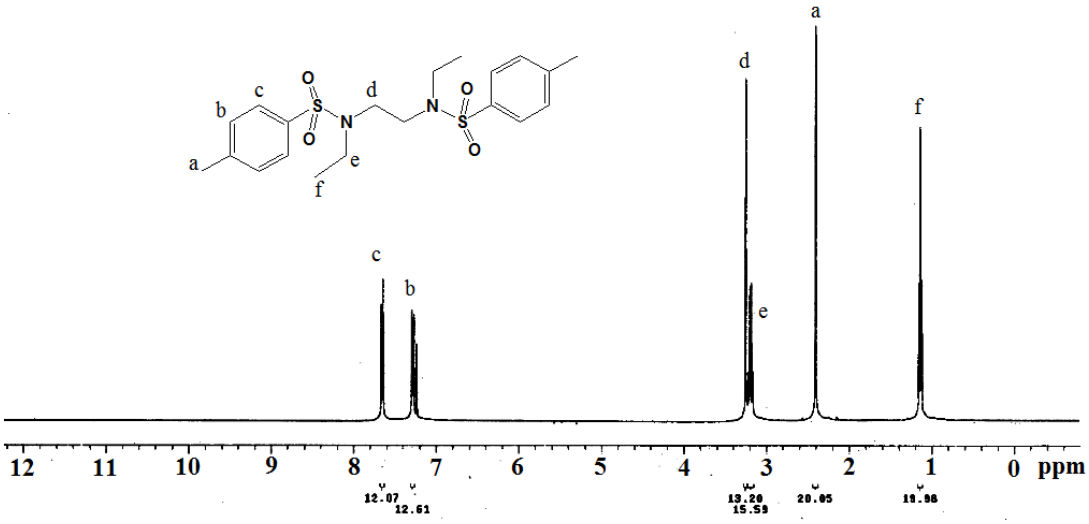

Figure A3.6: ^{1}H-NMR spectrum of **T-2** in $CDCl_3$.

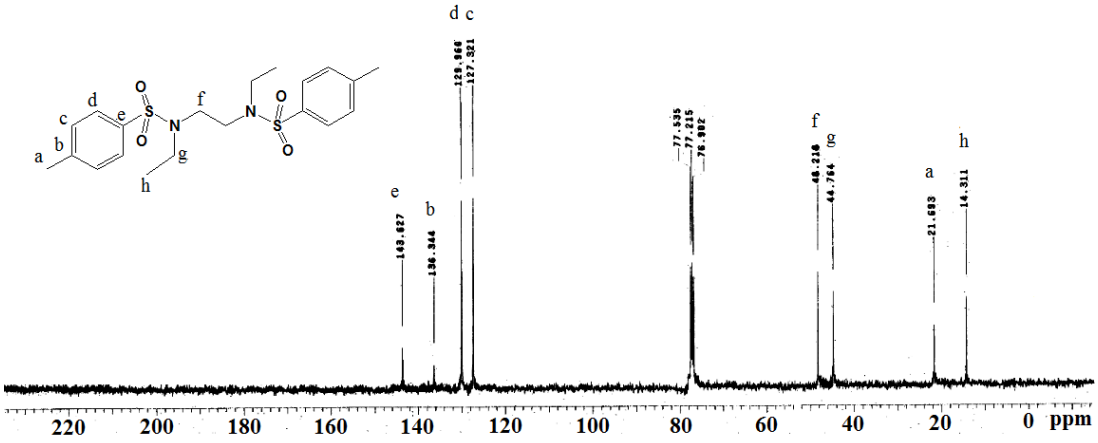

Figure A3.7: ^{13}C-NMR spectrum of **T-2** in $CDCl_3$.

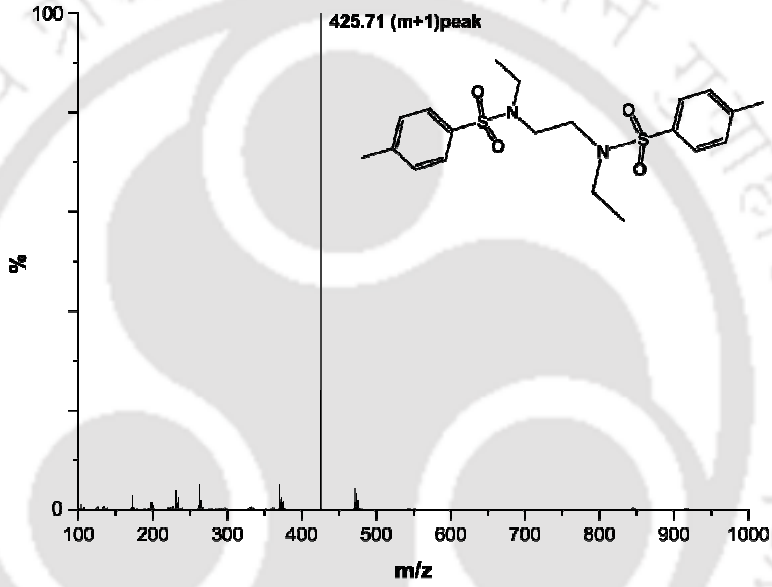

Figure A3.8: ESI-Mass spectrum of **T-2** in methanol.

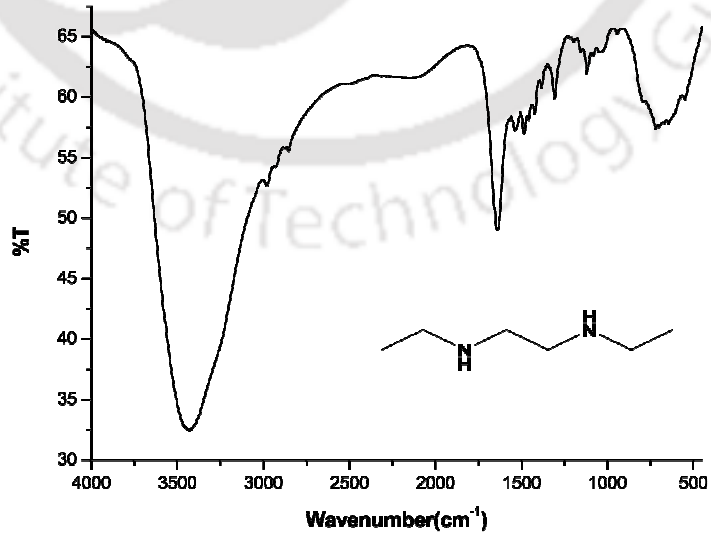

Figure A3.9: FT-IR spectrum of $\mathbf{L_5}$ in KBr pellet.

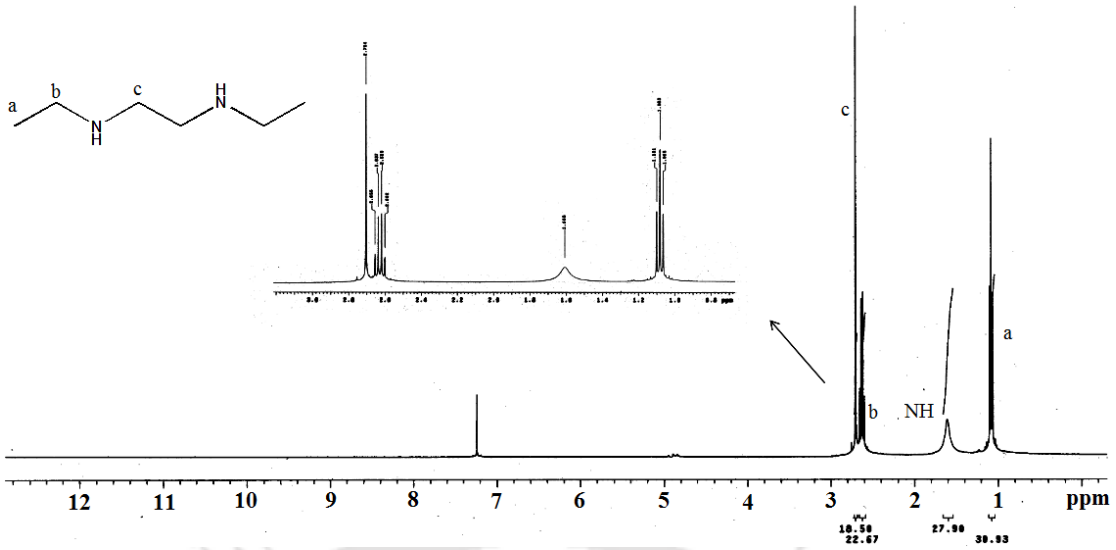

Figure A3.10: ^{1}H-NMR spectrum of $\mathbf{L_5}$ in $CDCl_3$.

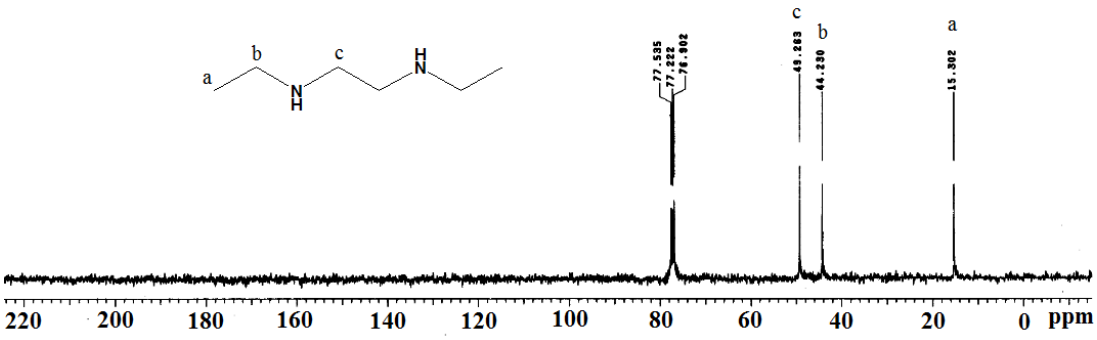

Figure A3.11: ^{13}C-NMR spectrum of $\mathbf{L_5}$ in $CDCl_3$.

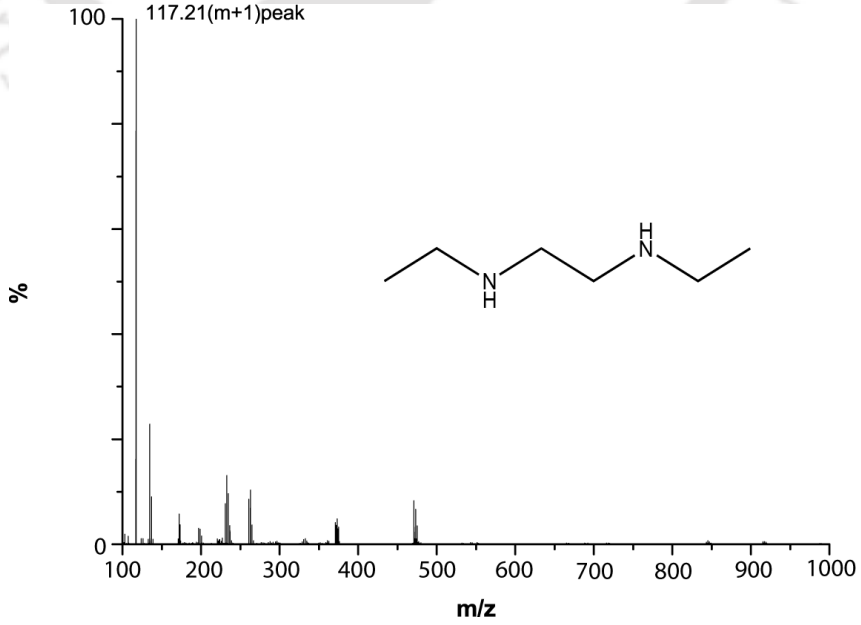

Figure A3.12: ESI-Mass spectrum of $\mathbf{L_5}$ in methanol.

Synthesis of ligands L_6

Ligand $\mathbf{L_6}$ was synthesized in three steps (scheme A3.2):

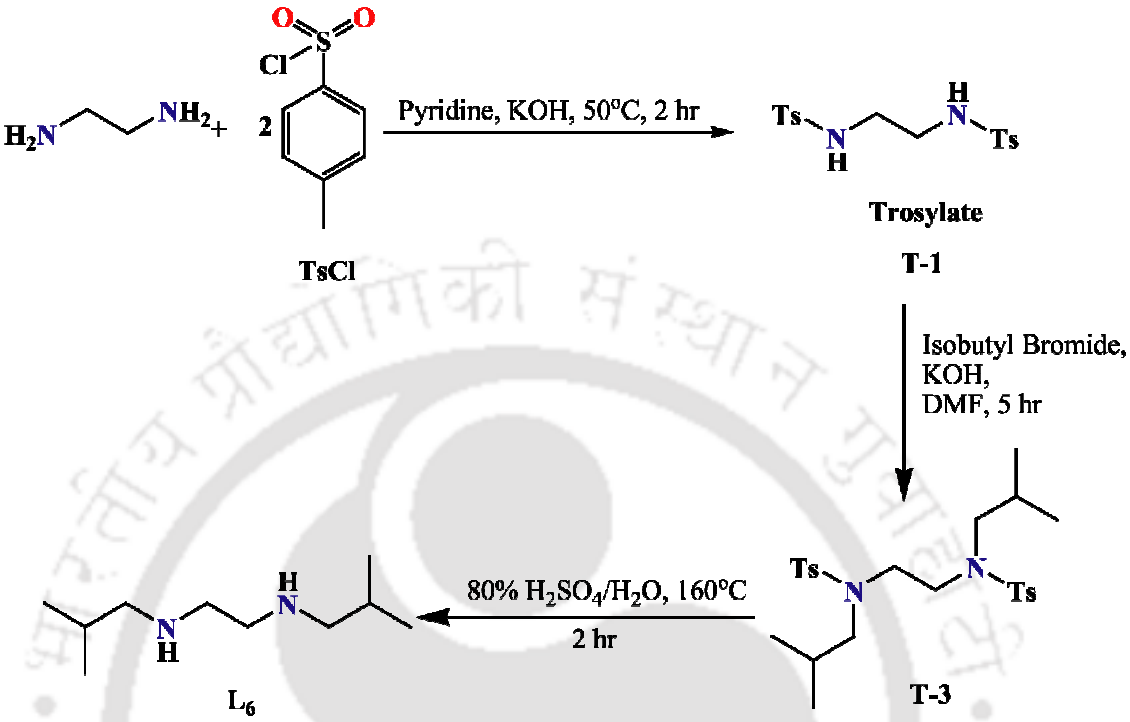

Scheme A3.2

Step I. Tosylation of ethylenediamine:

Same as in the case of synthesis of $\mathbf{L_5}$

Step II: Isobutylation of T-1:

The experimental procedure preparation of **T-3** is similar as the Step II in the case of $\mathbf{L_5}$. Only the difference is instead of ethyle iodide we have used here isobutyl bromide.

Yield: 2.65g (72%) of **T-3** as a colorless crystalline solid. Its structure was also determined by the X-ray single structure. FT-IR: 1344, 1157, 1005,725, 654 cm^{-1}. ^{1}H-NMR (400 MHz, $CDCl_3$): $\delta_{ppm,}$ 7.65(d, 4H) 7.30(d, 4H), 3.18(s, 4H). 2.83(d, 4H), 2.41(s, 6H), 1.86(m, 2H) 0.917d, 6H). ^{13}C-NMR (100 MHz, CDCl3): δ_{ppm}, 143.67, 135.71, 129.93, 127.45, 58.24, 49.38, 27.45, 20.191.

Hydrolysis of T-3:

Yield: 0.56 g (32%) of the desired amine $\mathbf{L_6}$. FT-IR: 2957, 2923, 2853, 1465, 1089 cm^{-1}. ^{1}H-NMR (400 MHz, $CDCl_3$): $\delta_{ppm,}$ 2.65 (s, 4H), 2.37 (d, 4H, J =8.0 Hz), 1.69(m, 2H), 0.85(d, 12H, J =8.0 Hz). ^{13}C-NMR (100 MHz, CDCl3): δ_{ppm}, 58.08, 49.47, 28.42, 20.80; (m+1)/z: 173.21.

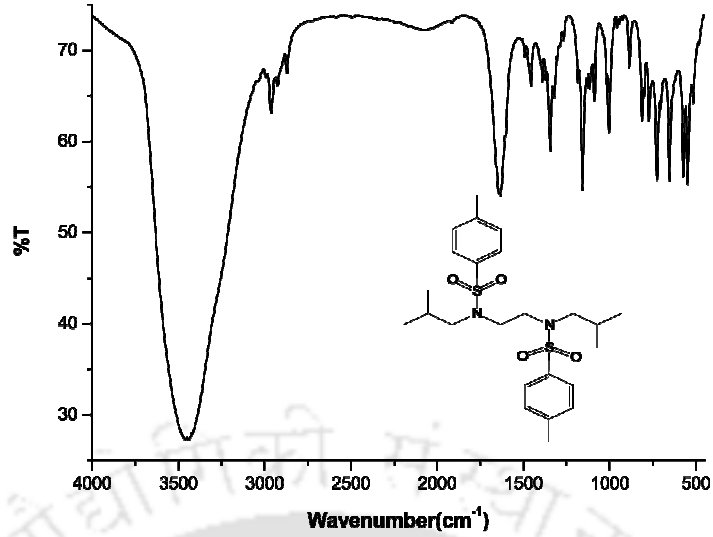

Figure A3.13: FT-IR spectrum of **T-3** in KBr pellet.

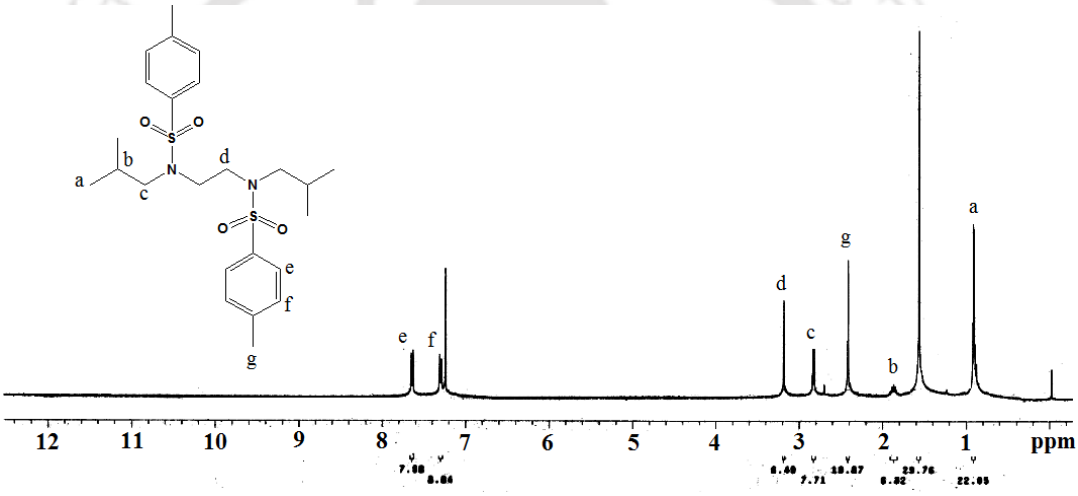

Figure A3.14: ^{1}H-NMR spectrum of **T-3** in $CDCl_3$.

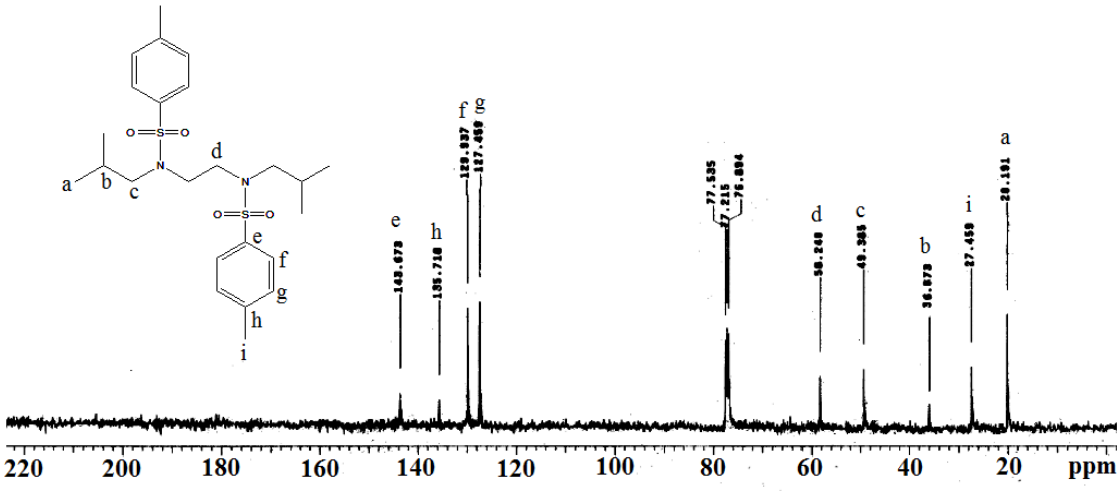

Figure A3.15: ^{13}C-NMR spectrum of **T-3** in $CDCl_3$.

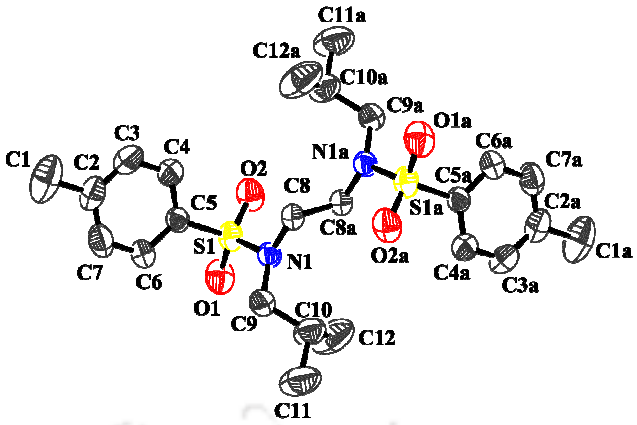

Figure A3.16: ORTEP diagram of **T-3** [a (-x, 1-y, -z) symmetry transformation is implied by each additional atom level] (50% thermal ellipsoid plot).

Table A5.1: Crystallographic Data for **T-3**.

	T-3
Formulae	$C_{24}H_{36}N_2S_2O_4$
Mol. wt.	480.67
Crystal system	Triclinic
Space group	P-1
Temperature /K	296(2)
Wavelength /Å	0.71073
a /Å	5.3633(2)
b /Å	9.9606(5)
c /Å	12.5886(5)
α/°	91.902(3)
β/°	98.241(3)
γ/°	97.192(3)
V/ Å^3	659.43(5)
Z	1
Density/Mgm^{-3}	1.210
Abs. Coeff. /mm^{-1}	0.232
Abs. correction	None
F(000)	258
Total no.of reflections	2151
Reflections, $I > 2\sigma(I)$	1545
Max. 2θ/°	25.00
Ranges (h, k, l)	-6 <= h <=6 -10<= k <=11 -14 <= l <= 14
Complete to 2θ (%)	92.5%

Refinement method	Full-matrix least-squares on F^2
Goof (F^2)	1.024
Flack parameter	-
Rint	0.0683
R indices [$I > 2\sigma(I)$]	0.0444
R indices (all data)	0.0611

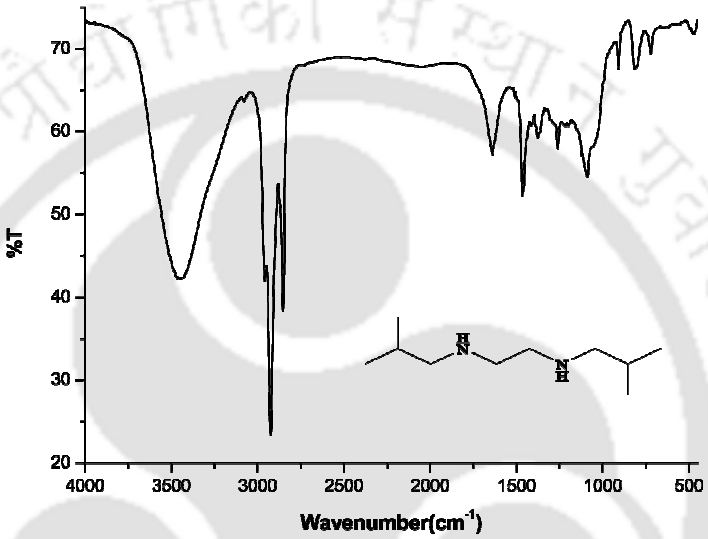

Figure A3.17: FT-IR spectrum of $\mathbf{L_6}$ in KBr pellet.

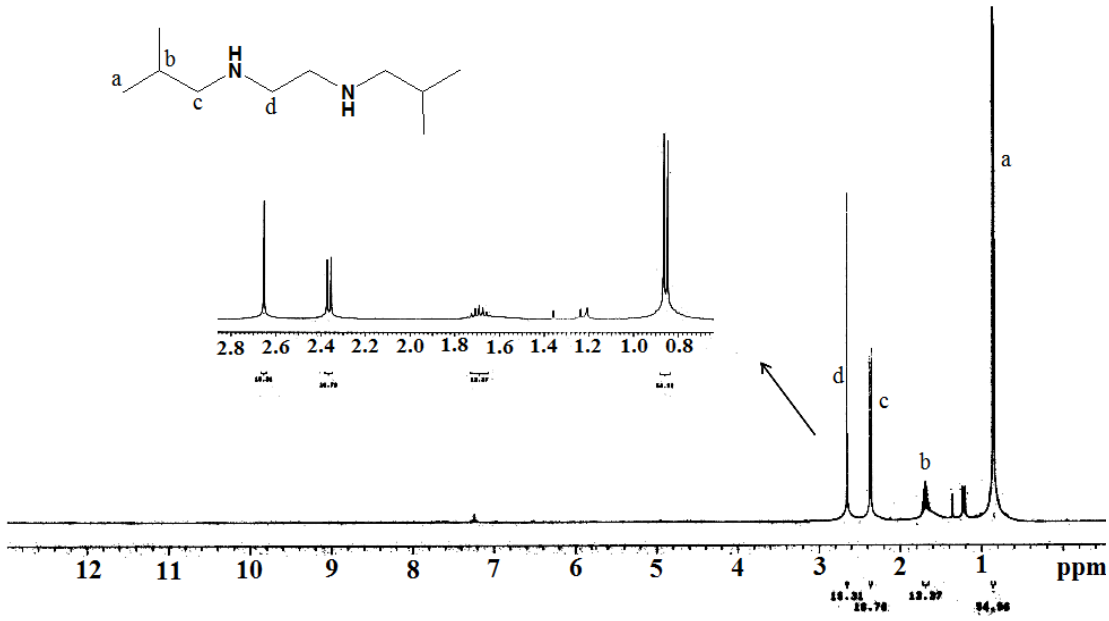

Figure A3.18: ^{1}H-NMR spectrum of $\mathbf{L_6}$ in $CDCl_3$.

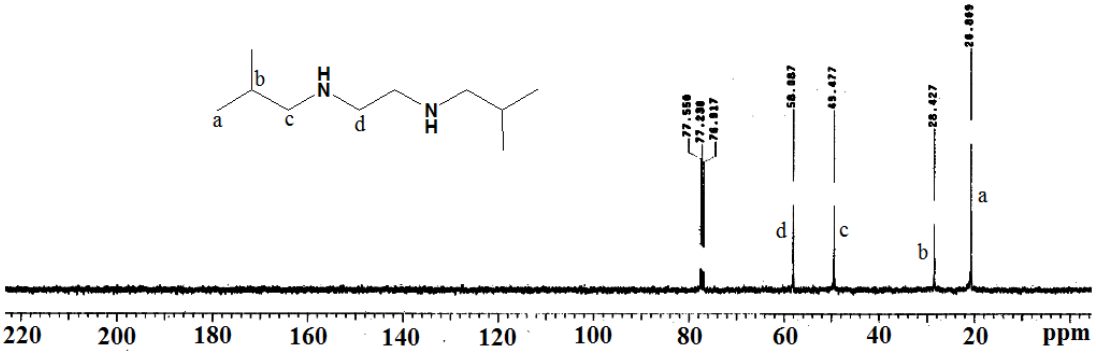

Figure A3.19: ^{13}C-NMR spectrum of $\mathbf{L_6}$ in $CDCl_3$.

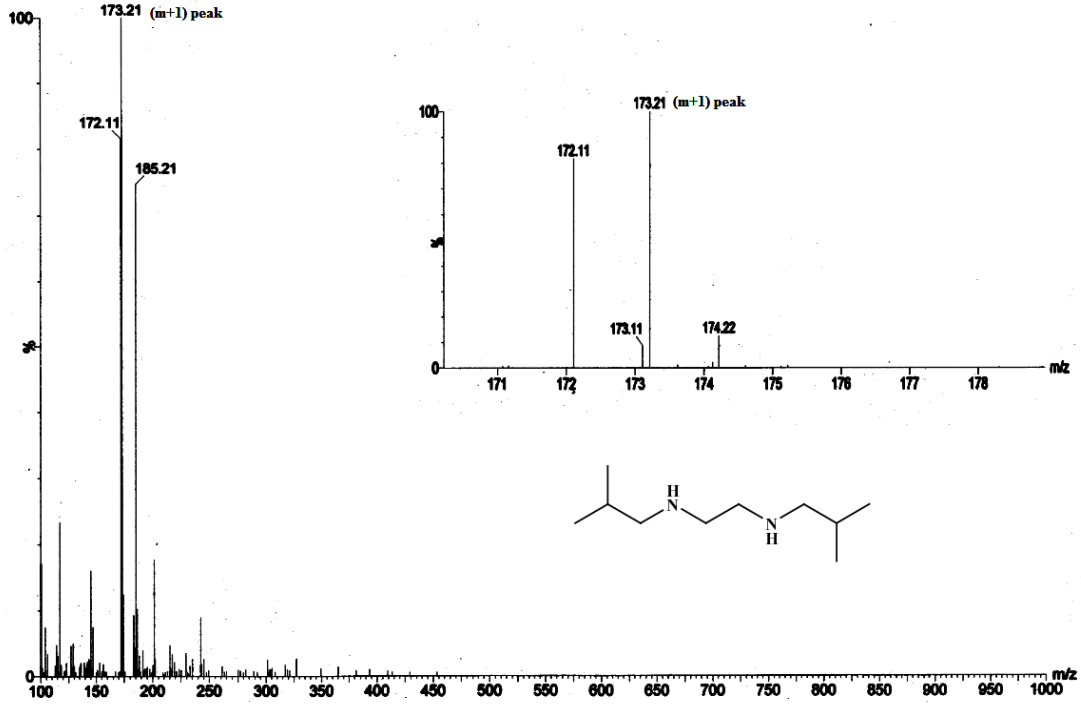

Figure A3.20: ESI-Mass spectrum of $\mathbf{L_6}$ in methanol.

Table A3.2. Crystallographic data for complexes **4.1**, **4.2** and **4.3.**

	Complex **4.1**	Complex **4.2**	Complex **4.3**
Formulae	$C_8\ H_{24}Cl_2\ Cu\ N_4\ O_8$	$C_{12}H_{36}Cl_2Cu\ N_4O_{10}$	$C_{20}\ H_{48}\ Cl_2\ Cu\ N_4\ O_8$
Mol. wt.	438.75	530.89	607.06
Crystal system	Monoclinic	Monoclinic	Orthorhombic
Space group	Cc	P2(1)/c	Pbca
Temperature /K	296(2)	296(2)	296(2)
Wavelength /Å	0.71073	0.71073	0.71073
a /Å	8.6311(3)	7.3704(5)	14.8346(5)
b /Å	13.7336(3)	9.9384(7)	16.8936(6)

c /Å	15.1029(5)	16.4246(10)	24.3560(8)
α/°	90.00	90.00	90.00
β/°	95.7460(10)	107.915(4)	90.00
γ/°	90.00	90.00	90.00
V/ Å^3	1781.24(9)	1144.77(13)	6103.9(4)
Z	4	2	8
Density/Mgm^{-3}	1.636	1.540	1.321
Abs. Coeff. /mm^{-1}	1.568	1.240	0.935
Abs. correction	None	None	None
F(000)	908	558	1992
Total no.of reflections	2786	2846	7590
Reflections, $I > 2\sigma(I)$	2734	2491	3567
Max. 2θ/°	25.49	28.36	28.31
Ranges (h, k, l)	-10 <= h <=8 -16<= k <=16 -17 <= l <= 18	-9 <= h <=9 -13<= k <=13 -21 <= l <= 21	-19 <= h <=19 -22 <= k <=22 -31 <= l <= 32
Complete to 2θ (%)	97.2%	99.4%	99.9%
Refinement method	Full-matrix least-squares on F^2	Full-matrix least-squares on F^2	Full-matrix least-squares on F^2
Goof (F^2)	0.935	1.064	1.006
R_{int}	0.0381	0.0225	0.0686
R indices [$I > 2\sigma(I)$]	0.0329	0.0397	0.0560
R indices (all data)	0.0335	0.0446	0.1379

Table A3.3. Selected bond lengths (Å) for complexes **4.1**, **4.2** and **4.3**.

	Complex **4.1**	Complex **4.2**	Complex **4.3**
Cu1-N1	2.042(4)	2.069(2)	2.046(3)
Cu1-N2	2.045(4)	2.026(2)	2.055(3)
Cu1-N3	2.043(4)	-	2.058(3)
Cu1-N4	2.036(3)	-	2.056(3)
N1-C1	1.468(9)	-	-
N1-C2	1.505(8)	-	-
N1-C3	-	1.485(3)	-
N1-C5	-	-	1.479(5)
N2-C3	1.469(7)	-	-

N2-C4	1.483(8)	1.489(3)	-
N2-C6	-	-	1.479(4)
N3-C5	1.475(7)	-	-
N3-C6	1.501(6)	-	-
N3-C15	-	-	1.490(5)
N4-C7	1.477(6)	-	-
N4-C8	1.466(6)	-	-
N4-C16	-	-	1.471(4)
C2-C3	1.49(1)	-	-
C3-C4	-	1.501(4)	-
C5-C6	-	-	1.493(6)
C6-C7	1.479(7)	-	-
C15-C16	-	-	1.480(6)

Table A3.4. Selected bond angles for complexes **4.1**, **4.2** and **4.3**.

	Complex **4.1**	Complex **4.2**	Complex **4.3**
N1-Cu1-N2	84.9(2)	85.6(7)	85.1(1)
N1-Cu1-N4	95.1(1)	-	-
N1-Cu1-N3	-	-	97.5(1)
N2-Cu1-N3	94.3(1)	-	-
N2-Cu1-N4	-	-	93.4(1)
N3-Cu1-N4	85.7(1)	-	85.3(1)
Cu1-N1-C2	105.5(3)	-	-
Cu1-N1-C3	-	105.6(2)	-
Cu1-N1-C5	-	-	105.9(2)
Cu1-N2-C3	107.8(3)	-	-
Cu1-N2-C4	-	107.0(1)	-
Cu1-N2-C6	-	-	107.2(2)
Cu1-N3-C6	106.3(3)	-	-
Cu1-N3-C15	-	-	104.8(2)
Cu1-N4-C7	105.8(3)	-	-
Cu1-N4-C16	-	-	107.2(2)
N1-C2-C3	108.2(5)	-	-
N1-C3-C4	-	108.6(2)	-
N1-C5-C6	-	-	108.9(3)
N2-C3-C2	108.1(5)	-	-
N2-C4-C3	-	108.7(2)	-
N2-C6-C5	-	-	109.4(3)
N3-C6-C7	108.9(4)	-	-
N3-C15-C16	-	-	109.9(3)
N4-C7-C6	108.8(4)	-	-
N4-C16-C15	-	-	109.2(3)

Table A3.5. Crystallographic data for $\mathbf{L_4''}$.

	$\mathbf{L_4''}$
Formulae	$C_4\ H_{10}\ N_4\ O_2$
Mol. wt.	146.16
Crystal system	Monoclinic
Space group	2/c
Temperature /K	296(2)
Wavelength /Å	0.71073
a /Å	5.7944(6)
b /Å	10.0079(6)
c /Å	13.3326(11)
α/°	90.00
β/°	97.710(6)
γ/°	90.00
V/ Å^3	766.16(11)
Z	4
Density/Mgm^{-3}	1.267
Abs. Coeff. /mm^{-1}	0.102
Abs. correction	None
F(000)	312
Total no.of reflections	879
Reflections, $I > 2\sigma(I)$	482
Max. 2θ/°	27.43
Ranges (h, k, l)	-5 <= h <=7 -12<= k <=7 -17 <= l <= 17
Complete to 2θ (%)	99.8%
Refinement method	Full-matrix least-squares on F^2
Goof (F^2)	1.145
R indices [$I > 2\sigma(I)$]	0.0638
R indices (all data)	0.0984

Table A3.6: Selected bond length (Å) and angle (°) of $\mathbf{L_4''}$.

Bond lengths(Å)		**Bond angles (°)**	
N1-N2	1.323(3)	N1-N2-O1	112.8(3)
N2-O1	1.220(4)	N2-N1-C1	115.2(2)
N1-C1	1.442(3)	N2-N1-C2	122.1(2)
N1-C2	1.442(3)	-	-

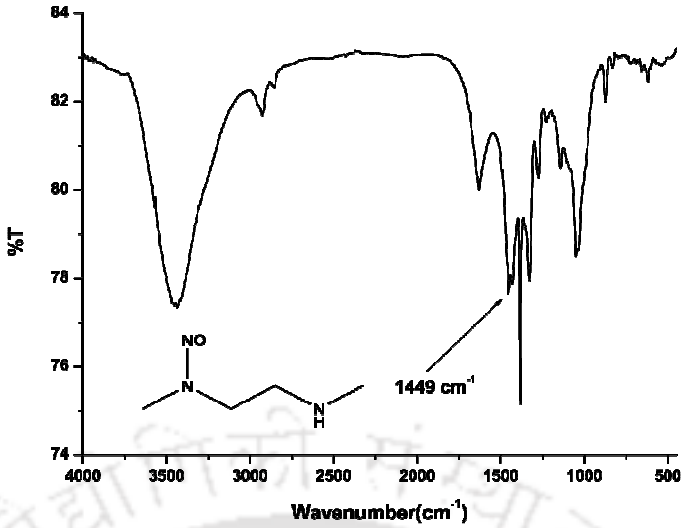

Figure A3.21: FT-IR spectrum of L_4' in KBr pellet.

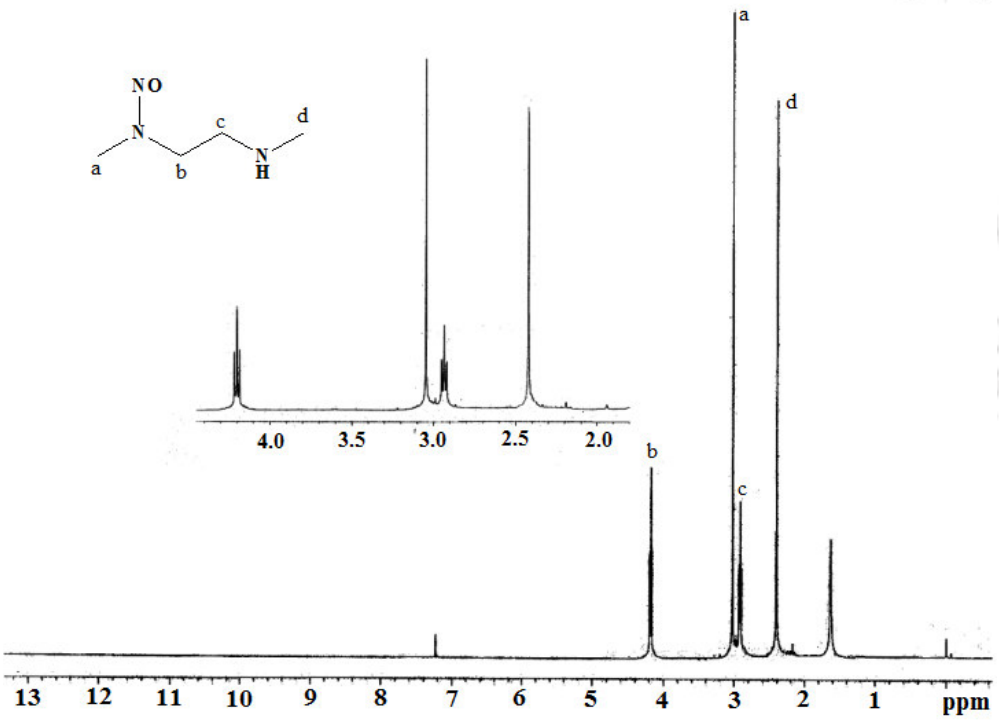

Figure A3.22: ^{1}H-NMR spectrum of L_4' of in $CDCl_3$.

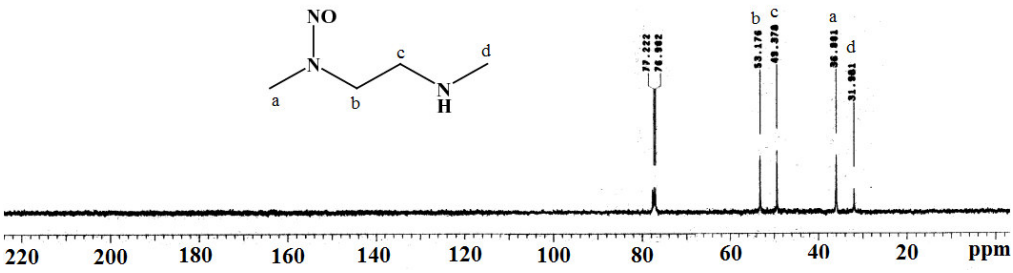

Figure A3.23: ^{13}C-NMR spectrum of L_4' of in $CDCl_3$.

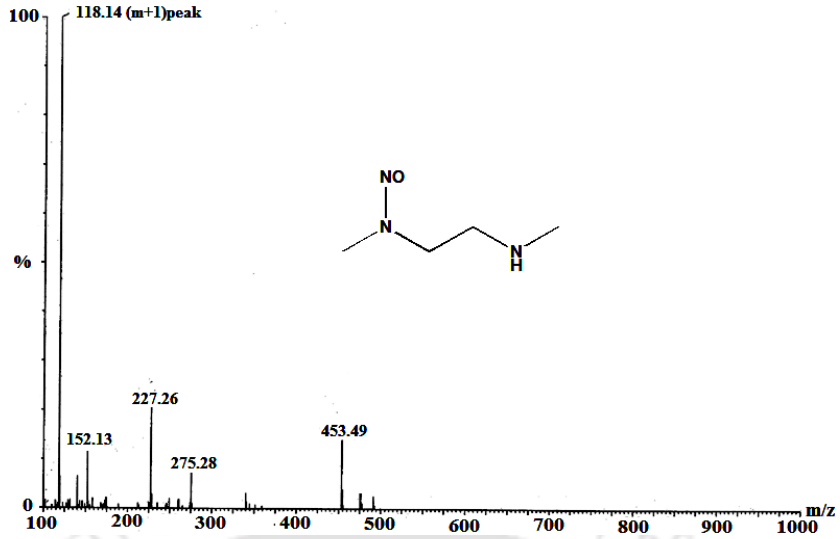

Figure A3.24: ESI-mass spectrum of L_4' in methanol.

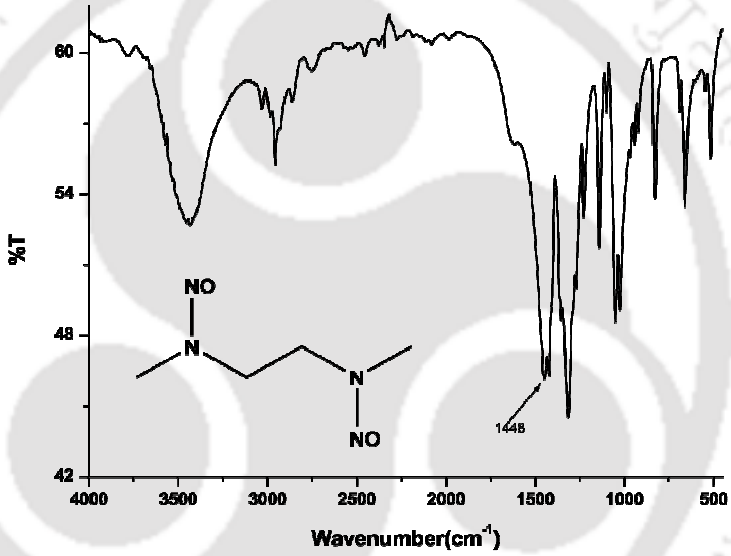

Figure A3.25: FT-IR spectrum of L_4'' in KBr pellet.

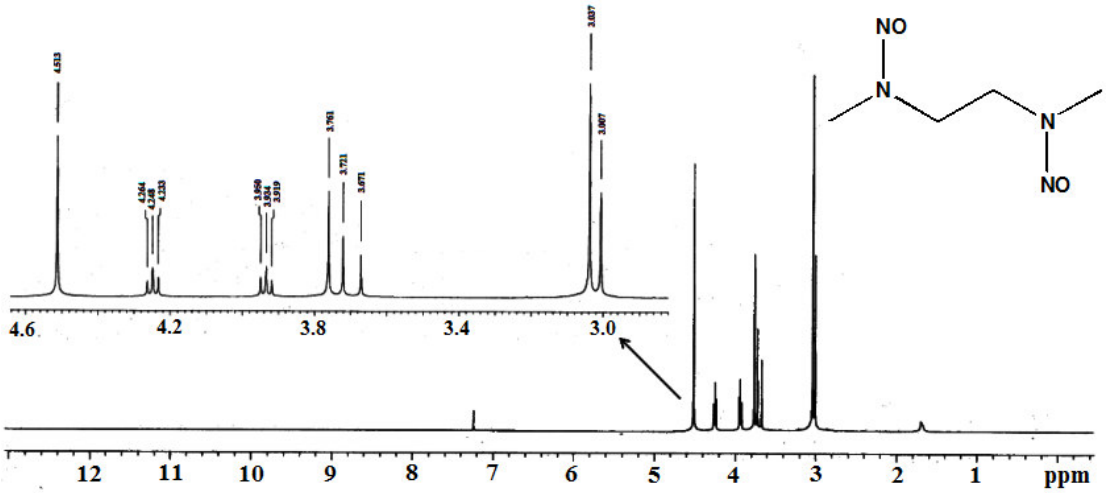

Figure A3.26: ^{1}H-NMR spectrum of L_4'' of in $CDCl_3$. The presence of extra signals in ^{1}H- and ^{13}C- NMR spectra are due to isomeric impurities.[1]

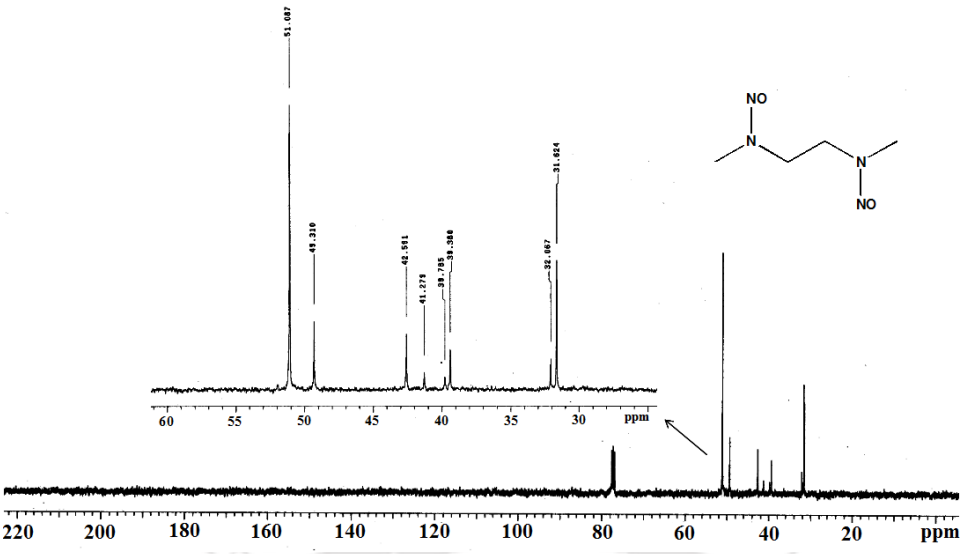

Figure A3.27: ^{13}C-NMR spectrum of $\mathbf{L_4''}$ of in $CDCl_3$. The presence of extra signals in ^{1}H- and ^{13}C- NMR spectra are due to isomeric impurities.[1]

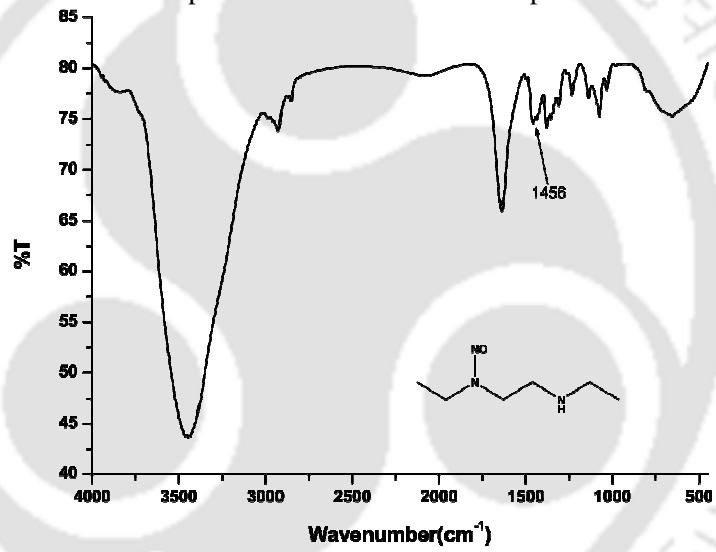

Figure A3.28: FT-IR spectrum of $\mathbf{L_5'}$ in KBr pellet.

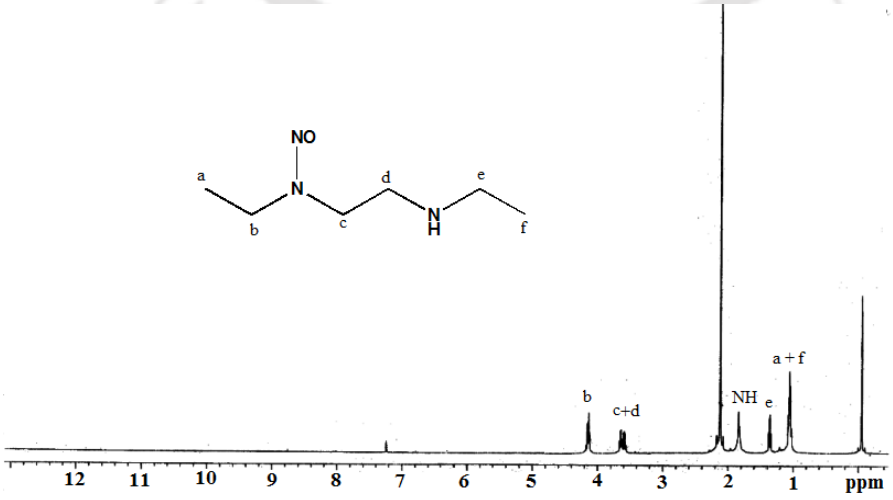

Figure A3.29: ^{1}H-NMR spectrum of $\mathbf{L_5'}$ of in $CDCl_3$.

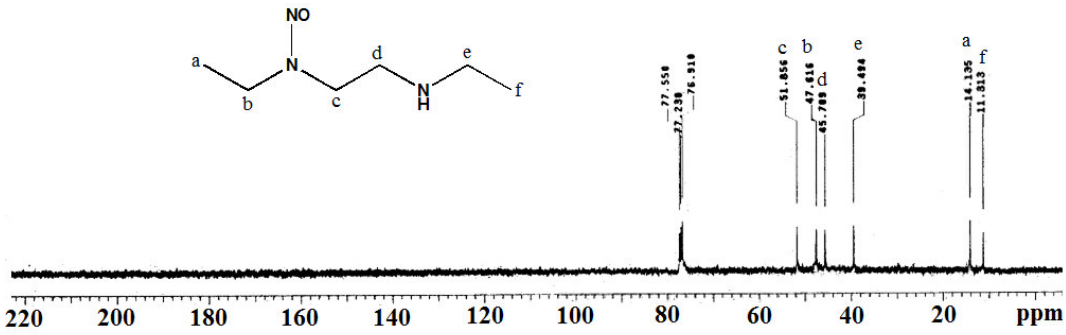

Figure A3.30: ^{13}C-NMR spectrum of $\mathbf{L_5}'$ of in $CDCl_3$.

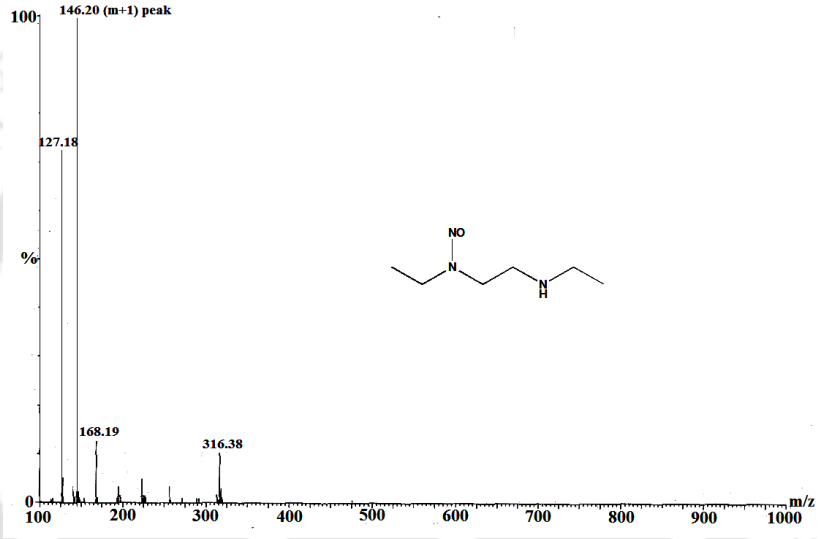

Figure A3.31: ESI-mass spectrum of $\mathbf{L_5}'$ in methanol.

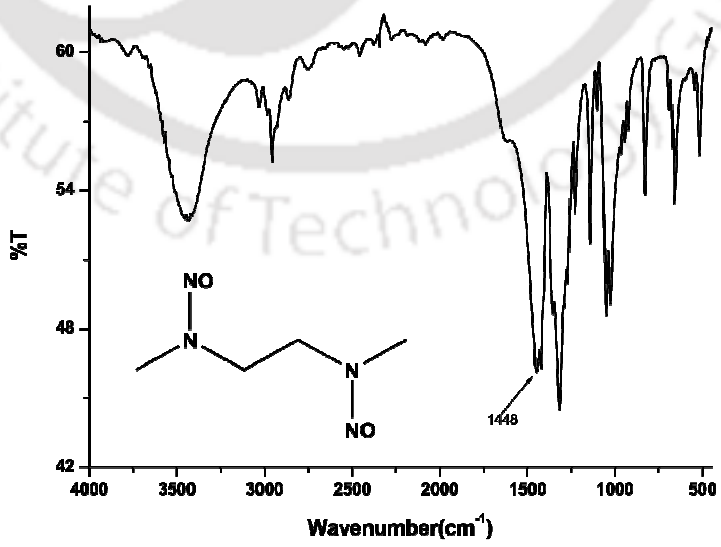

Figure A3.32: FT-IR spectrum of $\mathbf{L_5}''$ in KBr pellet.

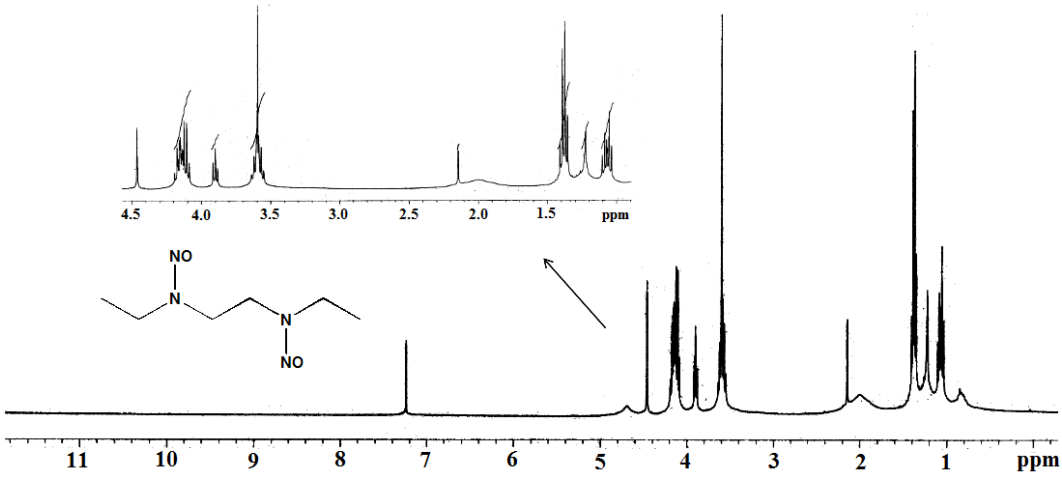

Figure A3.33: ^{1}H-NMR spectrum of $\mathbf{L_5''}$ of in $CDCl_3$. The presence of extra signals in ^{1}H- and ^{13}C- NMR spectra are due to isomeric impurities.[1]

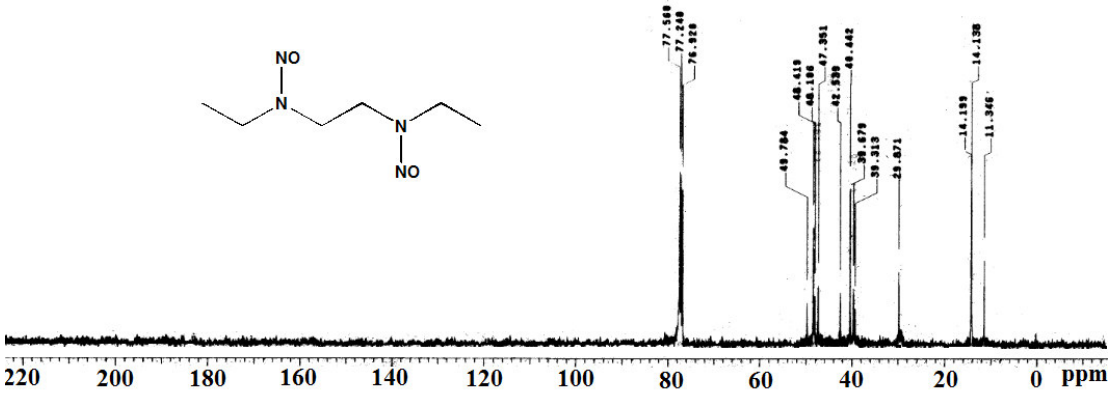

Figure A3.34: ^{13}C-NMR spectrum of $\mathbf{L_5''}$ of in $CDCl_3$. The presence of extra signals in ^{1}H- and ^{13}C- NMR spectra are due to isomeric impurities.[1]

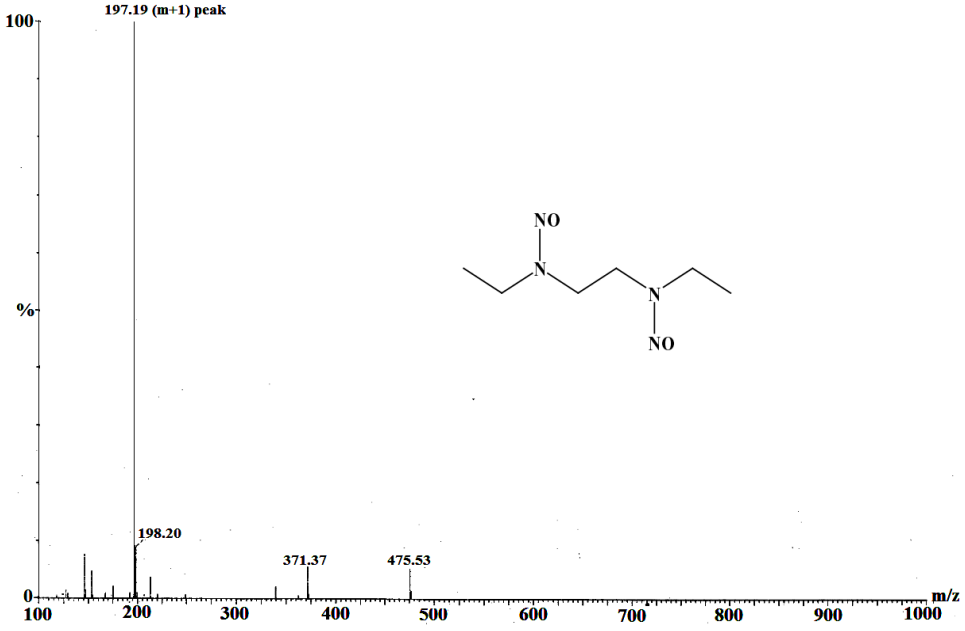

Figure A3.35: ESI-Mass spectrum of $\mathbf{L_5''}$ in methanol.

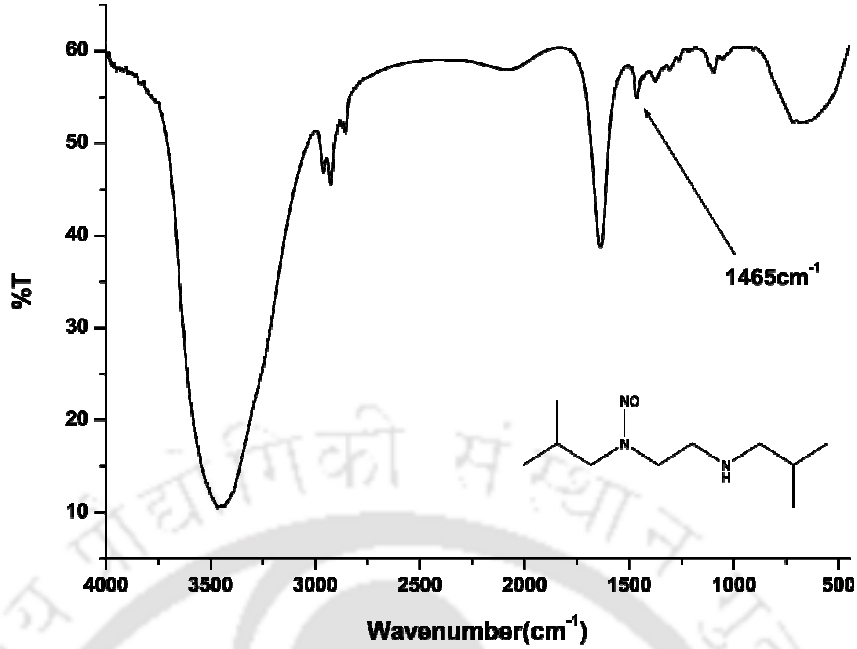

Figure A3.36: FT-IR spectrum of L_6' in KBr pellet.

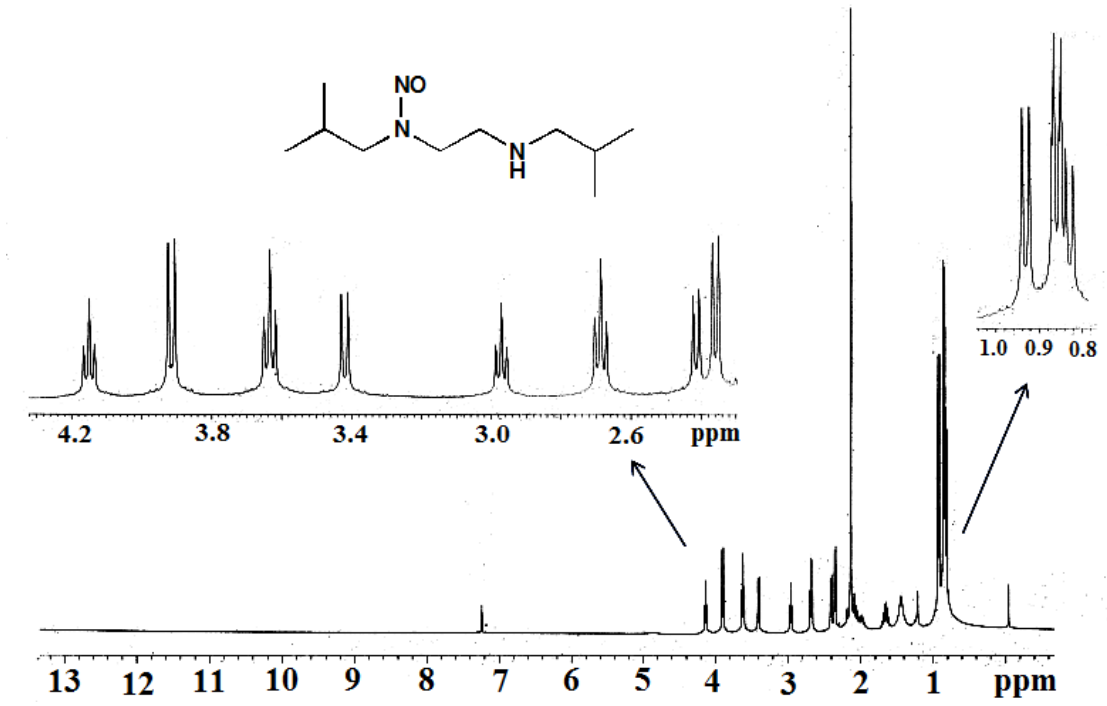

Figure A3.37: ^{1}H-NMR spectrum of L_6' of in $CDCl_3$. The presence of extra signals in ^{1}H- and ^{13}C- NMR spectra are due to isomeric impurities.[1]

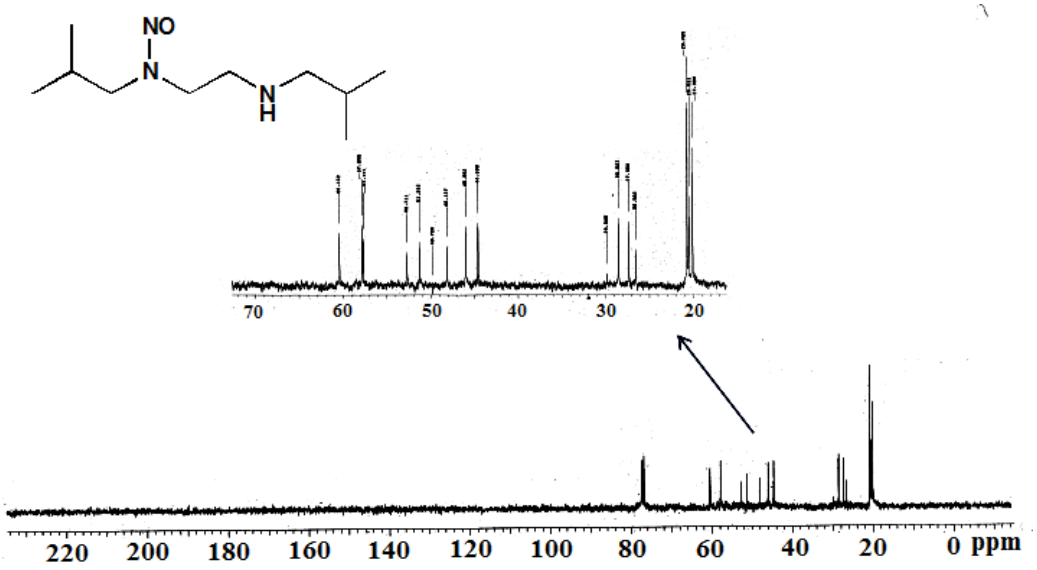

Figure A3.38: ^{13}C-NMR spectrum of $\mathbf{L_6'}$ of in $CDCl_3$. The presence of extra signals in ^{1}H- and ^{13}C- NMR spectra are due to isomeric impurities.[1]

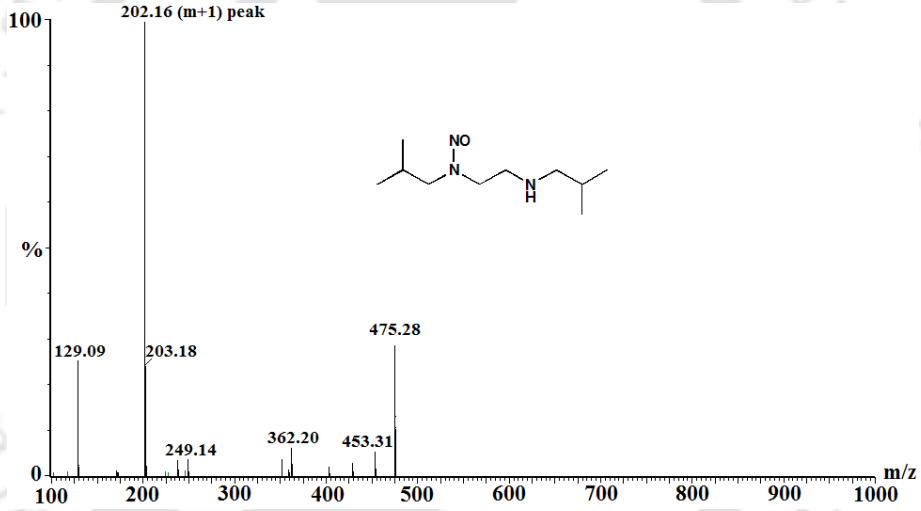

Figure A3.39: ESI-Mass spectrum of $\mathbf{L_6'}$ in methanol.

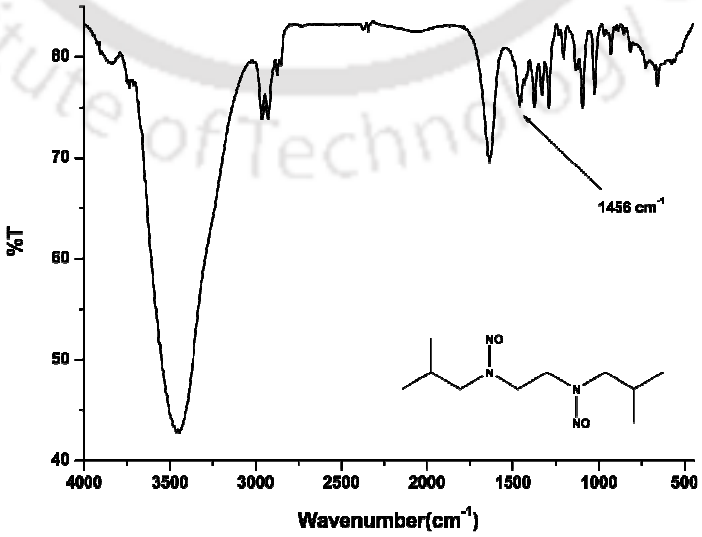

Figure A3.40: FT-IR spectrum of $\mathbf{L_6''}$ in KBr pellet.

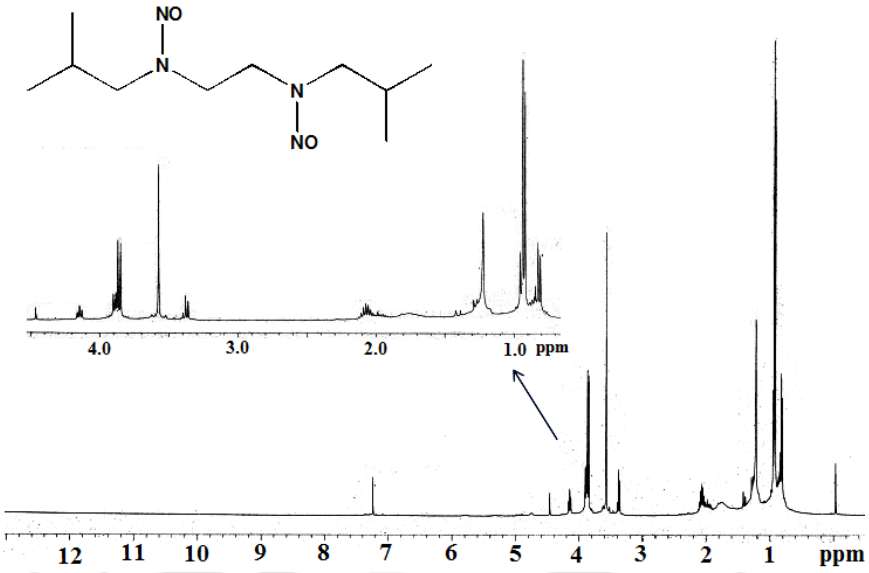

Figure A3.41: ^{1}H-NMR spectrum of $\mathbf{L_6}^{//}$ of in $CDCl_3$. The presence of extra signals in ^{1}H- and ^{13}C- NMR spectra are due to isomeric impurities.[1]

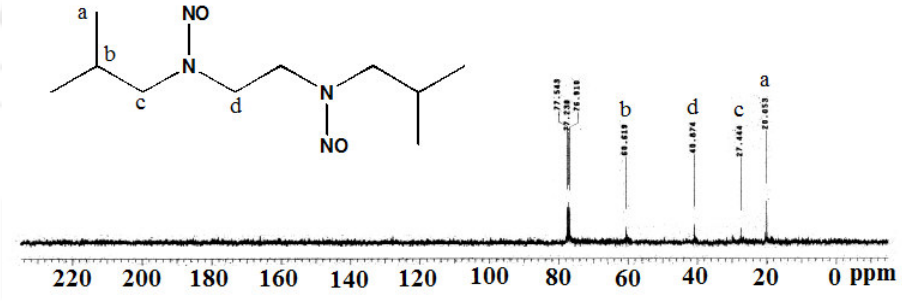

Figure A3.42: ^{13}C-NMR spectrum of $\mathbf{L_6}^{//}$ of in $CDCl_3$.

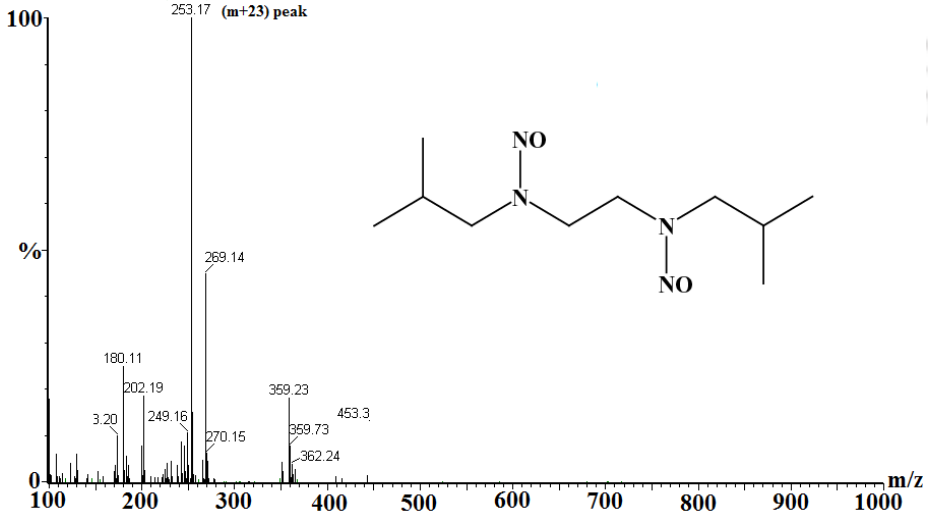

Figure A3.43: ESI-Mass spectrum of $\mathbf{L_6}^{//}$ in methanol.

Reference:

1. Harris, R. K.; Spragg, R. A. *J. Mol. Spect.* **1969**, *30*, 77.

Appendix IV

Table A4.1. Crystallographic data for complex **5.1**

	Complex **5.1**
Formulae	C_{12} H_{16} Cl_2 Cu N_4 O_8
Mol. wt.	478.78
Crystal system	Triclinic
Space group	P-1
Temperature /K	296(2)
Wavelength /Å	0.71073
a /Å	7.6342(6)
b /Å	7.9821(6)
c /Å	7.9904(7)
α/°	106.742(4)
β/°	95.757(4)
γ/°	108.833(3)
V/ $Å^3$	431.15(6)
Z	1
Density/Mgm^{-3}	1.844
Abs. Coeff. /mm^{-1}	1.629
Abs. correction	None
F(000)	243
Total no.of reflections	1265
Reflections, $I > 2\sigma(I)$	1155
Max. 2θ/°	25.00
Ranges (h, k, l)	-7 <= h <=9 -9<= k <=8 -6 <= l <= 9
Complete to 2θ (%)	82.8%
Refinement method	Full-matrix least-squares on F^2
Goof (F^2)	1.274
R indices [$I > 2\sigma(I)$]	0.0607
R indices (all data)	0.0642

Table A4.2: Selected bond length (Å) and angle (°) of complex **5.1**

Bond lengths(Å)		**Bond angles (°)**	
Cu1-N1	2.000(8)	N1-Cu1-2N	81.0(3)
Cu1-N2	2.022(8)	Cu1-N1-C5	115.0(6)
N1-C5	1.333(9)	Cu1-N2-C6	109.5(7)
N2-C6	1.46(1)	N1-C5-C6	115.4(8)
C5-C6	1.50(2)	N2-C6-C5	109.6(8)

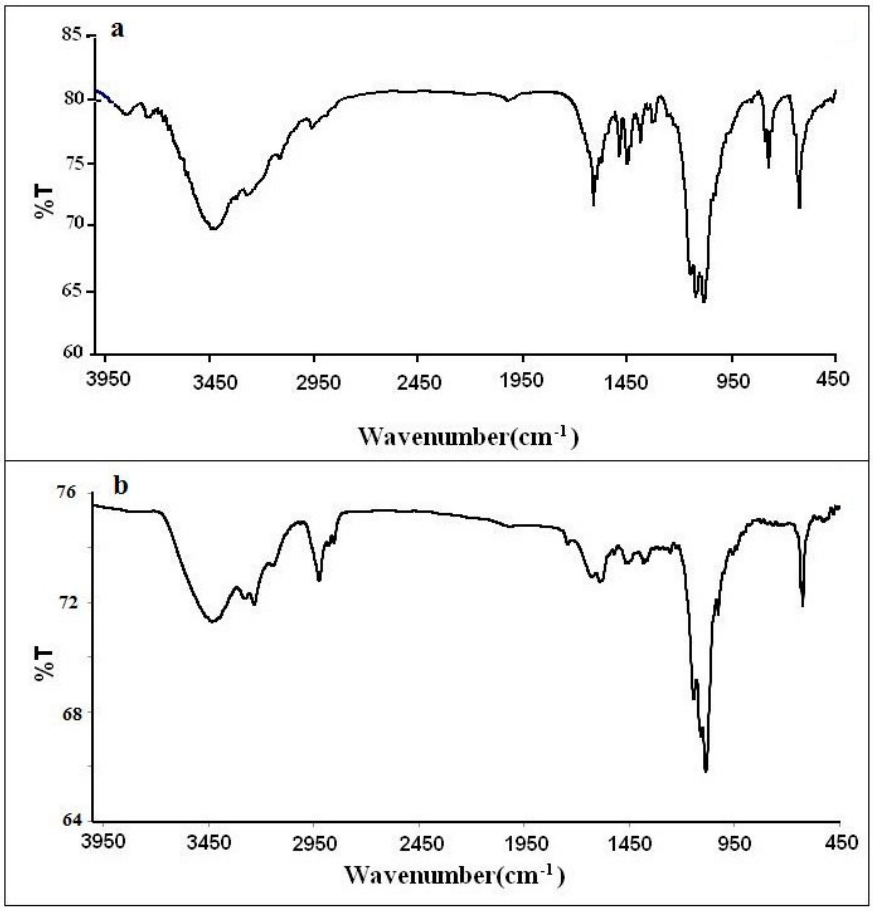

Figure A4.1: FT-IR spectra of complexes (a) **5.1** and (b) **5.2** in KBr pellet.

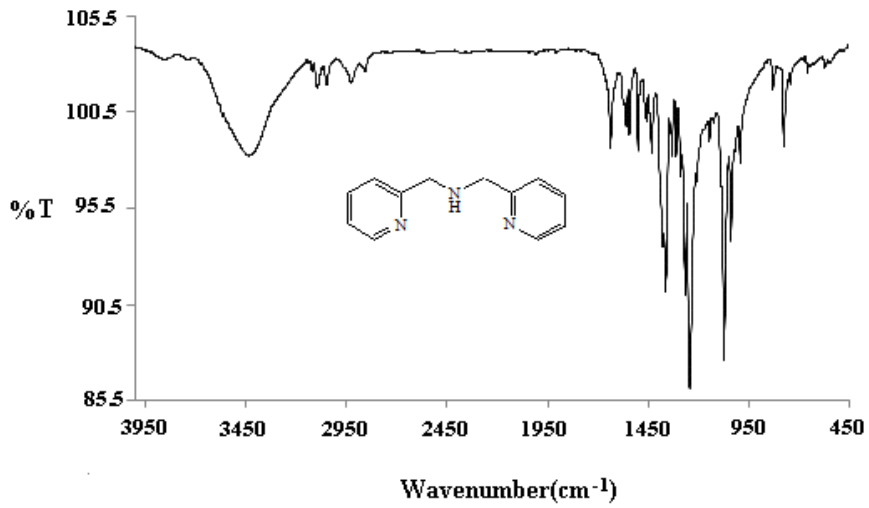

Figure A4.2: FT-IR spectrum of $\mathbf{L_7}'$ in KBr pellet.

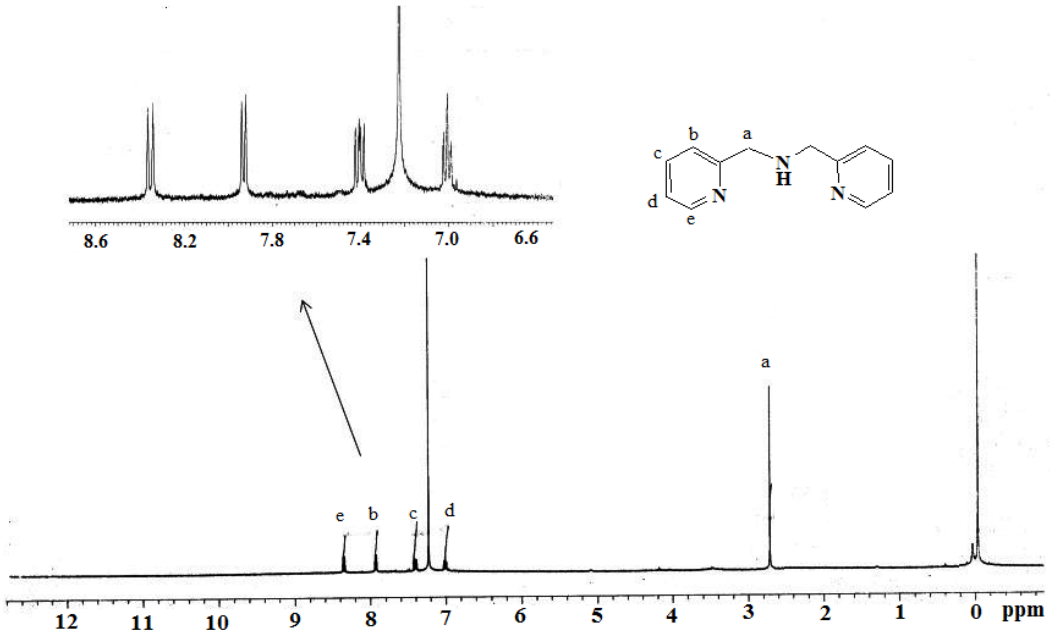

Figure A4.3: ^{1}H-NMR spectrum of $\mathbf{L_7}'$ in $CDCl_3$.

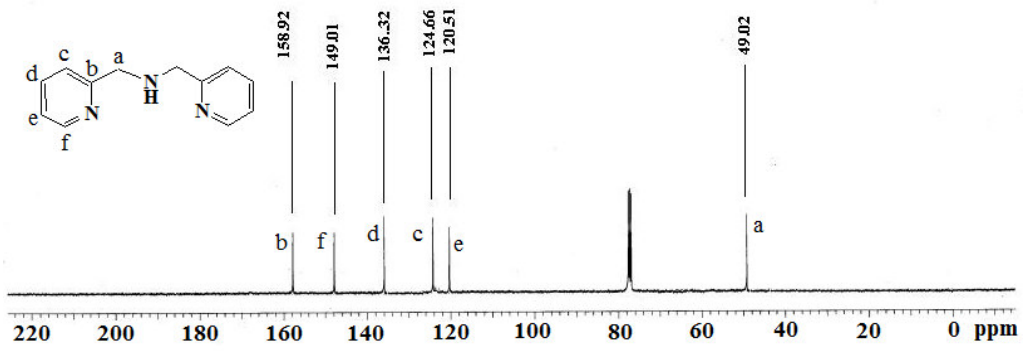

Figure A4.4: ^{13}C-NMR spectrum of $\mathbf{L_7}'$ in $CDCl_3$.

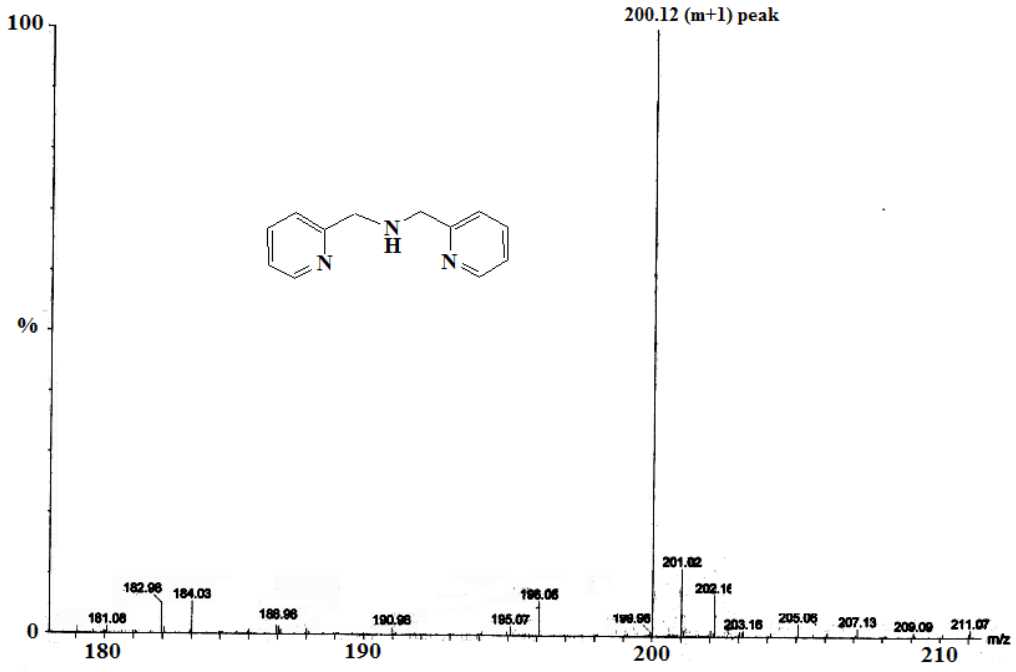

Figure A4.5: ESI-Mass spectrum of $\mathbf{L_7'}$ in Methanol.

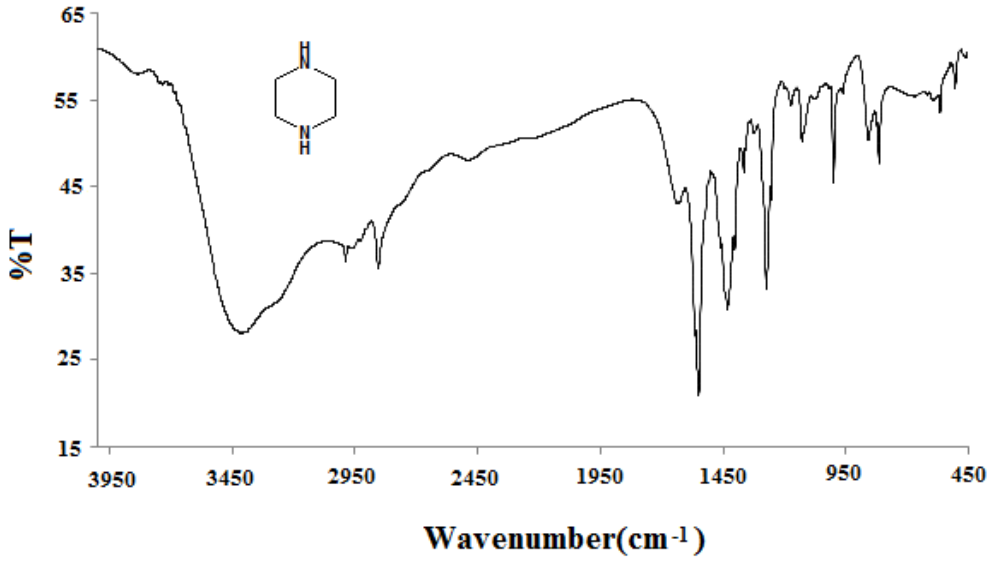

Figure A4.6: FT-IR spectrum of $\mathbf{L_8'}$ in KBr pellet.

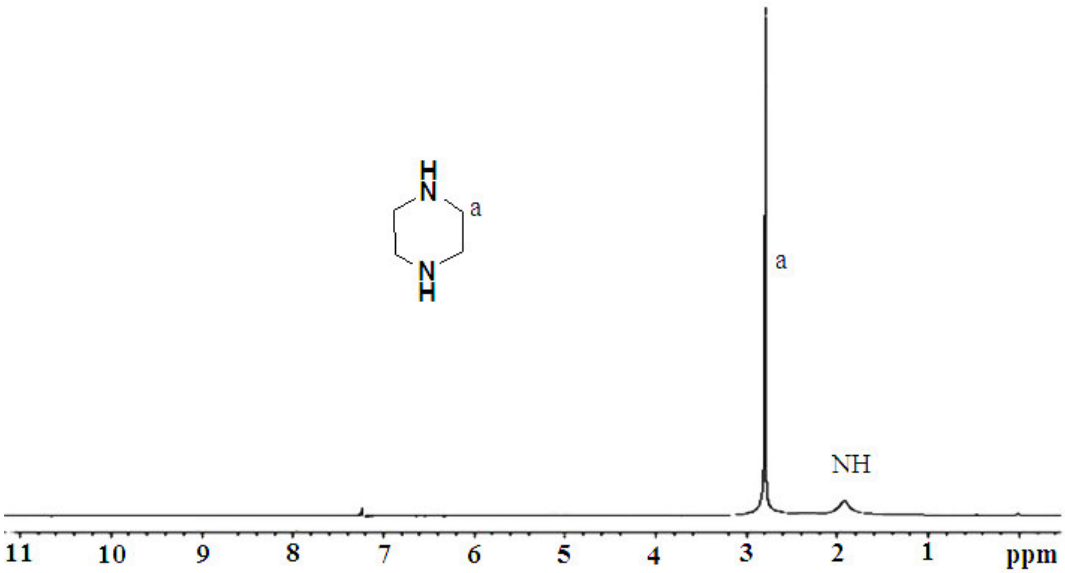

Figure A4.7: ^{1}H-NMR spectrum of $\mathbf{L_8'}$ in $CDCl_3$.

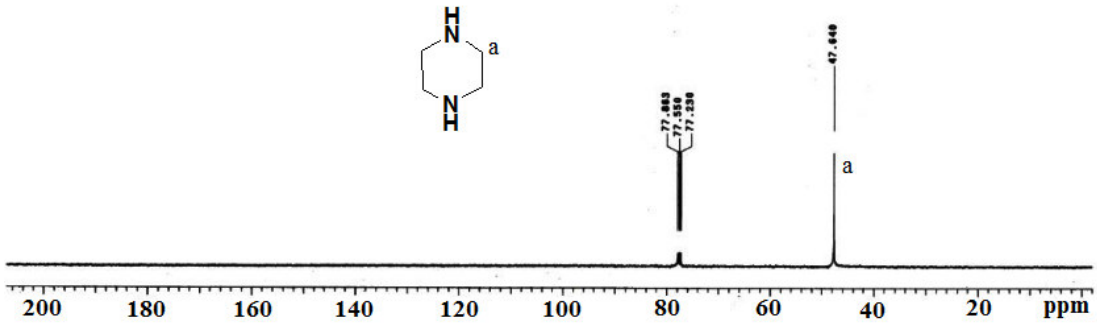

Figure A4.8: ^{13}C-NMR spectrum of $\mathbf{L_8'}$ in $CDCl_3$.

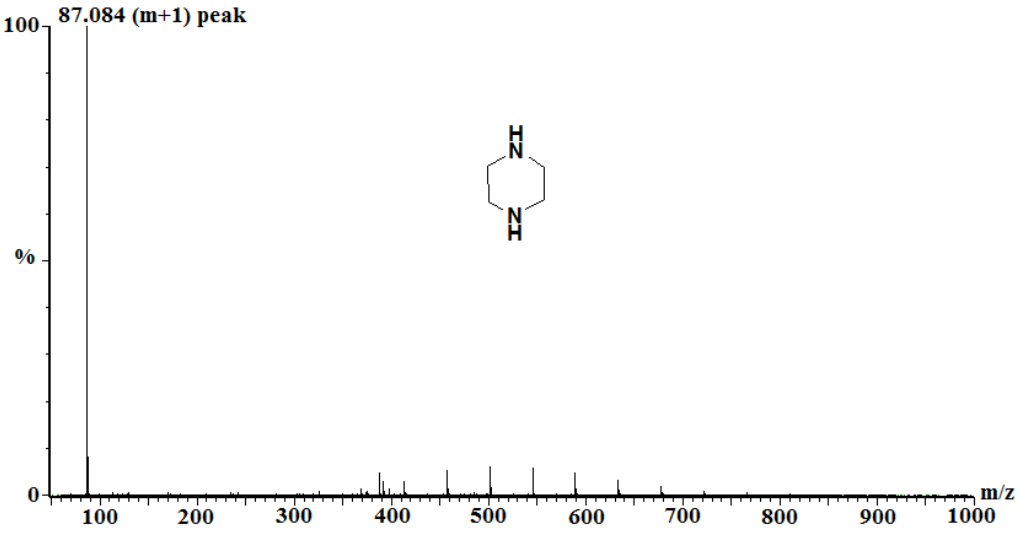

Figure A4.9: ESI-Mass spectrum of $\mathbf{L_8'}$ in methanol.

Appendix V

Synthesis of ligand L_{10}:

The ligand $\mathbf{L_{10}}$ was synthesized using the following procedure.

Ligand $\mathbf{L_{10}}$ was synthesized in three steps (scheme A5.1):

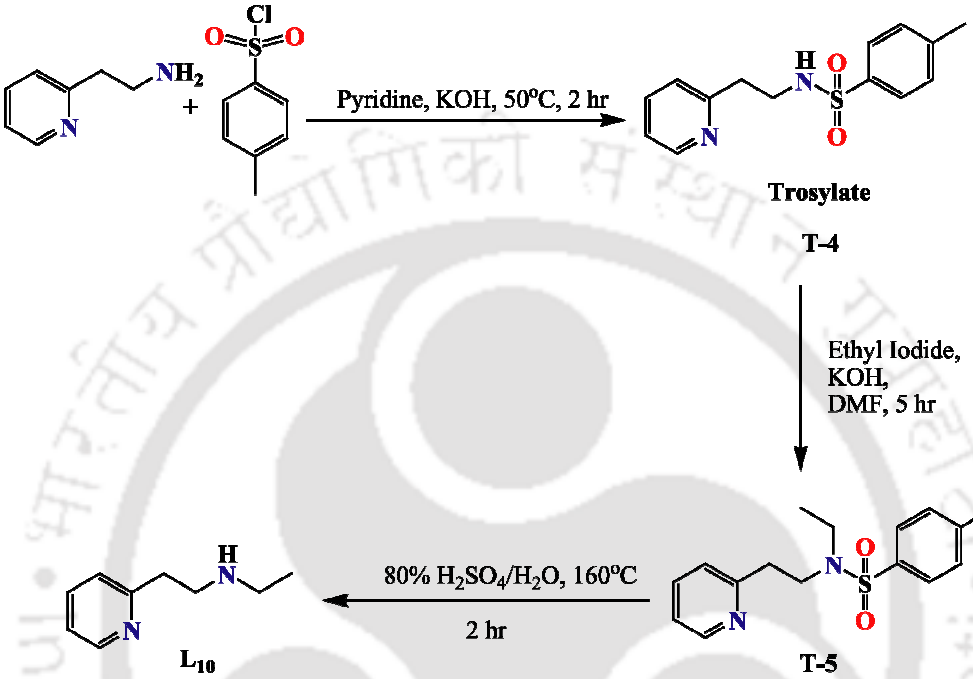

Scheme A5.1

Step I. Tosylation of 2-(2-aminoethyl)-pyridine:

A 250-ml two-necked round-bottomed flask equipped with a magnetic stirring bar, reflux condenser and a rubber septum was charged with 2-(2-aminoethyl)-pyridine (0.736 g; 6.0 mmol), pyridine (20 ml) and potassium hydroxide (1.01 g; 18.0 mmol). The mixture was stirred and cooled in an ice bath while 3.43 g (18.0 mmol) of tosyl chloride was added over a period of 5 min. After 5 min, the ice bath was removed and the reaction mixture was heated to 50 °C in an oil bath for 2 h with constant stirring. The reaction mixture was allowed to cool to room temperature was then poured into 20 ml ice-cold water. The crude tosylated product was obtained as whitish precipitate. The precipitate was purified by column chromatography using hexane to give 1.45 g (~ 87%) of 2-(N-*p*-methylbenzenesulfonamide-2-aminoethyl)-pyridine (**T-4**). FT-IR: 3064(m), 1597(m), 1325(s), 1156(m), 1082(s), 550(s) cm^{-1}. ^{1}H-NMR (400 MHz, $CDCl_3$): δ_{ppm}, 8.43(d, 1H), 7.70(d, 2H), 7.55(t, 1H), 7.24(d, 2H), 7.11(t, 1H), 7.05(d,1H), 3.32(q, 2H), 2.90(t, 2H), 2.37(s, 3H) . ^{13}C-NMR (100 MHz, $CDCl_3$): δ_{ppm}, 159.04,

149.19, 143.30, 137.32, 136.93, 129.79, 127.22, 123,72, 121.92, 42.43, 36.42, 21.65. (m+23)/z: calculated 299.07; found 299.14.

Step II: Ethylation of T-4:

A 250-ml two-necked round-bottomed flask equipped with a magnetic stirring bar, reflux condenser and a rubber septum was charged with 0.829 g (3.0 mmol) of **T-4,** 1.1 g (21.0 mmol) of potassium hydroxide, and 20 ml of anhydrous dimethylformamide (DMF). To this 2 g (12.0 mmol) ethyl iodide was added over a period of 5 min and the resulting mixture was heated at 60 °C in an oil bath for 4h. The reaction mixture was then allowed to cool to room temperature, diluted with 250 ml of water, and extracted with $CHCl_3$ (100 ml x 3 portions). The combined organic extracts were washed with brine (100 ml), dried over anhydrous sodium sulphate and concentrated under reduced pressure to give pale yellow oil. The oil was purified by column chromatography on neutral alumina to give 0.69 g (~86%) of **T-5** as a viscous pale yellow liquid. FT-IR: 2925(m), 1594(m), 1336(s), 1156(s), 550(s) cm^{-1}. ^{1}H-NMR (400 MHz, $CDCl_3$): δ_{ppm}, 8.46(d, 1H), 7.65(d, 2H), 7.56(t, 1H), 7.24(d, 2H), 7.16(d, 1H), 7.08(t, 1H), 3.47(t, 2H), 3.16(q, 2H), 3.02(t, 2H), 2.12(s. 2H), 0.99(t, 3H). ^{13}C-NMR (100 MHz, $CDCl_3$): δ_{ppm}, 156.65, 149.30, 143.19, 136.98, 136.58, 129.65, 127.11, 123.76, 121.64, 47.50, 43.421, 38.07, 21.48, 13.91. (m+1)/z: calculated 305.12; found 305.18.

Step III. Hydrolysis of T-5:

A 100-ml two-necked round-bottomed flask equipped with a magnetic stirring bar, reflux condenser, and a rubber septum was charged with 3.04g (10.0 mmol) of **T-5**, 17 ml of 80% H_2SO_4, and the resulting mixture was heated at 160 °C in an oil bath with constant stirring till solid goes into solution. The reaction mixture was then allowed to cool to room temperature, diluted with 30 ml of water and neutralized with 20% NaOH solution. The resulting amine was then extracted with 3 x 50 ml portions of dichloromethane. The combined organic extracts were washed with brine (100 ml), dried over anhydrous sodium sulphate and concentrated under reduced pressure. The residue was purified by column chromatography on neutral alumina to give 0.65 g (~43%) of the desired amine $\mathbf{L_{10}}$. FT-IR: 2971(m), 1595(m), 1382(s) cm^{-1}. ^{1}H-NMR (400 MHz, $CDCl_3$): δ_{ppm}, 8.48(d, 1H), 7.56(t, 1H), 7.15(d, 1H), 7.08(t, 1H), 3.02(t, 2H), 2.99(t, 2H), 2.70(q, 2H), 1.09(t, 2H). ^{13}C-NMR (100 MHz, CDCl3): δ_{ppm}, 159.75, 148.75, 135.81, 122.73, 120.56, 48.69, 43.42, 37.92, 14.71; (m+1)/z: calculated 151.12; found 151.11.

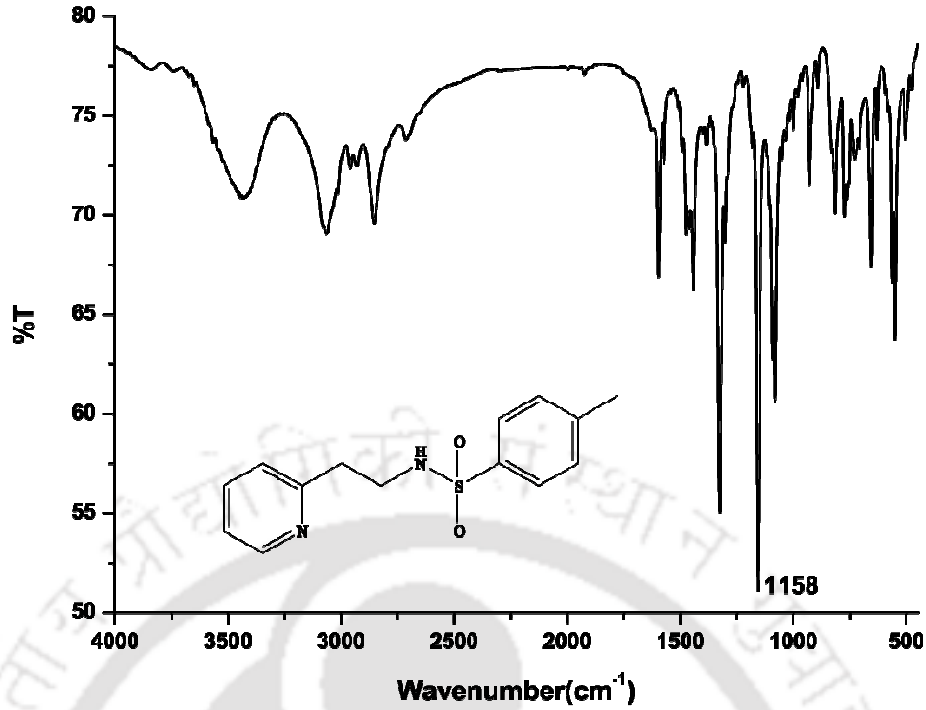

Figure A5.1: FT-IR spectrum of **T-4** in KBr pellet.

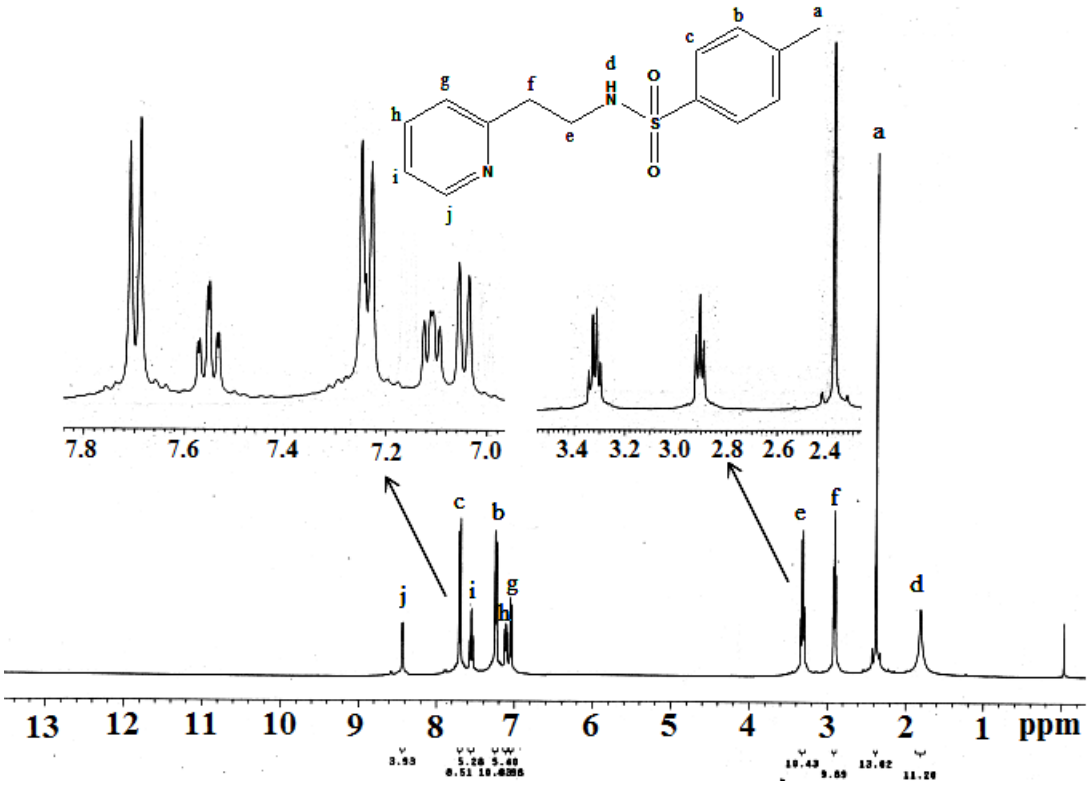

Figure A5.2: ^{1}H-NMR spectrum of **T-4** in $CDCl_3$.

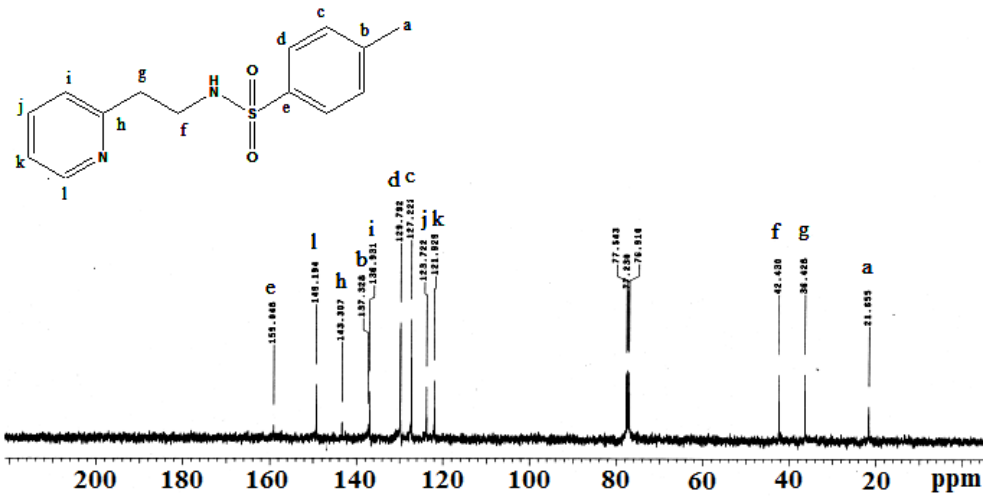

Figure A5.3: ^{13}C-NMR spectrum of **T-4** in $CDCl_3$.

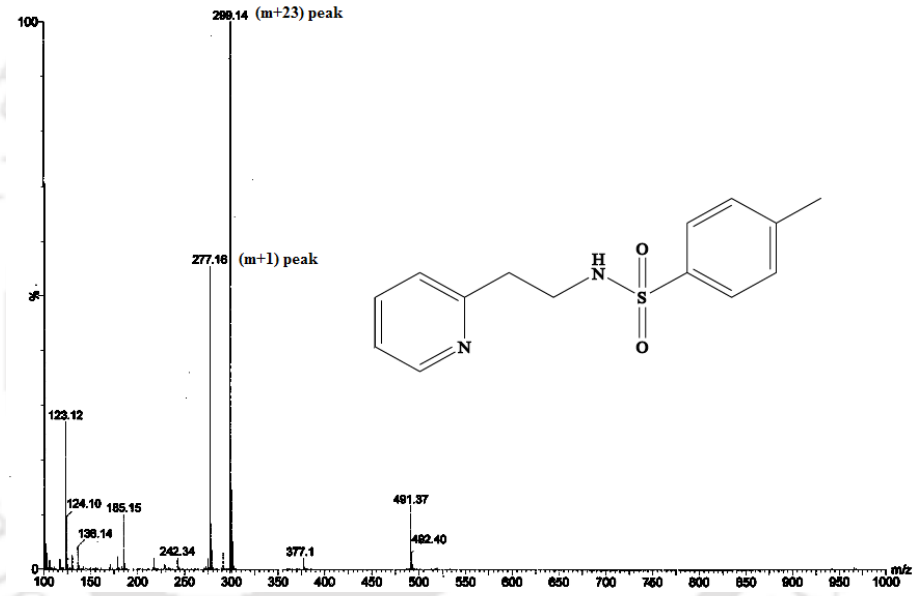

Figure A5.4: ESI-Mass spectrum of **T-4** in methanol.

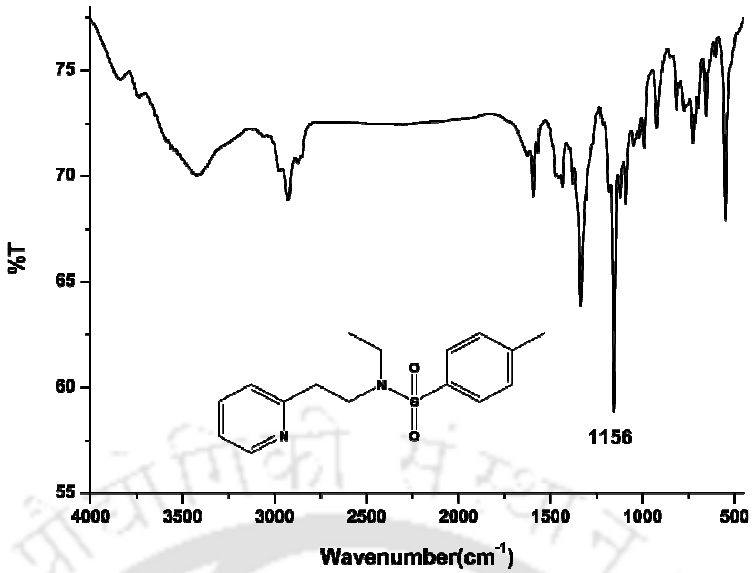

Figure A5.5: FT-IR spectrum of **T-5** in KBr pellet.

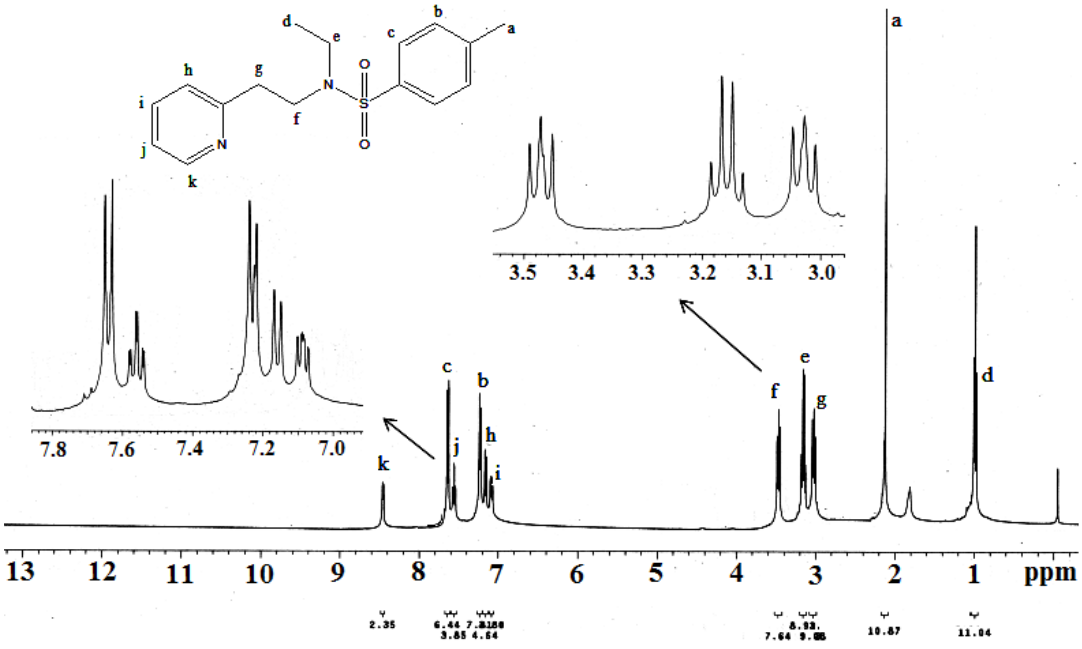

Figure A5.6: ^{1}H-NMR spectrum of **T-5** in $CDCl_3$.

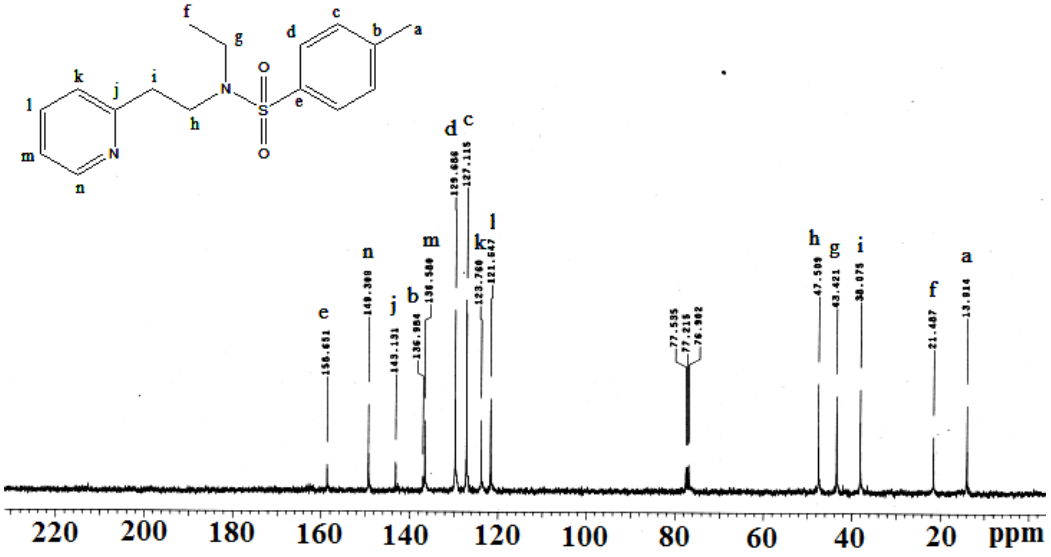

Figure A5.7: ^{13}C-NMR spectrum of **T-5** in $CDCl_3$.

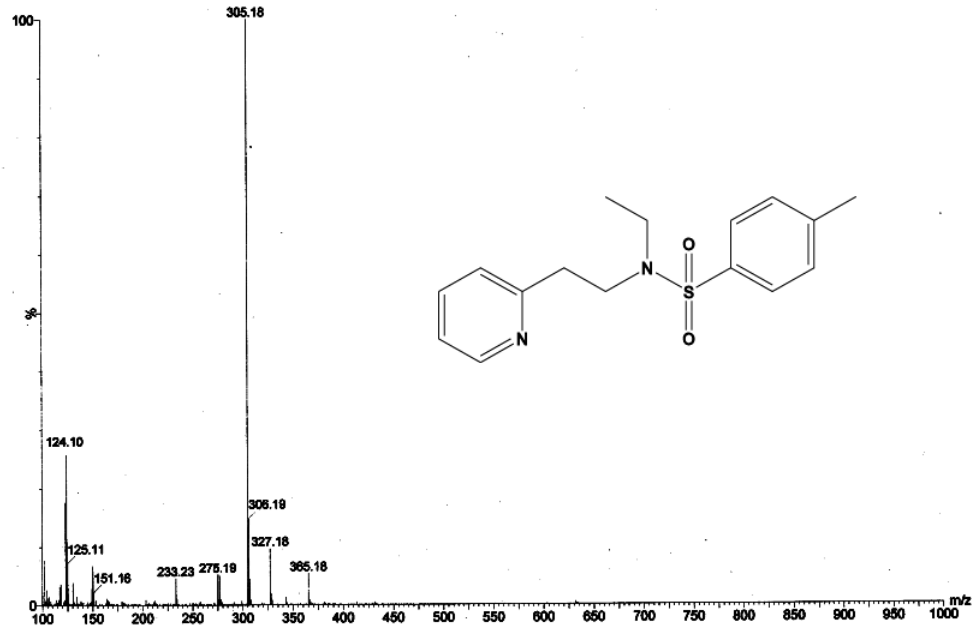

Figure A5.8: ESI-Mass spectrum of **T-5** in methanol.

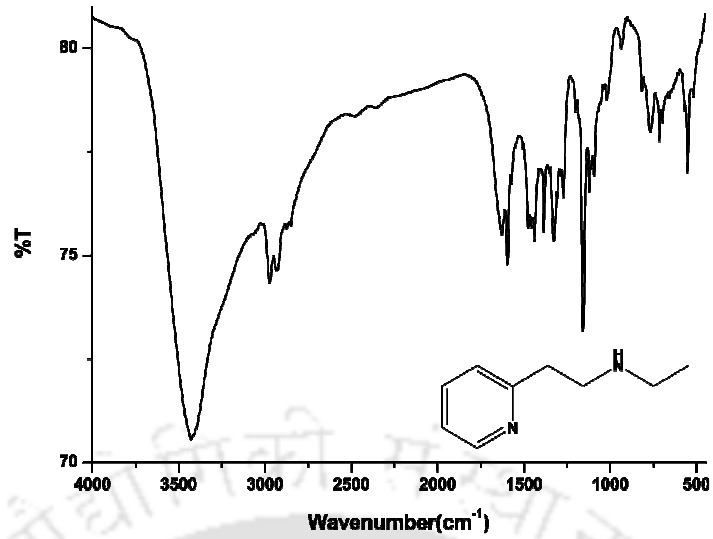

Figure A5.9: FT-IR spectrum of $\mathbf{L_{10}}$ in KBr pellet.

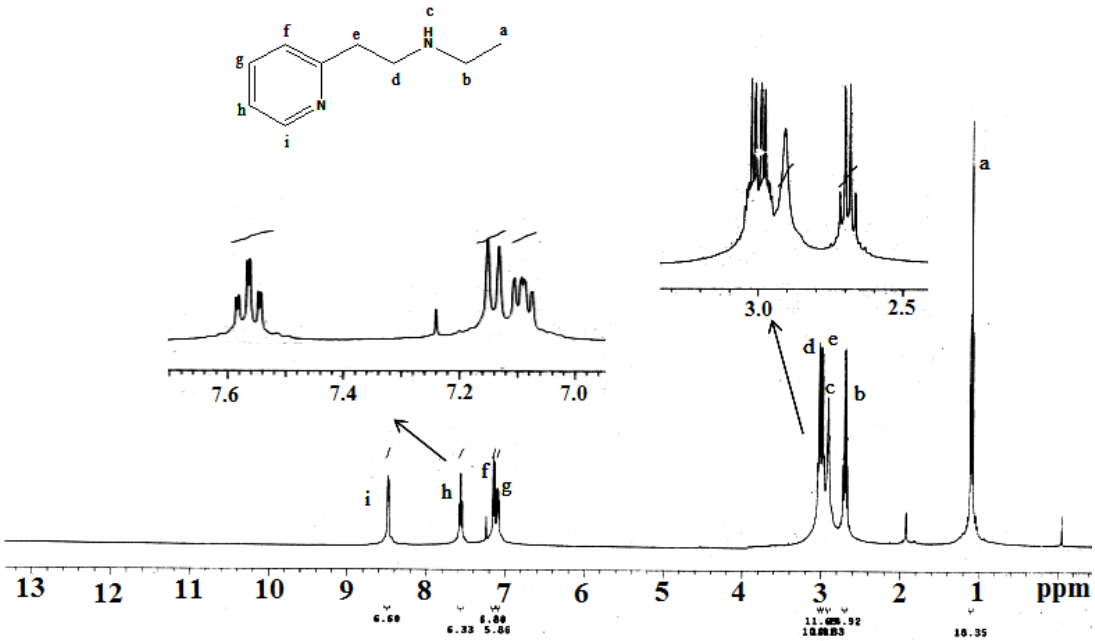

Figure A5.10: ^{1}H-NMR spectrum of $\mathbf{L_{10}}$ in $CDCl_3$.

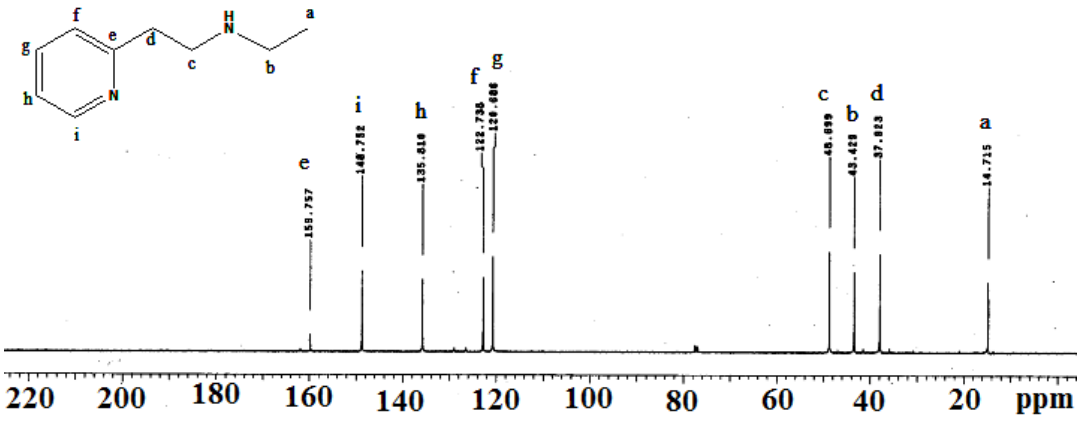

Figure A5.11: ^{13}C-NMR spectrum of $\mathbf{L_{10}}$ in $CDCl_3$.

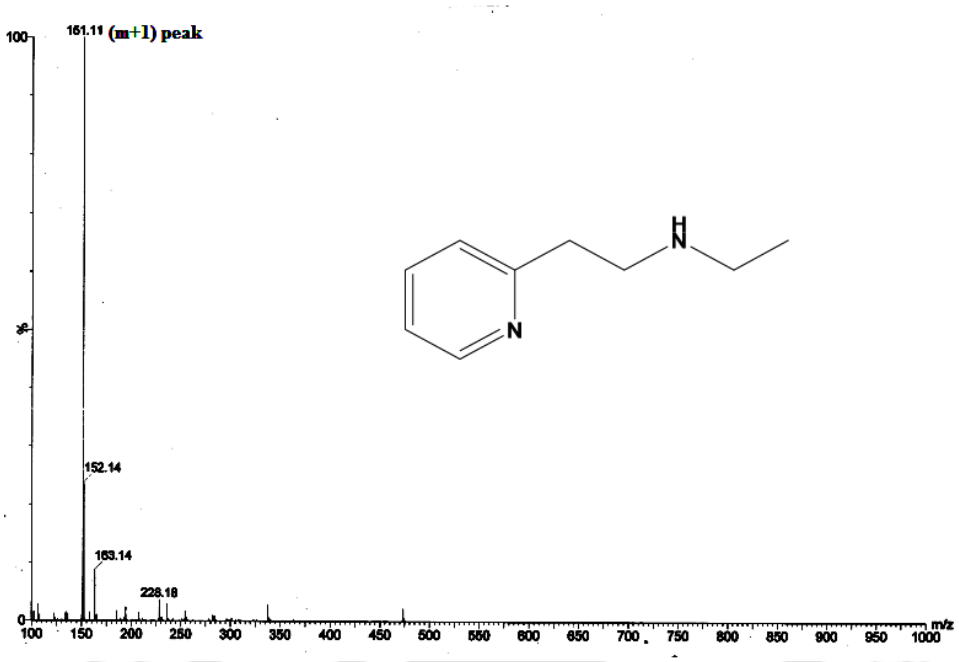

Figure A5.12: ESI-Mass spectrum of $\mathbf{L_{10}}$ in methanol.

Table A5.1. Crystallographic data for complex **6.1**

	Complex 6.1
Formulae	$C_{14}\ H_{16}\ Cl_2\ Cu\ N_4\ O_8$
Mol. wt.	502.76
Crystal system	Triclinic
Space group	P1
Temperature /K	296(2)
Wavelength /Å	0.71073
a /Å	7.9150(11)
b /Å	8.1101(13)
c /Å	8.3258(15)
α/°	107.969(11)
β/°	97.906(11)
γ/°	104.422(10)
V/ $Å^3$	478.84(14)
Z	1
Density/Mgm^{-3}	1.743
Abs. Coeff. /mm^{-1}	1.303
Abs. correction	None
F(000)	206
Total no.of reflections	2541
Reflections, $I > 2\sigma(I)$	1956
Max. 2θ/°	28.57

Ranges (h, k, l)	-10 <= h <=10 -8<= k <=10 -9<= l <= 8
Complete to 2θ (%)	72.6%
Refinement method	Full-matrix least-squares on F^2
Goof (F^2)	1.102
R indices [$I > 2\sigma(I)$]	0.0579
R indices (all data)	0.0819

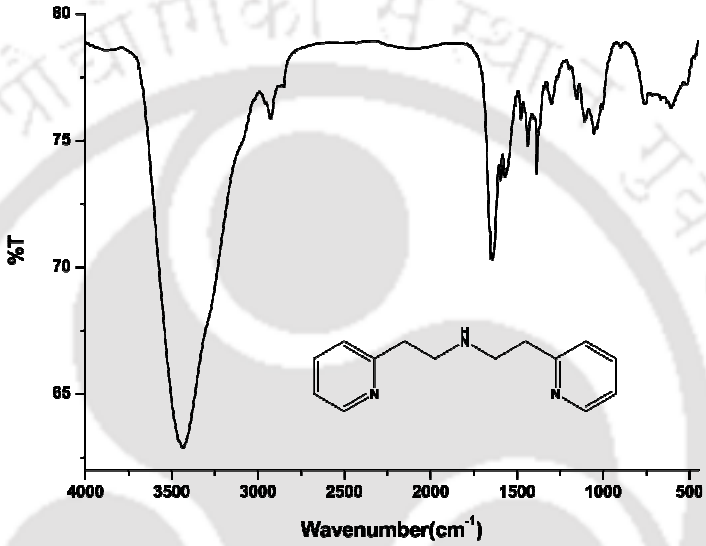

Figure A5.1: FT-IR spectrum of $\mathbf{L_9}'$ in KBr pellet.

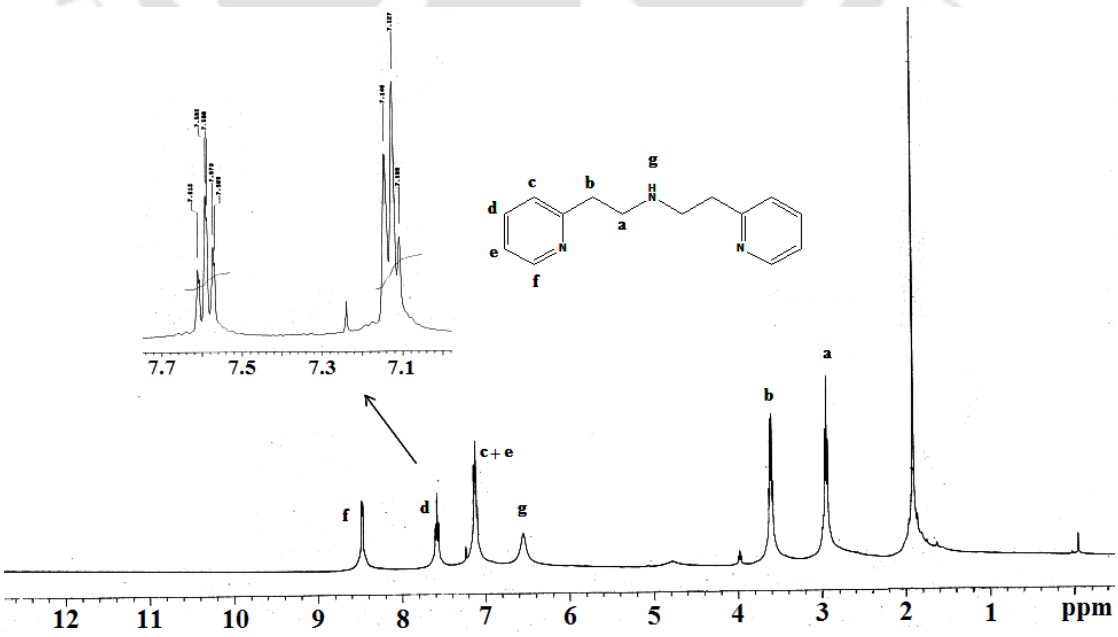

Figure A5.2: ^{1}H-NMR spectrum of $\mathbf{L_9}'$ in CD_3Cl.

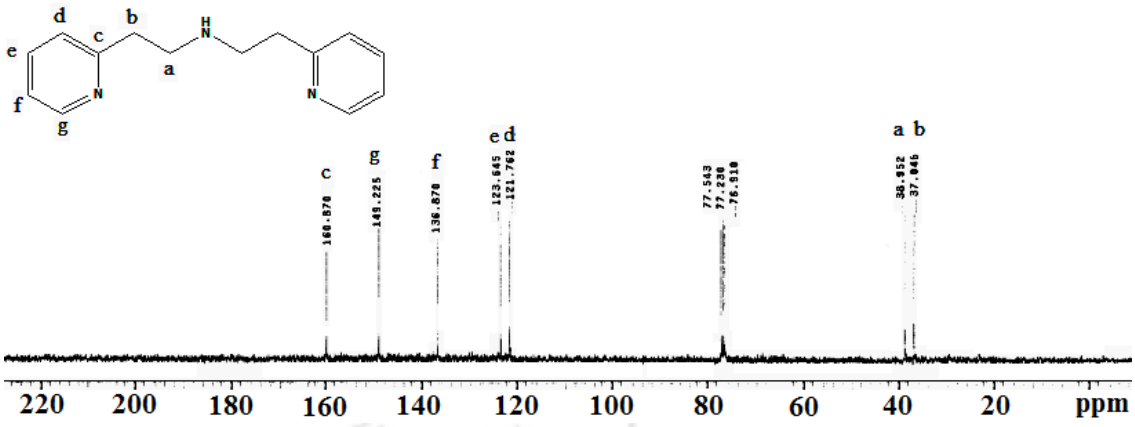

Figure A5.3: ^{13}C-NMR spectrum of $\mathbf{L_9'}$ in CD_3Cl.

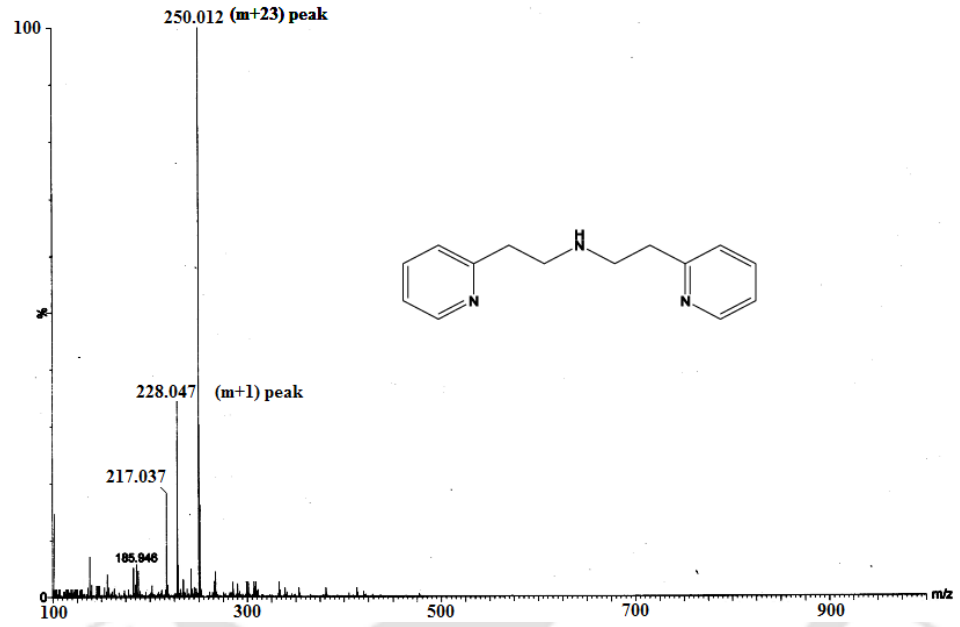

Figure A5.4: ESI-Mass spectrum of $\mathbf{L_9'}$ in methanol.

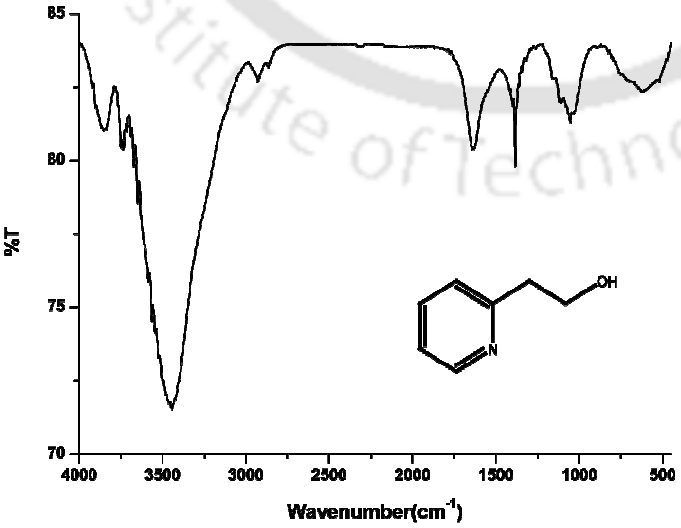

Figure A5.5: FT-IR spectrum of $\mathbf{L_9''}$ in KBr pellet.

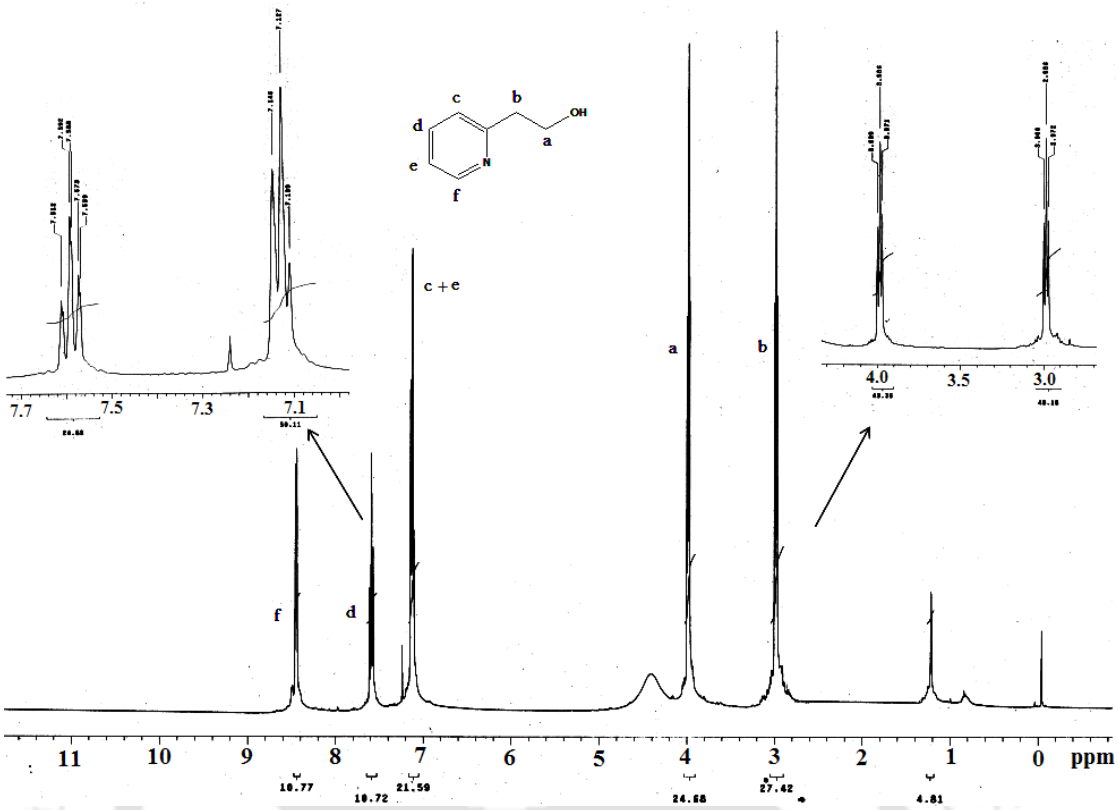

Figure A5.6: ^{1}H-NMR spectrum of $\mathbf{L_9''}$ in CD_3Cl.

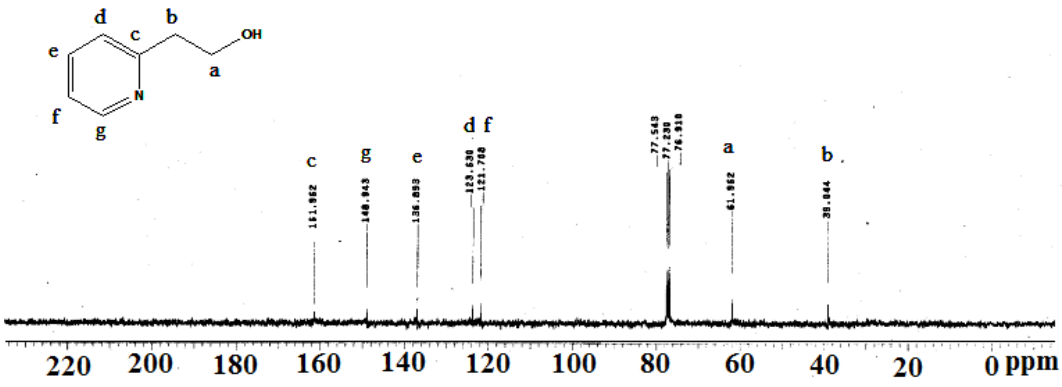

Figure A5.7: ^{13}C-NMR spectrum of $\mathbf{L_9''}$ in CD_3Cl.

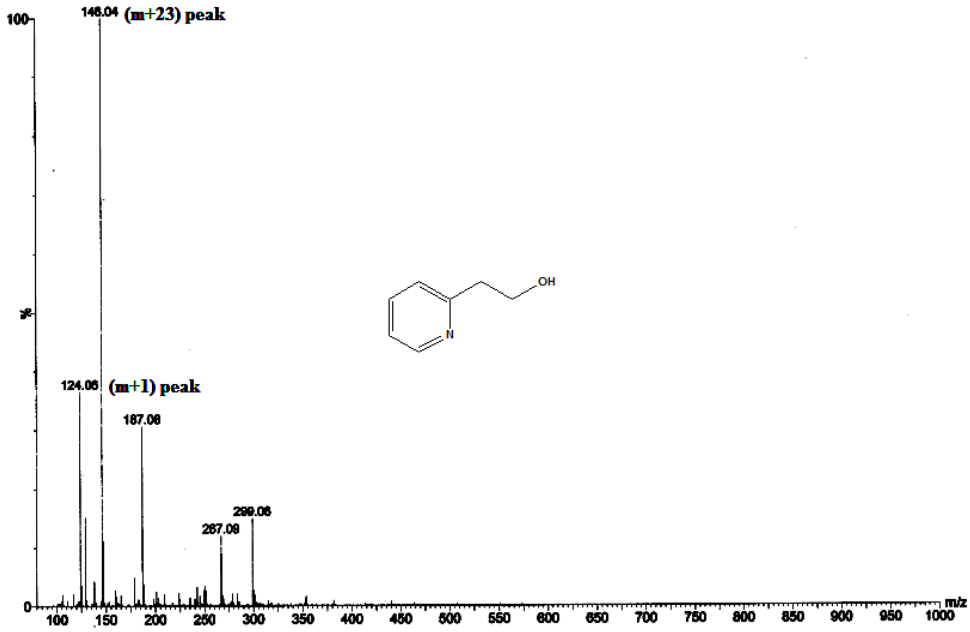

Figure A5.8: ESI-Mass spectrum of $\mathbf{L_9''}$ in methanol.

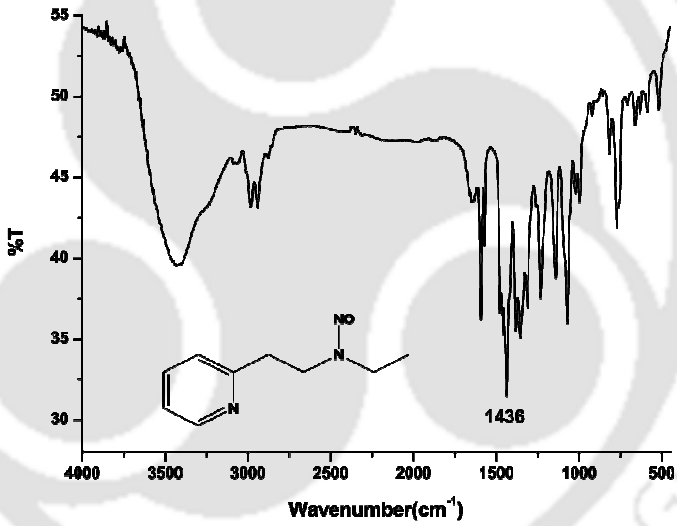

Figure A5.9: FT-IR spectrum of $\mathbf{L_{10}'}$ in KBr pellet.

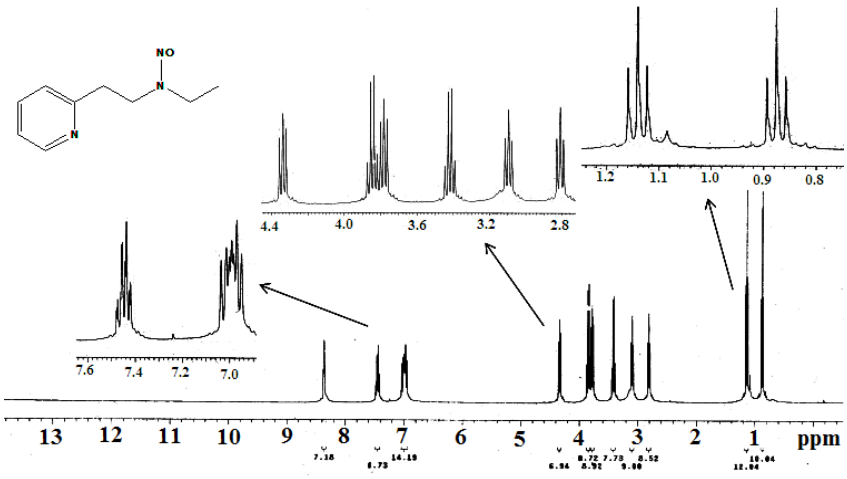

Figure A5.10: ^{1}H-NMR spectrum of $\mathbf{L_{10}'}$ in CD_3Cl.

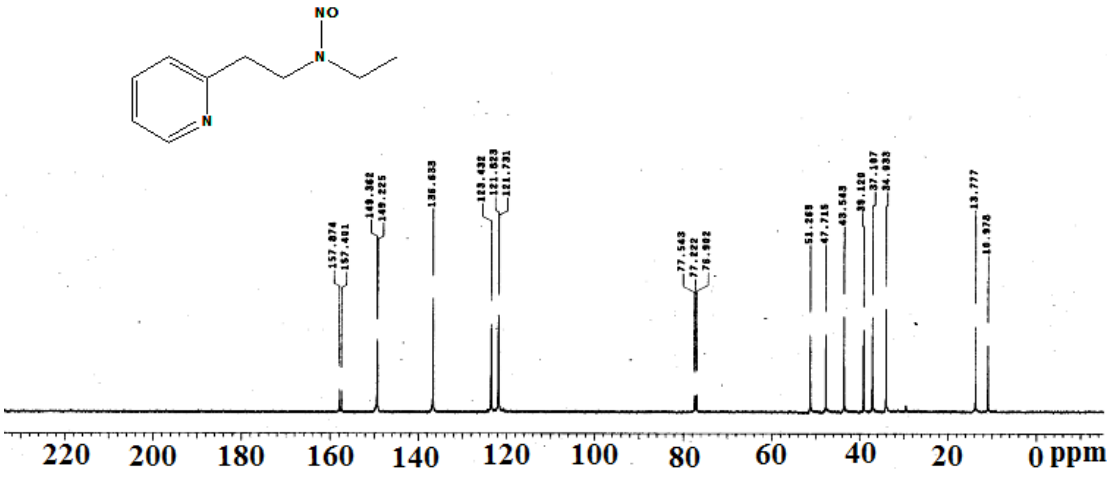

Figure A5.11: ^{13}C-NMR spectrum of $\mathbf{L_{10}}'$ in CD_3Cl.

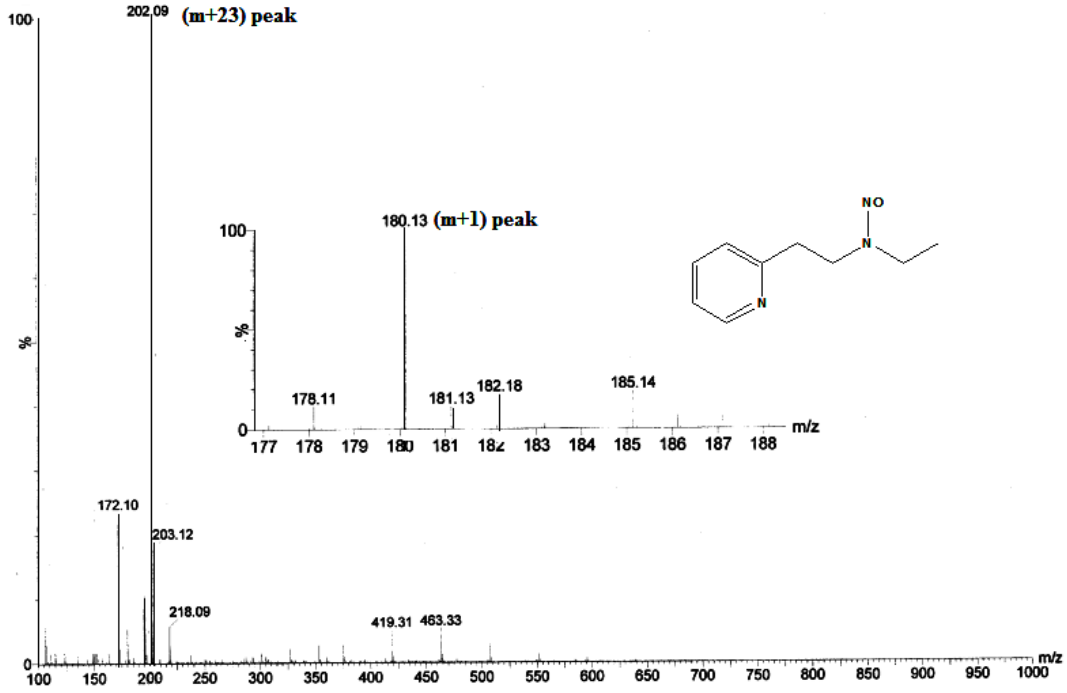

Figure A5.12: ESI-Mass spectrum of $\mathbf{L_{10}}'$ in methanol.

List of Publications

1. Reduction of copper(II) complexes of tripodal ligands by nitric oxide and trinitrosation of the ligands.

   Sarma, **M**.; Kalita, A.; Kumar, P.; Singh, A.; Mondal, B. *J. Am. Chem. Soc.* **2010**, *132*, 7846.

2. Nitric oxide reduction of copper(II) complex with tetradentate ligand followed by ligand transformation.

   Sarma, **M**.; Singh, A.; Mondal, B. *Inorg. Chim. Acta*, **2010**, *363*, 63.

3. Nitric oxide reduction of copper(II) complexes: spectroscopic evidence of copper(II) nitrosyl intermediate.

   Sarma, **M**; Mondal, B. *Inorg. Chem.* **2011**, *50*, 3206.

4. An asymmetric dinuclear copper(II) complex with phenoxo and acetate bridges: synthesis, structure and magnetic studies.

   Dutta, G.; Debnath, R. K.; Kalita, A.; Kumar, P.; **Sarma**, **M**.; Shankar, R. B.; Mondal, B. *Polyhedron* **2011**, *30*, 293.

5. Nitric oxide reactivity of copper(II) complexes of bidentate amine ligands: Effect of substitution on ligand nitrosation

   Sarma, **M**.; Mondal, B. *Dalton Trans*. DOI:10.1039/C2DT11082B

6. Nitric oxide reactivity of copper(II) complexes of bidentate bigands having aliphatic and aliphatic amine site : Effect of ring size on stability of [Cu^{II}-$NO^{\bullet}$] intermediate.

   Sarma, **M**.; Mondal, B. (*Manuscript under preparation*).